

**IDENTIFICATION OF ECG ANOMALIES
THROUGH DEEP DETERMINISTIC LEARNING**

UZAIR IQBAL

**FACULTY OF COMPUTER SCIENCE AND
INFORMATION TECHNOLOGY
UNIVERSITY OF MALAYA
KUALA LUMPUR**

2020

**IDENTIFICATION
OF ECG ANOMALIES THROUGH DEEP
DETERMINISTIC LEARNING**

UZAIR IQBAL

**THESIS SUBMITTED IN FULFILMENT OF THE
REQUIREMENTS FOR THE DEGREE OF DOCTOR
OF PHILOSOPHY**

**FACULTY OF COMPUTER SCIENCE AND
INFORMATION TECHNOLOGY
UNIVERSITY OF MALAYA
KUALA LUMPUR**

2020

UNIVERSITY OF MALAYA

ORIGINAL LITERARY WORK DECLARATION

Name of Candidate: UZAIR IQBAL

Registration/Matric No: 17050458/1

Name of Degree: Doctor of Philosophy

Title of Thesis: IDENTIFICATION OF ECG ANOMALIES THROUGH DEEP DETERMINISTIC LEARNING

Field of Study: Data mining (Computer Science)

I do solemnly and sincerely declare that:

- (1) I am the sole author/writer of this Work;
- (2) This Work is original;
- (3) Any use of any work in which copyright exists was done by way of fair dealing and for permitted purposes and any excerpt or extract from, or reference to or reproduction of any copyright work has been disclosed expressly and sufficiently and the title of the Work and its authorship have been acknowledged in this Work;
- (4) I do not have any actual knowledge nor do I ought reasonably to know that the making of this work constitutes an infringement of any copyright work;
- (5) I hereby assign all and every rights in the copyright to this Work to the University of Malaya ("UM"), who henceforth shall be owner of the copyright in this Work and that any reproduction or use in any form or by any means whatsoever is prohibited without the written consent of UM having been first had and obtained;
- (6) I am fully aware that if in the course of making this Work I have infringed any copyright whether intentionally or otherwise, I may be subject to legal action or any other action as may be determined by UM.

Candidate's Signature

Date:

Subscribed and solemnly declared before,

Witness's Signature

Date:

Name:

Designation:

IDENTIFICATION OF ECG ANOMALIES THROUGH DEEP DETERMINISTIC LEARNING

ABSTRACT

Electrocardiography (ECG) is a primary diagnostic tool for measuring the malfunctioning of the heart muscles in the context of morbidity of different cardiac diseases and arrhythmia. Different existing techniques and methods delivered accurate cardiac diseases myocardial infarction (heart stroke) and atrial fibrillation recognition. However, there are still some flaws in existing methods like recognition of special myocardial infarction situation flattened T wave in “Non-Specific ST-T Changes (*nsst-t*)” and reduction of computational cost in cardiac diseases recognition. Accurate recognition of cardiac diseases along with least computational complexity and feature analysis of *flattened T wave* in myocardial infarction remains an open job. In this research, three different datasets were used for experimental activities. Two datasets are publicly available namely; Massachusetts Institute of Technology-Beth Israel Hospital (MIT-BIH) arrhythmia database and Physikalisch-Technische Bundesanstalt (PTB), and the third dataset are exclusively obtained from the University of Malaya Medical Center (UMMC), Kuala Lumpur, Malaysia. This thesis presents the major contributions in perspective of, accurate as well as least computational complex in recognition of atrial fibrillation and flattened T wave situation in myocardial infarction detection and prediction. Two new deterministic methods are proposed namely; deep deterministic learning (DDL) and model driven deep deterministic learning (MDDDL) which delivered impressive results in recognition and predictive classification of atrial fibrillation and *flattened T wave* situation in myocardial infarction (i.e., $\leq 99.97\%$). Finally, both the proposed

models DDL and MDDDL are further useful for recognition and predictive classification of the other malfunctions of the heart.

Keywords: Deep Deterministic Learning, Classification, Wavelet Analysis, Myocardial Infarction, Electrocardiography.

Universiti Malaya

PENGENALAN ANOMI EKG MELALUI PEMBELAJARAN DETERMINISTIK

ABSTRAK

Elektrokardiografi (ECG) adalah alat diagnostik utama untuk mengukur kerosakan otot jantung dalam konteks morbiditi penyakit jantung dan aritmia yang berbeza. Pelbagai teknik dan kaedah yang ada memberikan penyakit jantung yang tepat infark miokard (strok jantung) dan pengiktirafan fibrilasi atrium. Walau bagaimanapun, masih terdapat beberapa kekurangan dalam kaedah yang ada seperti pengakuan keadaan infark miokard khas yang meratakan gelombang T dalam "Perubahan ST-T Tidak Spesifik (nsst-t)" dan pengurangan kos pengiraan dalam pengiktirafan penyakit jantung. Pengiktirafan penyakit jantung yang tepat bersamaan dengan kerumitan komputasi dan analisis ciri gelombang T yang rata dalam infark miokard tetap menjadi pekerjaan terbuka. Dalam penyelidikan ini, tiga set data yang berbeza digunakan untuk aktiviti eksperimen. Dua set data tersedia untuk umum iaitu; Pangkalan data aritmia Massachusetts Institute of Technology-Beth Israel Hospital (MIT-BIH) dan Physikalisch-Technische Bundesanstalt (PTB), dan kumpulan data ketiga diperoleh secara eksklusif dari Pusat Perubatan Universiti Malaya (UMMC), Kuala Lumpur, Malaysia. Tesis ini memberikan sumbangan utama dari sudut komputasi tepat, tepat dan paling tidak untuk mengiktiraf fibrilasi atrium dan keadaan gelombang T yang rata dalam pengesanan dan ramalan infark miokard. Dua kaedah deterministik baru dicadangkan iaitu; pembelajaran deterministik mendalam (DDL) dan pembelajaran deterministik mendalam yang didorong oleh model (MDDDL) yang memberikan hasil yang mengagumkan dalam pengiktirafan dan klasifikasi ramalan fibrilasi atrium dan keadaan gelombang T yang rata dalam infark miokard (iaitu, .999.97%). Akhirnya, kedua-dua model yang dicadangkan DDL dan MDDDL lebih berguna untuk pengiktirafan dan klasifikasi ramalan kerosakan fungsi pendengaran yang lain.

Kata kunci: Pembelajaran Deterministik Dalam, Klasifikasi, Analisis Wavelet, Infarksi miokardium, Elektrokardiografi

Universiti Malaya

ACKNOWLEDGEMENTS

First, thanks to almighty ALLAH for endowing me with enough strength, wisdom and courage and bestowing upon me His blessings to do my PhD. Next, I would like to express my deepest gratitude to my supervisor, Professor Dr. Teh Ying Wah for his continuous support, supervision and encouragement throughout my PhD progression. I also extend my profound thanks to Dr. Muhammad Habib-ur-Rehman for his invaluable guidance and advice.

On a personal level, my wife Sidra Attique deserves a special mention, who provided me with unrelenting emotional sustenance and superb motivation. Without her constant help, reassurance and patience, it would have been hard for me to bring this project to fruition.

Finally, this Thesis is dedicated to my father Muhammad Iqbal, my mother Azra Parveen and my elder brother Umair Iqbal for their continual care and encouragement.

TABLE OF CONTENTS

ABSTRACT.....	III
ABSTRAK.....	V
ACKNOWLEDGEMENTS.....	VII
TABLE OF CONTENTS.....	VIII
LIST OF FIGURES.....	XIII
LIST OF TABLES.....	XV
LIST OF SYMBOLS AND ABBREVIATIONS.....	XVII
LIST OF APPENDICES.....	XX
CHAPTER 1: INTRODUCTION.....	1
1.1 Background.....	1
1.2 Research Motivation.....	5
1.3 Problem Statement.....	7
1.4 Aims and Objectives.....	9
1.5 Research Questions.....	10
1.6 Research Methodology and Design:.....	11
1.6.1 Problem Identification:.....	11
1.6.2 ECG Dataset Collection.....	12
1.6.3 Signal Pre-Processing.....	12
1.6.4 Feature Engineering.....	12
1.6.5 Recognition and Prediction Models Construction.....	12
1.6.6 Evaluation of Recognition and Prediction Models.....	13
1.7 Research Significance.....	13
1.8 Research Contribution.....	14
1.9 Research Scope.....	15
1.10 Thesis Outline.....	16

CHAPTER 2: LITERATURE REVIEW	18
2.1 Introduction.....	18
2.2 Heart diseases detection: A Biomedical Domain	18
2.2.1 Data acquisition.....	21
2.2.2 Data pre-processing.....	22
2.2.3 Feature Extraction and Selection	24
2.2.4 Recognition and Predictive Classification techniques	30
2.3 Review of Modular Based Techniques.....	33
2.3.1 Data Driven Classification	33
2.3.2 Regressive Modeling.....	35
2.3.3 Current Trend	35
2.4 Review of MI Detection Methods	37
2.4.1 T wave anomalies through a T-onset feature	38
2.4.2 Impact of T wave Dependencies	40
2.4.3 MI and NSST-T	41
2.5 Review of Classification through Multilayer Perceptron (MLP)	43
2.5.1 Deep Learning Models	44
2.5.1.1 Convolutional Neural Network	45
2.5.1.2 Recurrent neural network	45
2.5.1.3 Probabilistic neural network.....	46
2.5.2 Deterministic Learning MLP Models	46
2.6 Performance Evaluation Strategy	49
2.7 Limitations in Related Literature.....	50
2.7.1 Limitations Related to Features Selection.....	51
2.7.2 Limitation in recognition of MI Cases	52
2.8 Research gap Analysis.....	53
2.9 Conclusion	56
CHAPTER 3: RESEARCH METHODOLOGY	57
3.1 Introduction.....	57

3.2	ECG Dataset Collection:.....	58
3.3	Data Preprocessing	59
3.4	Proposed Effective R peaks detection algorithm:.....	60
3.4.1	Identification model of flatten T wave.....	60
3.5	Feature Engineering.....	62
3.5.1	The Proposed deep deterministic learning model:	63
3.5.2	The Proposed Model-Driven Deep Deterministic learning model:	64
3.6	Construction of the DDL Classification Model.....	64
3.7	Evaluation of DDL Classification Model.....	65
3.8	Construction of MDDDL Predictive Classification Model.....	66
3.9	Evaluation of MDDDL Predicative Classification Model.....	67
3.10	Conclusion:	68
CHAPTER 4: PROPOSED DETERMINISTIC TECHNIQUE FOR IDENTIFYING FLATTENED T-WAVE.....		69
4.1	Introduction.....	69
4.2	Deterministic Method for Flattened T-wave	70
4.3	Experimental Model	71
4.4	Results of Effective R –peaks Detection Algorithm.....	75
4.4.2	Result of both Leads.....	78
4.4.3	Comparative Analysis of Lead II and Lead III	79
4.5	Evaluation Schema	80
4.5.1	State-of-the-art Comparison.....	80
4.6	Conclusion	81
CHAPTER 5: PROPOSED DEEP DETERMINISTIC LEARNING MODEL.....		83
5.1	Introduction.....	83

5.2	Deep Deterministic Learning Model	84
5.3	Experimental Setup.....	89
5.3.1	Feature Extraction	92
5.3.2	Feature Selection and Multilayer Perceptron.....	93
5.4	Experimental Results	96
5.4.1	Setting I Results	96
5.4.2	Setting II Results	105
5.4.3	Setting III Results.....	112
5.4.4	Setting IV	116
5.5	Deep Critical Analysis	118
5.5.1	Discussion	120
5.6	Complexity evaluation via mathematical model	124
5.6.1	Feed Forward Propagation.....	125
5.6.2	Backward propagation	128
5.6.3	Determinate Cost function:	136
5.6.4	Big O Notation Calculation.....	139
5.7	Conclusion	143
	CHAPTER 6: PROPOSED MODEL-DRIVEN DEEP DETERMINISTIC LEARNING FOR PREDICTIVE CLASSIFICATION.....	144
6.1	Introduction.....	144
6.2	Model-Driven Deep Deterministic Learning.....	145
6.3	Experimental Setup.....	147
6.3.1	Feature Engineering	148
6.4	Experimental Results	149
6.4.1	Data Streams Fusion	153
6.4.1.1	Setting I	154
6.4.1.2	Setting II.....	163
6.5	Feature Critical Analysis	173

6.6	MDDDL Evaluation Schema:.....	179
6.6.1	Statistical Diagnostic Test Evaluation	179
6.6.2	State-of-the-art Comparison.....	182
6.7	Conclusion	184
	CHAPTER 7: CONCLUSION.....	186
7.1	Introduction.....	186
7.2	Recap of Research Objectives and Research Questions.....	188
7.3	Limitations	196
7.4	Future Directions	197
7.4.1	Early detection of Neurogenic Stunned Myocardium via nsst-t.....	197
7.4.2	Prediction of Sudden Cardiac Arrest via MLP learning	198
7.4.3	Robust Recognition of Ventricular Arrhythmias via Optimal CNN model	199
7.5	Conclusion	200
	REFERENCES.....	201
	LIST OF PUBLICATIONS AND PAPERS PRESENTED	220
	Appendix A: DDL FEATURE SELECTION	221
	Appendix B: Expert Remarks	223
	Appendix C:Source link:.....	224

LIST OF FIGURES

Figure 1.1. Basic Structure of ECG Morphology	2
Figure 1.2. QRS Complex abnormalities	5
Figure 1.3. Hypokalemia (nsst-t) in different T wave anomalies	6
Figure 1.4. Different anomalous episodes of ST segment	6
Figure 2.1. Different Components of ECG Wavelet.....	19
Figure 2.2. Representation of Positive, negative, biphasic and flattened T wave.....	21
Figure 2.3. Noisy ECG wavelet	23
Figure 2.4. Block model of the primary ECG classification process.....	34
Figure 2.5. Different anomalies of T wave (a).flattened T wave (b) inverted T wave ...	39
Figure 3.1. Detailed structure of research methodology and design.....	57
Figure 3.2. Work directions of Identification of Ton feature of Flattened T-wave	61
Figure 4.1. Block Representation of Proposed Deterministic Method	71
Figure 4.2. Operated flattened T wave signal	76
Figure 5.1. Systematic work flow of deep deterministic learning	85
Figure 5.2. Internal operational execution of deep deterministic learning	88
Figure 5.3. UMMC ECG sample of flattened T wave subject.....	90
Figure 5.4. MIT-BIH ECG sample of <i>ST-T Change</i> subject	91
Figure 5.5. Neural network Architecture for DDL	95
Figure 5.6. UMMC: features mapping of <i>flattened T wave</i> subjects	99
Figure 5.7. UMMC: Features mapping of normal sinus rhythm subjects.....	102
Figure 5.8. UMMC: features mapping of atrial fibrillation subjects	104
Figure 5.9. MIT-BIH: features mapping of <i>ST-T change</i> subjects.....	107
Figure 5.10. MIT-BIH: features mapping of Stage 2 <i>nsr</i> subjects.....	109
Figure 5.11. MIT-BIH: features mapping of atrial fibrillation subjects	111
Figure 5.12. Efficiency gauges of CASE 1 at Stage 3.	113
Figure 5.13. Efficiency gauges of CASE 2	114
Figure 5.14. Efficiency gauges of CASE 3	115
Figure 5.15. Deterministic pattern recognition of both scenarios.....	116
Figure 5.16. Case 1: Complexity between flattened T waves and <i>ST-T changes</i>	119
Figure 5.17. Case 2: Complexity between both <i>nsr</i> subjects (UMMC and MIT-BIH)	120
Figure 5.18. Case 3: Complexity between both <i>afib</i> subjects (UMMC and MIT-BIH)	120

Figure 5.19. Stage 2 (MIT-BIH): Complexity measurement and pattern matching of all levels (<i>ST-T changes, nsr, and afib</i>).....	122
Figure 5.20. Stage 2 (UMMC): Complexity measurement and pattern matching of all levels (<i>flattened T wave, nsr, and afib</i>)	123
Figure 5.21. View of input and hidden layers in feed forward propagation	125
Figure 5.22. View Output layer in feed forward propagation.....	127
Figure 5.23. Computation Complexity representation of DDL	137
Figure 5.24. Computational Complexity representation of DL	138
Figure 6.1. Architecture of MDDDL	147
Figure 6.2. Complete MDDDL testbed classification.....	153
Figure 6.3. Efficiency gages of fusion process one with old features combination.....	156
Figure 6.4. Efficiency gages of fusion process one with new features combination ...	158
Figure 6.5. Efficiency gages of fusion process two with old features combination ...	161
Figure 6.6. Efficiency gages of fusion process two with new features combination....	163
Figure 6.7. Efficiency gages of fusion process three with old features combination ...	166
Figure 6.8. Efficiency gages of fusion process three with new features combination..	168
Figure 6.9. Efficiency gages of fusion process four with old features combination.....	170
Figure 6.10. Efficiency gages of fusion process four with new features combination .	172
Figure 6.11. Features analytics of fusion process one (<i>fc1</i>).....	174
Figure 6.12. Features analytics of fusion process two (<i>fc1</i>).....	174
Figure 6.13. Features analytics of fusion process three (<i>fc1</i>).....	175
Figure 6.14. Features analytics of fusion process four (<i>fc1</i>).....	176
Figure 6.15. Features analytics of fusion process one (<i>fc2</i>).....	177
Figure 6.16. Features analytics of fusion process two (<i>fc2</i>).....	177
Figure 6.17: Parametric analytics of fusion process two (new	178
Figure 6.18. Features analytics of fusion process four (<i>fc2</i>)	178
Figure 6.19. Confidence level comparison between parameters.....	182

LIST OF TABLES

Table 2.1: Standard Readings of ECG Features.....	20
Table 2.2: Different factors of nsst-t.....	20
Table 2.3: Resources of different ECG datasets	22
Table 2.4: Comparative summary of different noise removal methods.....	24
Table 2.5: Summary of R peaks dependencies on different cardiac diseases.....	26
Table 2.6: Performance Analysis different feature selection schemes	27
Table 2.7: Computational complexity comparison between different feature sets	28
Table 2.8: Comparative summary of machine learning techniques.....	32
Table 2.9: .Key features of T wave in ECG.....	40
Table 2.10: Summary of different flattened T wave studies.....	41
Table 2.11. Recognition Summary of cardiac diseases through deterministic learning .	48
Table 2.12: Comparison of deep learning and deterministic learning	55
Table 3.1: ECG Streams fetching resources	59
Table 3.2: ECG features used in this research study.....	63
Table 4.1: Demographic characteristics of flattened T wave subjects.....	72
Table 4.2: Findings of different parameters of ten flattened T wave subjects.....	76
Table 4.3: Compartive Summary of both leads Result.	79
Table 4.4: Difference between lead II and lead III	80
Table 4.5: Comparison unit with state-of-the-art Algorithms.....	81
Table 5.1: Efficiency parameters of flattened T wave cases (UMMC)	97
Table 5.2: Extracted time domain features of flattened T wave cases (UMMC)	97
Table 5.2(Continued): Extracted time domain features of flattened T wave cases (UMMC)	98
Table 5.3: Accuracy of normal sinus rhythm cases (UMMC).....	100
Table 5.4: Extracted features from normal sinus rhythm cases (UMMC).....	101
Table 5.5: Efficiency parameters of atrial fibrillation cases (UMMC).....	103
Table 5.6: Extracted time domain features of atrial fibrillation cases (UMMC).....	103
Table 5.7: Efficiency parameters of ST-T change cases (MIT-BIH).....	105
Table 5.7(Continued): Efficiency parameters of ST-T change cases (MIT-BIH)	106
Table 5.8: Time-domain feature extraction of ST-T change cases (MIT-BIH).....	106
Table 5.9: Accuracy of normal sinus rhythm cases (MIT-BIH)	108
Table 5.10: Features of normal sinus rhythm cases (MIT-BIH).....	108

Table 5.10(Continued): Features of normal sinus rhythm cases (MIT-BIH).....	109
Table 5.11: Accuracies of atrial fibrillation cases (MIT-BIH)	110
Table 5.12: Features of atrial fibrillation cases (MIT-BIH).....	110
Table 5.12(Continued): Features of atrial fibrillation cases (MIT-BIH)	111
Table 5.13: Summary of the accuracies of the deterministic pattern recognition method(DDL).....	117
Table 5.14: Comparison of the proposed deterministic pattern recognition method....	117
Table 5.15: DDL computation complexity comparison.....	138
Table 5.16: Big O notations of existitng approcahes	140
Table 5.17: Comparison of Big O notations for MI and afib.....	141
Table 6.1: Accuracy parameters of flattened T wave cases (UMMC).....	150
Table 6.2: Feature extraction unit of flattened T wave cases (UMMC)	150
Table 6.3: Accuracy parameters of TWA cases (PTB).....	151
Table 6.4: Feature extraction showcase of TWA cases (PTB)	151
Table 6.5: Fusion activity process one with different feature streams.....	154
Table 6.6: Fusion activity process two with different feature streams	159
Table 6.7: Fusion activity process three with different feature streams	164
Table 6.8: Fusion activity process four with different feature streams.....	169
Table 6.9: Data streams of UMMC evaluation through statistical test evaluation.	181
Table 6.10: Data streams of PTB evaluation through statistical test evaluation.....	181
Table 6.11: MDDDL Comparison with state-of-the-art.	182
Table 6.11(Continued): MDDDL Comparison with state-of-the-art.	183

LIST OF SYMBOLS AND ABBREVIATIONS

ECG	:	Electrocardiography
CVDs	:	Cardiovascular diseases
ML	:	Machine Learning
MI	:	Myocardial infarction
Afib	:	Atrial Fibrillation
PVC	:	Premature Ventricular Contraction
WT	:	Wavelet Transform
ANN	:	Artificial Neural Network
WTSEE	:	Wavelet transform and Shannon emery envelope
MITBIH	:	Massachusetts Institute of Technology-Beth Israel Hospital
PTB	:	Physikalisch-Technische Bundesanstalt
DDL	:	Deep Deterministic Learning
DDPG	:	Deep deterministic policy gradient
DWT	:	Discrete Wavelet transform
DL	:	Deep Learning
MDDL	:	Model Driven Deep Learning
MDDDL	:	Model Driven Deep Deterministic Learning
fp1	:	Fusion process one
fp2	:	Fusion process two
fp3	:	Fusion process three
fp4	:	Fusion process four
fc1	:	Traditional features combination
fc2	:	New features combination

Nsst-t	:	Non Specific ST-T Changes
STEMI	:	ST Segment Elevation Myocardial Infarction
STNEMI	:	ST Segment Non Elevation Myocardial Infarction
SCD	:	Sudden Cardiac Death
NSM	:	Neurogenic Stunned Myocardium
CAD	:	Coronary Artery Disease
SCG	:	Scale Conjugate Algorithm
RA	:	Right Arm
LA	:	Left Arm
RL	:	Right Leg
LL	:	Left Leg
RBBB	:	Right Bundle Branch Block
LBBB	:	Left Bundle Branch Block
RAAD	:	Robust Accurate Anomaly Detection
Se	:	Sensitivity
PCG	:	Phonocardiogram
Sp	:	Specificity
CNN	:	Convolutional Neural Network
RNN	:	Recurrent Neural Network
SVM	:	Support Vector Machine
LDA	:	Linear Discriminant Analysis
PCA	:	Principal Component Analysis
DWT	:	Discrete Wavelet Transform
DCT	:	Discrete Cosine Transform
MDE	:	Model Driven Environment
MDA	:	Model Driven Architecture

<i>hl</i>	:	Hidden layer
<i>d</i>	:	Delay
TWA	:	T- wave Alternans
RAD	:	Ratio of Accurate Detection
Acc	:	Accurcay
<i>mhrv</i>	:	Mean Heart Rate Variability
<i>rr-rms</i>	:	Root Mean Square Value of RR intervals
<i>sddn</i>	:	Standard Deviation of RR Intervals
<i>nnrr</i>	:	The Number of RR intervals greater than fifty
<i>mt_{on}</i>	:	Mean T-onset Value
<i>mt_{off}</i>	:	Mean T-offset Value
<i>mt_{pk}</i>	:	Mean T-peak Value
ML	:	Machine Learning
eph	:	Epoch
CF	:	Cost Function
Perf	:	Performance
Vad	:	Validation
Tim	:	Time
BOSS	:	Bag-of-SFA-Symbols
TSC	:	Time series classification

LIST OF APPENDICES

Appendix A: DDL FEATURE SELECTION	221
Appendix B: EXPERT REMARKS	223
Appendix C: GITHUB SOURCE FILES.....	224

Universiti Malaya

CHAPTER 1: INTRODUCTION

In this chapter, the theme of this study is outlined in the background, research objectives, problem statement, and research significance. Furthermore, the scope of the study is discussed in the perspective of identification of the different cardiac diseases (including *flattened T wave* in the special case of Myocardial Infarction (MI)) or Cardiovascular Diseases (CVDs) by using artificial neural network.

1.1 Background

Over the last two decades, the use of ever more advanced technology has resulted in the enhancement of many working models, in different domains of human affairs. Healthcare is one such domain where the use of technology is increasing steadily. Healthcare systems have always attracted considerable attention due to their significance for the well-being of the people and the involved risk factors. Given these two factors, not even the minutest detail ought to be ignored at any stage of the diagnostic and health monitoring process. Therefore, the importance of incremental work on the improvement of the accuracy and rising of the sensitivity level with regards to diagnostic and health monitoring process cannot be underrated. Utilization of technologies in health monitoring systems have greatly improved the quality and reliability of analytical results that are used for different diagnostic purposes. Electrocardiography (ECG) is one of those healthcare diagnostic tools that are used for monitoring the electrical activities of heart. While performing an ECG, electrodes are attached to different parts of the human body for measuring the electrical impulse of heart signals. These electrodes are the key source for monitoring the electrical and other activities of the heart. ECG is the primary diagnostic tool used for measuring many types of malfunction of the heart including different cardiac diseases and arrhythmia. The cycle of ECG monitors the electrical activities of the heart with respect to time

period by attaching electrodes to the outer skin of the human body. In normal routine 12 leads are used for measuring the electrical activities of the human heart. In a way of reduction the computational complexity uses 5-lead ECG instead of 12-lead ECG (Koga, Kawamura, Ito, Iseki, & Ikari, 2016) . Parameters of 5-lead ECG are (RA) right arm, (RL) right leg, (LA) left arm, (LL) left leg, and one of the V1 to V5 leads. The septal leads V1 or V5 are typically chosen for analyzing 5-lead signals. Each electrode on human body captures a different angle of the heart's electrical activity (Patient & Group, 2014). These angles are represented in the form of different wavelet segments. These segments are represented as a P wave, ST segment, QRS complex, and T wave on ECG Wavelet. Each segment represents heart's different kinds of activities like P wave represents atrial depolarization, QRS complex represents the ventricular depolarization, ST segment represents the interval between ventricular depolarization, repolarization, and the last T wave represents the repolarization of ventricles. The unusual deviations in these segments are highlighted as a cardiac diseases or CVDs. Figure 1.1 highlights the complete structural view of ECG wavelet.

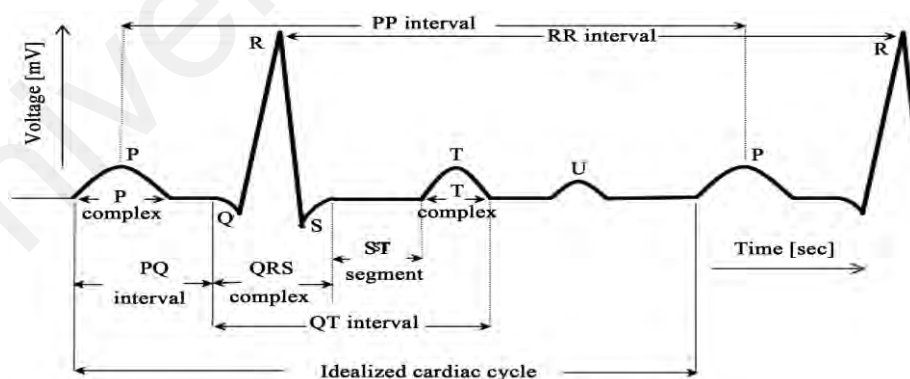


Figure 1.1. Basic Structure of ECG Morphology

The most critical part of ECG analysis is highlighting the ST segment and T wave section. Automated classification of T wave episodes is of high value to the cardiologists and medical professionals for the purpose of determining the exact intensity of MI. Anomalous episodes of T wave are the primary factor in causing the

MI (Rai, Trivedi, & Shukla, 2013) (Touma, Tafreshi, & Khan, 2016). Accurate classification of T wave clears the concept of anomalous nature like *flattened T*, *inversion T wave*, and *negative T wave* in MI. The nature of *flattened T wave* identification is still an intractable problem for cardiologists. Similarly, MI detection algorithm is better in determining accuracy level than previous algorithms. MI detection algorithm achieves the accuracy rate at 98% and is specially developed for the detection abnormalities in ST segment and T wave (Zheng et al., 2013)(Hadjem & Naït-Abdesselam, 2015)(Sivaraks & Ratanamahatana, 2015). The MI detection algorithm is characterized on the basis of ST-segment elevation (STEMI) and non-ST segment elevation (NSTEMI) (Raj, 2011).

Definition 1.1.1: Deep Deterministic Learning: A few studies in literature show that the ECG features classification, integrates the different wavelet analysis approaches with extensive feature engineering and machine learning; thus pre-defined methods are used for identification of the different malfunctions of the human heart, especially the *flattened T wave* case (Acharya, Fujita, Adam, et al., 2017; J. S. Park, Lee, & Park, 2017; Wu et al., 2019). Here, deep deterministic learning is defined in terms of tune up of the pre-defined conditions for pattern recognition of the ECG features. Such matching of patterns helps to recognize different cardiac diseases in the least complex manner as well as identifying such cardiac disease that have no previous track record; namely, *flattened T wave* (Iqbal, Wah, Habib Ur Rehman, Mujtaba, & Imran, 2018). Furthermore, the effectiveness of deep deterministic learning completely relies on the extracted features of the cardiac diseases. For instance (Iqbal, Wah, Habib Ur Rehman, & Mastoi, 2019), the efficiency of state-of-the-art T wave alternans algorithm is tested in a deterministic way for extraction of the basic features of *flattened T wave* that play a vital role in the accurate recognition of *flattened T wave* in deep deterministic learning. Moreover, deep deterministic learning is evaluated through comparison of state-of-the-

art traditional recognition methods of cardiac diseases, that justifies the significance of deep deterministic learning approach in patterns recognition. The proposed deterministic solution is presented in Chapter 5.

Definition 1.1.2: Model based deep deterministic learning: Different studies show that the structure of model driven architecture integrates with deep learning models for identification and prediction of different ECG data samples (Limaye & Adegbija, 2018; Yakovlev, 2016). The effective integration of model driven approaches with different machine learning methods delivers fruitful results in healthcare system, especially in ECG analytics (Acharya, Oh, et al., 2017; Miotto, Wang, Wang, Jiang, & Dudley, 2017). Here, model driven deep deterministic learning is defined in terms of applying the deep deterministic learning in the context of different T wave cases for feature pattern recognition as well as predictive classification (Iqbal, Wah, Habib Ur Rehman, & Shah, 2019). Additionally, the back tracking parameter of model driven architecture is properly embedded in feature fusion processes of deep deterministic learning along with best predictive machine learning algorithm (scale conjugate algorithm) (Iqbal, Wah, Habib Ur Rehman, & Mastoi, 2018). The production of such embedded portion delivers the accurate and robust predictive classification of different T waves. The production units of model based deep deterministic learning are evaluated through statistically diagnostic test evaluation scheme and state-of-the-art predictive classification methods of myocardial infarction. These evaluation schemas generate efficient results in predictive classification of different T waves, especially *flattened T wave*. Moreover, the empirical features selection critical analysis delivers some fruitful outcomes in terms of reduction of the computational complexity factors. The complete structural architecture and components of the proposed model driven deep deterministic method is presented in Chapter 6.

1.2 Research Motivation

Worldwide, CVDs are one of the main causes of cardiac deaths. Human death ratio has continuously increased over the years due to these CVDs. In the year 2010 alone, 17.4 million human deaths were reported that were caused by these CVDs (World Health Organization, 2011). Of these human deaths, approximately 7.4 million occurred due to Coronary Artery Disease (CAD). In 2013, the US reported 74,000 human deaths due to CAD which is equivalent to 1 of every 7 Americans (World Health Organization, 2014). Early classification of these heart diseases may improve the survival rate of human life and also assist in determining proper diagnostic solutions. Thus, a number of achievements in better classification or recognition of different CAD are recorded in literature (Baloglu, Talo, Yildirim, Tan, & Acharya, 2019). Along with these achievements, continued existences of some uncertainties in analytics of ECG are still an open challenge. These uncertainties related to the segments of QRS complex, ST segment and T wave abnormalities. Figure 1.2 highlighted the two common anomalous episodes of QRS complex namely, wide QRS complex and narrow QRS complex.

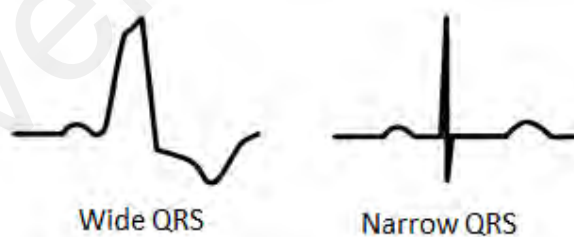


Figure 1.2. QRS Complex abnormalities

Some of the uncertainties are high in priority, due to risk factors involving different situations of myocardial infarction. Literature on the subject reveals that the recognition of the flattened cases in Non Specific ST-T Changes (nsst-t) remains an open question for the researchers (Naseer & Nazeer, 2017; Stub et al., 2015). Figure 1.3 captured the

hypokalemia factor of *nsst-t* in perspective of flattened T wave case, inversion T wave and biphasic T wave.

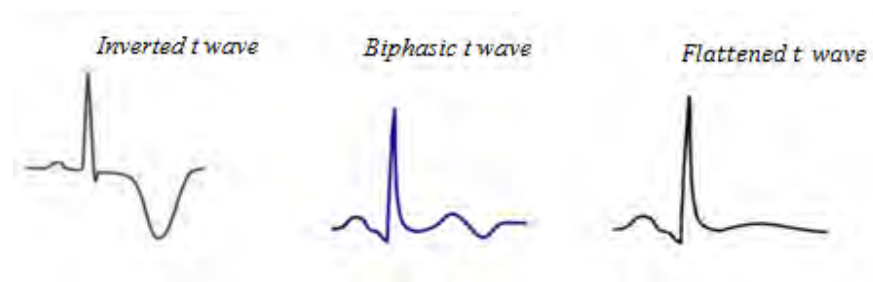


Figure 1.3. Hypokalemia (nsst-t) in different T wave anomalies

Existing clinical studies highlight the least discussed feature of flattened T wave that made the conflict with inverted T wave and other T wave anomalies. According to different clinical studies, the link between hypokalemia and hyperkalemia is traceable through identifying the feature analysis of flattened T wave. In some instances (Fukuda, Kanazawa, Aizawa, Ardell, & Shivkumar, 2015; Hadjem & Naït-Abdesselam, 2015), cardiologists refer to the negative or inversion T waves as *flattened T waves*. Similarly, sometimes the cases of STEMI and NSTEMI are also referred to as cases of flattened ST segment. Figure 1.4 represented waveform of STEMI and NSTEMI.

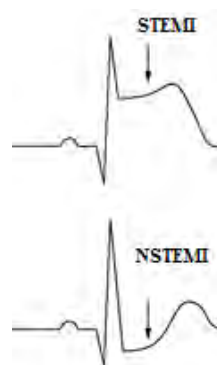


Figure 1.4. Different anomalous episodes of ST segment

Researchers and medical professionals are constantly exploring literature (Koga et al., 2016; Stub et al., 2015) to find a suitable algorithm that could be used for better

detection of ST Segment and T wave anomalous behaviors in ECG. For instance (Blanco-Velasco, Goya-Esteban, Cruz-Roldán, García-Alberola, & Rojo-Álvarez, 2017; Kaiser, Findeis, & Young, 2004), T-wave alternans (TWA) is found to be a suitable algorithm, used for measuring the anomalous behaviors of T wave. Literature shows the TWA algorithm is used for measuring the factors of T-onset and T-peak with high level of sensitivity 92.32% to 92.68 % (Blanco-Velasco et al., 2017). Similarly, a number of other algorithms have also been developed for tracing and classifying the different anomalies ST segment and T wave in ECG (Limaye & Adebija, 2018; Sivaraks & Ratanamahatana, 2015).

Traditional wavelet analysis techniques are also valuable for finding the abnormal features of ECG. Like other features, wavelet transformation technique is also used for finding the some abnormal features of T wave (Acharya, Fujita, Adam, et al., 2017; Banerjee & Mitra, 2014; Patro & Kumar, 2017; Zheng et al., 2013). Different feature engineering techniques are used for extracting the different time and frequency domain features for classifying the abnormalities factors that may cause myocardial infarction. However, identification of the exact nature of flattened anomalies is still a question that needs to be answered adequately (Bao et al., 2017).

1.3 Problem Statement

The current generations of automated classification techniques for cardiac morbidities are efficient and helpful for further diagnosis purposes in case of the malfunctions of human heart activities. However, considering the deep learning models for robust classification of different cardiac diseases especially afib and MI cases is the challenging task. These deep learning models utilize the large sample size of data for training phase that are enhanced the computational or time complexity. Enlarge iterations in training phases has the primary cause of failure the robustness factor in

deep learning models. Other classification techniques that used different neural models along with feature extraction also face enhancement of computational complexity issue during training phase of model. Despite, recognition of afib and MI cases through deterministic learning neural models are highlighted as least computational complexity as compared to deep learning due to constant weights upgradation. However, the extensive level feature analysis is acquired as an input for deterministic learning neural models. Moreover, deep learning models and other traditional classification techniques only support the defined situational of MI cases namely, STEMI and STNEMI. Different studies used the series of ECG wavelet analysis and the Wavelet Transform Modulus Maxima (WTMM) play a critical role in MI detection algorithm in the context of derivation of the slope, amplitude, and time coverage of T wave (Fukuda et al., 2015). Accurate measurement of T wave changes is also a significant part in an MI situation. For instance, in (Kaiser et al., 2004) discussed the qualitative as well as quantitative sections of TWA algorithm as being useful for measuring the ambiguities of *T wave* changes. However, the MI detection and TWA algorithm fail in such cases of MI recognition that belong to non-specific ST-T changes (*nsst-t*), which include the anomalies of *flattened ST segment* and *flattened T wave* (Blanco-Velasco et al., 2017). The significant values of *nsst-t* in terms of flattened anomalies are frequently highlighted in the domain literature (Bao et al., 2017; Kang, Chang, Su, Kim, & Shin, 2018).

However, recognition of flattened T wave MI situation is still a challenging task for current classification techniques. The impact of flattened T wave recognition reboots the recognition of other factors of *nsst-t*. The range of *nsst-t* lies between STEMI and STNEMI but lack to support the features analysis of flattened T wave. According to clinical interpretations, the exact situation of hypokalemia recognition in context of inverted T wave and flattened T wave is still a hard task. Existing clinical studies

highlighted hypokalemia and hyperkalemia are the factors of *nsst-t* and linkage between these factors are least discussed. Existing classification techniques have failed to support the complete feature analysis of flattened T wave and the correlation between other the T wave anomalies. The complete feature analysis and correlation of flattened T wave enrich the exact situation of *nsst-t* factor hypokalemia.

1.4 Aims and Objectives

The aim of this research is to investigate the state-of-the-art ECG signal classification or pattern recognition techniques so as to come up with a highly efficient technique that would accurately determine what happens if some unseen and ambiguous part in the ECG signal occurs (Ousaka, Obara, & Fujiwara, 2018). To this end, this research proposes and develops an efficient model for classification or pattern recognition of different cardiac diseases and then evaluates this model by comparing it with the existing state-of-the-art classification techniques. Secondly, the structure of proposed model is constructed on the basis of mode-driven solution (Ramirez, Melin, & Prado-arechiga, 2019; Sankaran et al., 2017). Such methodology helps in selection of features that deliver suitable and efficient results. Furthermore, the research analyses whether the implementation of the proposed model is workable or not, though critically analyzing different features selection. The research objectives are summarized below:

1. To extract the different features of flattened T wave cases from UMMC dataset through investigating the state-of-the-art techniques of feature engineering.
2. To develop efficient R peaks detection algorithm; for recognition of different ECG anomalies that are helpful for detection of *afib* and MI cardiac diseases.
3. To highlight the correlation between flattened T waves and other anomalies of T waves.

4. To develop (minimum time or computational complexity) models for recognition and predictive classification of different *afib* and MI cases.
5. To evaluate the performance of proposed models through efficiency measurement matrices.

1.5 Research Questions

Objective 1: To extract the different features of flattened T wave cases from UMMC dataset through investigating the state-of-the-art techniques of feature engineering

RQ1: What are the existing methods of feature engineering for recognition of cardiac diseases?

RQ2: How useful are the existing feature extraction techniques for extraction of different features of UMMC dataset?

RQ3: What are the limitations in existing features selection schema for recognition of the cardiac diseases and how such schemas effect the performance and complexity factor?

Objective 2: To develop efficient R peaks detection algorithm; for recognition of different ECG anomalies that are helpful for detection of *afib* and MI cardiac diseases.

RQ4: What are the limitations in traditional R peaks detection algorithms?

RQ5: How can the performance of the developed R peaks detection algorithm be evaluated?

Objective 3: To highlight the nature of flattened T wave anomaly and explore the similarities between flattened T waves and other anomalies of T waves.

RQ6: What is the importance of flattened T wave abnormality in the context of medical or clinical ontologies?

RQ7: How useful are the existing techniques to identify the *flattened T wave* features?

RQ8: How much do the features of the flattened T wave depend on the other ECG Wavelet segments?

Objective 4: To develop (minimum time or computational complexity) models for recognition and predictive classification of different *afib* and MI cases.

RQ9: How much of the recognition and prediction performance of cardiac diseases can be enhanced through developed recognition and prediction models?

RQ10: What are the limitations of the developed models of recognition and predictive classification of different cardiac diseases?

RQ11: What are the limitations in existing recognition models in the context of complexity factor?

Objective 5: To evaluate the performance of proposed models through efficiency measurement matrices.

RQ12: To what extent is the performance of the proposed recognition and predictive models improved relative to existing state-of-the-art techniques?

RQ13: Why the proposed recognition or classification and prediction models are efficient??

RQ14: How can the time complexity factor be evaluated?

1.6 Research Methodology and Design:

The general structure of this research study is shown in figure 3.1. As presented, this research study consists of five steps. These steps are briefly discussed in the subsequent sections. In Chapter 3, the structure of this research study is covered in brief.

1.6.1 Problem Identification:

This phase identifies the research problem by conducting a comparative review of the existing literature of recognition techniques of different cardiac diseases especially *afib* and MI cases. The results of comparative review are briefly discussed in Chapter 2.

1.6.2 ECG Dataset Collection

This stage discusses the real-world ECG datasets used in the experiments. These datasets were collected from the University of Malaya Medical Center (UMMC) exclusively and PhysioNet database that contains the Physikalisch-Technische Bundesanstalt (PTB) and Massachusetts Institute of Technology-Beth Israel Hospital (MIT-BIH). The detail of this stage is discussed in Chapter 3.

1.6.3 Signal Pre-Processing

This phase considers the various signal pre-processing tasks applied on collected ECG datasets, to remove different kinds of noises that reflect irrelevant features. These removal tasks includes the removal of *baseline wander* and *power* line interference in ECG, removal of upper limit noise, and removal of lower limit noise. This phase is elaborated further in Chapter 3.

1.6.4 Feature Engineering

In this phase, the effective feature engineering approach is applied on each datasets for extraction of different time domain features. Therefore, the accuracy of any classification or recognition and prediction models relies on the accurate extraction and selection of features. Additionally, the quality of extracted and selected features reflects the performance of any machine learning algorithm. The details of feature engineering phases are discussed in Chapter 5 and Chapter 6.

1.6.5 Recognition and Prediction Models Construction

This phase constructs the recognition and predictive classification models through formation of artificial neural networks, using various machine learning algorithms (levenberg-marquardt algorithm and scaled conjugate gradient algorithm). The specifics of this phase are discussed in Chapter 5 and Chapter 6.

1.6.6 Evaluation of Recognition and Prediction Models

This phase evaluates the performance of the proposed models by using the evaluation metrics including the performance of proposed effective R peaks detection algorithm. The evaluation metrics consists of measuring performance of proposed R peaks detection algorithm, time duration, epoch value, error ratio, and overall accuracy. Finally, this phase identifies the best recognition and prediction models, via proposed effective R peaks detection algorithm and machine algorithms. The completed detailed results are discussed in Chapter 4, Chapter 5, and Chapter 6.

1.7 Research Significance

The significance of this research helps in telehealth system which provides end-to-end classification in perspective of urgent cardiac issues. Furthermore, this research help rests deep investigation of *nsst-t* in the context of *flattened T wave* recognition. On the other hand, several computational algorithms and approaches have already been proposed for analysis of ECG signals but still some imperfections undermine these approaches namely, compromised the robust factor in context of computation or time complexity and recognition of the flattened T wave. Robust and accurate recognition of *flattened T wave* uncertainty and well defined afib cases are the core deliverables of this research. According to literature, evaluation of the ECG signals started after the development of Pan Thompkins QRS detection(Pan & Willis, 1985). Several state-of-the-art approaches use the methods of this algorithm and integrate it with the particular proposed method (Banerjee & Mitra, 2014; J. S. Park et al., 2017; Stub et al., 2015). It is constantly observed in all types of methodologies that features are extracted on the basis of accurate detection of R peaks and then further features are extracted (Elgendi, 2013; J. S. Park et al., 2017). In the extraction phase of features, time, and frequency domain features are extracted and then further used for recognition of the behaviors of signals to determine whether they are normal or abnormal. The most significant

segment in ECG is T wave which indicates the ventricular repolarization. Such ventricular repolarization indicates the healthy or unhealthy status of the heart (Ghoraani et al., 2019). In particular MI case, Flattened ST segment and Flattened T wave are important issues for cardiologists (Bhuiyan, Graff, Kanters, Thomsen, & Struijk, 2013; Sedova et al., 2017). Robotic detection of the ST segment and T wave changes may lead to the survival of human life (Cesari, Mehlsen, Mehlsen, Bjarup, & Sorensen, 2016).

1.8 Research Contribution

The contributions of this research are as follows

- **Literature Analysis:** The conducted review of literature focused on the limitation of current recognition and prediction techniques of different cardiac diseases. In the literature reviewed, five different aspects were studied, namely, different model based techniques in recognition and prediction of cardiac diseases, various feature selection approaches, different R-peaks detection algorithms, machine learning algorithms, and performance metrics.
- **Flattened T wave Identifier:** This research proposes better techniques for identification of the features of *flattened T wave* that are used as a resource for the clinical classification in the special case of myocardial infarction (*nsst-t*).
- **Pattern Recognition of Cardiac Diseases:** This research develops a model for recognition of features patterns of different cardiac diseases through deterministic method by using multilayer perceptron. Moreover, this pattern recognition model enables recognition of *flattened T wave* at low computational complexity in the context of effective feature selection.
- **Predictive Analytics of cardiac diseases:** This research presents the predictive analytics of different cardiac diseases through model based approach. The formation of model based deterministic method uses the machine learning

algorithm for prediction of high priority cardiac diseases (especially *flattened T wave*). Furthermore, this predictive method ensures low computation complexity through the usage of the effective feature selection.

All the proposed methods in this thesis have been published in reputable ISI-indexed journals (for the list of publications, refer to page 220). In Appendix-B, recommendation letter of cardiac expert in support of this research work (refer to page 223). In Appendix-C, GitHub source file link is also available for further observations (refer to page 224).

1.9 Research Scope

To make sure all the defined research objectives are met within a particular time frame, the scope of this research is summarized below:

1. In this research, we are using three datasets for global endorsement of the proposed methods. Moreover, the executions of the proposed methods are based and operated on public datasets as well as exclusive datasets.
2. The major focus of this research is categorized into two subsets. First, to recognize the unseen patterns of features that may cause unpredictable heart stroke (the special type of myocardial infarction that contains *flattened T wave*). Second, to enhance the recognition accuracy of high priority cardiac diseases. This includes myocardial infarction and different forms of cardiac arrhythmia.
3. The main sets of activities in this research are built on the basis of state-of-the-art techniques.
4. Evaluation of the results of the proposed novel methods are performed by the comparison of different state-of-the-art cardiac diseases pattern recognition approaches and predictive classification methods.

5. The proposed models of recognition and predictive classification are suitable for different signal processing area that includes automated detection of neurologic diseases and communication signals area namely, cognitive radio networks and channel optimization.

1.10 Thesis Outline

The remaining Chapters of this thesis are categorized as follows:

Chapter 2: This Chapter discusses the outcome of the survey of different computational ECG analytics. A brief outline of the field is given which describes the different ECG analytics processes. Moreover, this Chapter covers the literature review of various model based on classification or recognition, prediction techniques, and feature engineering techniques used for recognizing the different cardiac diseases.

Chapter 3: This Chapter covers the methodology used in this research to develop the proposed recognition and predictive classification models for different high priority cardiac diseases. Additionally, it discusses the performance measures schemes that were used to measure the efficiency of proposed models. Finally, the evaluation schema used to evaluate the performance of proposed models are also discussed.

Chapter 4: This Chapter discusses the proposed deterministic way for identification of *flattened T wave* features that are helpful in recognition and prediction processes. Moreover, it covers the experimental setup; results obtained through proposed R-peaks detection algorithm and evaluates the proposed algorithm by comparison with state-of-the-art R peaks detection algorithms. Finally, the Chapter discusses the findings of this proposed method.

Chapter 5: This Chapter discusses the details of proposed recognition or classification model through derivation of new and traditional time domain features. It

also presents results obtained through proposed methods and evaluates them through state-of-the-art methods. Finally, the Chapter discusses the findings of this proposed model.

Chapter 6: This Chapter presents the details of the proposed predictive classification model of different high priority cardiac diseases through deterministic way. Furthermore, it covers the results through experimental formation of this proposed model and its evaluation through comparison with state-of-the-art predictive methods. In the end, the Chapter discusses the findings of this model in the context of different features combination.

Chapter 7: This Chapter concludes this thesis by fulfilling the research objectives. The major contributions are summarized. This Chapter also discusses the limitations of this research and proposed future directions for further research.

CHAPTER 2: LITERATURE REVIEW

2.1 Introduction

This chapter delivers a detailed review of the existing related literature on recognition and predictive classification techniques of different cardiac diseases. Section 2.2 covers the general introduction of Electrocardiography (ECG) analytics and fundamental ways to diagnoses different heart diseases in ECG through computational techniques. Subsections 2.2.1 to 2.2.3 briefly discuss the different steps of ECG analytics. Similarly, Subsection 2.2.4 covers the automated recognition and predictive classification techniques. Sections 2.3 to 2.5 cover a compressive review of model based techniques in recognition and prediction of cardiac diseases. Such techniques include supervised machine learning techniques, different state-of-the-art MI detection methods and deep learning models. Section 2.6 highlights the performance evaluation strategies of the classification techniques. Next, section 2.7 covers the limitations in different classification and predictive classification techniques. Section 2.8 presents the research gap in this thesis. Finally, section 2.9 concludes this chapter.

2.2 Heart diseases detection: A Biomedical Domain

Detection of different kinds of heart diseases is a sensitive as well as complex process and is not possible without any monitoring apparatus or tool. Different activities of heart are monitored through phonocardiogram (PCG) or ECG (Nabih-Ali, El-Dahshan, & Yahia, 2017). However, in so far as the accuracy factor is concerned, ECG is the most suitable tool for diagnosis of different heart diseases. Different electrical signals are monitored in the form of information that is useful for providing any diagnostic solution. The complete electric signals of ECG is segmented into P wave,

QRS Complex, R peak, ST segment and T wave which is already shown in [figure 1.1](#) (See Chapter 1). There are three components of ECG wavelet namely, waveform, intervals and segments. The waveform includes the P wave, QRS Complex, T- Wave, and Intervals component contains PR interval, QT Interval, RR interval, ST interval. Similarly, the segment covers the PR segment and ST segment. Figure 2.1 highlighted the ideal and noise free ECG Wavelet structure with its components for better understanding (S. T. Chen et al., 2014).

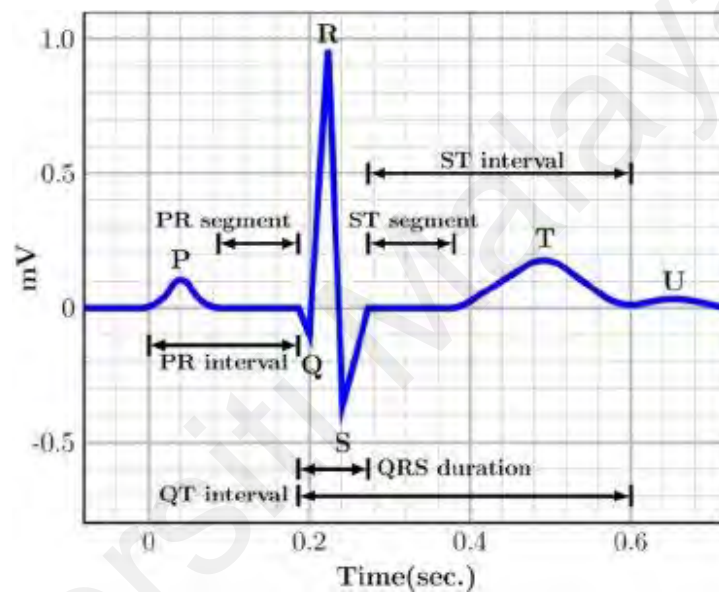


Figure 2.1. Different Components of ECG Wavelet

According to above components of ECG, anomalous parts in ECG waveform declare the cardiac diseases in perspective of different clinical studies (Harkness et al., 2019; Koivikko, Kenttä, Salmela, Huikuri, & Perkiömäki, 2017; Phillips, Wang, Celi, Zhang, & Feng, 2019; Rivero et al., 2019).

To support these observations, one study (Saritha, Sukanya, & Murthy, 2008) highlights the standard readings of different features that are useful for further classification process. Table 2.1 presents the standard reading of those different features (Saritha et al., 2008).

Table 2.1: Standard Readings of ECG Features

<i>Peak Values</i>	<i>Amplitude</i>	<i>Intervals</i>	<i>Duration</i>
P-Wave	0.75mV	P_R Interval	0.12 to 0.20 Sec
R-Wave	1.60mV	QT Interval	0.35 to 0.49 Sec
Q-Wave	25% of R-Wave	ST Segment	0.05 to 0.15 Sec
T-Wave	0.1 to 0.5mV	P wave Interval	0.11 Sec
		QRS Complex	0.09 Sec
		PR Segment	0.06 to 0.15 Sec
		T wave	Varies

It was observed through existing studies, the recognition techniques delivered the accurate results in context of the identification of anomalous information in heart activities like recognition of Atrial Fibrillation (afib), Atrial Flutter, Tachycardia, Bradycardia and different Myocardial Infraction (MI) situations. However, there are some MI situations that are still undetectable and may be cause of risky situation of human's life namely, *flattened T wave* in Non Specific ST-T Changes (*nsst-t*). Table 2.2 highlights the different factors of *nsst-t*.

Table 2.2: Different factors of nsst-t

ECG Wavelet	Abnormalities	Clinical presentation
ST Segment	ST Segment Elevation	MI
ST Segment	Non-ST Segment Elevation	MI
ST Segment	ST Segment Inversion	MI
T-Wave	Biphasic T wave	Hypokalemia (MI)
T wave	Flattened T wave	Hypokalemia(MI)
T wave	Hyperacute T wave	Hyperkalemia(MI)
T wave	Inversion T wave	Hypokalemia(MI)
T wave	Tall T wave	Hypermagnesemia

These highlighted factors of *nsst-t* in Table 2.2 represent the anomalies relation with clinical notations in context of cardiac morbidities. Like, hypokalemia through T wave inversion or flattened T wave anomalies, hypermagnesemia through tall T wave

anomaly(Koivikko et al., 2017; Rivera-Juárez et al., 2019; Vinyoles, Soldevila, Torras, Olona, & de la Figuera, 2015; Yoon et al., 2018). According to clinical studies, the exploitation of hypokalemia are valuable for exploration of other *nsst-t* factors (Harkness et al., 2019; Phillips et al., 2019). Figure 2.2 highlights the different cases of hypokalemia (MI) in context of inverted T wave, *flattened T wave* and biphasic T wave(Ponomariov et al., 2017)

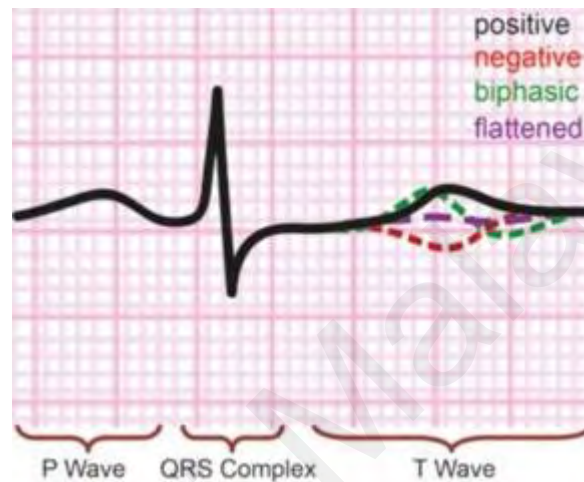


Figure 2.2. Representation of Positive, negative, biphasic and flattened T wave

Moreover, literature supported the analytics of ECG is segmented into a few modules which include the patient's ECG record acquisition, data pre-processing and segmentation, implementation of feature engineering techniques and finally, deployment of the classification or recognition techniques with the help of extracted features (Osowski & Linh, 2001; Prasad & Sahambi, 2003; Rai et al., 2013)

2.2.1 Data acquisition

To examine the patient's cardiac condition, real time ECG records are required for providing the diagnostic solution in case of any malfunction of the heart's structure. These ECG records are held in the form of datasets that are useful for medical physicians, cardiologists and researchers. The use of these ECG datasets for research purposes is steadily paving the way for improved detection of cardiac diseases. Table

2.3 lists in detail the public databases namely, MIT-BIH and PTB datasets. Table 2.3 describes the number of subjects which includes different cardiac diseases, number of channels that shows the number of input leads, sampling rate of ECG signal, and gender's information along with the different age ranges. Similarly, information of different diagnostic classes that help in classification process.

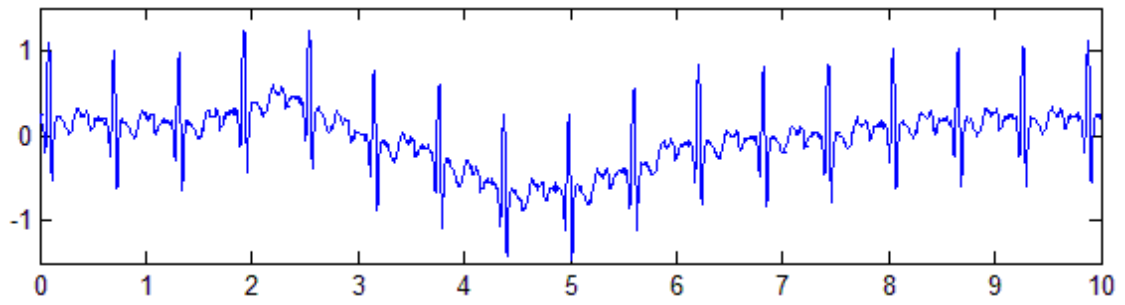
Table 2.3: Resources of different ECG datasets

References	No. of Subjects	No.of Channels	Sampling rate	Gender (Male/Female)	D_class	ECG Signal nature and Dataset
(Goldberger et al., 2000)	148 MI cases and 142 Others	14 Input channels	1000Hz	Both <i>Age range: 18 to 87</i>	9	T wave Alteranans <i>Public dataset</i> PTB Dataset
(Goldberger et al., 2000)	23 afib cases and 2 others	2 Input channels	250Hz	Both	4	Atrial Fibrillation MIT-BIH dataset
(Goldberger et al., 2000)	79 MI cases,	2 Input Channels	250Hz	Both <i>Men Aged: 30 to 84</i> <i>Women Aged: 55 to 71</i>	2	ST-T Changes MIT-BIH dataset

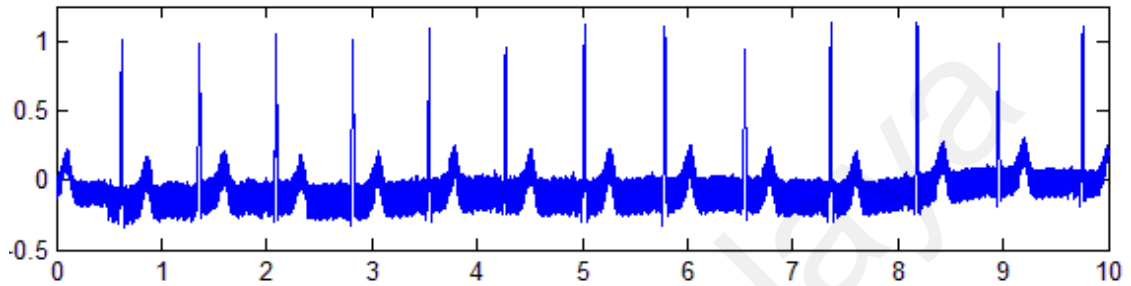
** D_Class(Diagnostic Class)

2.2.2 Data pre-processing

Data pre-processing involves the collection of patient's heart data by using sensors on the human body which contain different noises. Such raw data contain noises which include power line interference, baseline wandering, muscle movement noise and few minor noises that have an effect on monitoring the original condition (Bodisco, Netto, Kelson, Banks, & Hayward, 2014; Engin, 2004). Existing studies reported that different filtration techniques of baseline noise and power line noise are handy for features extraction phase(Acharya, Oh, et al., 2017; Blanco-Velasco et al., 2017). Figure 2.3 represents baseline noise, power line noise and muscular noise (Maggio, bonomini, Leber, & Arini, 2012)



(a) Baseline noise



(b) Power and muscle noise

Figure 2.3. Noisy ECG wavelet

At the stage of data pre-processing, raw signals are filtered out by using filtration processes such as low pass filter, high pass filter, Notch filter and Butterworth filter etc.(Acharya, Oh, et al., 2017; Elgendi, 2013; Jayant, Rana, Kumar, Nair, & Mishra, 2015; Yan, Geng, Deng, & Wang, 2019). The data cleaning process in ECG signal helps in extraction of exact features that are useful for the recognition of different cardiac problems.

Table 2.4 is a comparative summary of different noise reduction through filtration processes. Additionally, the impact of de-noising the signal through power, baseline and muscular noises are useful in context of cardiac morbidities identification. The smoothness of ECG signals through different filtration process play a critical role in feature extraction phase.

Table 2.4: Comparative summary of different noise removal methods.

References	Power Noise	Baseline Noise	Muscle Noise	FIR filter	High pass filter	WT	MIT-BIH Dataset	PTB Dataset
(Aloia, Longo, & Rizzi, 2019)	YES	YES	YES	NO	NO	YES	YES	NO
(Han & Shi, 2019)	YES	NO	NO	NO	NO	YES	NO	YES
(J. S. Park et al., 2017)	YES	YES	YES	NO	YES	YES	YES	NO
(Cheng & Dong, 2017)	YES	YES	YES	NO	YES	YES	YES	NO
(Raj, 2011)	YES	YES	NO	NO	YES	YES	NO	NO
(Lemire, Pharand, Rajaonah, Dubé, & Leblanc, 2000)	YES	YES	NO	YES	NO	YES	NO	NO
(Patient & Group, 2014)	YES	YES	NO	NO	NO	YES	NO	YES
(Qin, Li, Yue, & Liu, 2017)	YES	YES	YES	NO	NO	YES	YES	NO

** WT(Wavelet Transform)

2.2.3 Feature Extraction and Selection

This section represents the review part of different feature extraction and selection schemes that plays a vital role in recognition process. A number of studies are found on different ECG analysis schemes for accurate and early identification of abnormalities in ECG signals (Acharya, Oh, et al., 2017; Arabasadi, Alizadehsani, Roshanzamir, Moosaei, & Yarifard, 2017; Ravi et al., 2017). The most significant part of ECG morphology is the QRS complex (Cheng & Dong, 2017), and since 1985, Pan-Tompkins based QRS detection algorithms had high detection accuracies on ECG database (Pan & Willis, 1985). Therefore, the analysis of ECG relies mainly on the accurate QRS complex detection. QRS complex is partitioned into two key parts, i.e., feature extraction and identification of the nature of the feature in terms of classification (Gothwal, Kedawat, & Kumar, 2011; Sansone, Fusco, Pepino, & Sansone, 2013; Zheng et al., 2013). Furthermore, accurate detection of R peaks also play a vital role in accurate detection of QRS complex and RR intervals which represents the status of afib, atrial flutter, tachycardia and bradycardia(Acharya, Fujita, Lih, et al., 2017;

Desai, Nayak, Seshikala, Martis, & Fernandes, 2018; Rivero et al., 2019). Similarly, different feature sets of time domain, frequency domain and statistical features of ST segment and T waves are extracted through detected R peaks (Blanco-Velasco et al., 2017; Kaiser et al., 2004; Koga et al., 2016; Tramèr, Becker, Hochstrasser, Marsch, & Hunziker, 2018). In ECG analytics, the ST segment and T wave changes are another significant part of ECG which describes the critical information in different MI situation.

R-Peak Analysis: As it is apparent from the above discussion, recent trend indicates the significance of the extraction of different features relying on the accurate and robust detection of R-peaks. Different types of cardiac malfunctions are identified through such features that also rely on accurate R-peaks detection. Different types of arrhythmia are also detected through these R-peaks. Thus, atrial fibrillation are picked through irregular rhythm of RR intervals, premature ventricular contraction are detected through irregularity of QRS complex on ECG wavelet and different myocardial ischemias are identified through ST changes, features of T wave by considering the R peaks as a fiducial point (Blanco-Velasco et al., 2017; Elgendi, Eskofier, & Abbott, 2015; Hadjem & Naït-Abdesselam, 2015; Zheng et al., 2013). Identification of these irregular cardiac behaviors followed by highlighting the features that are derived from detected R peaks (He et al., 2017; J. S. Park et al., 2017; Yu et al., 2019).

The major concern discernable in the surveyed literature relates to reviewing the majority of R peaks detection techniques and methods that are suitable for all types of datasets. It is observed that the efficiency parameters of these R peaks detection algorithms would vary according to changes in the threshold values (He et al., 2017; Kew & Jeong, 2011; Lee, Park, Dong, & Youn, 2018). Table 2.5 represents the summary of different R peaks detection method that supports to recognize different cardiac diseases.

Table 2.5: Summary of R peaks dependencies on different cardiac diseases

References	R-peaks detection method	Dependent Cardiac Diseases	Public Dataset	Performance	Outcome
(J. S. Park et al., 2017)	Wavelet Transform Shannon Energy entropy(WTSEE) algorithm extracts the R peaks points from down sampling the ECG signal	Arrhythmia detection (PVC, afib, RBBB, LBBB)	MIT-BIH arrhythmia database	Acc=99.89% Se= 99.93% P ⁺ = 99.91%	WTSEE algorithm is handy for detection of different arrhythmia.
(Yu et al., 2019)	QRS Detection and segmentation of QRS detection	Heart rate leads to atrial fibrillation arrhythmia	MGH/MF Waveform	Acc=98.89% Se= 99.39% P ⁺ = 99.49%	Fusion of BP detection and ECG R peaks detection
(Qin et al., 2017)	Wavelet multiresolution analysis	Arrhythmia detection(afib, LBBB, pvc)	MIT-BIH arrhythmia database and QT database	<i>MIT-BIH:</i> Acc=98.89% Se= 99.39% P ⁺ = 99.49% <i>QT Database:</i> Acc=99.73% Se= 99.90% P ⁺ = 99.83%	First-order forward differential approach through truncated the amplitude time intervals thresholds for R peaks
(Sadhukhan & Mitra, 2012)	Derivative approach for highlighting QRS regions then R peaks detection	Different Myocardial infraction through ST segments changes and T wave changes	PTB diagnostic ECG database (PTB-db)	Se=99.8%	This approach is implemented on embedded platform of wearable cardio-respiratory systems
(He et al., 2017)	QRS Detection through KNN and PSO	Arrhythmia detection(afib, pvc)	MIT-BIH	Acc=99.43% Se= 99.69% P ⁺ = 99.72%	Dimensional reduction in noise ECG signal
(Lee et al., 2018)	R peaks detection through signal envelop filtering (SEF) and Shannon energy envelope along with the Savitzky-Golay filter (SEE-SG).	Arrhythmia detection and different myocardial infarction situations	MIT-BIH QTdatabase (QTDB) ,Noise Stress Test Database (NSTDB)	Se= 99.39% P ⁺ = 99.49%	Noval approach is implemented on real world noisy ECG signal

Acc (Accuracy), Se(Sensitivity), P+(Positive Prediction Value), **RBBB(Right Bundle Branch Block), **LBBB**(Left Bundle Branch Block), **PVC**(Premature Ventricular Contraction)

Extraction and Selection Schemes: Banerjee,Mitra (Banerjee & Mitra, 2014) and Gutiérrez (Gutiérrez-Gnecchi et al., 2017) developed two different techniques for extracting the features of ECG signals by using Wave transform (WT), Principal Component Analysis (PCA), discrete Wavelet transform (DWT) and discrete cosine transform (DCT). Different sets of features are extracted from these traditional techniques namely, ECG wavelet or morphologies features, time domain features,

frequency domain features, and power features and statistical features. Table 2.6 showed the performance analysis of different features set along with traditional features selection scheme for classification of different cardiac diseases.

Table 2.6: Performance Analysis different feature selection schemes

References	Features set	Feature selection schema	Classification Method	Performance	Public Dataset
(Yeh, Wang, & Wun, 2010)	morphological features, statistical features	Range-Overlaps Method (ROM), A qualitative feature selection	Cluster Analysis method and fuzzy logic	Cluster Analysis: Acc= 93.57% fuzzy logic: Acc= 93.17%	MIT-BIH Arrhythmia
(Ebrahimzadeh, Manuchehri, Amoozegar, & Araabi, 2018)	Time domain features, frequency domain and statistical features	Time local subset feature selection	Multi Layered Perceptron(MLP)	Acc=88.29%	MIT-BIH labeled with Sudden Cardiac Death Holter and Normal Sinus Rhythm
(Llamedo & Mart, 2011)	Morphological features, statistical features	Sequential floating feature selection algorithm (SFFS)	Model based automatic classification between the three AAMI	Supraventricular class: Se= 77% P+= 39% Ventricular class: Se= 81% P+= 87%	MIT-BIH Arrhythmia, MIT-BIH Supraventricular Arrhythmia, St. Petersburg Institute of Cardiological Technics (INCART)
(Patro & Kumar, 2017)	Time domain features	Onset and Offset detection of PQRST points	Customized Artificial Neural network	Acc= 98.1481%	MIT-BIH ECG id signal
(Y. Chen & Yu, 2012)	Statistical features	Nonlinear correlation measures the effective features in different pairs of features	Customized feed-forward back-propagation neural network (FFBNN) is used as a classifier	Acc= 96.34%%	MIT-BIH
(Jinho Park, Pedrycz, & Jeon, 2012)	Time domain features and Statistical features	Detect the time positions of Onset and Offset QRS complex position	Classification through SVM	Se= 95.7% Sp=95.3%	European ST-T database

Furthermore, different state-of-the-art methods are used for classification of different features set with different feature selection polices (Acharya, Fujita, Sudarshan, et al., 2017; Gothwal et al., 2011), such as K-means neighbor method, support vector machine (SVM), linear discriminant analysis (LDA), fuzzy logic and ANN, Wavelet transformation methods, and deep leaning models(Devi, Karpagam, & Kumar, 2017; Naseer & Nazeer, 2017; Osowski & Linh, 2001). However, it is observed in some studies that classification through deep learning models, Wavelet transformation and Machine learning approaches deliver different sort of computational complexity information. Table 2.7 represents the comparison summary in context of computational complexity information through collection of different studies that use different domain of features along with different adequately classification methods.

Table 2.7: Computational complexity comparison between different feature sets

References	Recognition approach	TD info	FD info	PWR info	Statistical features info	Public Dataset	CC info	Efficiency Rate
(Baloglu et al., 2019)	Deep learning	NO	NO	NO	NO	YES	YES	HIGH
(Dang, Sun, Zhang, & Qi, 2019)	Deep learning	NO	NO	NO	NO	YES	YES	HIGH
(Aloia et al., 2019)	WT approach	YES	NO	NO	YES	YES	NO	HIGH
(Acharya, Fujita, Adam, et al., 2017)	WT approach	YES	YES	NO	NO	YES	NO	HIGH
(Qin et al., 2017)	WT approach	YES	NO	NO	YES	YES	NO	HIGH
(J. S. Park et al., 2017)	WT approach	YES	NO	YES	YES	YES	NO	HIGH
(Jinho Park et al., 2012)	ML approach	YES	NO	NO	YES	YES	YES	HIGH
(Sadhukhan & Mitra, 2012)	WT approach	YES	NO	NO	YES	YES	NO	HIGH
(Zheng et al., 2013)	ML approach	YES	YES	YES	YES	YES	YES	HIGH
(Acharya, Fujita, Lih, et al., 2017)	WT approach	YES	YES	NO	YES	YES	NO	HIGH
(Xia et al., 2018)	ML approach	NO	NO	NO	YES	YES	YES	HIGH
(Hannun et al., 2019)	Deep learning	NO	NO	NO	NO	YES	YES	HIGH
(Martis, Acharya, & Min, 2013)	ML approach	YES	NO	NO	NO	YES	YES	HIGH
(Banerjee & Mitra, 2014)	Cross WT approach	YES	NO	NO	NO	YES	NO	HIGH

****TD** (time domain features), **FD** (frequency domain features), **PWR** (Power domain features), **CC** (Computational complexity, **ML** (Machine learning), **WT**(Wavelet Transform)

Opportunities: The deployment of effective feature selection creates multiple opportunities. Literature supports the recognition of *afib* and MI cardiac diseases are relied on different time domain features and statistical features(Acharya, Fujita, Adam, et al., 2017; J. S. Park et al., 2017; Savalia, Acosta, & Emamian, 2017). Existing studies show the use of minimal features sets for accurate recognition of *afib* and MI cardiac diseases with least computational or time complexity value(J. S. Park et al., 2017; Juyoung Park & Kang, 2014; Qin et al., 2017). Conversely, different deep learning approaches in literature claimed the high efficient results in recognition of cardiac diseases but it compromised on computational or time complexity value(Acharya, Fujita, Lih, et al., 2017; Acharya, Oh, et al., 2017; Pourbabae, Roshtkhari, & Khorasani, 2017)

Challenges: In perspective of complexity reduction, selection of right features set is still a hard job in recognition of *afib* and MI either it belongs to machine learning or wavelet analysis approaches. It is constantly observed in existing studies; the correlations exist between different features set and cardiac diseases recognition reliability on these feature sets(Blanco-Velasco et al., 2017; Kaiser et al., 2004; J. S. Park et al., 2017; Sedova et al., 2017). In context of correlation existence, the accurate detection of R peaks and RR intervals are significant for recognition of different shapes of *afib*, and *MI*.

Additionally, reduction of R peaks detection dependences is difficult job due to involvement of different features extraction. These extracted feature sets perform a vital role in recognition cardiac diseases namely, *afib* cardiac event recognize through detected R peaks and different feature domain sets. Similarly, different shapes of MI are also recognized through detected R peaks and feature sets of time domain-statistical features(Blanco-Velasco et al., 2017; Kaiser et al., 2004).

2.2.4 Recognition and Predictive Classification techniques

This section covers the compressive review of different recognition and predictive classification techniques of cardiac diseases through extracted features of ECG signal. ECG is the main diagnostic tool for monitoring the different and unusual activities of the heart muscle for detecting different heart diseases and arrhythmia. Such type of diagnostic tools requires perfection in terms of accuracy, sensitivity, and positive prediction value and error rate. Several studies highlight better ECG features classification results (Cheng & Dong, 2017; Xia et al., 2018)(Han & Shi, 2019; Nabar, Banerjee, Gupta, & Poovendran, 2011) For instance (Savalia et al., 2017) developed the automated classification technique that achieved the overall accuracy level of 82.5 % by fine-tuning the ANN. (J. S. Park et al., 2017) proposed the Wavelet transform and Shannon emery envelope (WTSEE) that works for different heartbeats on the basis of R-peak detection and achieves overall accuracy at 99.838 % level.

Along with different cardiac diseases and arrhythmia, accurate and robust identification of MI is also critical for cardiologists. In that context, the intensity markup of MI plays a vital role for the accurate and robust identification of different situations of MI(K. Feng, Pi, Liu, & Sun, 2019; Fukuda et al., 2015). The intensity of MI further depends on the changes in amplitude and time duration of ST segment and T wave. To support this method, trapezium's area (TRA) approach works as a location tracer through finding the maxima and minima value of T-peak by using the window-based method (Cesari et al., 2016). In TRA method, three vertexes are fixed and one vertex is mobile which is shifted over the ECG signal (Cesari et al., 2016). TRA approach is a useful tool for detection of T waves in ECG signals with the presence of different noise factors. One of the drawbacks in this method is that it works only for the detection of biphasic T wave. Existing literature on the subject lays constant emphasis on the importance of different ECG features classification and identification (Cheng &

Dong, 2017; Sansone et al., 2013). For instance, in (Bhuiyan et al., 2015), the beat-to-beat analysis deals with QT interval; the time interval between Q wave onset (start time of Q wave) and T wave offset (end time of T wave). A second study (Lemire et al., 2000) proposes another approach of mathematical modeling that is applied on ECG signal for calculations of the time duration and amplitude of different segments like ST segment, QT interval, RR interval and T wave. Wavelet Transform Modulus Maxima (WTMM) approach represents the characteristic behaviors of heart signals in ECG and is a part of T wave detection algorithm which works with the combination of the wavelet transforms regarding amplitude and slope of T wave (Krimi, Ouni, & Ellouze, 2006). Predictive recognition of the abnormal behavioral status of ST segment and T wave leads towards the MI formation. ST segment elevation myocardial infarction (STEMI) and ST segment depression or non-elevation of myocardial infarction (STNEMI) are the most crucial situations of MI (Qayyum, Hemaya, Squires, & Adam, 2018; Stub et al., 2015).

Furthermore, the contemporary deep learning techniques are normally used for recognition and predicative classification of different ECG features. In a prediction scenario, a model driven deep learning (MDDL) approach is the most suitable option for the prediction of defined parameters (Xu & Sun, 2018). For instance, in (Yakovlev, 2016), the concept of defined parameters is helped for prediction of different cardiac diseases like *afib* cases, known cases of MI (STEMI and STNEMI). Similarly, Paroxysmal atrial fibrillation (*paraf*) is a kind of cardiac arrhythmia that requires timely treatment otherwise it transforms into permanent atrial fibrillation which leads to a high rate of morbidity in the heart's structure (Yamada, Fukunami, Shimonagata, & Kumagai, 2000). In predictive classification, numerous studies have been proposed for the prediction of PAF (Acharya, Fujita, Lih, et al., 2017; Rao & Rao, 2016; Shin et al., 2006). Additionally, in their study (Shin et al., 2006) presented a model based machine

learning approach that proposed a truly positive approach, leading to a high accuracy ratio. Table 2.8 is a comparative summary of different machine learning techniques for recognition of *afib* and MI cases. Additionally, Table 2.8 also highlights the information of computational complexity and sample size that plays a vital role for understanding the robustness factor.

Table 2.8: Comparative summary of machine learning techniques

References	Deep Learning	R-Peaks ML	Other than ML	Large SS	CC Info	afib	MI	Public dataset
(Acharya, Oh, et al., 2017)	CNN	NO	NO	YES	NO	YES	NO	YES
(Hannun et al., 2019)	NO	YES	NO	YES	NO	YES	NO	NO
(Patro & Kumar, 2017)	NO	YES	NO	NO	NO	YES	NO	YES
(Aloia et al., 2019)	NO	NO	YES	NO	NO	YES	YES	NO
(Roza, De Almeida, & Postolache, 2017)	NO	YES	NO	YES	YES	YES	NO	YES
(Han & Shi, 2020)	NO	YES	NO	NO	NO	NO	YES	YES
(Wu et al., 2019)	NO	YES	NO	YES	NO	NO	YES	NO
(Übeyli, 2009)	RNN	NO	NO	YES	YES	YES	NO	YES
(Baloglu et al., 2019)	CNN	NO	NO	YES	YES	NO	YES	YES
(Engin, 2004)	NO	YES	NO	NO	NO	YES	NO	YES
(Acharya, Fujita, Lih, et al., 2017)	NO	YES	NO	NO	NO	NO	YES	YES
(Ellenius & Groth, 2000)	NO	YES	NO	NO	YES	NO	YES	NO
(Dang et al., 2019)	YES	YES	NO	YES	NO	YES	YES	YES
(Lobodzinski, 2013)	NO	NO	YES	NO	NO	YES	NO	NO

**ML(Machine Learning),SS(Sample Size), CNN(Convolutional Neural Network), RNN(Recurrent Neural Network), DNN(Deep Neural Network)

Open issues: Recent automated techniques of recognition or predictive classification of *afib* and MI cases shows some margin of improvement in optimization parameters (Baloglu et al., 2019; Dang et al., 2019).Classification of cardiac diseases through different models of deep learning or multi-layer perceptron's delivers the accurate results. However, in recognition process the number of iterations (epochs) is high in deep learning models and as well as different multilayer perceptron's(Acharya, Oh, et al., 2017; Kara & Okandan, 2007). The high range of epoch value enhances the

computational time that creates a hurdle in robustness in recognition process. Moreover, it's a challenging task in perspective of deployment the defined feature selection schemes for recognition the cardiac morbidities which reduces the number of iterations (computational time).

2.3 Review of Modular Based Techniques

This section presents the review of different modular ECG features classification solution that are recognized the cardiac diseases with different epoch values. According to previous studies, extensive level of feature engineering is performed to get the better recognition of cardiac diseases results(J. S. Park et al., 2017; Soria & Martínez, 2007). Furthermore, it's constantly observed in literature, deep neural models (deep learning models and different structural ANN's) reported high accurate results in recognition along with high epoch values (high Computational time)(Acharya, Fujita, Lih, et al., 2017; Acharya et al., 2019; Dang et al., 2019). Conversely, the impact of deterministic ANN structures delivered the efficient result with low sample size that may reduce the epoch values range. In deterministic structure of ANN, the least features are used for recognition process that's why such solution shows low epoch's value. Moreover, it's also observed in literature that the models of deep learning and other deterministic models of ANN followed the estimation parameters of model driven environment (MDE)(Engin, 2004; Sansone et al., 2013)

2.3.1 Data Driven Classification

The MDE induction in the field of healthcare systems constitutes what can be considered a game changer. The ECG is considered the most sensitive and effective method in the diagnosis of different heart diseases. For the purpose of diagnostic solutions of different heart diseases, the category of diseases needs to be classified. Estimation parameters of MDE support the traceability factors that are helpful for ECG

features classification. In perspective of MDE, several studies discuss the ways of improving the ECG classification techniques and algorithms (Cheng & Dong, 2017; Krimi et al., 2006; J. S. Park et al., 2017). Some studies discuss this classification in the form of a modular solution (Acharya, Fujita, Lih, et al., 2017; Miotto et al., 2017; Sankaran et al., 2017; Xia et al., 2018). Figure 2.4 showcases a typical example of a model based ECG classification.



Figure 2.4. Block model of the primary ECG classification process

During the review of literature, classification of ECG features through modular forms is observed in several studies (Baloglu et al., 2019; Faust, Hagiwara, Jen, Shu, & Acharya, 2018; Soria & Martínez, 2007). However, the aim of the MDE is to deliver the structure of the defined solution in such form that the elements of traceability, and reusability are possible. Based on these elements, several studies are found that highlight the model-based classification of ECG features (Acharya, Fujita, Oh, et al., 2017; Ravi et al., 2017; Yuan, Yang, Kang, Xu, & Li, 2018). This model based classification indicates the MDE involvement in modeling by embedding the elements of traceability, and reusability allow for a more effective classification including the backtracking feature. All the data models are also categorized in MDE, based on the fact that they incorporate the said elements (traceability, maintainability, and reusability). The autoregressive modeling and Hidden Markov model constitute ideal examples of the form of solution-oriented data modeling. According to the existing literature, these models possess a good trackback record in ECG feature classification (Sansone et al., 2013). One study discusses the classification of the features of *afib* in ECG signals by

adopting the autoregressive modeling (Padmavathi & Ramakrishna, 2015). Similar to autoregressive modeling, Markov's hidden model is also used in ECG analysis in order to calculate the prediction factor along with the classification of different features (Li, Pan, Jiang, & Liu, 2018)

2.3.2 Regressive Modeling

Some studies propose superior algorithmic techniques to classify ECG features, yet stop short of discussing their dependencies (Kaplan et al., 2018; C Wang & Guo, 2019). In such context, the defining elements (traceability, and reusability) are useful in dependencies calculation. Some studies use the methodology of classifying the ECG features with the help of data models (Benhar & Idri, 2019; Sun & Cheng, 2012). Different data models are used to classify the different ECG features; for example, model driven urgent ambulance control systems, autoregressive modeling for *afib* detection, and web-based health monitoring tool (Limaye & Adegbija, 2018; Yakovlev, 2016). In such systems, a part of the feature classification of ECG demonstrates that the MDE and Model Driven Architecture (MDA) are usable for every stakeholder (Bodisco et al., 2014). Autoregressive modeling for the classification of *afib* is also included in the proposed data modeling studies (Acharya, Oh, et al., 2017; Miotto et al., 2017).

2.3.3 Current Trend

Based on modular techniques in ECG, human heart monitoring has continuously improved as compared to other tools like phonocardiogram (PCG). ECG is a more efficient diagnostic tool. Diagnostic tools for this purpose require high accuracy and sensitivity. Reasonable results on the classification of different ECG features have been demonstrated (Acharya, Fujita, Adam, et al., 2017). Model based automated classification approaches have been proposed to identify cardiac problems in ECG. Unfortunately, some model based methods like deterministic policy gradient algorithms,

do not highlight the complete structure of the internal layers of the classification model (Shi, Sun, & Li, 2018). Moreover, the method of robust accurate anomaly detection (Robust Accurate Anomaly Detection (RAAD) algorithm) reduces false alarm rates and improves accuracy levels to up to 100% (Sivaraks & Ratanamahatana, 2015). However, RAAD algorithm cannot recognize data in ECG signals that do not past record, such as *flattened T wave*. Similarly, in their study, when (Blanco-Velasco et al., 2017) used the T- Wave Alternans (TWA) algorithm to recognize T wave anomalies with the help of the T-onset feature, the inability to recognize unseen features was encountered. Prior research (Savalia et al., 2017) developed an automated classification technique employing feature extraction and a finely tuned ANN. This technique was used to classify tachycardia and bradycardia with 82.5% accuracy, which is generally unacceptable in healthcare systems. Authors in (J. S. Park et al., 2017) proposed the WTSEE technique, which employs R-peak detection and then implements Wavelet Transform (WT) to classify features. This technique classified different heartbeats and achieved an overall accuracy of 99.838%; but this technique did not consider the computational complexity factor that is also a concern in robotic classification of cardiac diseases.

Some studies on different ECG analysis schemes have highlighted the accurate and early identification of abnormalities in ECG (Acharya, Fujita, Adam, et al., 2017)(Krimi et al., 2006; Limaye & Adegbija, 2018). For robust and accurate ECG features classification, the relevant literature continuously highlights the most significant component of the ECG morphology as the QRS complex (Elgendi, 2013). Since the 1985 Pan-Thompkins QRS detection algorithm (Elgendi, 2013), analysis of ECG has relied on accurate QRS complex detection. Accurate detection of the QRS complex is partitioned into two key components: extraction of features and identification of the nature of features for classification (Qayyum et al., 2018). Two different techniques for

extracting ECG feature signals have been developed by using WT, PCA, DWT, and DCT (Banerjee & Mitra, 2014) (Gutiérrez-Gnecchi et al., 2017). Similarly, different state-of-the-art methods have been used to classify different features (Naseer & Nazeer, 2017; J. S. Park et al., 2017; Patro & Kumar, 2017), such as K-means neighbor method, support vector machines, linear discriminant analysis, fuzzy logic, and Artificial Neural Network (ANN) (Acharya, Fujita, Adam, et al., 2017; Devi et al., 2017; Engin, 2004; Zheng et al., 2013).

Identification of cardiac irregularities is followed by the highlighting of the features derived from the detected R peaks (J. S. Park et al., 2017). Several accurate and robust R peak detection algorithms have been proposed, like the effective R peak detection algorithm, variable threshold values for R peak detection, and Shannon energy transform, which are remain common techniques for R peak detection (J. S. Park et al., 2017; Qin et al., 2017; Yu et al., 2019). Recent trends indicate that extraction of different features relies on the accurate and robust detection of R peaks. Different types of cardiac malfunctions can be identified through these features (J. S. Park et al., 2017), including arrhythmia, *afib* (through irregular RR intervals), PVC (through irregularities of the QRS complex in ECG wavelets), and myocardial ischemias (through ST changes). Furthermore, different studies reported that the anomalous portions of RR interval and ST changes rapidly lead towards the risky cardiac situations namely atrial flutter, continuous tachycardia, acute myocardial infarction, hypokalemia, hyperkalemia and factors of *nsst-t* in MI (Gothwal et al., 2011; Harkness et al., 2019; Yoon et al., 2018).

2.4 Review of MI Detection Methods

This section presents brief review of different shapes of MI and its cause through the anomalous portions of ST changes and T wave changes. MI situations are the top

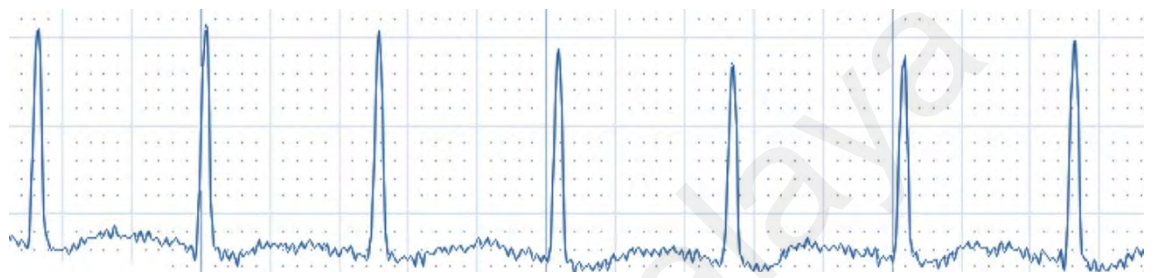
risk in survival of human life. In diagnosis of MI, the cause and human life survival factor are most significant terms, ST segment elevation, ST segment depression, ST segment inversion and different T wave anomalies are the leading cause of different MI situations (Nagao et al., 2015; Okin et al., 2002; Qayyum et al., 2018). For diagnostic purposes, the MI nature must be determined, such factor is covered by robust and accurate recognition of different T waves that helps to recognize the different situations of MI. Additionally, accurate recognition of T waves normal and abnormal categories are more significant and primary step for different critical situations of MI. Anomalous episodes of T wave are known to be the primary cause of the MI (Alathr, Smith, & Vinocur, 2017; Hadjem & Naït-Abdesselam, 2015). Robust detection of T waves anomalies are the game changer in recognition of MI situations (Elgendi et al., 2015; Han & Shi, 2019; Lemire et al., 2000).

Classification of different T waves episodes with minimal ambiguity rate has become highly desirable for ECG researchers and cardiologists (Bhuiyan et al., 2015; Elgendi et al., 2015). According to the existing literature, the parametric factors are dependent on the external or internal factors which may be called features dependencies (Cesari et al., 2016; Hadjem & Naït-Abdesselam, 2015; Vázquez-seisdedos, Neto, Reyes, Klautau, & De Oliveira, 2011). Additionally, different state-of-the-art classification techniques of different T waves are fetched and examined from literature (Alathr et al., 2017; Elgendi et al., 2015; Hadjem & Naït-Abdesselam, 2015) that are useful for detection of different MI shapes especially in case of *nsst-t*.

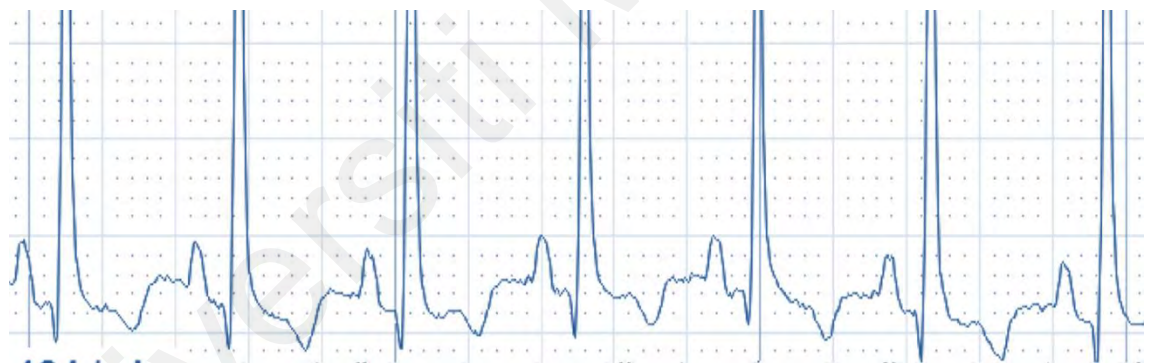
2.4.1 T wave anomalies through a T-onset feature

For efficient MI detection, proper identification of MI situation is helpful for diagnostic purposes, as it addresses the high-risk factors. For diagnostic purposes, the most critical part of MI is to recognize the sudden non-invasive changes of T wave

where the primary step that needs to be taken is to highlight the abnormal T wave episodes. Previous studies reported that accurate classification of T wave anomalies depends on a features recognition solution(Ghoraani et al., 2019; Krimi et al., 2006). Different wavelet features set of T wave are already discussed in Table 2.2 that help to identify the nature of T wave's anomalies. Figure 2.5 is captured form study (Tramèr et al., 2018) that highlights the different anomalies of T waves.



(a) Case of flattened T wave



(b) Case of Inverted T wave

Figure 2.5. Different anomalies of T wave (a).flattened T wave (b) inverted T wave

TWA algorithm is one of the techniques that is discussed and examined in literature (Blanco-Velasco et al., 2017). Such algorithm primarily works for the extraction the T-onset feature. Execution of the TWA algorithm works on the basis of R peak as fiducial point and then considers the RR intervals (Elgendi et al., 2015). The significant part of the TWA algorithm is RR interval displayed in the equation 2.1 below. This equation

indicates the energy intensity of T wave either in the form of standard or anomalies dependent on a T-onset parameter of T wave (Blanco-Velasco et al., 2017)

$$T_{on} = 40 + 1.33\sqrt{RR} \quad (2.1)$$

Features discussion of T wave always revolves around four subparts, namely, T *onset*, T *offset*, T *dur* and T *amp* which is highlighted in Table 2.3 (Goldberger et al., 2000)

Table 2.9: .Key features of T wave in ECG

DIFFERENT T WAVE FEATURES	
<i>T wave Features</i>	<i>Description</i>
T <i>onset</i>	Start time of the T wave in ECG
T <i>offset</i>	End time of the T wave in ECG
T <i>amp</i>	Peak value between T onset and T offset
T <i>dur</i>	T wave duration between T onset and T offset

2.4.2 Impact of T wave Dependencies

For recognition of features patterns, especially in case of MI, the foremost step is to identify the root cause of MI generation. Identification of such root cause is possible if we can highlight the dependencies factor of T wave changes. Calculations of the dependencies of T wave are only possible if we can get all the features of T wave. Proper tagging of T wave anomalies is dependent upon the T offset, the time duration of T wave, the amplitude of T wave and T onset values(Kaiser et al., 2004).

To analyze dependencies calculation of T wave changes, further studies were explored in the existing literature. Various studies have contributed to feature analysis in ECG such feature analysis is performed by using different methods like Wavelet Transform Module Maxima (WTMM) and WT with detected R peaks (Legarreta, Addison, Grubb, & Engineering, 2003; Legarreta et al., 2005; Soria & Martínez, 2007). T wave detection algorithm works in the context of usage of the WTMM for detection of T waves (Hadjem & Naït-Abdesselam, 2015). Such algorithm works on the basis of

different parameters of T waves (combination of amplitude parameter of T wave and slope of the T wave). Another state-of-the-art approach is used for detection of T wave through amplitude (T peak) features of T wave (Bhuiyan et al., 2015). The above two state-of-the-art methods are also practiced indirectly for finding the dependencies. As for the particular case of two anomalies, i.e., T wave inversion and flattened T wave, both of these anomalies have a placed in the same slot, but both are known to behave differently in a situation of MI(Okin et al., 2001; Sedova et al., 2017). Table 2.10 is a short comparative summary in context of clinical and experimental studies on *flattened T wave*.

Table 2.10: Summary of different flattened T wave studies

References	Clinical study	Experimental study	Flattened information
(Tramèr et al., 2018)	NO	YES	NO
(Koivikko et al., 2017)	YES	NO	YES
(Blanco-Velasco et al., 2017)	NO	YES	NO
(Kerro, Woods, & Chang, 2017)	YES	NO	YES
(Isaksen et al., 2018)	YES	NO	YES
(Vinyoles et al., 2015)	YES	NO	YES
(Ghoraani et al., 2019)	NO	YES	NO

2.4.3 MI and NSST-T

The significant part of any MI detection is the identification of cause through changes involvement ST segment and T wave. Different studies reported that ST segment and T wave changes rely on two categories namely, major ST-T wave changes and minor ST-T wave changes(Schillaci et al., 2004; Vinyoles et al., 2015). It's reported in different studies that major ST-T wave changes happened when the ST segment depression is greater than 0.1mV(Ishikawa, Hirose, Schwartz, & Ishikawa, 2018; Koga et al., 2016). These major ST-T changes lead towards the MI with due to the cause of hypertension and smoking. Similarly, the minor ST-T wave changes are reported that

ST segment depression is less than 0.1mV. Additionally, the cause of minor ST-T changes belong to the hypertensive factor and the risk impact of minor ST-T changes are high as compared major to ST-T changes.

However, there is a third category in MI situation that belongs to non-specific ST –T changes. Such non-specific ST-T changes are relying between the major and minor ST-T changes. It's observed in literature the range of ST segment depression is very minimal for highlighting the difference between major and minor ST–T changes(Ishikawa et al., 2018; Schillaci et al., 2004). Despite the range of ST segment depression, there are some flatness or T- wave inversion reported in some studies that belong to *nsst-t*(Bhuiyan et al., 2013; Yoon et al., 2018). The flatness factor of ST segment and T waves are very low range and lead towards the risky MI situation. The conflict of T- wave inversion and flattened anomalies in *nsst-t* are still an ongoing research work(Yoon et al., 2018).

Opportunities: In recognition of MI situation that belongs to the *nsst-t* are the current area of workable for ECG researchers(Vinyoles et al., 2015). The anomalies of flatness are the leading cause of *nsst-t* that shows the conflict between major and minor ranges of ST-T changes(Ishikawa et al., 2018; Koga et al., 2016). According to existing studies, there is some room of research works that relates to explore features of *flattened T wave*(Bhuiyan et al., 2013; Sedova et al., 2017). Exploration of the features of onset, offset, time duration and peak value are the initial steps for identifying the other factors of *nsst-t*(Kang et al., 2018; Vinyoles et al., 2015). Moreover, the recognition of correlation between *flattened T wave* and other T wave anomalies are helpful for identification of the cause of MI situation(Okin et al., 2001)

Challenges: Existing studies reported the recognition of *flattened T wave* through non-deterministic way is a hard task either if use deep learning models and other

wavelet approach. It was observed through previous studies the ratio of feature analysis on *flattened T wave* and *nsst-t* was quite low as compared to clinical review studies (Bao et al., 2017; Schillaci et al., 2004; Sedova et al., 2017). Previous Clinical studies reported that the existence of *nsst-t* is a rare scenario and flattened T wave is the most significant part of *nsst-t* (Bhuiyan et al., 2013; Ishikawa et al., 2018; Koga et al., 2016).

2.5 Review of Classification through Multilayer Perceptron (MLP)

This section briefly discusses the two unique way of ECG features classification through MLP namely, deep learning models and deterministic leaning techniques. The classification process is typically used for the identification of irregularity or unusual patterns (novelty detection) in ECG (Patro & Kumar, 2017). Such a process splits the regular and irregular patterns. Traditionally, different ionic classification techniques are used for splitting the irregular responses except for the prediction element (Gothwal et al., 2011; Sivaraks & Ratanamahatana, 2015). In contrast, ANN were used for the scenario of rapid accurate predictive classification of different cardiac diseases (Karthik, Tyagi, Raut, & Saxena, 2019; Prasad & Sahambi, 2003; Shin et al., 2006) .

a. Artificial neural network

Conduction of operational investigations in every ANN structure involves some sort of organized structure. ANN employs the three main layer structures. These layer structures consist of the input layer, the output layer and the hidden layer. The input and output layers utilize a number of nodes, but the output layer has one mode. The nodes circuit of neural network contains the activation function. By using the patterns of neural network, which interacts with hidden layers and patterns are generated with the help of input layer. The actual operational activities of neural network are processed in the hidden layers which allocate different weights to the edges. The hidden layers are

fully connected with input and output layers till the final answer is computed (Devi et al., 2017).

The primary task is to train the neural network by adjusting the weights of each unit. This step helps condense the error ratio between the desired output and actual output. Error derivation of the outputs is a critical phase that displays the changes in error by varying the weights slightly in the manner of increasing or decreasing (Roza et al., 2017). Back Propagation (BP) algorithm is mostly used to determine the error (Hameed, Karlik, & Salman, 2016). In obtaining true results of the ECG features classification, usage of feed forward multi-layer neural network works along with back propagation algorithm. In an ideal case, the target values of the neural network approximately equal the expected output value. The Levenberg-Marquardt(LM) algorithm was found the best for obtaining results in this phase (Lourakis, 2005). The most successful deliverable of such an algorithm is a reorganization of the apparent difference between two heartbeats, i.e., regular heartbeats and PVC (Gutiérrez-Gnecchi et al., 2017). Additionally, deep learning models are more useful for classification of different ECG features

2.5.1 Deep Learning Models

In deep learning models, the recognition of different cardiac diseases is done by skipping the feature engineering phases which help for reduction of the complexity factor. However, the complete requirement of a particular paradigm for the identification of these cardiac diseases might increase the complexity factor, because a bundle of time is required for the complete execution of convolutional neural network (CNN), Recurrent neural network (RNN) and Probabilistic neural network (PNN) models (Acharya, Fujita, Oh, et al., 2017; Acharya, Oh, et al., 2017; Ravi et al., 2017).

2.5.1.1 Convolutional Neural Network

Since the early part of 21st century, deep learning models have played a vital role in different domain analytics. Structural representations of CNN exploit the correlation that exists between adjusted layers, e.g., the neurons architecture of human brain. Technically, the different architectures of CNN usually train and test the object's data. Each data is shared into convolution layers with filters, pooling, fully connected layers and subsequently, by application of the defined softmax function to classify the objects with the probabilistic representation of values between 0 and 1. However, the complexity factor is always increased in processing data with CNN. In ECG analytics the model of CNN is a useful tool for recognition of different cardiac diseases. Domain literature constantly demonstrates that different structure of CNN models are a robust and accurate way to recognize the different cases of high priority cardiac diseases (Acharya, Oh, et al., 2017; Pourbabaee et al., 2017)(K. Feng et al., 2019; C Wang & Guo, 2019). These diseases includes the different forms of *MI*, *afib*, *PVC* and different categories of *HRV*.

2.5.1.2 Recurrent neural network

Normally, the analysis of any time series problems uses the concepts of time domain features, frequency domain features, and k-near neighbor analysis for prediction purposes in data analytics. Before the era of deep learning commenced, the prediction parameters were measured through the famous mathematical modelling of SARMA model (Comp & Sumathi, 1997). Induction of this mathematical modeling involved human error; therefore, using the solution of deep learning became imperative for error-free predictive analytics. Another most promising deep learning model is RNN that is usually used for predictive analytics of sequential data like the speech recognition, natural language processing and biomedical data predictive analytics. Similarly, like the usage of RNN for other analytics, such model of deep learning is also used for different

types of ECG analytics, such as automated and robust measurement for HRV through induction of extra hidden layers in RNN(Übeyli, 2009; Wu et al., 2019). Similarly, Predictive classification of recognized forms of *MI* and *afib* are also performed through RNN (Dorffner, Leitgeb, D, & Polten, 1994; Ellenius & Groth, 2000).

2.5.1.3 Probabilistic neural network

PNN model is a feedforward neural network, which was derived from a statistical algorithm called a Kernel Fisher Discriminant Analysis and Bayesian network (Mika, Ratsch, Weston, Scholkopf, & Mullers, 1999; Nir FriedmanDan ,GeigerMoises, 1997). The PNN model works critically for recognition of the cardiac diseases, especially in the probability context. Various existing studies on the subject use the PNN model for recognition or classification of cardiac diseases on the basis of probability (Elhaj, Salim, Harris, Tian, & Ahmed, 2016; N. Feng, Xu, Liang, & Liu, 2019). For instance, (Martis et al., 2013) delivered the novel method of beat recognition through PNN in combination with the Independent Component Analysis (ICA). The feedforward neural network model assesses the probability of myocardial infarction in a deterministic way through proper use of feature selection. However, the PNN model is unsuccessful if the features are aggregated in improper way.

2.5.2 Deterministic Learning MLP Models

This subsection briefly discusses those ANN approaches that are used to classify the anomalies in ECG with defined way. Literature supports few studies that belong to recognize the different anomalies (cardiac diseases) in ECG signal on deterministic manner(Deng, Wang, Tang, & Zheng, 2018; Dong, Si, & Huang, 2018). These studies support the deterministic learning theory; such theory is developed for recognition and controls the different features based application(Lai, Deng, Tang, & Wang, 2019; C Wang et al., 2016; Cong Wang & Hill, 2007).These studies show the recognition of

different cardiac diseases through deterministic learning with integration traditional of classification techniques. Moreover, it's also observed that deterministic method is also used with ANN for recognition of different cardiac diseases(Cervellera & Muselli, 2004; Yang, Devine, & Macfarlane, 1994).

Different studies delivered the deterministic learning theory in detail that shows the data representation, definition of similarity index and how to recognize the patterns in rapid way(Dong et al., 2018; C Wang et al., 2016).For instance (Dong, Wang, & Si, 2017), in beat recognition through deterministic learning, delivers the efficient results with minimum features. In beat to beat recognition, the workflow categorizes into two parts namely; identification phase and recognition phase. These phases of identification and recognition were mapped with constant weight of ANN. Moreover, for beat recognition through deterministic learning, the design of two types of classifiers namely globally classifier and patient adaptive classifier(Dong et al., 2017). Recognition with global classifier highlights the accurate results in perceptive of recognizing all defined cardiac diseases namely, Right Bundle Branch Block (RBBB), Left Bundle Branch Block (LBBB) and PVC. Similarly, patient adaptive classifier recognizes the patient specific cardiac problems that highlight least computational time.

In clinical interpretations, the beat recognition is significantly helpful for recognition of the arrhythmia's namely *afib*, Ventricular Fibrillation(VF) , and Tachycardia leads to MI(Koivikko et al., 2017; Phillips et al., 2019). Table 2.11 presents the summary of recognition of cardiac diseases through hybrid of deterministic learning with traditional techniques.

Table 2.11: Recognition Summary of cardiac diseases through deterministic learning

References	Cardiac issues	TD	FD	PWR	SF	D-FSS	Public Dataset	R_R
(Dong et al., 2017)	Afib	YES	NO	NO	YES	YES	MIT-BIH	Acc=97.78%
(C Wang et al., 2016)	MI	YES	NO	NO	YES	YES	PTB	Se=90% Sp=80%
(Dong et al., 2018)	MI	YES	NO	NO	YES	YES	PTB and Others	Acc=100%
(Lai et al., 2019)	MI	YES	NO	NO	YES	YES	NO	Acc=83.12% Se=87.5% Sp=78.75%
(Yang et al., 1994)	Afib	YES	NO	NO	NO	YES	NO	Se=92% Sp=92.3%
(Deng et al., 2018)	MI	YES	NO	NO	YES	YES	PTB	Acc=83.9% Se=83.9% Sp=84.4%
(Deng, Wu, Cao, Tang, & Wang, 2019)	MI	YES	NO	NO	YES	YES		Acc=91.2%
(Yan et al., 2019)	MI	YES	NO	NO	YES	YES	PTB	Acc=85%

**TD (time domain features), FD (frequency domain features), PWR (Power domain features), D-FS (defined features set), SF (Statistical features learning), R_R(Recognition Result),SP(Specificity)

.Opportunities: There is the opportunity to deploy the logical structure of ANN model in deterministic way which supports to identify the correlation between different ECG anomalies(Yan et al., 2019). Therefore, there must be a set of constant weight in ANN model for finding the correlation between different anomalies(Dong et al., 2018). The impact of deterministic logic helps to analyze the different features that are further control the recognition process in least computational time.

Challenges: It's hard job to avoid the overfitting in deployment of ANN deterministic logic(Deng et al., 2019). Usage of minimum ECG features stream is the cause of overfitting that may affect the validation of recognition process. Therefore, the cardiac event based feature selection is the changeling job in the deterministic ANN model. Furthermore, adaptive feature selection for deterministic logic of ANN requires extra effort in feature extraction phase(Dong et al., 2018; Sun & Cheng, 2012).

2.6 Performance Evaluation Strategy

This section discusses the performance evaluation policy of previous classification or recognition techniques whose impact directly relates to different ECG features. Different structures of deep learning model are used in existing studies for recognition of different situations of afib and MI. In existing studies, different CNN structures are used to recognize the STEMI and NSTEMI situations of MI that delivered the impressive accurate result but compromise on the robustness factor due to high computational or time complexity. For training the deep learning models, the huge input feeds are required to tune the models for recognition of cardiac diseases that enhance the computational cost with number of iterations (epoch value). Additionally, the factors of nsst-t especially flattened T wave is not recognized through deep learning models because these models are not supported by the feature analysis. Conversely, few studies highlighted the recognition of *afib* and MI via deterministic learning ANN models that require defined feature sets with constant weights. The computational complexity and efficiency of deterministic learning are dependent on the defined features set that supported the feature analysis. However, literature does not support the depth feature analysis of flattened T wave, expects to discuss the range of nsst-t that specified range of ST segment depression(Harkness et al., 2019; Phillips et al., 2019). Existing studies highlighted the extraction of different domains and statistical features, dependent on R peaks detection which delivered the better analysis of features(Ebrahimzadeh et al., 2018; Lee et al., 2018; Lemire et al., 2000)

Several studies highlight the significance of accurate detection of R peaks imposed the huge impact of recognition of cardiac diseases through different ECG anomalies namely, irregular RR interval, STEMI, NSTEMI, and T wave anomalies(Blanco-Velasco et al., 2017; Hadjem & Naït-Abdesselam, 2015; Stub et al., 2015). The variation in RR intervals highlights the heart rate variability which delivers the

information of *afib* situation(Lobodzinski, 2013). Additionally, rapid heart rate variety in *afib* leads towards the heart strokes and heart failure. Similarly, previous studies reported that different situations of MI are dependent on accurate R peaks detection(Ebrahimzadeh et al., 2018; Lee et al., 2018; Lemire et al., 2000). With MI concern, some studies discussed that TWA algorithm are used for detection of T wave variations and these variations measure through calculation of RR intervals(Blanco-Velasco et al., 2017; Kaiser et al., 2004; Krimi et al., 2006).

A survey of domain literature reveals one constant concern of the cardiologists and researchers alike, that with the accurate recognition of T wave episodes, the shape and nature of *flattened T wave* that are identified through the different features of T wave (time duration, peak value, start and end time)(Elgendi et al., 2015; Hadjem & Naït-Abdesselam, 2015). Another common observation highlights the dependencies of different features on T wave episodes, like the R peak as a fiducial point for the calculation of T-onset parameter (Blanco-Velasco et al., 2017). Such dependencies factors play a vital role in the recognitions of different T wave episodes. Contemporary research, therefore, concurs that achieving accurate and robust recognitions of different T wave episodes is an unresolved issue, especially in the case of flattened T wave (Elgendi et al., 2015). A number of studies found in the literature surveys that are focused directly or indirectly on T wave classification (Cesari et al., 2016; Hadjem & Naït-Abdesselam, 2015; Naseer & Nazeer, 2017).

2.7 Limitations in Related Literature

This section shows the limitations and challenges observed during the review of literature. The major limitation and challenge in literature related to the selection of features for recognition of cardiac diseases. The second major limitation and challenge

was as to how to recognize the unseen cardiac diseases like different factors of non-specific ST-T changes (*nsst-t*).

2.7.1 Limitations Related to Features Selection

The literature survey brought out some useful facts, one of which was the improper feature selection for recognition of the cardiac diseases. Table 2.6 reported the different features selection techniques for recognition of the *afib* and MI cardiac issues. However, it is also observed in literature that supports the accuracy factor in recognition of cardiac diseases instead of other factor like impact of computational complexity. Previous studies highlighted the large set of different wavelet features, time domain features, and frequency domain features are used for recognition of different cases of *afib* and MI(Aloia et al., 2019; J. S. Park et al., 2017; Qin et al., 2017). Different studies claimed the robustness in recognition of *afib* and MI are actually least when discussing the computational complexity factor especially the models of deep leaning and hybrid techniques of ANN and wavelet transform(Acharya, Oh, et al., 2017; K. Feng et al., 2019; Kara & Okandan, 2007). In section 2.2.4, Table 2.8 is highlighted the accurate results and computational or time complexity information, however the impact of complexity lacks in existing studies. Similarly, different feature selection techniques in Table 2.6 highlighted the high efficient rate without knowing the computational values. It is continuously observed in literature that computational complexity is not considered as significant factor in recognition especially in deep learning models(Acharya, Fujita, Lih, et al., 2017; N. Feng et al., 2019; Han & Shi, 2020).The usage of large features sets or feather selection in non-deterministic way enhances the computational complexity. The non-deterministic way of feature selection is the limitation in recognition of cardiac diseases, if uses the deep learning models or other hybrid approaches with ANN. Beyond doubt, the significance of the complexity factors is high in cases of urgent and high priority cardiac diseases recognition.

Conversely, the usage of deterministic way in features selection helps in predictive classification of cardiac diseases. Timely diagnoses of these cardiac problems help the physicians in providing better and often life-saving treatment for cardiac patients.

Different sets of features were used in literature for recognition of different sets of cardiac diseases, for recognition of cardiac diseases, a series of time domain and frequency domain features include a number of detected R-peaks, number of RR intervals, the root mean square values of RR interval (*rr-rms*), standard derivation of RR intervals (*sdnn*), energy entropy of detected R peaks, onset and offset values of different segments ECG signal. Different studies used the combination of these features sets for recognition of the *afib* cases, and MI different cases(Blanco-Velasco et al., 2017; Y. Chen & Yu, 2012; Kaiser et al., 2004).

2.7.2 Limitation in recognition of MI Cases

The second major concern in the context of limitation is the recognition of MI that belongs to *flattened* anomalies of *nsst-t*. The operation research on recognition of *flattened T wave* is limitation in literature. However, few case studies highlight the significant values of *flattened T wave* in perceptiveness of *nsst-t*(Isaksen et al., 2018; Tramèr et al., 2018; Vinyoles et al., 2015). Table 2.10 in section 2.4.2 summarizes the previous work on *nsst-t* especially on *flattened T wave*. Previous studies support minimal feature analysis of flattened T wave that's why the conflict of T wave inversion and flattened T wave anomalies still exist in hypokalemia(Harkness et al., 2019; Phillips et al., 2019). Complete feature analysis of *flattened T wave* is a limitation; therefore the recognition of hypokalemia(MI) in perceptiveness of T wave inversion and *flattened T wave* is a challenging job. Moreover, MI Detection algorithmic method, QT detection techniques, RAAD algorithmic for identification of MI cases in the context of T wave

anomalies, and quantitative as well as qualitative shapes of TWA algorithm for T wave anomalies (Blanco-Velasco et al., 2017; Sivaraks & Ratanamahatana, 2015). TWA algorithm depends on the accurate detection of R peaks in ECG signal for identification of the abnormal range of T wave. With this concern the quantitative portion of TWA algorithm reflects R peaks as the fiducial point for measurement of the T-onset of T wave. However, the recognition of flattened anomalies are entirely dependent on the correlation on other anomalies of ST segment and T wave anomalies. (Wu et al., 2019). The features correlation findings on flattened T wave and other T wave anomalies are also a limitation in literature (Bhuiyan et al., 2013; Okin et al., 2001).

These limitations in section 2.7.1 and section 2.7.2 were already highlighted in problem statement above (Chapter 1), especially the recognition of flattened T wave and complexity reduction in recognition of these cardiac diseases. This thesis tries to deliver the complete combo method as a solution of these issues and also highlights some useful future directions for future research opportunities.

2.8 Research gap Analysis.

This section briefly discusses the limitation in literature that defines the gap between current state of cardiac recognition techniques and target state of cardiac recognition approach. The detail survey of literature highlighted the efficiency rate in recognition process, as dominated as compared to the computational complexity factor. Different studies showed the automated recognition completely relied on deep learning models due to high efficient recognition results in context of cardiac diseases (Acharya, Oh, et al., 2017; Han & Shi, 2020; Pourbabae et al., 2017). However, the deep learning models in Table 2.8 highlighted the factor of computational complexity which is high due to usage of large sample size for training and testing the data for classification purposes. A number of studies examine and discuss different tier structures of CNN that are used for classifying *afib* and MI cases but the impact of the high value of epochs

are not addressed properly in perspective of recognition robustness(Acharya et al., 2019; Acharya, Oh, et al., 2017; Han & Shi, 2020). The enhancement of epochs values actually gear up the computational complexity that directly imposed the negative impact in robustness factor of recognition. (Daraei & Hamidi, 2017; K. Feng et al., 2019). Conversely, according to Table 2.11 in section 2.5.2, the deterministic learning with ANN plays a vital role in reduction of computational complexity that utilized the low sample sizes as compared to deep learning models. For deterministic learning with ANN, the extraction and selection of ECG features vary effectively that delivered the value results. The review of different deterministic learning studies is highlighted in the two phases that belongs to identification and recognition phase(Deng et al., 2019; Dong et al., 2017) .These two phases along with effective feature selection are valuable combination for recognition of flattened T wave.

Furthermore, literature supports the clinical studies on flattened T wave as compared to minimal worked in feature analysis on *flattened T wave*(Bhuiyan et al., 2013; Isaksen et al., 2018; Vinyoles et al., 2015). To support the feature analysis factor, identification the correlation between T wave inversion and flattened T wave enhances the knowledge of hypokelima in nsst-t(Phillips et al., 2019; Sedova et al., 2017). According to ECG clinical studies , the existence of *nsst-t* is rare due to defined range of major ST-T changes and minor ST changes(Ishikawa et al., 2018; Koga et al., 2016). Therefore, the existence of flattened T wave cases may be in low ratio for examination. Previous studies belonging to the categories of case studies and clinical reviews of flattened T wave clearly highlight area of feature analysis (see Table 2.10 in Section 2.4.2)

It's observed after the detailed review of literature that optimization in recognition processes of cardiac diseases, feature analyses along with recognition of *flattened T*

wave are the open area for researchers. In section 2.2.3, Table 2.6 highlights the different feature selection techniques for recognition of cardiac diseases which lacks to define the information of computational complexity. Moreover, for effective feature selection, in Section 2.2.3 Table 2.7 clearly mentions the statistics which indicate the time domain features with the combination of statistical features delivers the efficient results along with low computational values.

In last, for robust recognition of cardiac morbidities, the comparison between deep learning and deterministic learning delivers the valuable statistics in context of the strengths and weakness of two automation approaches. Table 2.12, shows the comparative summarized of deep learning and deterministic learning.

Table 2.12: Comparison of deep learning and deterministic learning

Approach	Weakness	Strength	References
Deep Learning	<ol style="list-style-type: none"> 1. Requires large sample size for training, testing and validation of the model for classification 2. Lack of feature analysis opportunity (not supportable for flattened T wave) 3. High computational complexity (high number of epochs) 	<ol style="list-style-type: none"> 1. Highly accurate classification result 2. Highly suitable in automated classification 3. Performance rate is high prediction of defined cardiac diseases. 4. No need for pre-processing and filtration 	(Acharya, Fujita, Lih, et al., 2017; Acharya et al., 2019; Acharya, Oh, et al., 2017; Faust et al., 2018; Miotto et al., 2017; Pourbabae et al., 2017; Ravi et al., 2017)
Deterministic Learning	<ol style="list-style-type: none"> 1. Requires constant weights in training and testing the ANN 2. Requires basic level of pre-processing and filtration 3. Feature engineering required in flattened T wave cases. 	<ol style="list-style-type: none"> 1. Low computational complexity (low number of epochs) 2. Suitable for correlation identification between cardiac diseases 3. Feature analysis opportunity (supportable for flattened T wave). 4. Low sample size is required for processing 	(Cervellera & Muselli, 2004; Deng et al., 2019; Dong, Wang, Hu, & Ou, 2014; Dong et al., 2017; Lai et al., 2019; Cong Wang & Hill, 2007; Yan et al., 2019)

2.9 Conclusion

This chapter delivers the critical review/observations in context of recognition or classification of different cardiac morbidities in ECG signals. Six main aspects of ECG signal classification were explored: the characteristics of dataset, pre-processing methodologies, different deployed feature engineering techniques, traditional wavelet analysis techniques for classification, machine learning algorithms, and different architectures of deep learning models. Thorough review of the different studies of ECG analytics which are highlight the two core open issues; Firstly, recognition of cardiac morbidities in perspective of *flattened T wave*. Secondly, it was further observed that the existing primary studies used the public datasets, which mostly compromised of the global acceptance values as well as optimization on computational complexity (time complexity). It was also found that before proceeding to the classification or recognition phase, the induction of the feature engineering techniques played a vital role in classifying the cardiac disease. By using the state-of-the-art feature engineering techniques, different features were extracted that represent these key segments of the ECG signal. These extracted features were further used in wavelet transformation techniques and machine learning which was further categorized in deep learning models and deterministic learning models for recognition of different cardiac diseases

Moreover, the factors of *flattened T wave* recognition and robustness are discussed in perspective deep leaning models and deterministic learning models. The weakness and strengths comparison of these two machine learning approaches are helpful in formulation of flattened T wave recognition and computation or time complexity issues.

CHAPTER 3: RESEARCH METHODOLOGY

3.1 Introduction

This chapter discusses the complete schema of methods of this study. The chapter is further subdivided into two subsets that highlight the different methods for achievement of defined research objectives discussed in Chapter 1 (see section 1.4). These subsets cover-up the areas of collection different datasets for globally recognized proposed methods, data pre-processing and segmentation, extraction of different features on ECG signal, development of proposed models and evaluation of the performance of proposed models. All the subsets of this research are comprehensively represented in figure 3.1.

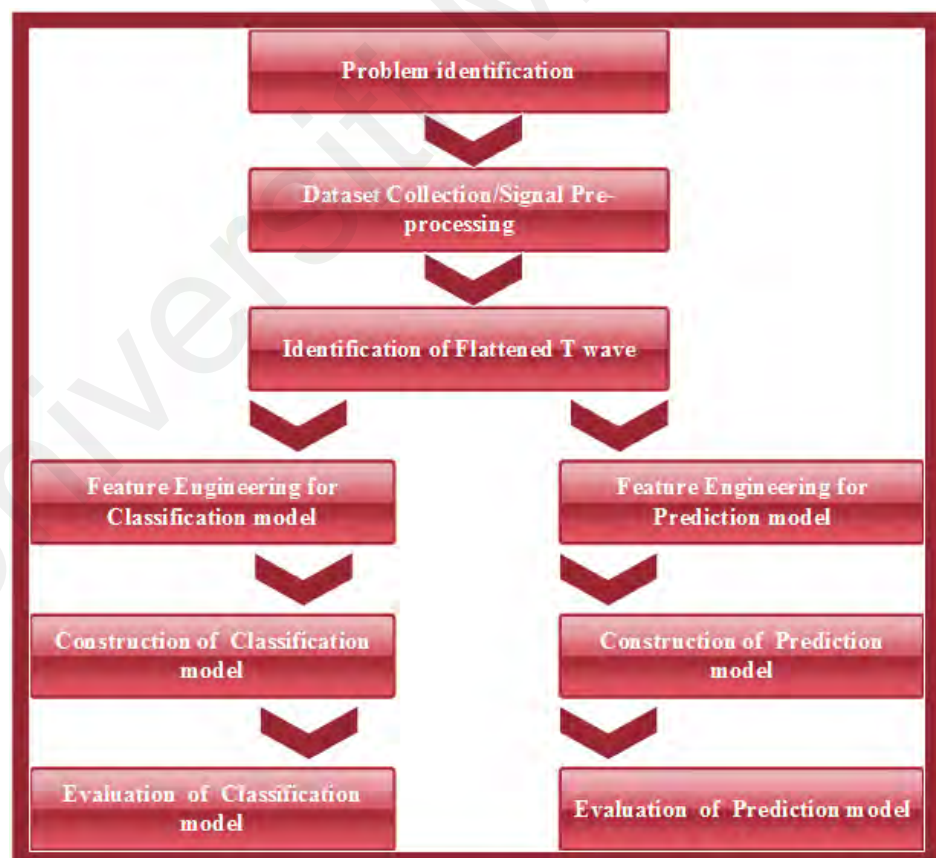


Figure 3.1. Detailed structure of research methodology and design

3.2 ECG Dataset Collection:

The surveyed literature shows that normally, the ECG records were collected by using the datasets of MIT-BIH and PTB that are publicly available. For this research study, we have used three datasets that contain a different nature of cardiac records or subjects. Two of these datasets are publicly available for research purposes (MIT-BIH dataset and PTB dataset). Along with these two public datasets, the third dataset we have used is the one from the University of Malaya Medical Center (UMMC). This exclusive dataset was collected after the ethical approval of the medical center of the university. The characteristics of different ECG subjects and details of datasets are summarized in a tabular form in Table 3.1 that are used in this research study. This Table 3.1 discusses the summary of ECG subject's nature, elected subjects that are used in proposed models, size of datasets in context of total number of subjects in each dataset, number of input channels which are used for ECG signal acquisition, dataset collection resource and availability. According to Table 3.1, 10 subjects of flattened T wave (MI) are used in this research for recognition of features pattern matching with other T wave anomalies through proposed models. Different clinical studies supported that existence of flattened T wave cases in MI situation of non-specific ST-T changes (*nsst-t*) are rare as discussed in Section 2.4.3 of Chapter 2 (Ishikawa et al., 2018; K. B. Lin, Shofer, McCusker, Meshberg, & Hollander, 2008; W. Lin, Teo, & Poh, 2013; Schillaci et al., 2004). Moreover, the existence of only 6 atrial fibrillation (*afib*) and 20 normal sinus rhythm (*nsr*) out of 306 total ECG subjects of UMMC are completely used in this research. Similarly, the existence of all ST-T changes (MI), T-wave alternans (MI), *afib* and *nsr* subjects of public datasets (MIT-BIH and PTB) are completely utilized in the research. All elected subjects of Table 3.1 are utilized for features pattern matching operations in proposed models that discussed in Chapter 5 and Chapter 6.

Table 3.1: ECG Streams fetching resources

<i>ECG Signal nature</i>	<i>Elected subjects</i>	<i>Dataset size (total Subjects)</i>	<i>No .of Channels</i>	<i>Dataset Availability</i>	<i>Resource of dataset</i>
Flatten T wave(MI)	10	306	2 Input Channels	Exclusive	UMMC
Atrial Fibrillation(afib)	6	306	2 Input Channels	Exclusive	UMMC
Normal Sinus Rhythm(nsr)	20	306	2 Input Channels	Exclusive	UMMC
ST-T Changes (MI)	10	79	2 Input Channels	Public	MIT-BIH (stdb)
T-wave Alternans(MI)	10	148 (MI)	14 Input Channels	Public	PTB (ptbdb)
Atrial Fibrillation(afib)	10	25	2 Input Channels	Public	MIT-BIH (afdb)
Normal Sinus Rhythm(nsr)	10	18	2 Input Channels	Public	MIT-BIH (nsrdb)

**UMMC(<https://www.ummc.edu.my>),

** MIT-BIH(stdb) (<https://physionet.org/physiobank/database/stdb/>)

** PTB (ptbdb) (<https://physionet.org/physiobank/database/ptbdb/>)

** MIT-BIH (afdb) (<https://physionet.org/physiobank/database/afdb/>)

** MIT-BIH(nsrdb) (<https://physionet.org/physiobank/database/nsrdb/>)

3.3 Data Preprocessing

The most significant step in the analytics of different ECG signals is to prepare the signal correctly for further operations. Reduction of different noises in the signal is the key for detection of different peaks in a signal and magnitude of the different features that will be discussed in next section. Raw form of ECG signals are of not much use for exploiting any information and also signals corrupted due to the occurrence different noises render the information useless. Therefore, preprocessing methods are used for refining and clarifying the ECG signal. The following preprocessing methods were applied on the ECG signals before moving over to the feature extraction phase.

- Segmenting the ECG signal data with the sliding window method by adjusting the window size 0.2 seconds(K. I. Minami, Nakajima, & Toyoshima, 1999; K. Minami, Nakajima, & Toyoshima, 1997).
- Induction of the basic filtration methods on ECG signal; such methods reduces the different low frequency and high frequency components.

3.4 Proposed Effective R peaks detection algorithm:

This section highlights the pre-primary step before the execution of feature extraction operations. After the preprocessing methods have been applied on the ECG signal, the next step is to highlight the R peaks of the signal. This research contributes to the existing body of knowledge a novel and efficient R peaks detection algorithm that works on globally accessible datasets. The main theme of the effective R peaks detection algorithm is reflected in the form of fixed threshold points for measurement of the operational efficiency. These threshold points work for accuracy calculation with regard to the ratio of accurate detection (RAD) of R peaks, sensitivity (S_e), positive prediction index (P_+) of T_{on} by detected R peaks, and error rate calculation (E).

3.4.1 Identification model of flatten T wave

The detected R peaks through proposed effective R peaks detection algorithm are further used for the purpose of identification of *flattened T wave*. A deterministic method is used for identification of the *flattened T wave* features with the help of T-Wave Alternans (TWA) algorithm.

This section on the identification model discusses the determination of T-onset (T_{on}) feature and T-offset (T_{off}) feature of the *flattened T wave* which will be further helpful in the deep deterministic learning (DDL) in the second phase of this research. In the context of attaining a solution to the problem, the first stage is finding the T_{on} features of the *flattened T wave* by considering the ten different subjects of the *flattened T wave* (using UMMC dataset). Such finding constitutes a first step toward knowledge extraction of the *flattened T wave*. The figure 3.2 on next page highlights the identification model for T_{on} feature of the *flattened T wave* subjects. In the first part of the identification model is a representation of marking the T_{on} feature of the *flattened T wave* by using the R peak analysis and then state-of-the-art TWA detection algorithm by

considering the R peak as a fiducial point. The second part of the identification model is the derivation of T_{off} feature of the *flattened T wave* by using the T_{on} feature of the *flattened T wave* subjects. The equation 2.1 in Chapter 2 is a core part of our model that is adopted from TWA detection algorithm (Blanco-Velasco et al., 2017)

According to the flow of first part of the identification model, the segmentation process is applied to ten different subjects of ECG data (the *flattened T wave*) which splits data lead wise, into lead II and lead III. Raw Data of these two leads are further helpful for analysis after pre-processing for identification of the different features of *flattened T wave*. Afterwards, noise filtration is achieved by using the notch filter for removal of low-frequency and high frequency components and discovering the peak values. These highlighted peak values are further investigated by a proposed effective R peak detection algorithm which deals with the detected R peak values along with the RR intervals.

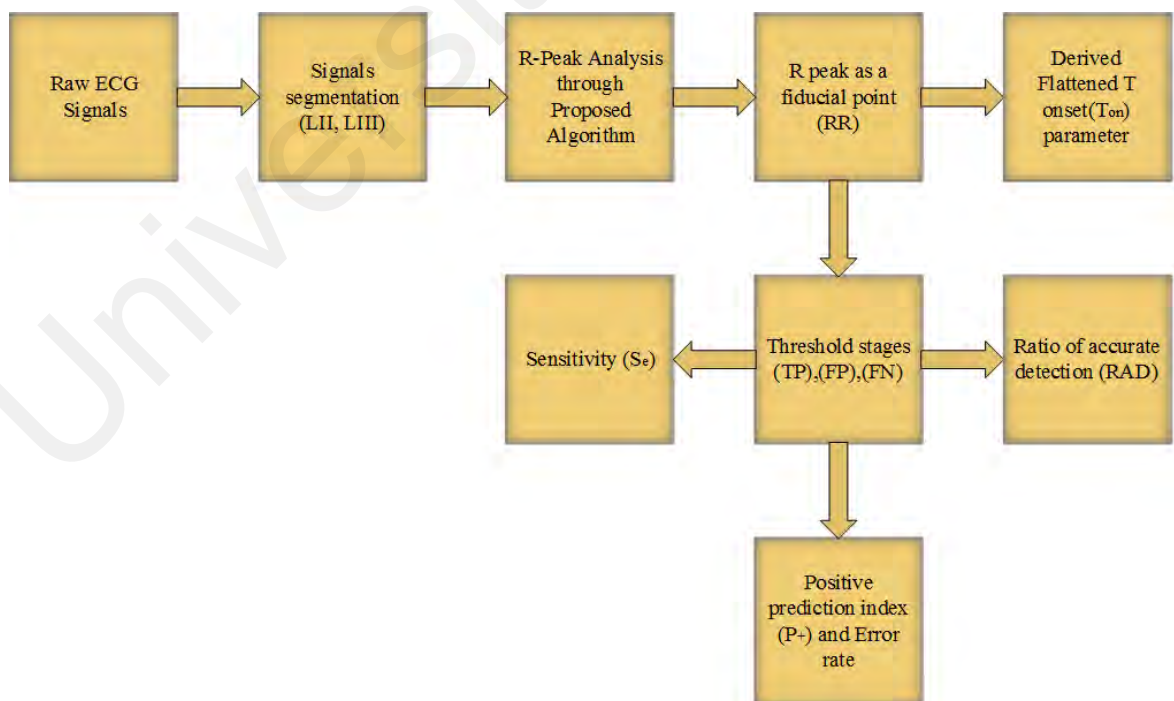


Figure 3.2. Work directions of Identification of T_{on} feature of Flattened T-wave

Derivation of these operational factors for tracing the T_{on} feature of the *flattened T wave* totally depends on the detected R peak values. Such derivation clearly, imposes the involvement of dependencies factor of the ECG features. The proposed deterministic technique uses ten different subjects of the *flattened T wave* of the UMMC dataset that is found useful for the subsequent proposed recognition method. By using such a deterministic method, we can derive the average value of T_{on} of the *flattened T wave* by the analysis of the T_{on} values of ten different subjects. First, this proposed method detects the number of R peaks in the filtered segmented signal of the ECG by using window filtration. In its second phase, this method highlights the maximum RR intervals and then finally uses the core part of TWA detection algorithm by considering the last RR interval. Such RR interval embeds equation 2.1(see subsection 2.4.1) for the derivation of T_{on} value. The implication of these phases works on both leads that are further helpful for comparative analysis. With the help of such analysis further qualitative improvement will also be possible in future.

3.5 Feature Engineering

In the execution stage of the proposed effective R-peak detection algorithm, seven different time domain features are extracted on each dataset. These are mean heart rate variability ($mhrv$), root mean square value of RR intervals ($rr-rms$), standard deviation of RR intervals ($sddn$), the number of RR intervals greater than fifty ($nnrr$), mean T-onset value (mt_{on}), mean T-offset value (mt_{off}), and mean T-peak value (mt_{pk}). These extracted features are further used in proposed deep deterministic learning (DDL) and model driven deep deterministic learning (MDDDL).

The extracted features through extensive feature engineering play a vital role for recognition of the heart's condition to determine if there is any morbidity or not. A list of features with their abbreviations is presented in Table 3.2 which are used in this

thesis. Existing studies also supported the features of Table 3.2 for identification the different ECG anomalies which plays a vital role in recognition of *afib* and MI cases(Arif, Malagore, & Afsar, 2012; Czabanski et al., 2020; Mathews, Kambhamettu, & Barner, 2018; Yaghouby, Ayatollahi, Bahramali, & Yaghouby, 2012)

Table 3.2: ECG features used in this research study

Abbreviations	Description
<i>hrv</i>	Mean of heart rate
<i>sddn</i>	Standard deviation of RR interval
<i>rmsrr</i>	Root mean square difference of RR interval
<i>nnrr</i>	Number of RR intervals more than 50
<i>hr</i>	Heart rate
<i>mtoff</i>	Mean value of T-wave offset
<i>mton</i>	Mean value of T-wave onset
<i>mtpk</i>	Mean value of T-wave peak

3.5.1 The Proposed deep deterministic learning model:

The first contribution of this research is to design the pattern recognition of different cardiac diseases (especially the *flattened T wave*) and arrhythmias with the help of the exclusive dataset from UMMC and the public dataset from MIT-BIH. Our research defines a deep deterministic learning (DDL) model for recognizing the patterns of different cardiac problems. The starting point of DDL is just the execution of the proposed effective R peak detection algorithm that works on different ECG data streams (UMMC and MIT-BIH). This deterministic model is a three-stage process that works separately on two datasets. Features fusion is performed in the last stage for matching the patterns of the two datasets with the help of feature engineering. The role of the proposed effective R-peak detection algorithm is to extract the best possible time domain features for recognizing patterns with the help of a finely tuned ANN and deliver the different features aggregated cases for further features fusion processes (data fusion). This research mainly contributes the significant value of Non Specific ST-T

Changes (*nsst-t*) through patterns matching of the *flattened T waves* with *ST-Segment* changes. The overall operational processes of DDL will be discussed in Chapter 5.

3.5.2 The Proposed Model-Driven Deep Deterministic learning model:

The second major contribution of this study deals with the predictive analytics of different cause of MI by using the public dataset from PTB database and exclusive dataset from UMMC database. Our research claims to develop and present the novel classification method in the form of Model driven deep deterministic learning (MDDDL) for the predicative classification of the *flattened T wave*. In MDDDL, the theme and concept of DDL is used for the predictive classification of the *flattened T wave* with the help of fusion activities. In MDDDL, the effective R peaks detection algorithms are executed on both datasets and then with the help of these detected R peaks, the feature extraction steps are performed. The seven extracted features (*rr-rms*, *sddnn*, *nn50*, *hrv*, *mt_{ons}*, *mt_{off}* and *mt_{pk}*) are categorized in two groups; one is the traditional features combination and the other is new features combination. Through these extracted features, the next core part of MDDDL is the fusion activities part which is performed in the form of four fusion processes. Additionally, these four fusion processes are operated in two different formats of settings. The complete MDDDL experimental operational activities will be presented in Chapter 6.

3.6 Construction of the DDL Classification Model

Computer Assisted Design (CAD) experts in the ECG analytics domain continuously work for developing robust and accurate recognition models for detection of different cardiac diseases. Accurate ECG signal analysis can improve and save human life in many cases, from diagnosing diseases among cardiac patients to better managing the lifestyles of diabetic patients. Abnormalities in the heart's activities lead to different cardiac diseases and arrhythmia. However, some cardiac diseases like different

situations of myocardial infarction (MI) and atrial fibrillation (*afib*), require special attention due to the risk involved and their direct impact on human life. Recognition of the *flattened T wave* cases (especially MI type of cases) and the extent to which these cases are similar to the other ST segment and T wave anomalies can be performed through novel methods.

This research presents a novel contribution to classify the *flattened T wave* of MI and *afib*. To this end, the formation of a novel model in the form of DDL is proposed that works by combining predefined heart activities with fused datasets. In this research, two different datasets are used, namely, the dataset from MIT-BIH, which is publicly available, and the dataset from UMMC which is exclusively obtained for the purposes of this research. Under the DDL classification model, the predefined activities of the heart are initiated on each individual dataset to recognize the patterns between the *ST-T change* and the *flattened T wave* cases and the fusion activities are used to merge both datasets in a manner that delivers the most accurate pattern recognition results. The proposed DDL model is a systematic stage-wise methodology that relies on the accurate detection of *R* peaks in the ECG signals, time domain features of the ECG signals, and the fine tune-up of artificial neural networks. The proposed pattern recognition model is a significant contribution to the diagnosis of special cases of MI (*the flattened T wave*) that relates to the *nsst-t*. Additionally, this theme of pattern recognition model is applicable for further predictive classification of cardiac diseases by using the different customized neural network models.

3.7 Evaluation of DDL Classification Model

The performance of DDL classification model is evaluated through different evaluation schemas that include self-evaluation of DDL, evaluation through comparison with state-of-the-art classification models, and evaluation through deep features critical

analysis. The self-evaluation scheme includes the performance analysis of the proposed effective R peaks detection algorithm and then comparing the effective R peaks detection algorithm with state-of-the-art R peaks detection algorithms (such comparison will be discussed in complete detail in Chapter 4). Under the next evaluation scheme, the whole deep deterministic learning model is evaluated through efficiency metrics and global acceptance. Such metrics belong to the efficiency gauges that include the performance, epoch value, time duration, and error ratio. With the help of these efficiency gauges, the operational activities of DDL are further evaluated on two different datasets that reflect the concept of global acceptance. According to global acceptance, the same operational procedures of DDL are applied in two different datasets (the exclusive dataset and the public dataset).

The most significant schema of evaluation of DDL is its comparison with state-of-the-art classification models that include the typical feature engineering methods, automated diagnosis of cardiac diseases, and automated detection of *MI*. The last evaluation schema of the performance of DDL model is the deep features critical analysis. The performance of DDL model is observed and analyzed by using different features combination in the DDL model for operational investigations. Such features combination includes the traditional time domain features as well as two new derived time domain features (mt_{on} and mt_{off}).

3.8 Construction of MDDDL Predictive Classification Model

Early prediction of such MI cases that have no past record is a challenging task, especially the classification of flattened anomalies. This research study delivers the second major novel contribution in terms of predictive classification of the *flattened T wave*. To this end, the study proposes the MDDDL Predictive Classification Model, that works for general recognition and predictive classification of different cardiac diseases

under the rubric of DDL and theme of model driven deep learning (MDDL). In the MDDDL model, two different datasets are used for the operational activities, namely, the dataset from PTB which is publically available, and the dataset from UMMC that is obtained exclusively for the purpose of this research. The MDDDL model presents the systematic behavior in terms of recognition the extracted features patterns between *T wave alternans* and the *flattened T wave* subjects and then merges both the datasets by way of the fusion activities and the pre-defined conditions. Furthermore, the proposed MDDDL model is a systematic and highly accurate methodology that relies on the architecture of DDL. Empirical methods are adopted in the MDDDL evaluation in terms of implementation of the different features combination and comparison of the MDDDL model with state-of-the-art methods. The complete operational investigations and architectural aspects of the MDDDL model will be covered in Chapter 6.

3.9 Evaluation of MDDDL Predicative Classification Model

The evaluation schema of DDL is replicated for the evaluation of the MDDDL model. The MDDDL predicative classification model is evaluated thorough performance measures, which include the efficiency gauges of performance, time, epoch values, and error ratio. Moreover, the accuracy ratio of this prediction model is also evaluated through linear regression and then by comparison with the traditional prediction models. The most significant part of the evaluation of the proposed MDDDL model is through comparison with different traditional machine learning regression models which include state-of-the-art predicative classification models of MI.

Finally, an empirical method is adopted to evaluate the proposed MDDDL predicative classification model through features selection analysis performed on the basis of traditional feature combination and new derived feature combination. Through

this analysis, the time or computational complexity factor is better analyzed and delivers some useful future directions.

3.10 Conclusion:

This chapter covered the research methodology used to design and implement the recognition and predictive classification models of different high priority cardiac diseases, especially the *flattened T wave* cases of *MI*. Here, the different feature engineering methods were discussed in detail along with the datasets used. This chapter also offered a brief discussion of the proposed recognition and prediction models and provided the evaluation schemas of the proposed models through defined efficiency gauges, feature selection analysis and comparison with state-of-the-art methods. The specific details of the unique feature engineering techniques and their contributions are discussed in Chapter 4, Chapter 5, and Chapter 6.

CHAPTER 4: PROPOSED DETERMINISTIC TECHNIQUE FOR IDENTIFYING FLATTENED T-WAVE

4.1 Introduction

The proposed research methodology in Chapter 3 delivers the systematic approach for the identification of *flattened T wave* subjects. Various studies in Chapter 2 are reported that employ the different methods to classify and predict the different cardiac diseases. However, it's observed in traditional methods that the element of uncertainties removal are still a pending work in recognition and predictive classification of cardiac diseases, such uncertainties are reflected in terms of recognition of the unseen situations of Myocardial Infarction (MI) cases (*flattened anomalies*). This chapter presents the deterministic way to find the T-onset (T_{on}) feature of different *flattened T wave* subjects with the help of T-wave Alternans (TWA) algorithm, such derivation is an initial and crucial step for diagnostic purposes in unique situation of MI. Section 4.2 discussed the technical aspects of proposed deterministic technique for derivation the T_{on} of *flattened T wave*. Additionally, section 4.3 presents the experimental model for execution of this proposed deterministic technique. Section 4.4 covers the results of experimental model after the execution of proposed deterministic technique. Section 4.5 discusses the findings of experimental results in context of lead wise comparative analytics. Furthermore, subsection 4.5.1 presents the comparison of proposed effective R peaks detection algorithm with state-of-the-art R peaks detection algorithms. Finally, section 4.6 concludes this chapter with discussion of a significant contribution of this proposed the deterministic technique for derivation of T_{on} feature of the *flattened T wave* and further, discuss how these findings will be valuable for recognition and predictive classification of *flatten T wave*.

4.2 Deterministic Method for Flattened T-wave

Literature constantly reported the significant values of feature based solution of classification of the abnormalities in ECG. Analysis of beat-to-beat, heart rate variability, detection of Atrial Fibrillation (*afib*), detection of Premature Ventricular Contraction (*PVC*) and detection of MI are dependent on such feature based solutions (Gothwal et al., 2011; Gutiérrez-Gnecchi et al., 2017; Nikan, Gwady-Sridhar, & Bauer, 2017). The Features of amplitude, start time, end time, and time duration of different ECG signals always become handy for the diagnostic purpose of various diseases.

MI affected patient require special attention for the diagnostic purposes. Despite the significance/importance of the diagnostic purposes of MI affected patients, some special cases of MI in terms of *flattened* anomalies are still a pending work as discussed in Chapter 2. In Chapter 3, a complete methodology schema of recognition and predictive classification of different high priority cardiac diseases especially recognition of *flattened T wave* through features patterns matching with *ST-T changes* and *T wave alternans* cases. Therefore, before recognition of *flattened T wave*, at first the deterministic way is adopted for derivation the T_{on} feature of *flattened T wave* as discussed in Chapter 3.

This Chapter presents the execution of defined operational execution in terms of experimental design and model for the derivation of T_{on} feature of *flattened T wave* in deterministic way. Thus, the derivations of T_{on} feature for ten subjects of *flattened T wave* are derived through deterministic way through adopting central part of TWA algorithm. In addition, section 4.3 covers the complete deterministic experimental model for T_{on} feature for 10 subjects of the *flattened T wave*, section 4.4 highlights the findings of this experimental model and finally, section 4.5 covers the evaluation scheme of this deterministic method

4.3 Experimental Model

This section covers the first contribution of this study through a deterministic way in terms of finding the T_{on} feature of the *flattened T wave* that is helpful in diagnostic purposes of MI affected patients. According to this research module as discussed in Chapter 3, firstly deploy the segmentation phase on ECG signals and then apply the filtration process on the signals for removal of unnecessary components in the signal. Afterward, the detection of R peaks values and RR intervals through deployment of proposed effective R peaks detection algorithm, in next phase, the findings of detected R peaks and RR intervals are embedded with the core part of TWA algorithm. These two biphasic operations are executed individually on ten different subjects of *flattened T wave* and get the T_{on} feature of *flattened T wave*. Figure 4.1 highlights the summary model of derivation of T_{on} feature.

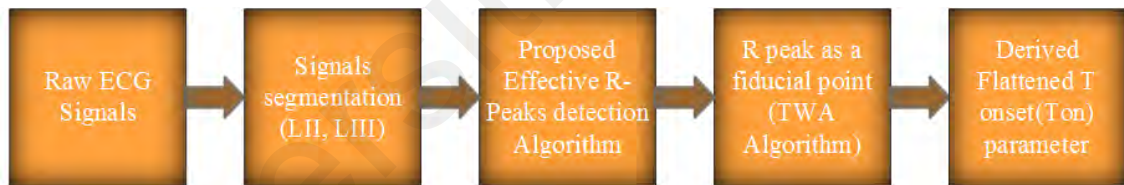


Figure 4.1. Block Representation of Proposed Deterministic Method

According to the flow of above model in figure 4.1, the segmentation process is applied to ten different subjects of ECG data (*flattened T wave*) which splits data into lead wise, *lead II* and *lead III*. Table 4.1 represents the demographic characteristics of these ten different subjects as different existing studies use the demography of UMMC dataset for different medical analysis (Alex et al., 2018; Goh, Ng, Kamaruzzaman, Chin, & Tan, 2017; Tan et al., 2019). Table 4.1 covers the gender info, adult aged patients above then 55 years and ethnic group which represents the combination of Malay, Indian, and Chinese patients.

Table 4.1: Demographic characteristics of flattened T wave subjects

Sr	M_Tag_patients	Sex (M/F)	Adult Age 55+ (y/n)	I_C	QRS (ms)	SF (Hz)	QT_I	RR (sec)	Noise	Ethnic Group patients
1	ecg10233	Female	y	2	119	250	-0.62	0.04	bn, pn	yes
2	ecg10235	Female	y	2	126	250	-0.43	0.01	bn, pn	yes
3	ecg10236	Female	y	2	138	250	-0.08	0.06	bn, pn	yes
4	ecg09426	Female	y	2	107	250	-0.26	0.05	bn, pn	yes
5	ecg1002	Male	y	2	126	250	-0.09	0.06	bn, pn	yes
6	ecg09934	Female	y	2	113	250	-0.21	0.04	bn, pn	yes
7	ecg09847	Male	y	2	132	250	-0.14	0.04	bn, pn	yes
8	ecg09824	Male	y	2	107	250	-0.04	0.04	bn, pn	yes
9	ecg09154	Female	y	2	100	250	-0.03	0.05	bn, pn	yes
10	ecg09470	Female	y	2	113	250	-0.24	0.09	bn, pn	yes

** I_C(Number of input Channels), QRS(QRS complex duration),QT_I(QT interval duration), RR(RR interval) SF(Sample frequency), Baseline Noise (bn), Power Noise (pn), Ethnic Group (Malay, Indian, Chinese)

Onwards implication of the noise filtration by using the notch filtration for removal of unnecessary components in terms of low and high frequency components and then dominate the peak values. These highlighted peak values are further investigated by a proposed effective R peaks algorithm that highlight the detected R peak points (include threshold points of R peaks) along with the RR intervals. Furthermore, the second part of the algorithm is to fix the threshold points for measurement of the operational efficiency of this algorithm. These threshold points work for accuracy calculation namely, the ratio of accurate detection (RAD) of R peaks, Sensitivity (S_e), Positive prediction index (P_+) of T_{on} through detected R peaks and error rate calculation (E). Additionally, after the execution of the proposed algorithm, at the final step of this proposed method is taking the R peak as the fiducial point and insert the final derived value of RR interval (RR_i) in equation 2.1 as discussed in Chapter 2

Moreover, in the context of operational efficiency of this proposed algorithm, the effective R peaks detection method is employed via a inclusion of fix threshold points. Three threshold levels of R peaks are assigned with fixed ranges employed in proposed

effective R peaks detection algorithm. Additionally, true positive detected R peak (tp), true negative detected R peak (tn), false positive detected R peak (fp), and false negative detected R peak (fn) are the threshold points of this proposed algorithm. Usage of below equations 4.1 to 4.4 regarding measurement of the operational efficiency of proposed algorithm under the consideration of these threshold points

$$S_e = tp / (tp + fn) * 100 \quad (4.1)$$

$$Sum = tp + fp + fn$$

$$RAD = tp / (Sum) * 100 \quad (4.2)$$

$$P_+ = tp / (tp + fn) * 100 \quad (4.3)$$

$$E = (fp + fn) / (tp + fn) * 100 \quad (4.4)$$

These above from Equation 4.1 to Equation 4.4 works for the derivation of sensitivity, the ratio of accurate detection, positive prediction index and error rate or ratio. Next page algorithmic model is clearly defined showing the systematic flow of the proposed effective R peak detection algorithm. The step1 of the algorithm defines; a particular ECG signal is loaded with a frequency of 250 Hz and adjusting the window size. Step 2 is the filtration phase, which filters the signal by applying a notch filter as well as wavelet filtration to remove different kinds of noises. Step 3 is the segmentation phase by that delivered useful signal information. After segmentation, the signals in the pre-defined setting are deployed in Step 4 by using the guidelines of Pan Thompkins QRS detection (Pan & Willis, 1985). Here, the threshold point is defined for identification of R peaks in the signal. Step 5 is the peak detection phase, which is performed whenever signals cross the threshold value representing the R peak. Finally, four fixed threshold points are set as tuning parameters and delivered the efficient results.

Algorithm: Proposed effective R peak detection algorithm

Step I: ECG signal loading and adjust window size

Load the ECG record, set the default frequency(fs) and window size(w) is 0.2sec

1. **INPUT:** $ecg = load('signal');$
2. **SET:** $fs = 250;$
3. $VA = length(ecg);$
4. $tim = [0:VA-1]/fs;$
5. **SET:** $w = 25/(fs/2);$
6. $bw = w$

Step II: Signal filtration and Wavelet Transformation

Apply a notch filter ($FILT$) for the removal of noisy components in signal and wavelet implementation (WI) to increase the performance of peak detection

7. **FILT:** $[num, den] = iirnotch(w, bw);$
8. $ecg_notch = filter(num, den, ecg);$
9. **WI:** $[n, o] = wavedec(ecg_notch, 10, 'db6');$
10. $g = wrcoef('a', n, o, 'db6', 8);$
11. $ecg_wave = ecg_notch - g;$
12. $ecg_smooth = smooth(ecg_wave);$

Step III: Signal Segmentation

After filtration step, signal is segmented.

13. **SET:** $Seg = length(ecg_smooth);$
14. $t1 = (0:Seg-1)/fs;$

Step IV: Pre-defined setting

Apply a pre-defined setting for peak detection by using the guidelines of the Pan Thompkins algorithm (By finding threshold (th) and loop initializing, with all values as zero in the array) % loop initializing, with all values as zero in the array

15. **SET:** $VAR = ecg_smooth; j = []; time = 0;$
16. $th = 0.45 * max(VAR);$

Step V: Peak detection

Implement the peak detection steps for highlighting the R_peaks through *filtered signal*. Condition, i should be greater than previous, next, and threshold point;

17. **FOR:** $i = 2: length\ of\ Seg - 1$
18. **IF:** $((VAR(i) > VAR(i+1)) \& \& (VAR(i) > VAR(i-1)) \& \& (VAR(i) > th))$
19. $j(i) = VAR(i);$
20. $time(i) = [i-1]/250;$
21. **END**
22. **END**

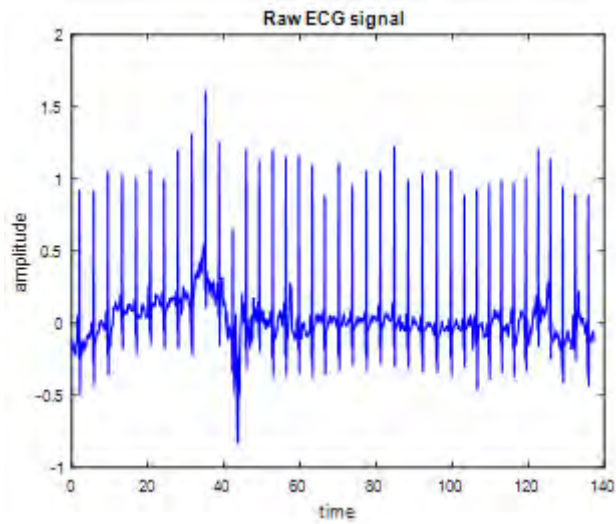
Efficiency Tuning Parameters definition

Next phase is set efficiency tuning parameters through fixed threshold points with statistical work namely, detection of true positive R peaks (0.3 to 0.4), detection of true negative R peaks (4.5 to 5), detection of false negative R peaks (11 to 12), detection of false positive R peaks (9.5 to 10.5)

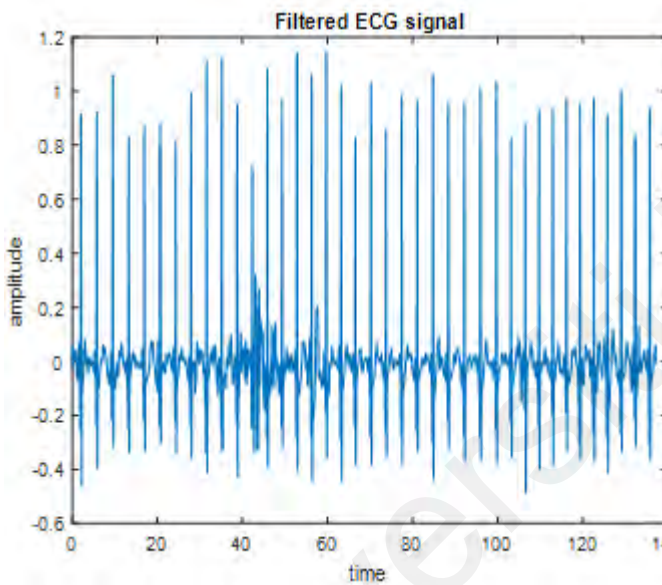
According to effective R Peak detection algorithm, the results of this proposed algorithm rely on the novel fixed threshold points (efficiency tuning parameters) namely; tp , tn , fp , and fn . These fixed threshold points are associated with window size ($w=0.2\text{sec}$) and frequency ($fs=250\text{hz}$) of the signal. Literature supported that existing R peaks detection algorithms are also used such association with different threshold points in defined true R peaks detection range(0.2mv to 1.8mv) namely, variable threshold points and energy threshold points(Kaur, Agarwal, Agarwal, & Kumar, 2019; Liu et al., 2014; J. S. Park et al., 2017). Moreover, adjustment of fixed threshold points in proposed algorithm are evaluated through datasets of UMMC, MIT-BIH and PTB in Chapter 5 and Chapter 6. The findings of effective R-peaks detection algorithm in Chapter 5 (see Section 5.4) and Chapter 6 (see Section 6.4) clearly highlight the global acceptance of this proposed R-peak detection algorithm

4.4 Results of Effective R –peaks Detection Algorithm

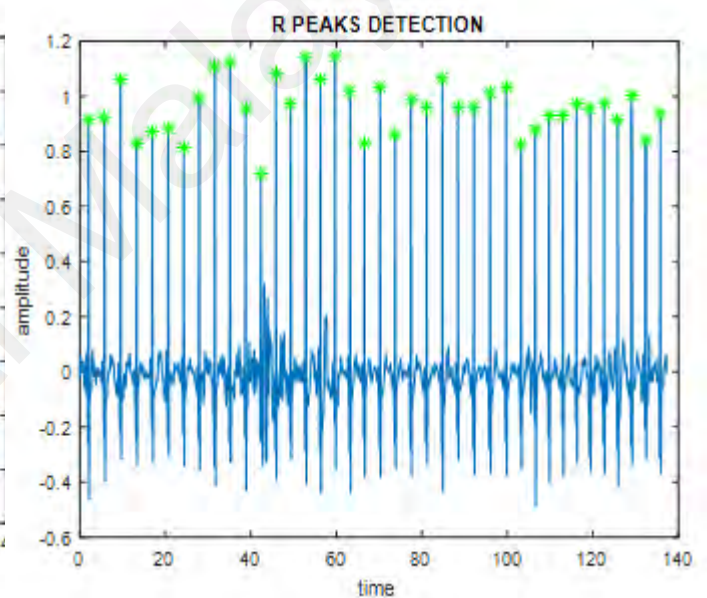
Identifying the T_{on} feature of the *flattened T wave* is the first step towards highlighting the exact nature of *flattened T wave*. In this deterministic approach raw signals are splitted into lead wise (*lead II* and *lead III* for maximum feature extraction) and then apply the notch filter for removal of noisy components in the signal by adjusting the frequency generation $fs=250\text{Hz}$. After the removal of noisy components then set the three threshold points as highlighted in proposed algorithm of R peaks detection for determining the tp , fp , fn . Figure 4.2 highlighted the processed flattened T wave subject in three different phases namely, (a) raw ECG signal which shows baseline and power noise factor, (b) such part represents the filtered ECG signal, and (c) highlight the detected R peaks through proposed algorithm.



(a) Raw ECG signal of flattened T wave



(b) Filtered ECG signal of flattened T wave



(c) Detected R-Peaks in flattened T wave

Figure 4.2. Operated flattened T wave signal

Furthermore, implementation of this efficient approach on ten different M_Tag_patient records which have *flattened T wave*, and summarized the results of T_{on} values, number of detected R peaks and last part of the RR interval (RR_i) in Table 4.2

Table 4.2: Findings of different parameters of ten flattened T wave subjects

Sr	M_Tag_patients	Segmentation	T-onset (milli sec)	T-onset (sec)	Detected R peaks	Detected RR interval	RRi
1	ecg10233	LII	40.33	0.04033	345	344	0.062

		LIII	40.36	0.04036	2836	2835	0.075
2	ecg10235	LII	40.35	0.04035	144	143	0.070
		LIII	41.16	0.04116	349	348	0.764
3	ecg10236	LII	40.61	0.04061	44	43	0.923
		LIII	41.27	0.0412	222	221	0.213
4	ecg09426	LII	40.34	0.04034	235	234	0.053
		LIII	40.3	0.0403	3455	3454	0.069
5	ecg1002	LII	40.47	0.0407	362	361	0.126
		LIII	40.47	0.0407	362	361	0.126
6	ecg09934	LII	41.14	0.04114	65	64	0.121
		LIII	40.46	0.04046	379	378	0.739
7	ecg09847	LII	40.37	0.04037	245	244	0.05
		LIII	40.29	0.04029	3012	3011	0.081
8	ecg09824	LII	40.3	0.0403	339	338	0.098
		LIII	40.41	0.04041	1632	1631	0.052
9	ecg09154	LII	40.34	0.0403	187	186	0.095
		LIII	40.4	0.0404	2773	2772	0.066
10	ecg09470	LII	40.45	0.0404	220	219	0.983
		LIII	40.31	0.041	232	231	0.118

As discussed in above experimental design section 4.3, the second part of effective R peaks detection algorithm is a calculation of threshold points for measurement of sensitivity, the ratio of accurate detection, positive prediction index, and error rate. With this concern, table 4.2 is a complete representation of detected R peaks and RR intervals through proposed effective R peaks detection algorithm. Afterward, next phase is to highlight the mean values of T_{on} values, sensitivity, and the ratio of accurate detection, positive prediction index and error rate of *lead II* and *lead III*. In ECG analytics domain, such deterministic method is an extensive method to exploit the features of the *flattened T wave* in perspective of feature analysis. This exploitation may require some deep comparative results between two leads (*lead II* and *lead III*). Furthermore, the findings of Table 4.2 are handy for comparative analysis between two leads.

4.4.2 Result of both Leads

Let's consider the *lead II* for deriving mean value T_{on} of *flattened T wave* in terms of milliseconds and seconds. In below equations 4.5 to 4.9, N represents the ten different subjects of *flattened T wave* (N=10).

$$Lead II T (T_{on}) = 1/N \sum_{i=1}^N T_{on}^i \quad (4.5)$$

Usage the results of Table 4.2, Equation 4.5 is implemented on T_{on} values of *lead II*. Get the result in the context of milliseconds and seconds, $lead II T (T_{on}) = 40.47$ ms and $lead II T (T_{on}) = 0.04097$ sec. The same process is executed on Sensitivity (S_e), Ratio of Accurate Detection (RAD), Positive prediction index (P_+) and Error rate (E) by using the results of table 4.2.

$$Lead II(S_e) = 1/N \sum_{i=1}^N S_e^i \quad (4.6)$$

Equation 4.6 represents the mean summation of ten sensitivity values

$$Lead II (RAD) = 1/N \sum_{i=1}^N \tau^i \quad (4.7)$$

Similarly, in above Equation 4.7, τ represents the mean ratio of accurate detection (RAD) of ten *flattened* subjects

$$Lead II (P_+) = 1/N \sum_{i=1}^N P_+^i \quad (4.8)$$

Equation 4.8 shows the mean value of the positive prediction index.

$$Lead II (E) = 1/N \sum_{i=1}^N \eta^i \quad (4.9)$$

Showcase of error ratio in Equation 4.9 represents in the form of η

Extracted mean values from Equation 4.5 to Equation 4.9 are Sensitivity (S_e) =99.29%, Ratio Accurate Detection (RAD) =99.29%, Positive Prediction Index (P_+) = 100% and Error rate (E) =0.74%. Similarly, the replica scenario is imposed on *lead III* values as applied to finding the *lead II* means values. we get the value *Lead III T* (T_{on}) = 40.54 ms, *Lead III T* (T_{on}) =0.0406 sec. Mean values of Sensitivity (S_e), Ratio Accurate Detection (RAD), Positive Prediction index (P_+), and Error rate (E) are of *Lead III* are S_e =99.56% , RAD =99.56%, (P_+)= 100% and E = 0.428

. The proposed deterministic method is an initial step towards other features determination of *flattened T wave*. The operational activities of this method follow the core part of the TWA algorithm by taking the R peak as a fiducial point. Such operational process reflects the involvement of dependencies factor during the investigation of T_{on} features of *flattened T wave*. Moreover, before proceeding to the evaluation schema, at first discuss the comparative analytics between *lead II* and *lead III* in terms of findings the T_{on} features.

4.4.3 Comparative Analysis of Lead II and Lead III

Derivation of Mean values of features T_{on} and operation efficiency factors are highlighted in Table 4.3 for comparative analysis. The findings of difference between mean values of *lead II* and *lead III* is a further step towards the investigation. Table 4.4 represent the difference between *lead II* and *lead III* findings.

Table 4.3: Compative Summary of both leads Result.

T-onset Parameter and Efficiency factors	Lead wise Comparison	
	<i>Lead II</i>	<i>Lead III</i>
T_{on}	40.47 ms, 0.04097s	40.54ms, 0.0406s
S_e (%)	99.29	99.56
RAD (%)	99.29	99.56
P_+ (%)	100	100
<i>Error rate</i> (%)	0.74	0.428

These findings clearly reflect that error rate between two leads is negotiable but further operational qualitative improvements are highly desirable in the context of derivation of the other features of *flattened T wave*.

Table 4.4: Difference between lead II and lead III

Leads Combination	Tonset(ms)	T-onset(s)	Se (%)	RAD (%)	(P₊)(%)	E(%)
Lead II	40.47	0.04097	99.29	99.29	100	0.74
Lead III	40.54	0.0406	99.56	99.56	100	0.428
<i>Difference</i>	<i>0.07</i>	<i>0.00037</i>	<i>0.27</i>	<i>0.27</i>	<i>0</i>	<i>0.312</i>

4.5 Evaluation Schema

The above section of this deterministic method is the most striking section in terms of getting the fruitful results for extracting the T_{on} feature of *flattened T wave*. After the findings of T_{on} feature, next step is to evaluate the actions of proposed method. Furthermore, the formation of evaluation schema is designed in comparative way namely; compare the efficiency gages of proposed effective R peaks detection algorithm with state-of-the-art R peaks detection algorithms

4.5.1 State-of-the-art Comparison

To explore the effectiveness of proposed R Peaks detection algorithm, construct a summarized tabular form which delivers the efficiency gages comparison of proposed effective R peaks algorithm with state-of-the-art R peaks detection algorithms.

Table 4.5 presents the complete display unit of such comparison. Table 4.5 delivers the interesting stats in perspective of positive predictively gages. The ideal efficiency of proposed algorithm is helpful for feature analysis as well as recognition of different cardiac diseases.

Table 4.5: Comparison unit with state-of-the-art Algorithms

R Peaks Detection Algorithms Comparison						
<i>Reference</i>	<i>Algorithm name</i>	<i>year</i>	<i>RAD</i>	<i>Se</i>	<i>P+</i>	<i>Error</i>
(Yu et al., 2019)	ECG R-wave peaks marking with simultaneously recorded continuous blood pressure	2019	97.30%	96.70%	97.40%	2.70%
(Qin et al., 2017)	An Adaptive and Time-Efficient ECG R-Peak Detection Algorithm	2017	98.89%	99.39%	99.49%	1.11%
(Lee et al., 2018)	A Novel R Peak Detection Method for Mobile Environments	2018	99.73%	99.95%	99.78%	0.27%
(J. S. Park et al., 2017)	R Peak Detection Method Using Wavelet Transform and Modified Shannon Energy Envelope	2017	99.84%	99.93%	99.91%	0.16%
<i>Proposed Algorithm</i>	<i>Effective R peaks Detection algorithm</i>	<i>2019</i>	<i>99.56%</i>	<i>99.56%</i>	<i>100.00%</i>	<i>0.43%</i>

Evaluation through state-of-the-art algorithms compared with proposed effective R peaks detection are further handy for recognition and predictive classification of different cardiac diseases. Such recognition and predictive classification of different cardiac diseases will be presented in Chapter 5 and Chapter 6 respectively

4.6 Conclusion

In this chapter, a deterministic method was adopted for identification of the feature behavior of T_{on} flattened T wave which belongs to the special cases of MI. Additionally, the proposed effective R peaks detection algorithm is the core section of this Chapter 4 that discussed how the fix threshold points and TWA alternans algorithm played a critical role for derivation the T_{on} feature of flattened T wave. For operational investigations, exclusive dataset of UMMC is used for derivation the T_{on} feature of ten different subjects of flattened T wave. It was observed in operational activities of the

proposed deterministic method, the ratio of error between two leads are low. In same context, a high rate result of T_{on} feature after the operation activities indicates the bigger achievement in terms of future findings of other features of *flattened T wave*. A feature base solution of *flattened T wave* opens the doors for further factors determination which play a vital role in a diagnostic purpose of MI affected patients especially dealing with the situation of Non Specific ST-T Changes (*nsst-t*). Evaluation of this deterministic method manifests the high-efficiency factors after experimental investigations and comparison of proposed effective R peaks detection algorithm with state-of-the-art R peaks detection algorithms. Hence, the proposed deterministic method delivers the way to improve the recognition and predictive classification of different cardiac diseases especially patterns matching of *flattened T wave* with other anomalies of *T wave*. Therefore, such improvement of recognition and predictive classification of these cardiac diseases are discussed in Chapter 5 and Chapter 6 respectively.

CHAPTER 5: PROPOSED DEEP DETERMINISTIC LEARNING MODEL

5.1 Introduction

The pattern recognition of *flattened T wave* plays a vital role to initialize and identify the different situations in Non Specific ST-T Changes (*nsst-t*). In order to recognize the patterns from *flattened T wave*, the T-onset feature sets were used which were earlier computed in Chapter 4. This Chapter 5 presents an effective pattern recognition model to recognize different cardiac diseases which includes *flattened T wave*, *ST-T Changes* cases of Myocardial Infarction (*MI*), different cases of Atrial Fibrillation (*afib*), and normal situation of heart's condition in the form of Normal Sinus Rhythm (*nsr*). The proposed model deep deterministic learning (DDL) explores the *flattened T wave* relation with *nsst-t*. Furthermore, this proposed effective model follows the deterministic learning theory (Dong et al., 2018) for the features pattern recognition of *MI*, *afib*, and *nsr*. Conversely, the other state-of-the-art classification model, especially the deep learning models (such as CNN,RNN,DNN) infuse the high computational cost or complexity . A brief summary of major contributions in context of proposed DDL are stated in below:

- 1) Recognition of the features pattern of *afib*, *nsr*, *flattened T wave*, and *ST-T changes* from ECG signals are computed with high efficiency by using a trained Artificial Neural Network (*ANN*) along with a combination of feature selection method.
- 2) Pattern matching of *flattened T wave* is achieved through *ST-T changes* at over 98% accuracy with the help of a deterministic fusion operation.
- 3) Two new time domain features, namely, mean T-onset(mt_{on}) and mean T-offset(mt_{off}) are derived after extensive feature engineering.

- 4) Deep features analysis are performed by considering the accuracy, time and computational complexity factors.
- 5) Mathematical modeling and performance evaluation of the proposed DDL is performed in terms of accuracy and computational complexity..

Rest of this Chapter is structured in different sections. Section 5.2 presents the technical aspects of proposed DDL model. Furthermore, section 5.3 covers the experimental setup details which include the extraction of different features in sub section 5.3.1. Subsection 5.3.2 discusses the selection of feature combination in operations of DDL. Section 5.4 presents the results of experimental design in the form of different settings. Setting I and II shows the findings of UMMC and MIT-BIH datasets in context of different ECG data streams. Similarly, findings of Setting III reflect the fusion activities results. Setting IV discusses the summarized report of all stage wise results of DDL and comparison of DDL with different state-of-the-art methods. Furthermore, Section 5.5 discusses different features combination analysis that covers different sort of results especially the two new derived features with low complex results and some unique results. Section 5.6 highlights the performance evaluation of DDL via mathematical modeling. Subsections 5.6.1 and 5.6.2 shows the error calculation of feed forward propagation and backward propagation of neural network. Finally Section 5.7 shows the conclusion of this Chapter. .

5.2 Deep Deterministic Learning Model

The architecture of the DDL delivers the fruitful results in pattern recognition of cardiac diseases especially useful for diagnostic purposes. The logical frame of DDL is constructed by the help of two main paradigms, i.e., deep level features engineering and usage of well trained neural networks for the recognition of the different feature patterns of ECG signal. Figure 5.1 illustrates the complete DDL structure.

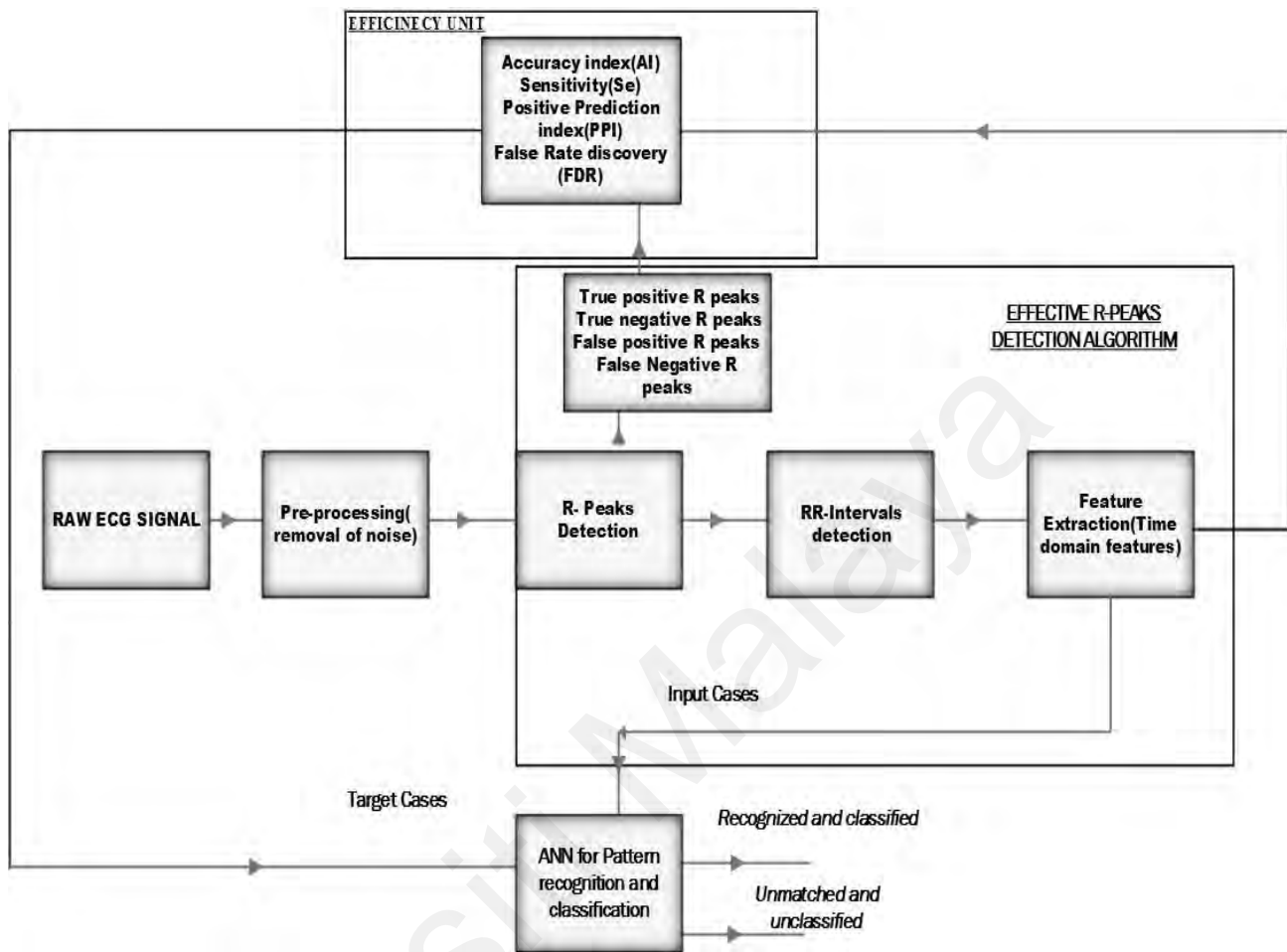


Figure 5.1. Systematic work flow of deep deterministic learning

The logical structure of the DDL considers the proposed effective algorithm of R peaks detection (see Table 4.1 in Chapter 4) that deliver the accurate results by deployment of fixed threshold points. For better understanding the workflow of DDL, a figure 5.2 presents the operational flow of the DDL model. At initial, pre-processing technique is deployed on raw ECG signals of each dataset for noise removal and time domain features extraction. By using the notch filter, remove the different sort of noises in the raw ECG signal. Removal of different noises plays a vital role for tracing the exact location of R peaks. According to figure 5.2 of DDL, the flow of different operations are systematic and highlight the multi-stage recognition technique. In recognition operations, standard levenberg-marquardt(LM) algorithm is used which take least

memory. Additionally, recognition process immediately stop in LM algorithm if the measure square error slightly increase (Lv et al., 2018) . Moreover, the operations of DDL are segmented into two parts, namely scenario one and scenario two. Scenario one deals with the different ECG subjects of UMMC dataset which is further classified into three levels, *Level A* contains the 10 *flattened T wave* subjects, *Level B* deals with the 20 *nsr subjects*, and *Level C* covers 6 *afib* subjects. Similarly, scenario two covers the different ECG subjects of MIT-BIH dataset which is also further segmented into three different levels, *Level A* deals with 10 *ST-T changes* subjects, *Level B* contains 10 *nsr subjects*, and *Level C* covers 10 *afib* subjects. Operational flow of DDL in figure 5.2 highlights the three different stages that are imposed on both scenarios (UMMC dataset and MIT-BIH dataset). At the beginning of DDL, Stage 1 belongs to the execution of proposed effective R –Peaks detection algorithm on each *level* of both scenarios, extracted seven different time domain features which plays a vital role in stage 2 and stage 3 of DDL. In stage 2 operations, these extracted features are arranged in six defined feature combinations (see Appendix A) and select best feature combination (*fc*) out of six features combination through the use of proposed feature selection algorithm (see Section 5.3.2). At *level A* of scenario one, the selected feature combination of mt_{on} and mt_{off} of *flattened T wave* are used in target and input classes, such classes are adjusted on the basis of efficiency gages of effective R peaks detection algorithm in previous Stage 1. The target class of *flattened T wave* subjects belongs to the most accurate results of detected R-peaks on the basis of efficiency gages of effective R peaks detection algorithm and selected mt_{on} , mt_{off} feature combination (see Section 4.3 for efficiency gages of effective R peaks detection algorithm). Similarly, the input class represents the *flattened T wave* subject which is the least accurate results of detected R peaks on the basis of efficiency gages of effective R peaks detection algorithm and selected feature combination (mt_{on} , mt_{off}). Moreover, both classes of

target and input are processed by a customized ANN that consume five hidden layers for self recognition the different feature patterns. Furthermore, the same operational investigations are applied on remaining *Level B* and *Level C* of scenario one. *Level B* contains the 20 different subjects of *nsr* which performs similar *Level A* operations, used the Stage 1 results of *Level B*. The findings of detected R peaks through efficiency gages of effective R-peaks algorithm along with selected feature combination (all seven extracted features) are partitioned into target and input classes. Similar to *Level A*, the target class and input class are adjusted, then processed with customized ANN with five hidden layers for self-recognizing the *nsr* features patterns. Like *Level A* and *Level B*, the same operations are performed on *Level C* that contains *afib* subjects with selected combination of feature. The corresponding findings of stage 1 of Level C are used in stage 2 for self-recognizing the features pattern.

Furthermore in Stage 2, the replica operations with same feature combinations of scenario one are executed on each level of scenario two. Recognition of the features pattern of *ST-T changes* subjects at *Level A*, *nsr* subjects at *Level B*, and *afib* subjects at *Level C* are used in next recognition stage which belongs to fusion stage (Stage 3 of DDL). Figure 5.2 shows the fusion stage or stage 3 of DDL are executed in the form of feature streams fusion in three different *CASES*, namely *CASE 1* covers the *Level A* of both scenarios, *CASE 2* belongs to *Level B* of each scenario, and *CASE 3* contains the *Level C* of each scenario. Moreover, in *CASE 1*, the Stage 2 results of *ST-T changes* in MIT-BIH(scenario two) and *flattened T waves* in UMMC (scenario one) are fused through combination of all extracted features. The most accurate results of stage 2 in both dataset is considered as a target file and conversely, the least accurate results are considered as input file. Both target and input files are processed through same customized ANN structure as used in Stage 2. The recognition of matching feature patterns of target and input streams of *CASE 1* delivers the recognized and unrecognized

status. The outcome of *CASE 1* in stage 3 narrates the similarity of features pattern between *ST-T changes* and *flattened T wave*. Finally, the accuracy of *CASE 1* is measured through the recognized status mean patterns are matched and unrecognized status, patterns are unmatched. Similarly, the same replicated procedures are applied on *CASES 2* and *3*. In *CASE 2*, the Stage 2 results of *nsr* in MIT-BIH and *nsr* in UMMC are fused through same customized ANN structure (five hidden layer) and get the results of patterns matching in context of recognized and unrecognized status. Same as the process for *CASE 3*, the Stage 2 results of *afib* of MIT-BIH and *afib* of UMMC are fused, then and get the recognized and unrecognized status.

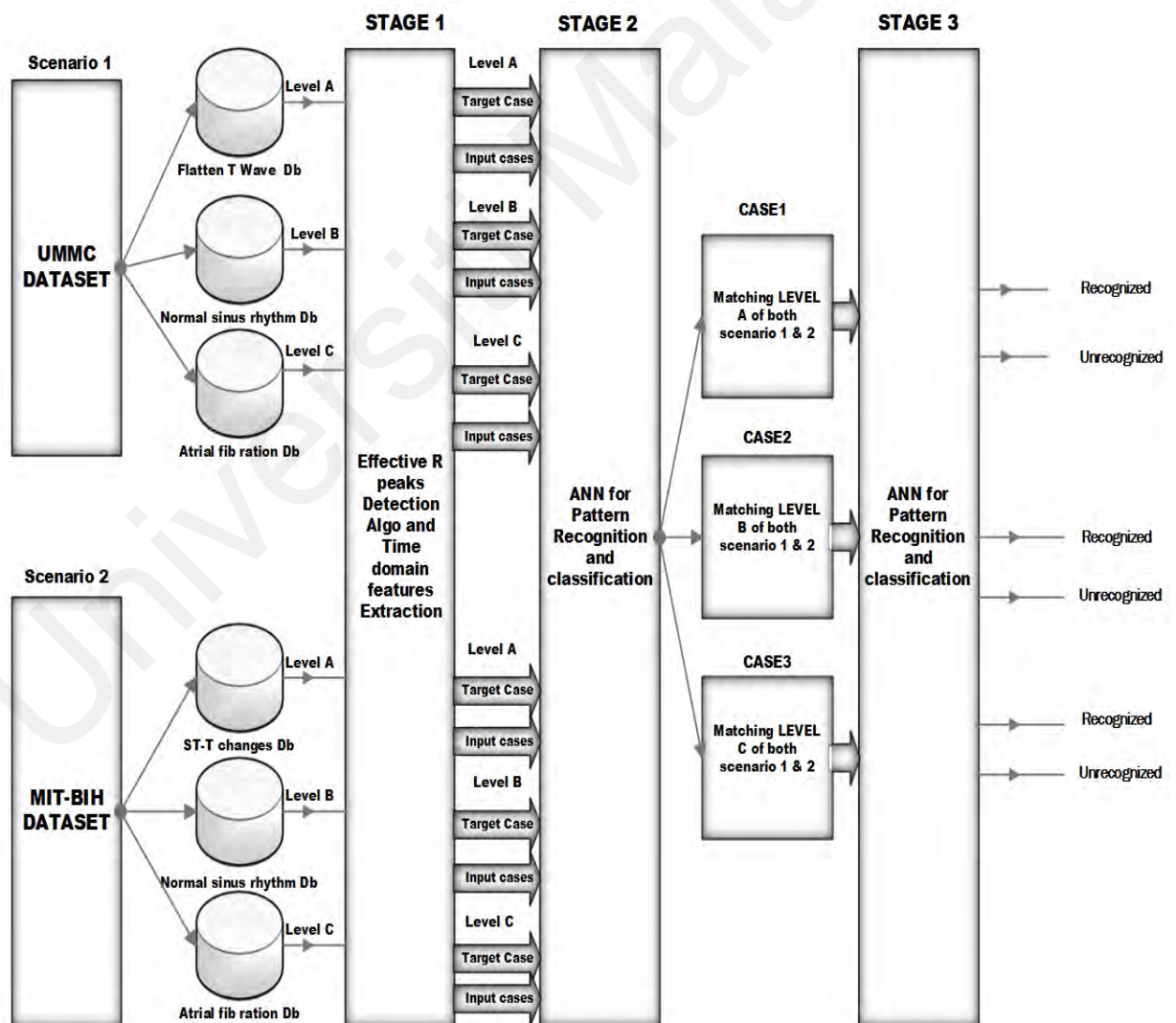
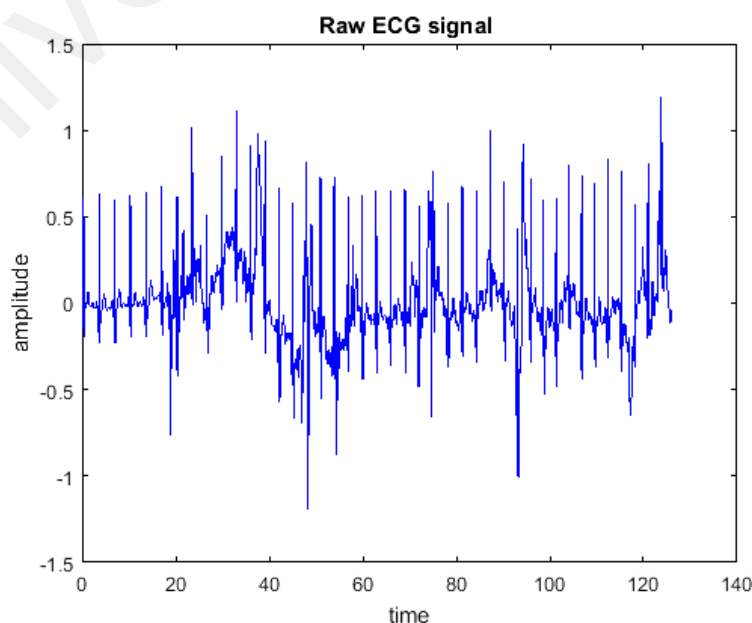


Figure 5.2. Internal operational execution of deep deterministic learning

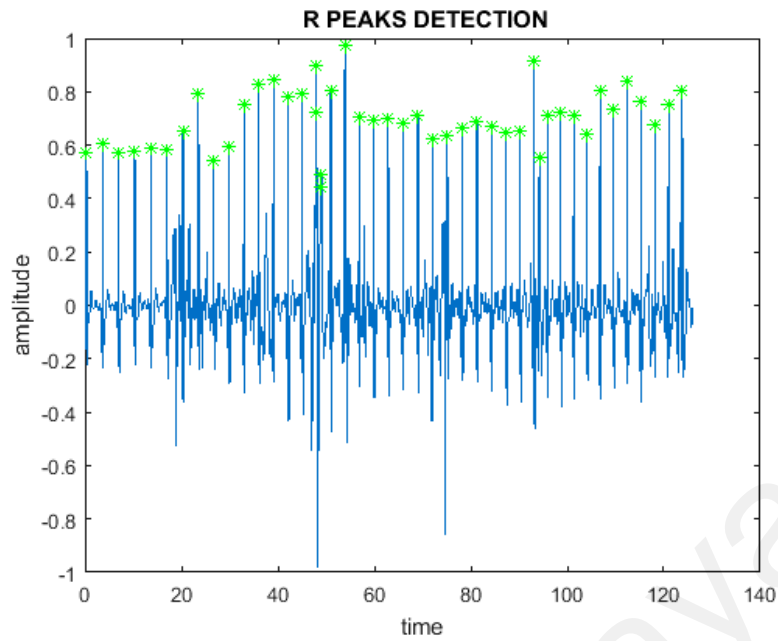
According to figure 5.2, the robust and accurate proposed DDL model is segmented into two modules, namely basic features knowledge of cardiac diseases through extensive feature engineering and then the patterns of extracted features are matched in defined way that delivers the significance of cardiac diseases dependencies through global acceptance. The detailed of basic feature extraction of *flattened T wave* are already covered in Chapter 4. The linkage of Chapter 4 with Chapter 5 is actually reflected in operational flow of the logical structure of DDL in terms of recognition the ECG features patterns. Such part is briefly discussed in next section 5.3.

5.3 Experimental Setup

The effectiveness of DDL is only measured after evaluation of this model. For the evaluation, the experimental step is launched by using the different ECG data streams of two datasets (MIT-BIH and UMMC). The operational activities are starting with the help of proposed effective R peak detection algorithm which is already discussed in Chapter 4. Figure 5.3 highlights the findings of R peaks in UMMC dataset through the use of the effective R-peaks detection algorithm after removal of power line and baseline wander noises



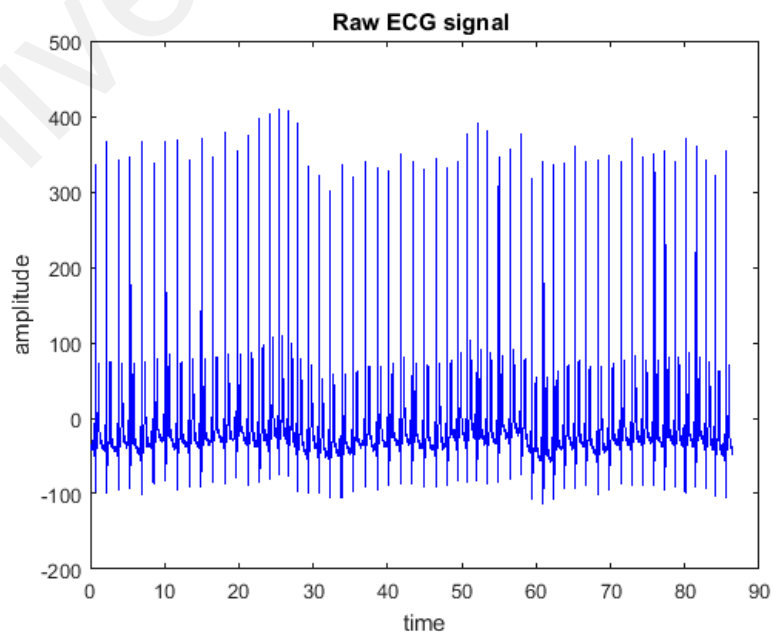
(a) Baseline and power noisy *flattened T wave* signal



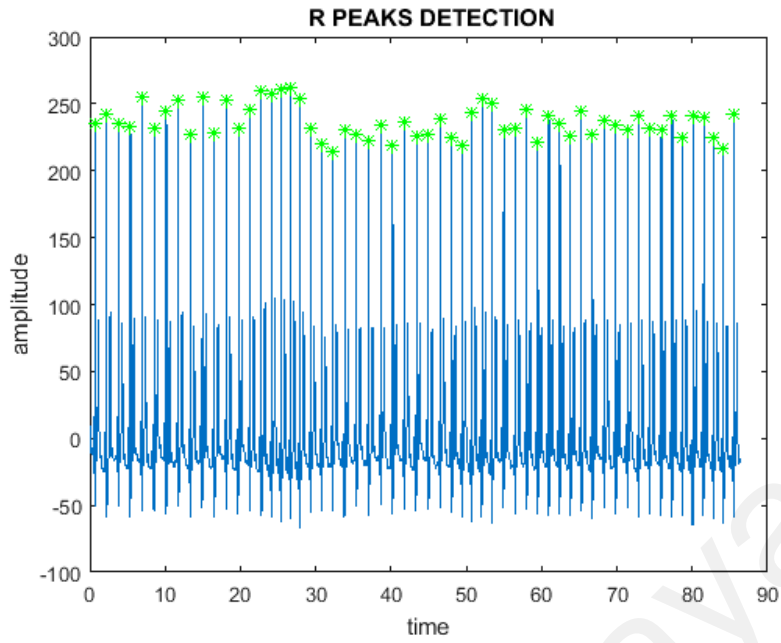
(b) R-peaks detection on filtered *flattened T wave* signal

Figure 5.3. UMMC ECG sample of flattened T wave subject

The above figure 5.3(a) represents the noisy raw form of *flattened T wave* ECG signal which include base wander line noise and power line noise. Whereas, figure 5.3(b) highlighted the detected R peaks in filtered signal through effective R peaks detection algorithm. Similarly, figure 5.4 represents the ECG patterns in terms of findings the R peaks in MIT-BIH dataset through proposed effective R –peaks detection algorithm.



(a) Baseline and power noisy *ST-T change* signal



(b) R-peaks detection on filtered *ST-T change* signal

Figure 5.4. MIT-BIH ECG sample of *ST-T Change* subject

Similar to *flattened T wave* subjects, figure 5.4(a) shows the *ST-T change* ECG signal which has powerline noise as well as baseline noise. Figure 5.4(b) indicates the detected R peaks of filtrated signal of *flattened T wave*.

The most important part of the proposed R peak detection algorithm is to fix the threshold points for getting the better efficiency(see Section 4.3). The parameters of true positive R peak detection (*tp*), true negative R peak detection (*tn*), false positive R peak detection (*fp*), and false negative R peak detection (*fn*) are key factors for measuring the efficiency of effective R peak detection algorithm. The efficiency measurement units are accuracy index (A_I), sensitivity (S_e), positive prediction value (P^+), and false discovery rate (F^{dr}). All of the keys factors for efficiency calculations are highlighted in Equation 5.1 to Equation 5.4.

$$\text{Accuracy Index } (A_I) = \frac{tp}{tp + fp + fn} \quad (5.1)$$

$$\text{Sensitivity } (S_e) = \frac{tp}{tp + fn} \quad (5.2)$$

$$\text{Positive prediction value } (P^+) = \frac{tp}{tp + fp} \quad (5.3)$$

$$\text{False discovery rate } (F^{dr}) = \frac{fp}{tp + fp} \quad (5.4)$$

According to proposed flow of DDL, in feature engineering phase, the extraction of different time domain features through the results of proposed effective R peaks detection algorithm. Seven different time domain features are extracted from ECG signals. Such features are the combination of state-of-the-art features and two new derived features (mt_{on} and mt_{off}). The extracted features include heart rate (hr), mean of HR (hrv), standard deviation of RR interval ($sdnn$), root mean square difference of RR interval ($rms-rr$), number of RR intervals more than 50 ($nnrr$), mean value of T-wave onset (mt_{on}), and mean value of T-wave offset (mt_{off}).

5.3.1 Feature Extraction

Moreover, the whole ECG signal length is presented in the form of ln . The detected R peaks and RR intervals are highlighted in the form of pi and $|(pi+1) - (pi)|$, respectively. In Equation 5.5, the mean value of the heart rate is:

$$hrv = 60 / (ln - 1) \sum_{i=0}^{ln} |(pi + 1) - (pi)| \quad (5.5)$$

Similar to Equation 5.5, the root mean difference value of RR intervals are presented in Equation 5.6.

$$rms - rr = \sqrt{1 / (Ln - 2) \sum_{i=3}^{ln} [|(pi + 1) - (pi)|] 1/2} \quad (5.6)$$

The same scenario is applied for calculating the four other features. Equations (5.7a) and (5.7b) present the $sdnn$, Equation 5.8 highlights the number of pairs of RR intervals more than 50, Equations (5.9a) and (5.9b) present the mt_{on} detection, and Equations (5.10a) and (5.10b) show the mt_{off} detection.

$$\gamma = 1/Ln \sum_{i=0}^n |(pi + 1) - (pi)| \quad (5.7a)$$

$$sdnn = \sqrt{1/(Ln - 1) \sum_{i=2}^n [|(pi + 1) - (pi)| - \gamma]} \quad (5.7b)$$

$$nnrr = [\sum_{i=0}^{ln} |(pi + 1) - (pi)|] > 0.05 \quad (5.8)$$

$$t_{on} = \vartheta = 40 + 1.33 \sum_{i=2}^n \sqrt{|(pi + 1) - (pi)|} \quad (5.9 a)$$

$$mt_{on} = 1/(Ln - 1) \sum_{i=2}^n |(\vartheta i + 1) - (\vartheta i)| \quad (5.9 b)$$

$$t_{off} = \delta = 40 + 1.33 \sum_{i=3}^{ln} [|(pi + 1) - (pi)|]1/6 \quad (5.10a)$$

$$mt_{off} = 1/(Ln - 1) \sum_{i=2}^n |(\delta i + 1) - (\delta i)| \quad (5.10b)$$

A significant component of the ECG signal is the QRS complex, and in-depth R peak is a fiducial point for all the features extraction. Thus, we build the efficient and accurate pattern recognition process through the neural network by considering seven different features (*hr*, *hrv*, *rms-rr*, *sdnn*, *nnrr*, *mt_{on}*, and *mt_{off}*) for matching the cardiac states (*nsr*, *afib*, *ST-T changes*, and *flattened T waves*). In DDL, selection of features is a core aspect for recognition of different patterns, such as *ST-T changes* and *flattened T wave* through the use of *mt_{on}* and *mt_{off}*, pattern matching of *afib* through *hrv*, *rms-rr*, and *sdnn*, and recognition of patterns for *nsr* through all seven extracted features. Next, proposed features selection algorithm supports the low computational complexity and enhances the pattern recognition efficiency of DDL.

5.3.2 Feature Selection and Multilayer Perceptron

This section covers the selection of feature sets and architectural view of ANN that used in DDL. After extraction of seven different features, these features are combined in

six different combinations. So, the selected features set against cardiac states are extracted from six different fc by using the proposed feature selection algorithm. The key parameters of proposed feature combination selection algorithm are the lowest computational cost or complexity, optimal gradient value and accuracy against the six different feature combinations (see Appendix-A for detail of fc). Algorithm of feature combination selection highlighted the selection criteria of different defined fc

Algorithm: Selection of Feature combination

<p> fe : Number of features x : Input feed that belongs to different features combination x_T : Target value fc : Defined features Combinations tot : Total number of features combinations cf : Computational cost or time complexity is measured through mean square error eph : Epoch value represents the number of iterations acc : Features patterns matching accuracy G : Gradient Opt: Optimal 1: LOAD input feed ($x \in fc$) 2: SET Target adjust x_T 3: FOR ($fc = 1; fc \leq tot; fc ++$) 4: compute: $fc \rightarrow target$ set x_T 5: IF ($acc \rightarrow Max_{value}$ && $eph \rightarrow Min_{value}$ && $G \rightarrow opt_{value}$) 6: compute: cf 7: ELSE compute other fc (Repeat 4 to 6) 8: END IF 9: END FOR </p>
--

Additionally, the algorithm of feature combination selection is fruitful to avoid the overfitting in neural network structure. The selected input feed in the form of selected fc is quite supportable in reduction of irrelevant features which narrates the low computational complexity in recognition operations of DDL. In algorithm of feature combination selection, adopted the optimal point of gradient along with accuracy and

epoch values in network is the way to reduce the over fitness. Algorithm flow in above clearly shows the defined six fc are tested under the condition of high accuracy, low epoch values and optimal gradient value for selection against the different cardiac states i.e. MI(flattened T wave and ST-T changes), *afib* and *nsr*.

In architectural view of ANN for DDL, figure 5.5 highlights the input "x" of one feature set that passes certain features stream in five different hidden layers with constant weights W_c in whole network for one input feed with different biased value b . However, the weights are constantly upgraded according to the next input feeds. These input feeds are arranged according to defined feature sets, means $x \in R$ where as R is a set of different feature combinations $R = \{fc_1, fc_2, fc_3, \dots, fc_n\}_i$, where i is the number of features. The target value is x_T compared to associate in given DDL stage. Moreover, the corresponding highlights recognized or un-recognized status indicates the correlation level on context of various features sets in DDL model (correlation between different ECG anomalies).

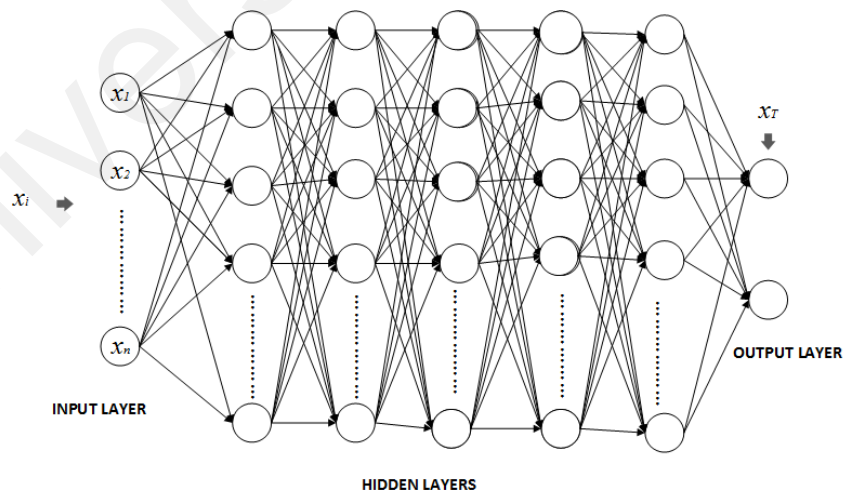


Figure 5.5. Neural network Architecture for DDL

Furthermore, the operational activities of DDL are constructed with the well tune of ANNs on Stages 2 and 3 for generation of accurate results of features pattern matching. In tuning phase of ANNs, consider the five hidden layers to improve efficiency after

observing the different combinations of the hidden layers. The second efficiency concern involves proper identification of the input and target cases. According to the systematic and stage-wise methodology of DDL, the experimental results are organized in different level of settings which discussed in Section 5.4. These settings depict all operational activities of scenarios one and two in DDL. Setting I is the measuring unit of all investigations of the Stage 2 which belongs to ECG subjects of UMMC dataset. Similarly, Setting II includes the investigational process of the Stage 2 which refers the ECG subjects of MIT-BIH dataset. Furthermore, Setting III deals feature fusion process of Stage 3 in context of matching the ECG features patterns of the MIT-BIH and UMMC. Finally, Setting IV discusses the comparative report of DDL, which includes a comparison of DDL with existing classification or pattern recognition methods.

5.4 Experimental Results

In this section, the evaluations of this methodology are performed in the form of different results and compared DDL with the different state-of-the-art classification techniques. Measurement of the efficiency of proposed DDL methodology relies solely on the operational execution plans. First, the plans are executed on the basis of selected feature combinations. Afterward, the DDL methodology is cross-checked through all defined combinations of features (cover up computational complexity). The most significant part of this thesis is the evaluation report of the experimental DDL setup. During evaluation, the efficiency of the individual and overall parts of the DDL model determines the success of this method.

5.4.1 Setting I Results

According to Stage 1 of DDL operational investigations, the results of the UMMC dataset (*scenario one* of DDL) were evaluated through using Setting I as per the evaluation plan. The *level A* of UMMC contains ten *flattened T wave* subjects. In *level A*

operation, the detection of the R peaks of the *flattened T wave* subjects were used to measure the efficiency units, and such findings are represented in Table 5.1. The parameters of Table 5.1 narrates the usage of ten flattened T wave subjects from UMMC dataset for finding the efficiency gages of A_I , P_+ , S_e , and F^{DR} with help of threshold points(tp , tn , fp and fn) of effective R peak detection algorithm. The overall efficiency gages of ten *flattened T wave* cases in Table 5.1 shows the accurate result and further helpful in self-recognition of *flattened T wave* patterns. Furthermore, table 5.2 highlighted the extracted seven different time domain features (hr , hrv , $rms-rr$, $sdnn$, $nnrr$, mt_{on} , and mt_{off}) which are futher used to select the perfect fc (mt_{on} and mt_{off} selected through proposed feature selection algorhtim) out of defined fc as discussed in Section 5.2 (see Appendix-A for defined fc).

Table 5.1: Efficiency parameters of flattened T wave cases (UMMC)

$M_Subjects$	$Lead$	$R-peaks$	tp	tn	fp	fn	RR	$A_I(\%)$	$P_+(\%)$	$S_e(\%)$	$F^{DR}(\%)$
ECGRLIIBD	LII	29	23	0	0	0	28	100	100	100	0
ECGRLIIFA	LII	25	21	3	1	0	24	95.455	95.455	100	4.5455
ECGRLIINAF	LII	22	20	3	1	0	21	100	100	100	0
ECGRLIISAT	LII	43	40	3	0	0	42	100	100	100	0
ECGRLIANSI	LII	26	24	1	1	1	25	92.308	96	96	4
ECGRLIIDAT	LII	21	19	4	2	2	20	82.609	90.476	90.476	9.5238
ECGRLIIHAJ	LII	39	37	0	0	0	38	100	100	100	0
ECGRLIIJUS	LII	46	43	0	0	0	45	100	100	100	0
ECGRLIIRAF	LII	20	18	0	0	0	19	100	100	100	0
ECGRLIIRAZ	LII	20	18	4	2	2	19	81.818	90	90	10

Table 5.2: Extracted time domain features of flattened T wave cases (UMMC)

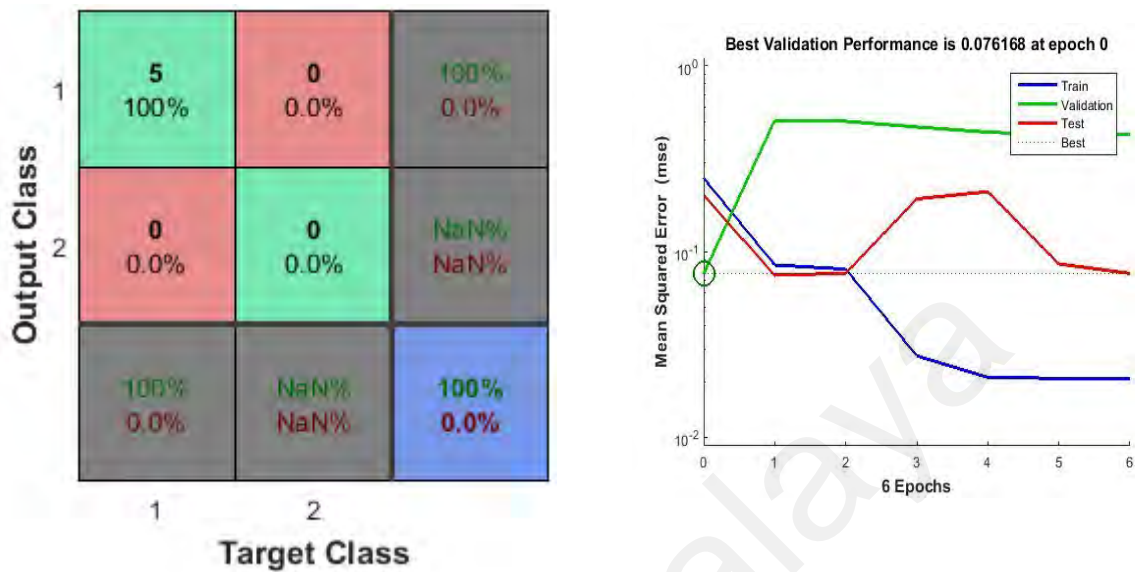
$M_Subjects$	$Lead$	hr	hrv	$sdnn$	$rmsrr$	$nn50$	mt_{on}	mt_{off}
ECGRLIIBD	LII	6.72	168.7371	1.1716	1.5636	25	41.5224	40.6215
ECGRLIIFA	LII	5.76	90.2261	2.9735	3.3506	23	41.7383	40.7097
ECGRLIINAF	LII	5.04	18.325	1.836	1.8485	19	42.5417	41.0376
ECGRLIISAT	LII	10.08	32.7426	1.0751	1.1393	13	42.1584	40.8812
ECGRLIANSI	LII	6	21.4911	2.9051	4.391	12	42.4071	40.9827

<i>M_Subjects</i>	<i>Lead</i>	<i>hr</i>	<i>hrv</i>	<i>sdnn</i>	<i>rmsrr</i>	<i>nn50</i>	<i>mt_{on}</i>	<i>mt_{off}</i>
ECGRLIIDAT	LII	4.8	25.9253	4.6688	6.077	18	42.5105	41.0249
ECGRLIIHAJ	LII	9.12	17.1005	0.19153	0.11042	21	42.4941	41.0182
ECGRLIIJUS	LII	10.8	29.8001	0.70886	0.73787	20	42.1729	40.8871
ECGRLIIRAF	LII	4.56	23.1606	0.72636	0.91433	13	42.2543	40.9203
ECGRLIIRAZ	LII	4.56	45.9334	3.9614	5.9362	18	42.1546	40.8796

The extracted seven different time domain features are arranged in six different *fc* and selected the perfect *fc* through highlighted proposed algorithm of feature combination selection (see Section 5.3.2). So, the next part of this stage is self-recognition of the patterns of *flattened T* subjects using the scheme of the most accurate results in terms of efficiency gages of Table 5.1 were referred as a target class, and the least accurate (efficiency gages of Table 5.1) results as an input class.

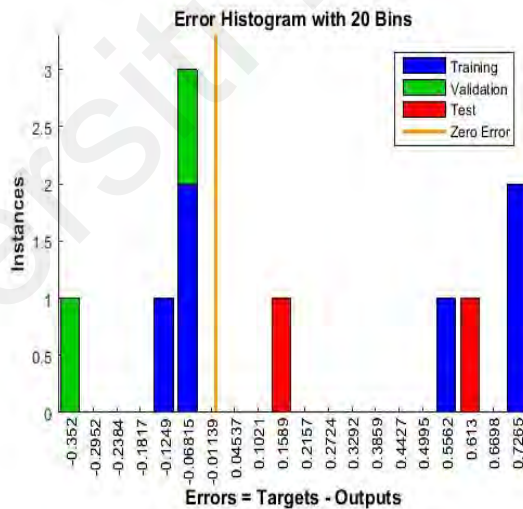
The combination of accurate R peaks detection, feature extraction of seven time domain features (see Section 5.3.1) and selected feature set through proposed feature selection combination (see Section 5.3.2) plays a vital role for adjusting the target class and input class. According to figure 5.2, the adjustment of target class and input class are relied on the previous stage which belongs to results of detected R peaks and its accuracy. The most accurate detected R peaks findings in terms of extracted feature set of stage 1 at *level A* UMMC dataset act as a target class, whereas the least accurate findings of stage 1 *level A* UMMC dataset reflected the input class. Furthermore, the scheme of target and input classes are mapped through selected *fc*, the *flattened T wave* patterns were matched with the features of *mt_{on}* and *mt_{off}* with accuracy above 99.95% and zero epoch value shows the least computational complexity in pattern recognition of features. The detail observations of epoch values, accuracy, and other parameters are presented in Appendix-A. However, other *fc* in appendix-A highlighted the least effective findings in terms of accuracy and computational complexity (epoch value) as

compared to selected fc (mt_{on} and mt_{off}). Figure 5.6 presents the complete evaluation of these features mapping.



(a) Confusion matrix

(b) Performance validation



(c) Error Histogram

Figure 5.6. UMMC: features mapping of flattened T wave subjects

In figure 5.6, the target class in confusion matrix highlights the desire result of *level A* UMMC dataset and output class shows the actual or gained result of UMMC *level A*. So, in Figure 5.6(a), confusion matrix represents the 100% accuracy of the *flattened T wave* patterns which means gained results 100% match with desire result. Figure 5.6(b)

represents the computational complexity in terms of epoch value that is equal to null value. Figure 5.6(c) highlights the error ratio of mismatched features between target class and output class, such error ratio is equal to zero level. Similarly, the same operational investigations were implemented on the *nsr* and *afib* subjects. At *Level B*, the different threshold R peaks points of the *nsr* subjects were identified by using the effective R peak detection algorithm. Through these threshold values of the R peaks, the efficiency parameters are derived in the form of A_I , P_+ , S_e and F^{DR} . Table 5.3 shows the efficiency gages obtained of twenty *nsr* subjects of UMMC dataset. These gages of A_I , P_+ , S_e and F^{DR} highlight the accurate result through using threshold points(fp, fn, tp and tn) of effective R peaks detection algorithm.

Table 5.3: Accuracy of normal sinus rhythm cases (UMMC)

<i>M_Subjects</i>	<i>Lead</i>	<i>R-peaks</i>	<i>tp</i>	<i>tn</i>	<i>fp</i>	<i>fn</i>	<i>RR</i>	A_I (%)	P_+ (%)	S_e (%)	F^{DR} (%)
ECGRLIIme10235	LII	20	18	0	0	0	19	100	100	100	0
ECGRLIIme10233	LII	20	8	4	2	2	19	81.8	90	90	10
ECGRLIIme10205	LII	22	20	1	0	0	21	100	100	100	0
ECGRLIIme10115	LII	25	23	0	0	0	24	100	100	100	0
ECGRLIIme10091	LII	16	14	4	0	0	15	100	100	100	0
ECGRLIIme10009	LII	15	13	2	0	0	14	100	100	100	0
ECGRLII10002	LII	46	43	0	0	0	45	100	100	100	0
ECGRLIIme09847	LII	29	23	0	0	0	28	100	100	100	0
ECGRLIIme09777	LII	33	29	0	0	0	32	100	100	100	0
ECGRLIIme09653	LII	17	15	6	0	0	16	100	100	100	0
ECGRLIIme09565	LII	10	8	0	0	0	9	100	100	100	0
ECGRLIIme09518	LII	23	21	1	0	0	22	100	100	100	0
ECGRLIIme09448	LII	35	33	2	0	0	34	100	100	100	0
ECGRLIIme09446	LII	41	35	12	0	0	40	97.2	97.2	100	2.777
ECGRLIIme09360	LII	20	18	0	0	0	19	100	100	100	0
ECGRLIIme09299	LII	13	11	0	0	0	12	100	100	100	0
ECGRLIIme09279	LII	21	19	0	0	0	20	100	100	100	0
ECGRLIIme09199	LII	95	84	1	0	0	94	100	100	100	0
ECGRLIIme09159	LII	16	14	0	0	0	15	100	100	100	0
ECGRLIIme09062	LII	12	10	0	0	0	11	100	100	100	0

Same above *flattened T wave* scenario is applied on *nsr* subjects, and extensive feature engineering is applied through above feature extraction (see Section 5.3.1). Table 5.4 presents the seven extracted features of twenty *nsr* subjects of UMMC dataset. In Table 5.4, the findings of *hr*, *hrv*, *rms-rr*, *sddnn*, *nn50*, *mt_{on}*, and *mt_{off}* seems valuable for selection of perfect *fc* as discussed in Section 5.2 . Additionally, the selected perfect *fc* delivers the accurate self-recognition of features pattern as performed in *level A*.

Table 5.4: Extracted features from normal sinus rhythm cases (UMMC)

<i>M_Subjects</i>	<i>Lead</i>	<i>hr</i>	<i>hrv</i>	<i>sddnn</i>	<i>rmsdd</i>	<i>nn50</i>	<i>mt_{on}</i>	<i>mt_{off}</i>
ECGRLIIme10235	LII	4.56	23.1606	0.72636	0.91433	13	42.2543	40.9203
ECGRLIIme10233	LII	4.56	45.9334	3.9614	5.9362	18	42.1546	40.8796
ECGRLIIme10205	LII	5.04	17.4705	0.64364	0.89312	17	42.4861	41.0149
ECGRLIIme10115	LII	5.76	17.9309	0.26099	0.06494	9	42.4379	40.9953
ECGRLIIme10091	LII	3.6	14.875	0.54742	0.2309	14	42.6877	41.0972
ECGRLIIme10009	LII	3.36	20.972	2.0185	2.2556	12	42.5934	41.0642
ECGRLIIme10002	LII	10.8	29.8001	0.70886	0.73787	20	42.1729	40.8871
ECGRLIIme09847	LII	6.72	168.737	1.1716	1.5636	25	41.5224	40.6215
ECGRLIIme09777	LII	7.68	39.9541	0.90594	0.82898	12	42.1111	40.8618
ECGRLIIme09653	LII	3.84	13.3771	0.85152	1.2755	10	42.843	41.1606
ECGRLIIme09565	LII	2.16	20.5429	0.18102	0.09372	5	42.2757	40.9291
ECGRLIIme09518	LII	5.28	19.4981	0.69062	0.9423	3	42.3526	40.9605
ECGRLIIme09448	LII	8.16	29.9125	1.052	1.5332	21	42.0488	40.8364
ECGRLIIme09446	LII	9.6	73.3223	3.0501	4.1812	38	42.024	40.8263
ECGRLIIme09360	LII	4.56	16.9408	0.17872	0.08221	13	42.5052	41.0227
ECGRLIIme09299	LII	2.88	23.8941	0.75836	1.0266	9	42.2974	40.9379
ECGRLIIme09279	LII	4.8	25.8655	0.40945	0.44295	3	42.0715	40.8457
ECGRLIIme09199	LII	22.5	103.845	0.82567	1.0153	81	41.1957	40.4882
ECGRLIIme09159	LII	3.6	17.8379	0.82004	1.0666	9	42.5693	41.0489
ECGRLIIme09062	LII	2.64	24.4479	0.04422	0.03951	2	42.0838	40.8507

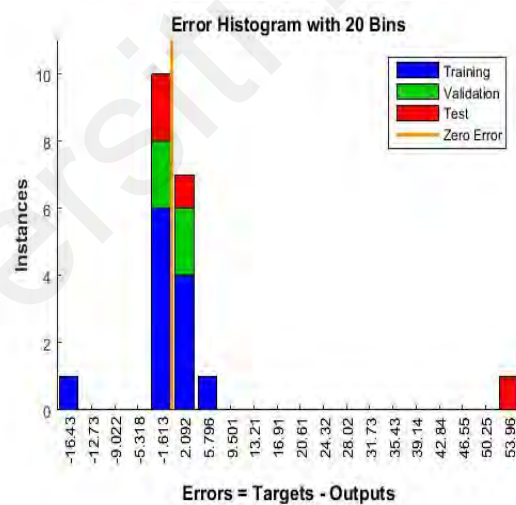
After extraction of seven time domain features, the *fc* of seven features are selected on the basis of feature combination selection algorithm (see Section 5.3.2) and then the *ANN* for self-pattern recognition of different *nsr* subjects was tuned, such as in the case of the *flattened T wave*. In operating the self-pattern matching process, we obtained an

accuracy of 80% using a combination of the seven pre-defined features. In Figure 5.7, an evaluation of the *Level B* operational investigations is provided.



(a) Confusion matrix

(b) Performance validation



(c) Error histogram

Figure 5.7. UMMC: Features mapping of normal sinus rhythm subjects

Figure 5.7(a) shows the confusion matrix of *nsr* subjects with 80% accuracy. Similar to above confusion matrix of figure 5.6(a), the target class highlights the desired result and output class refers the gain result in form of feature patterns matching. So, results of features pattern matching between desired (target) and gained (output) classes highlight 80% accuracy. Figure 5.7 (b) shows the least computational complexity at epoch level 6

where the features are recognized. Finally, Figure 5.7(c) shows the error ratio is equal to 2.092 which shows that 20% mismatch features exist between target class and output class.

The same procedure is applied at *Level C*, which deals with the six different *afib* subjects. The efficiency gages determined using the threshold values of the detected R peaks are highlighted in Table 5.5. The findings in Table 5.5 in aspect of efficiency gages indicate fair result except two subjects of *afib*, namely ECGRLII07344che and ECGRLIIme03332_lee. Similarly, Table 5.6 highlights the same steps for the extraction of seven different time domain features that were performed by using same extraction method as performed in above *Level A* and *level B*.

Table 5.5: Efficiency parameters of atrial fibrillation cases (UMMC)

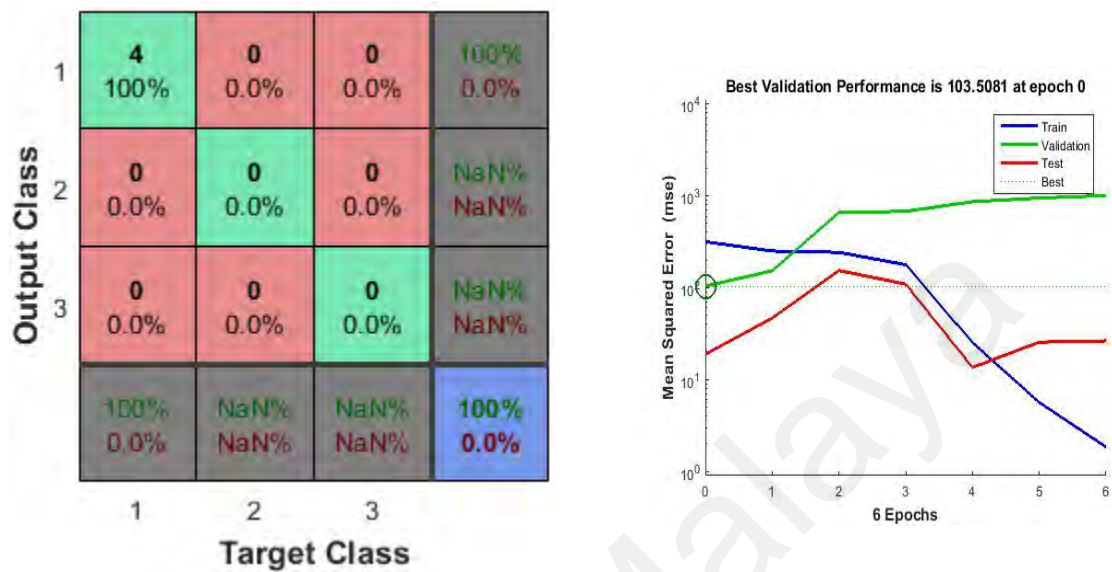
<i>M_Subjects</i>	<i>Lead</i>	<i>Rpeaks</i>	<i>tp</i>	<i>tn</i>	<i>fp</i>	<i>fn</i>	<i>RR</i>	<i>A_I</i> (%)	<i>P₊</i> (%)	<i>S_e</i> (%)	<i>F^{DR}</i> (%)
ECGRLII07344che	LII	373	371	199	80	74	372	70.6	82.2	83.3	17.7
ECGRLIIme0858abdul	LII	41	35	2	0	0	40	100	100	100	0
ECGRLIIme02416chee	LII	42	39	6	1	1	41	95.1	97.5	97.5	2.5
ECGRLIIme03332_lee	LII	19	17	3	1	1	18	89.4	94.4	94.4	5.5
ECGRLIIme06106	LII	8	6	0	0	0	7	100	100	100	0
ECGRLIIme06168	LII	12	10	0	0	0	11	100	100	100	0

Table 5.6: Extracted time domain features of atrial fibrillation cases (UMMC)

<i>M_Subjects</i>	<i>Lead</i>	<i>hr</i>	<i>hrv</i>	<i>sddnn</i>	<i>rmsdd</i>	<i>nn50</i>	<i>mt_{on}</i>	<i>mt_{off}</i>
ECGRLII07344che	LII	89.28	18.026	5.211	7.2451	333	43.1842	41.3
ECGRLIIme0858abdul	LII	9.6	74.698	1.3781	2.0852	38	41.6469	40.6723
ECGRLIIme02416chee	LII	9.84	46.7626	2.0375	2.7453	35	41.9455	40.7942
ECGRLIIme03332_lee	LII	4.32	23.9088	4.9432	7.8308	15	42.495	41.0186
ECGRLIIme06106	LII	1.68	31.8108	1.5139	1.6518	4	42.1826	40.891
ECGRLIIme06168	LII	2.64	15.3573	0.446	0.5885	9	42.6412	41.0782

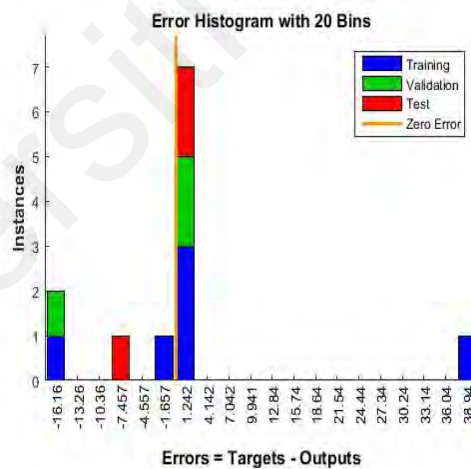
In the last instance, the same procedure for DDL is implemented among *afib* subjects using the finely tuned *ANN-like flattened T waves* and *nsr* subjects. Selected *fc* of three features(*hrv*, *rms-rr*, and *sddn*) are picked through selection of feature combination

algorithm. Furthermore, an accuracy of 100% was obtained as a result of self-pattern matching with help of selected fc . Figure 5.8 highlighted the evaluation of self pattern recognition of the UMMC *afib* subjects



(a) Confusion matrix

(b) Performance validation



(c) Error Histogram

Figure 5.8. UMMC: features mapping of atrial fibrillation

Figure 5.8(a) shows the confusion matrix of 100% accuracy in context of feature pattern matched between target class and output class. Similar to above representation, target class reflected the desired result and output class represents the gained or actual result. Figure 5.8(b); highlights the zero epoch value which reflects least computational cost

for recognition of the features pattern. Finally, figure 5.8(c), represents the error ratio is zero between target class and output class in feature recognition process. .

5.4.2 Setting II Results

The above experimental work was replicated in Scenario 2 through the concept of global acceptance (the same experimental workflow applied to two different entities, one entity must be state-of-the-art). Such concept indicates that the same scenario is imposed on the MIT-BIH dataset, which means the above methodology is deployed on the MIT-BIH dataset. At the first stage *Level A*, the R peaks of ten different streams or subjects of *ST-T changes* were identified using the effective R peak detection algorithm and then same time domain features were extracted. The feature extraction and efficiency attributes or gages are shown in different tables similar to Scenario 1. Table 5.7 represents the accuracy level of *ST-T changes* subjects regarding the detected R peaks along with the derivation units of efficiency measurements (*tp*, *tn*, *fp*, and *fn*). The efficiency attributes A_I , P_+ , S_e , and F^{DR} of this table are extracted from the derived efficiency units. Table 5.8 shows the extracted time domain features *hr*, *hrv*, *sddnn*, *rms-rr*, and *nn50* using state-of-the-art methods along with two new extracted features, mt_{on} and mt_{off} .

The findings of Table 5.7 clearly indicate the positive facts in terms of extraction of the R peaks. All *ST-T change* subjects` or ECG streams delivers the true results in terms of high efficiency attributes (findings of A_I , P_+ , S_e , F^{DR}).

Table 5.7: Efficiency parameters of ST-T change cases (MIT-BIH)

$M_Subjects$	<i>Lead</i>	<i>Rpeaks</i>	<i>tp</i>	<i>tn</i>	<i>fp</i>	<i>fn</i>	<i>RR</i>	$A_I(\%)$	$P_+(\%)$	$S_e(\%)$	$F^{DR}(\%)$
300	LII	93	91	0	0	0	92	100	100	100	0
301	LII	57	55	0	0	0	56	100	100	100	0
302	LII	63	62	0	1	0	62	98.41	98.41	98.4	1.5
303	LII	86	84	0	2	0	85	97.67	97.67	97.7	2.3
304	LII	54	52	0	0	0	53	100	100	100	0
305	LII	9	8	0	0	0	8	100	100	100	0

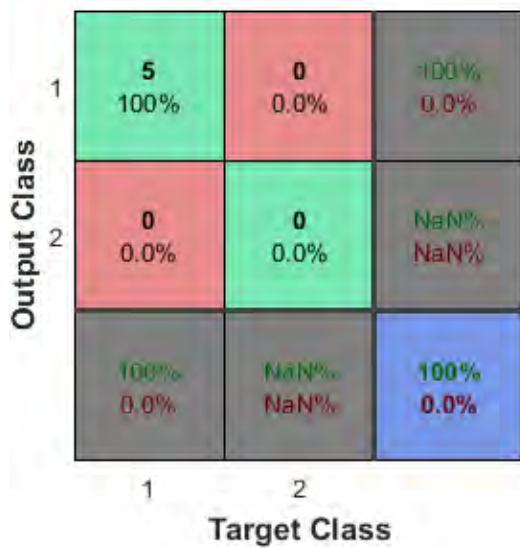
<i>M_Subjects</i>	<i>Lead</i>	<i>Rpeaks</i>	<i>tp</i>	<i>tn</i>	<i>fp</i>	<i>fn</i>	<i>RR</i>	<i>A_I(%)</i>	<i>P₊(%)</i>	<i>S_e(%)</i>	<i>F^{DR}(%)</i>
306	LII	64	62	0	0	0	63	100	100	100	0
307	LII	58	56	0	0	0	57	100	100	100	0
308	LII	116	115	0	0	0	115	100	100	100	0
309	LII	85	84	0	1	0	84	98.82	98.82	98.8	1.1

Furthermore, the extracted seven features from effective R peaks detection algorithm are highlighted in Table 5.8. According to figure 5.2, replicated operations is executed on *ST-T changes* subjects of MIT-BIH dataset as executed on *flattened T wave* subjects of UMMC dataset. The extracted features of *ST-T changes* is further selected in terms perfect *fc* out of six defined *fc* through using feature combination selection algorithm.

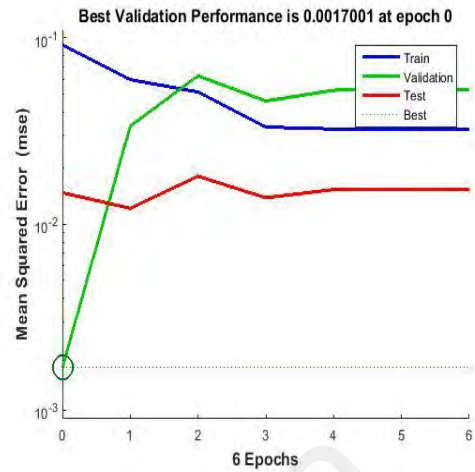
Table 5.8: Time-domain feature extraction of ST-T change cases (MIT-BIH)

<i>M_Subjects</i>	<i>Lead</i>	<i>hr</i>	<i>hrv</i>	<i>sddnn</i>	<i>rmsdd</i>	<i>nn50</i>	<i>mt_{on}</i>	<i>mt_{off}</i>
300	LII	22.08	64.6581	0.028591	0.010926	0	41.2816	40.5232
301	LII	13.44	39.7182	0.060377	0.090587	13	41.6355	40.6677
302	LII	14.88	49.2867	0.26685	0.34714	21	41.5456	40.631
303	LII	20.4	59.8273	0.048094	0.021162	4	41.333	40.5442
304	LII	12.72	37.2866	0.023913	0.022743	0	41.6873	40.6888
305	LII	1.92	1858.0371	1.4596	2.6188	6	40.9812	40.4006
306	LII	15.12	44.9227	0.10302	0.072341	31	41.5404	40.6289
307	LII	13.68	40.5358	0.10652	0.063915	17	41.6214	40.6619
308	LII	27.6	169.0049	0.38794	0.72483	114	41.0966	40.4477
309	LII	20.16	59.1951	0.062151	0.035737	10	41.3408	40.5474

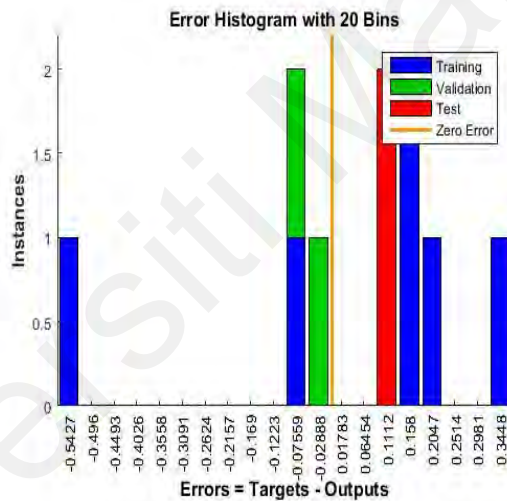
After selection of perfect *fc*, the results of *level A* of MIT-BIH(*Secario 2*) represents the impressive accurate result pattern matching same as the level A of UMMC(*Secario 1*). Figure 5.9 represents the evaluation of *ST-T change* subjects in terms of confusion matrix, performance validation, and error histogram. Additionally, the target class and input class of confusion matrix defines the accuracy of features mapping.



(a) Confusion matrix



(b) Performance validation



(c) Error histogram

Figure 5.9. MIT-BIH: features mapping of ST-T change subjects

The confusion matrix in figure 5.9(a) shows 100% accuracy of features mapping between target class and output class which means the desired result (target class) and actual result (output class) are completely mapped with zero loss in features matching. Similarly, figure 5.9 (b) narrates the best performance at epoch 0, which indicates the computation complexity value is zero. Figure 5.9 (c) presents an error histogram in terms of error ratio which defines zero error between pattern matching of target class and output class.

Moreover in Scenario 2, the same workflows are applied to *Levels B (nsr)* and *C (afib)* as applied on Scenario 1 (UMMC). The ten subjects of the *nsr* are used on *Level B* and the ten subjects of *afib* are used on *Level C*. *Level B* of Scenario 2 deals with *nsr* subjects and performed on same operational processes as in *Level B* of Scenario 1. Table 5.9 represents the efficiency attributes of A_I , P_+ , S_e , F^{DR} with the help of threshold values of effective R peaks detection algorithm. The high impact findings of efficiency parameters of Table 5.9 are valuable for extraction the features *nsr* subjects and further self-recognition patterns.

Table 5.9: Accuracy of normal sinus rhythm cases (MIT-BIH)

<i>M_Subjects</i>	<i>Lead</i>	<i>Rpeaks</i>	<i>tp</i>	<i>tn</i>	<i>fp</i>	<i>fn</i>	<i>RR</i>	$A_I(\%)$	$P_+(\%)$	$S_e(\%)$	$F^{DR}(\%)$
16265m	LII	95	93	0	0	0	94	100	100	100	0
16272m	LII	69	61	0	0	0	68	100	100	100	0
16420m	LII	95	93	0	0	0	94	100	100	100	0
16773m	LII	80	69	0	0	0	79	100	100	100	0
17052m	LII	70	68	0	0	0	69	100	100	100	0
19088m	LII	33	30	0	0	0	32	100	100	100	0
18177m	LII	54	49	0	1	0	53	98	98	100	2
19140m	LII	79	77	0	0	0	78	100	100	100	0
16483m	LII	198	194	0	2	0	197	98.97	98.97	100	1
19090m	LII	39	32	0	0	0	38	100	100	100	0

Similarly, Table 5.10 highlights the same extracted features (*hr*, *hrv*, *rms-rr*, *sddnn*, *nnrr*, *mt_{on}*, and *mt_{off}*) with the use of Table 5.9 efficiency attributes. These extracted features are further selected the perfect *fc* through using the feature combination algorithm as performed in above *Level B* of Setting I in section 5.4.1.

Table 5.10: Features of normal sinus rhythm cases (MIT-BIH)

<i>M_Subjects</i>	<i>Lead</i>	<i>hr</i>	<i>hrv</i>	<i>sddnn</i>	<i>rmsdd</i>	<i>nn50</i>	<i>mt_{on}</i>	<i>mt_{off}</i>
16265m	LII	22.56	186.2935	0.0093929	0.0068658	0	40.755	40.3082
16272m	LII	16.32	158.8482	0.12556	0.15188	21	40.8732	40.3565
16420m	LII	22.56	186.6801	0.0090762	0.0065583	0	40.7542	40.3079
16773m	LII	18.96	174.594	0.08189	0.092899	15	40.8178	40.3339

<i>M_Subjects</i>	<i>Lead</i>	<i>hr</i>	<i>hrv</i>	<i>sddnn</i>	<i>rmsdd</i>	<i>nn50</i>	<i>mt_{on}</i>	<i>mt_{off}</i>
17052m	LII	16.56	137.1256	0.024099	0.014912	0	40.8807	40.3596
19088m	LII	7.68	711.9254	0.4189	0.64647	9	40.9221	40.3765
18177m	LII	12.72	210.899	0.47634	0.72641	44	40.9144	40.3733
19140m	LII	18.72	183.181	0.12318	0.095162	17	40.816	40.3331
16483m	LII	47.28	690.2563	0.063836	0.1095	194	40.5097	40.2081
19090m	LII	9.12	408.7407	0.62905	0.70339	18	41.023	40.4176

These efficiency attributes of Table 5.9 along with selected fc are used for self-recognition the *nsr* subject's patterns. Figure 5.10 presents the evaluation gages of self-recognition the patterns of *nsr* subject's.

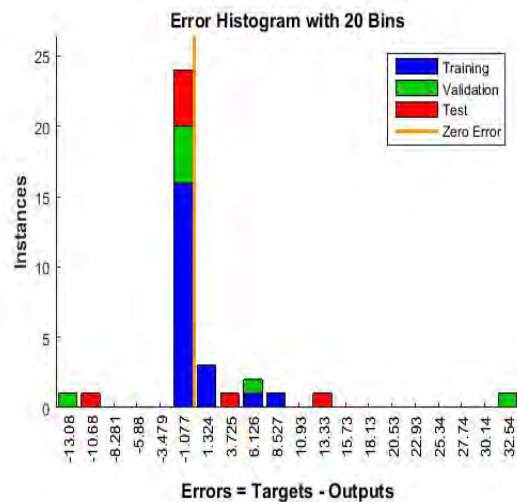
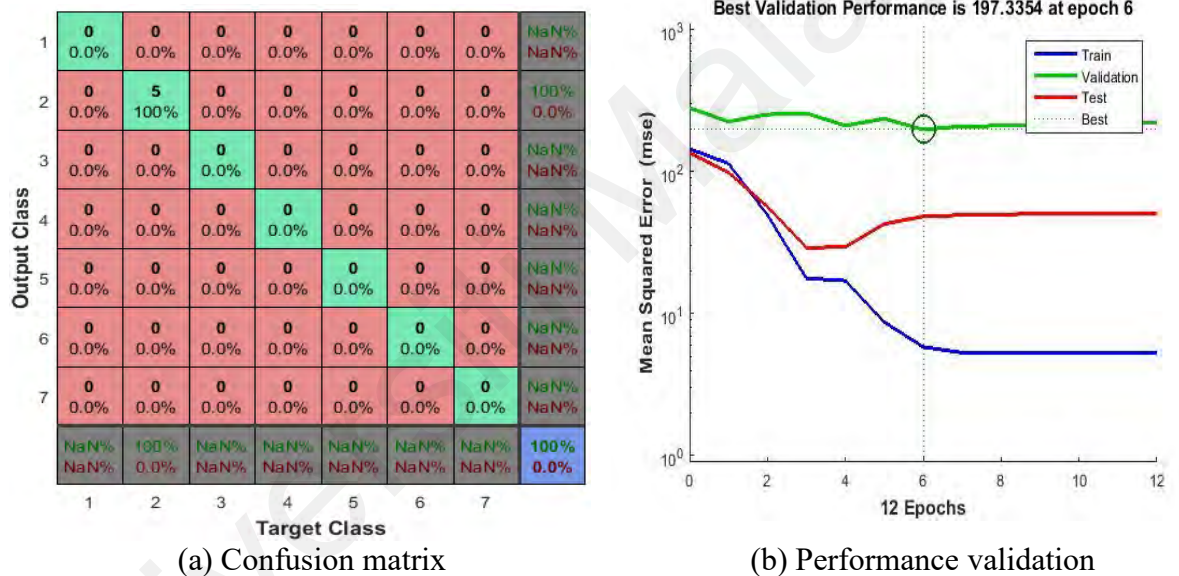


Figure 5.10. MIT-BIH: features mapping of Stage 2 *nsr* subjects

Figure 5.10(a), shows the confusion matrix of 100 % accuracy between target class and input class of selected fc (hr , hrv , $sddn$, $rr-rms$, $nn50$, mt_{on} and mt_{off}). Similar to *Scenario 1* operations, target class defines the desired result and output class indicates the actual gained result. Figure 5.10(b), represents the epoch value is 6 that highlights the least complexity value. Figure 5.10(c), shows the least error ratio of features mapping between target class and output class which shows null value.

Moreover, *Level C* represents the same operational activities performed in the above two levels. Table 5.11 shows the efficiency attributes A_I , P_+ , S_e , F^{DR} of *afib* subjects through threshold values of tp, tn , fp and fn of effective R peaks detecton algorithm. Additionally, Table 5.11 presents the accurate results in terms of efficiency attributes expect the 108 subject of *afib*. Further, Table 5.12 shows the extracted features of *afib* subjects.

Table 5.11: Accuracies of atrial fibrillation cases (MIT-BIH)

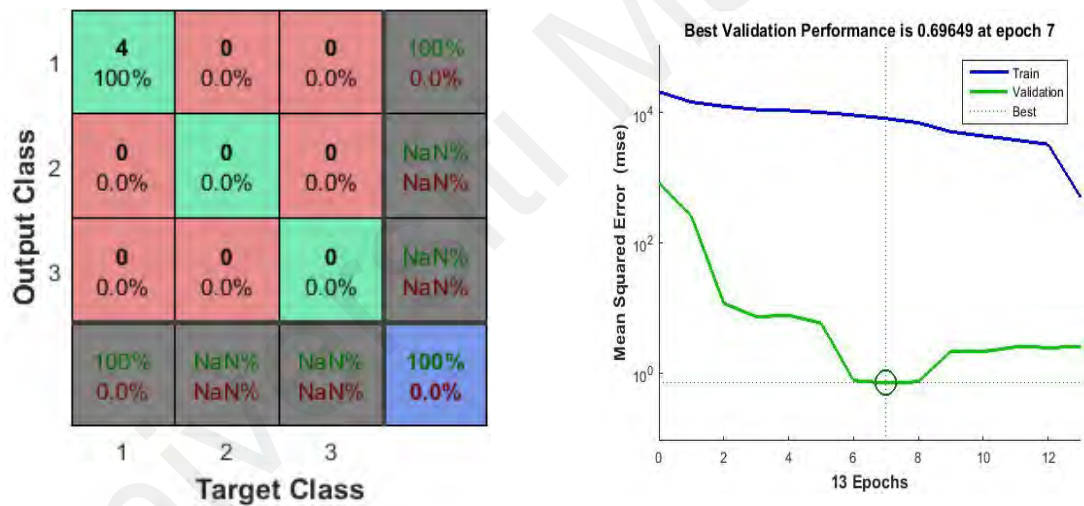
$M_Subjects$	$Lead$	$Rpeaks$	tp	tn	fp	fn	RR	$A_I(\%)$	$P_+(\%)$	$S_e(\%)$	$F^{DR}(\%)$
100	LII	74	72	0	0	0	73	100	100	100	0
101	LII	71	69	0	0	0	70	100	100	100	0
102	LII	112	109	0	0	0	111	100	100	100	0
103	LII	70	69	0	0	0	69	100	100	100	0
104	LII	21	20	0	1	0	21	95.23	95.23	95.23	4.7
105	LII	83	81	1	1	0	82	97.59	97.59	97.59	1.2
106	LII	60	59	0	0	0	59	100	100	100	0
107	LII	93	89	2	1	0	92	95.69	95.69	95.69	1.1
108	LII	1	0	0	0	0	0	nan	nan	nan	Nan
109	LII	89	89	0	0	0	88	100	100	100	0

Table 5.12: Features of atrial fibrillation cases (MIT-BIH)

$M_Subjects$	$Lead$	hr	hrv	$sddnn$	$rmsdd$	$nn50$	mt_{on}	mt_{off}
100	LII	17.52	51.4064	0.054368	0.08011	17	41.438	40.5871
101	LII	16.8	49.2025	0.072767	0.03796	12	41.4706	40.6004
102	LII	26.64	535.2258	0.53796	0.87545	87	41.0321	40.4213
103	LII	16.56	48.7734	0.047941	0.04257	21	41.476	40.6026

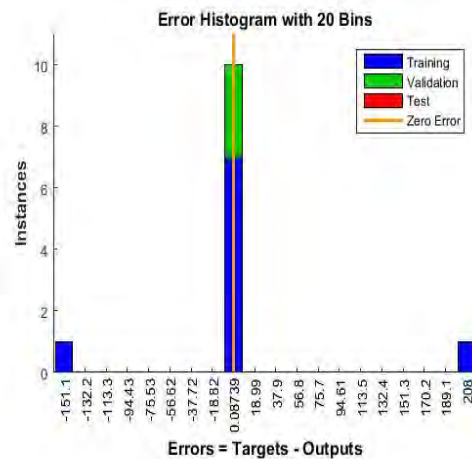
<i>M_Subjects</i>	<i>Lead</i>	<i>hr</i>	<i>hrv</i>	<i>sddnn</i>	<i>rmsdd</i>	<i>nn50</i>	<i>mt_{on}</i>	<i>mt_{off}</i>
104	LII	4.8	304.7539	3.5493	5.765	19	42.1962	40.8966
105	LII	19.68	58.5104	0.12991	0.212	16	41.3556	40.5534
106	LII	14.16	45.966	0.62653	0.87619	29	41.5614	40.6374
107	LII	22.08	140.6103	0.34143	0.37407	62	41.2511	40.5107
108	LII	0	nan	nan	nan	nan	nan	Nan
109	LII	21.12	63.1893	0.1215	0.15158	13	41.3001	40.5308

The extracted features are further selected the suitable fc through using the feature selection algorithm as discussed in above Section 5.2. Similar to above *levels* operations, self-recognition of *afib* subjects are clearly dependent on the findings Table 5.11 and Table 5.12. Figure 5.11 shows the result gages of self-recognition of *afib* subjects.



(a) Confusion matrix

(b) Performance validation



(c) Error histogram

Figure 5.11. MIT-BIH: features mapping of atrial fibrillation subjects

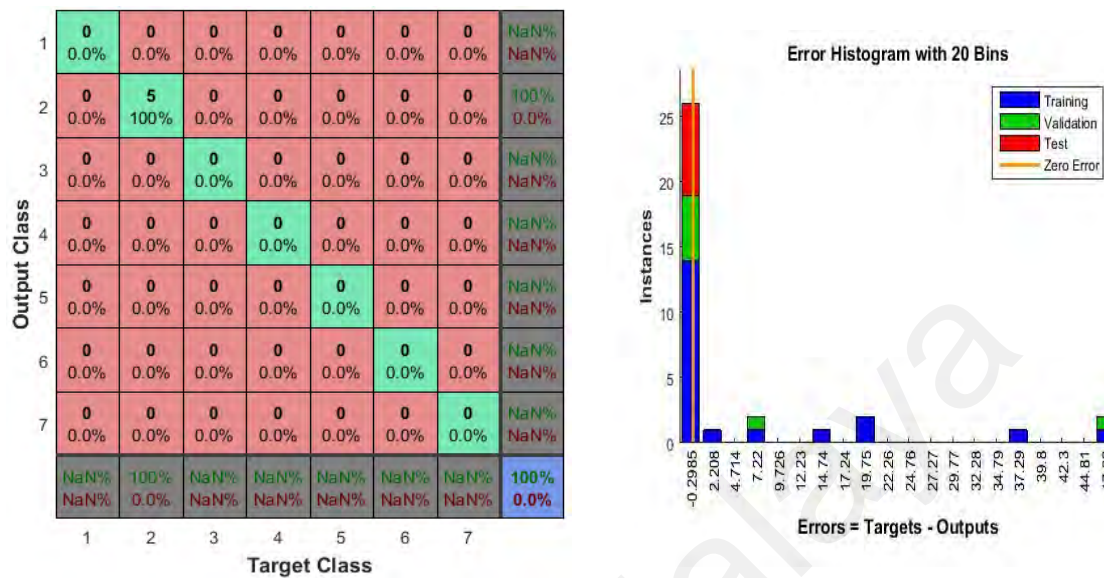
Similar to above *Level's*(*Level A* and *Level B*), The confusion matrix in figure 5.11(a) highlights 100% self-pattern matching accuracy between target class and output class under the usage of three features combination(*hrv, sdn, rr-rms*). Figure 5.11(b) highlights the best performance of *afib* in the form of pattern matching at epoch 7 (least complexity value). Finally, Figure 5.11(c) highlights the zero error ratio in feature matching between target class and output class.

5.4.3 Setting III Results

Moreover, according to proposed DDL model, the data fusion operation is a vital role in this model. The novelty of the DDL method is reflected in the form of the data fusion stage, which is highlighted in Figure 5.2 as Stage 3. The aim of this stage is to efficiently recognize the different feature patterns of the two datasets. In Stage 3, *CASE 1*, *CASE 2* and *CASE 3* belongs to the category of fusion stage where ECG feature streams are fused to highlight the similarities in both dataset. Additionally, in fusion process, target class represented the Stage 2 findings of MIT-BIH dataset (*Scenario 2*), whereas output class highlighted the Stage 2 results of UMMC dataset (*Scenario 1*).

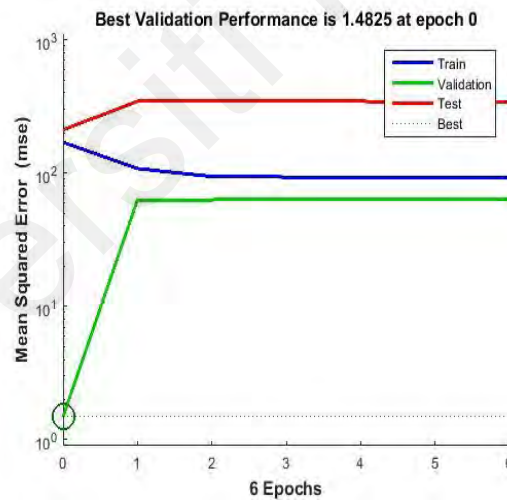
In fusion stage, *CASE 1* narrates the *Level A* of *Scenario 1* is pattern matched with *Level A* of *Scenario 2*. For similarity measurement in *CASE 1*, all extracted features of *flattened T wave* subjects and *ST-T changes* subjects are picked through again feature combination selection algorithm(see Section 5.2) . Furthermore, *CASE 1* delivered the accuracy of more than 99.95% in features pattern recognition through same ANN configuration as used in Stage 2. For other *fc* computational complexity, the detailed discussion is highlighted in next Section (See Section 5.5). *CASE 1* findings is the major contribution of this research which shows the most accurate patterns matching results of *flattened T wave* and *ST-T changes*. Figure 5.12 presents efficiency parameters that

highlight the similarity between *ST-T changes* and *flattened T waves* in context of features mapping between *ST-T changes* subjects and *flattened T wave* subjects



(a) Confusion matrix

(b) Error histogram



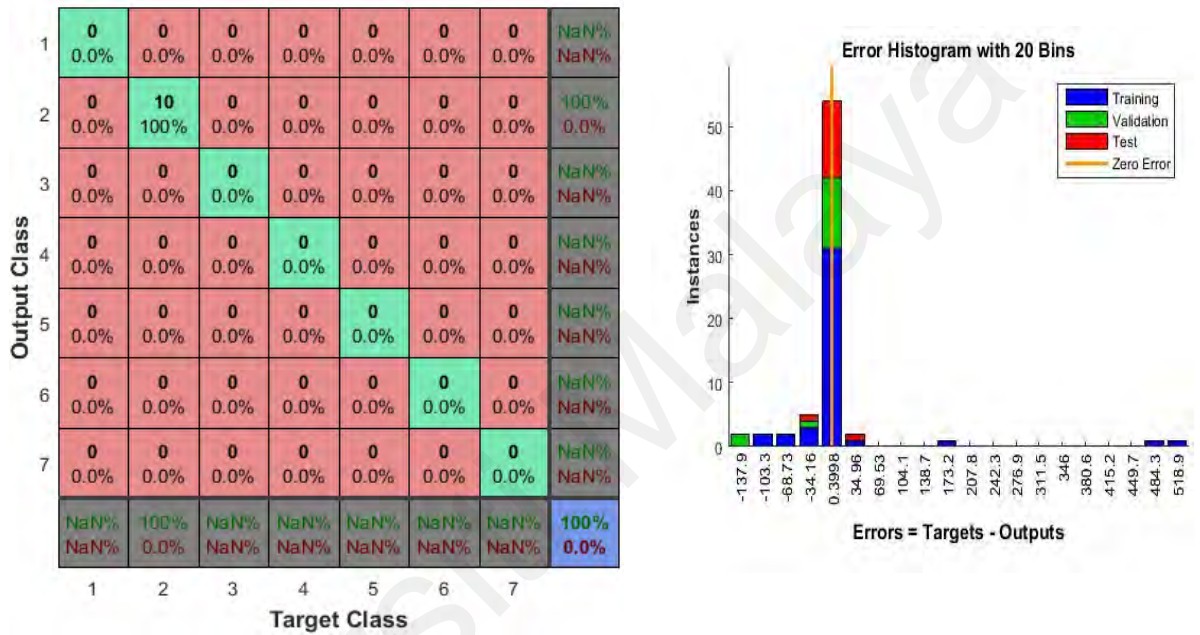
(c) Performance evaluation

Figure 5.12. Efficiency gauges of CASE 1 at Stage 3.

Figure 5.12(a) shows a confusion matrix revealing accuracy of 99.98% matching of feature pattern between target class and output class. Similarly, Figure 5.12(b) shows an approximate zero error ratios (0.02%) of this fusion activity which features accurate mapping between target class and output class. Next, figure 5.12(c) illustrates the

performance evaluation in terms of least computational complex value for features mapping which indicate 0 epoch value.

CASES 2 and 3 adopt the same data fusion process applied to CASE 1 and yielded accuracies of 100% and above than 99.97%, respectively. Figure 5.13 presents efficiency gauges of CASE 2.



(a) Confusion matrix

(b) Error histogram

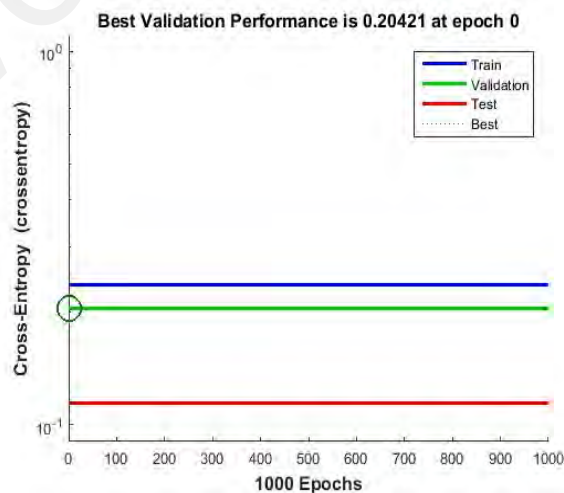


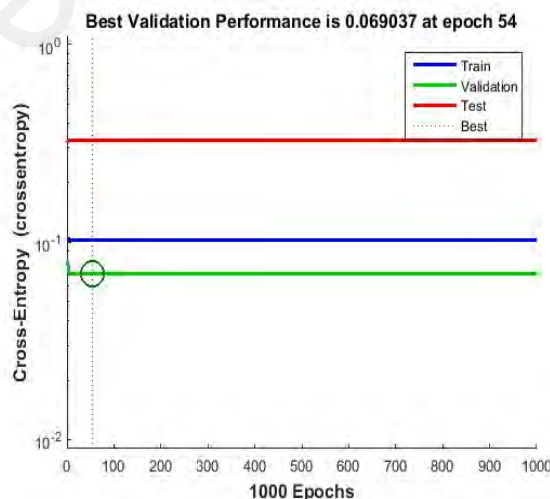
Figure 5.13. Efficiency gauges of CASE 2

In figure 5.13(a), accuracy of 100% in confusion matrix defines the feature matching between target class and output class. Similar to *CASE 1*, target class represents the feature streams of *level B* MIT-BIH dataset (*Scenario 2*) and output class highlights the feature streams of *level B* UMMC dataset (*Scenario 1*). Similarly, figure 5.13(b) present the error ratio features mapping. Figure 5.13(c), define the least computational complex value is epoch 0. Finally, Figure 5.14 highlight efficiency gauges for *CASE 3*.



(a) Confusion matrix

(b) Error histogram



(c) Performance evaluation

Figure 5.14. Efficiency gauges of CASE

The confusion matrix in figure 5.14(a) indicates 99.97% of accuracy which represent accurate map of fc (hrv , $sddnn$ and $rr-rms$) between target class and output class.

Similar to above *CASES 1 and 2*, the features stream of *level C* of MIT-BIT dataset (*Scenario 2*) belongs to the target class and features stream of *level C* of UMMC dataset (*Scenario 1*) represents the output class. Figure 5.14(b) presents the almost zero error ratios (0.03%) between target class and output class operations. Finally, figure 5.14(c), shows the epoch value is 54 which reflects the computation complexity value of feature mapping between target class and output class.

5.4.4 Setting IV

This research investigates how recognition accuracy for different cardiac disease patterns can be enhanced. With this concern, the proposed DDL model is compared with state-of-the-art methods of recognition of the different cardiac diseases (*afib* and MI). In Table 5.14, the result of this comparison clearly highlights the cardiac diseases recognition accuracy of DDL model is bit high as compared to existing methods. A major contribution of this DDL is the pattern matching of *ST-T changes* and *flattened T waves* with 99.98% accuracy and minimal complexity. Secondly, 99.97% accuracy is achieved in pattern recognition of *afib* cases. Moreover, figure 5.15 shows the stage wise accuracies of DDL model.

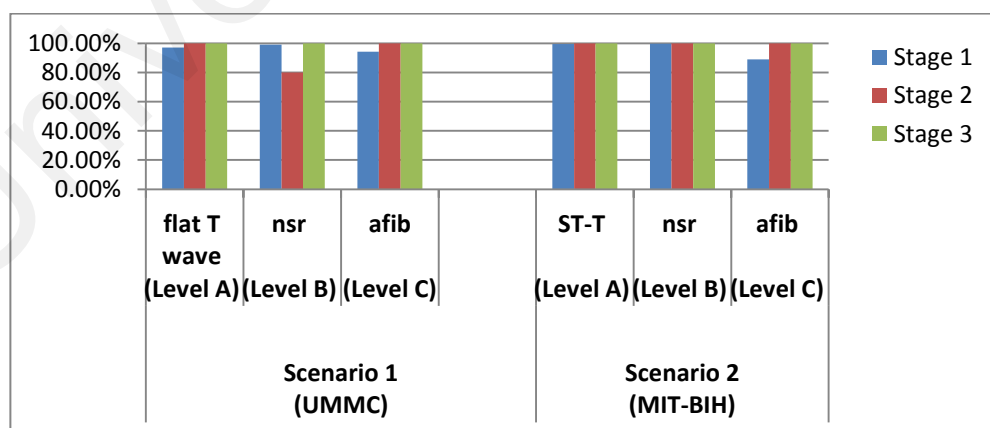


Figure 5.15. Deterministic pattern recognition of both scenarios

Similarly, Table 5.13 highlights all of the DDL results in a stage-wise manner. This table is the second form of a summarized report that describes the proposed DDL model is perfectly suitable for UMMC and MIT-BIH. The validation of this DDL is built on

the basis of global acceptance, namely all the operational investigations are operated on both datasets and get the accurate results.

Table 5.13: Summary of the accuracies of the deterministic pattern recognition method (DDL)

<i>Subjects</i>	<i>Scenario 1 (UMMC)</i>			<i>Scenario 2 (MIT-BIH)</i>		
	<i>Stage 1</i>	<i>Stage 2</i>	<i>Stage 3</i>	<i>Stage 1</i>	<i>Stage 2</i>	<i>Stage 3</i>
ST Segment Changes	-----	-----	-----	99.49%	100%	99.98%
Normal Sinus Rhythm	98.95%	80%	100%	99.69%	100%	100%
Atrial Fibrillation	94.29%	100%	99.97%	88.88%	100%	99.97%
Flattened T wave	97.04%	100%	99.98%	-----	-----	-----

In Table 5.14, results generated using the current DDL method were satisfactory which means the proposed method is far better than previous state-of-the-art methods.

Table 5.14: Comparison of the proposed deterministic pattern recognition method

<i>Comparative results of DDL with different methods</i>						
<i>Sr</i>	<i>Method</i>	<i>Type of malfunction detection</i>	<i>Dataset</i>	<i>Subjects Size</i>	<i>Year</i>	<i>Accuracy Level</i>
1	Feature Extraction-NN (Karthik et al., 2019)	Atrial Fibrillation	MIT-BIH	10 afib	2018	80.00%
2	BSS-Fourier (Prasad & Sahambi, 2003)	Atrial Fibrillation, Atrial Flutter, Myocardial Infarction	MIT-BIH	10 afib, 3 afl, 10MI	2003	85.04%
3	MOE (Hu, Palreddy, & Tompkins, 1997)	Atrial Fibrillation, Premature Ventricular Contraction, Myocardial Infarction	MIT-BIH	8 afib 19 pvc 5 MI	1997	94.00%
4	Deep CNN detection (Acharya, Fujita, Oh, et al., 2017)	Automated Myocardial infarction Detection	MIT-BIH	10 MI (st-t anomalies) 11 MI (t wave)	2017	95.22%
5	FFT-ANN (Gothwal et al., 2011)	Myocardial Infarction	MIT-BIH	10MI	2011	98.48%
6	Pattern Recognition App (Nikan et al., 2017)	Myocardial Infarction, Premature Ventricular Contraction	MIT-BIH	10 MI 19 pvc	2017	98.99%
7	<i>Proposed DDL</i>	<i>Myocardial Infarction (Flattened T wave and ST-T)</i>	<i>UMMC,</i>	<i>10 flattened T wave (MI)</i> <i>6 afib</i>	<i>2018</i>	<i>99.98%</i>
		<i>Normal Sinus Rhythm</i>	<i>MIT-BIH</i>	<i>10 St-t(MI)</i> <i>10 afib</i>		<i>100%</i>
		<i>Atrial Fibrillation</i>		<i>10 St-t(MI)</i> <i>10 afib</i>		<i>99.97%</i>

*** afl (atrial flutter), pvc (premature ventricular contraction)

5.5 Deep Critical Analysis

Results of the DDL method are significant only if the selection of features is accurate and least computational complex. Therefore, crosscheck the different feature combinations on Stage 2 and Stage 3 of DDL method. Overall, efficient results are produced after cross-checking both stages (Stages 2 and 3) by using different combination of features. The accuracy level in all stages almost reached a satisfactory level for diagnostic purposes of the three cardiac states. In Appendix-A, a table of the critical analysis (features selection) results based on different combinations of features is shown. The next discussion is about the time complexity in context of computational complex factor.

The results of DDL method are validating through deep critical analysis which means change the various factors to monitor the performance of the *ANN*. In terms of time complexity or computational complexity, the dependencies between the factors of performance (*perf*), time (*sec*), epoch(*eph*), gradient (*grad*), and validation (*valid*) are also a part of this critical analysis activity. Based on the literature and state-of-the-art methods, the relationship between performance (*perf*) and gradient (*grad*) is direct which means that if the performance is at a good level, the stage gradient is also a satisfactory one.

The discussion of critical analysis is performed in a systematic manner, which is similar to the experimental flow of the whole DDL method except that of Stage 1. Different feature combinations are applied on fusion cases which represent the validation of DDL results. A figure 5.16 to 5.18 shows the fusion cases.

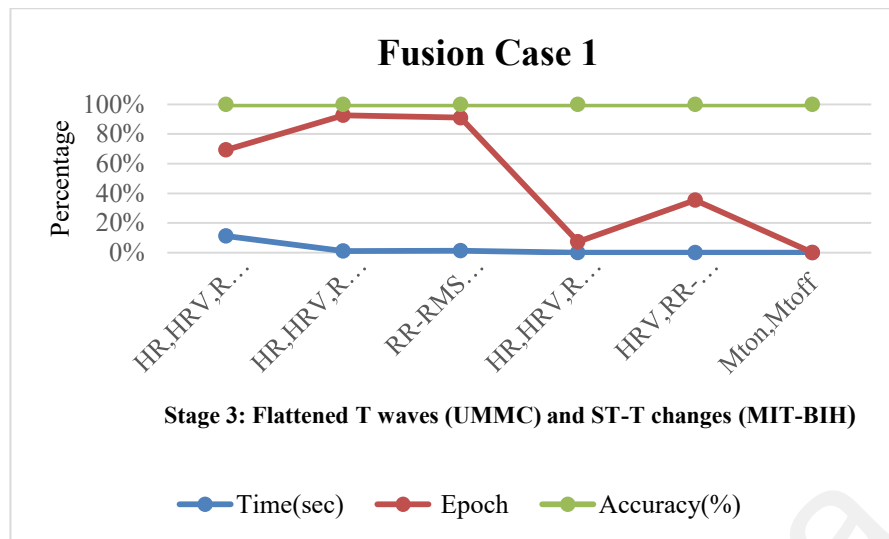


Figure 5.16. Case 1: Complexity between flattened T waves and ST-T changes

The first subset of the critical analysis of data fusion activity is reflected in Figure 5.16. In figure 5.16, the pattern matching with different time domain features almost reached a satisfactory level. The concern of this critical analysis is time complexity. The last mt_{on} and mt_{off} feature combination is the best in terms of time complexity (epoch rate is almost zero) and $grad$ factor is optimal. The combination of five features are the worst cases in terms of complexity factor due to the increased rate of the epoch.

Data fusion of Cases 2 and 3 highlight the same story in terms of best time complexity factors, such as in Figure 5.17. The least time complexity combination is mt_{on} and mt_{off} , which indicates the best result (epoch rate of almost zero). In the worst-case scenario, the combinations of five features, four features, and three features yield high rates of complexity factor (epochs with 1,000 peak level). In Figure 5.18, the combinations of seven, five, and three features are the worst due to their high rate of epochs. By contrast, the combination of two features is the best, similar to the above cases.

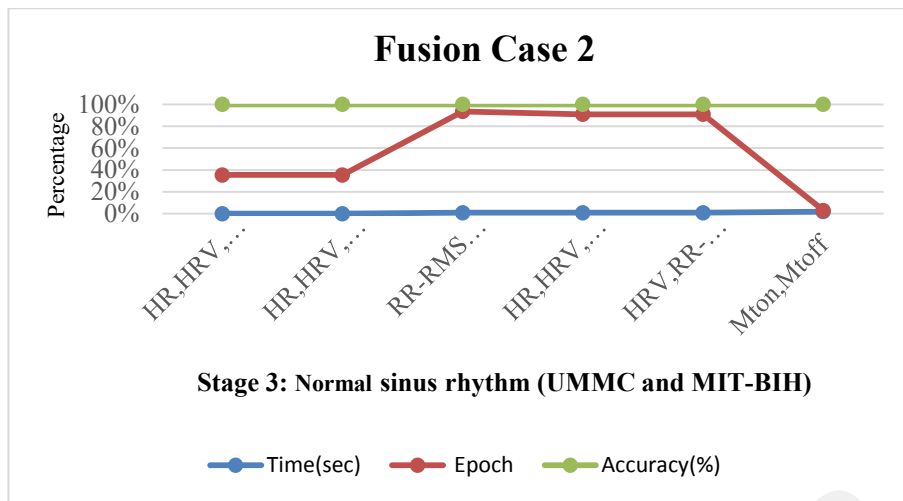


Figure 5.17. Case 2: Complexity between both *nsr* subjects (UMMC and MIT-BIH)

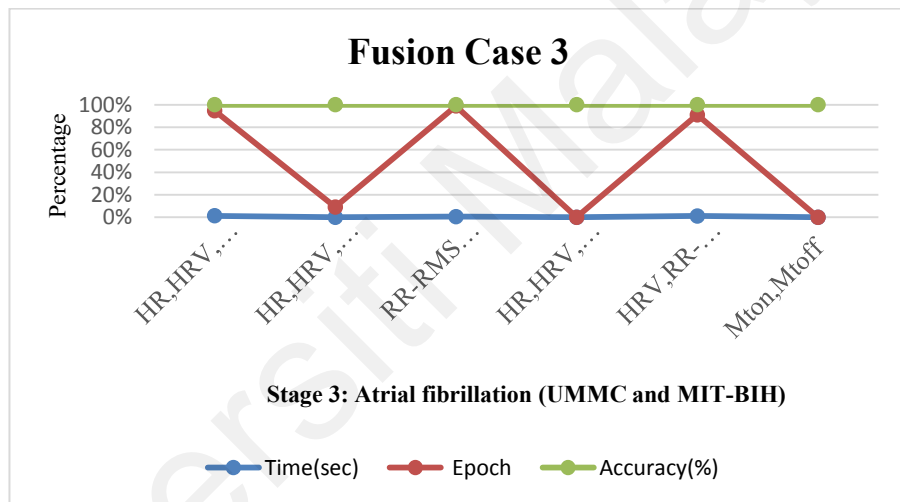
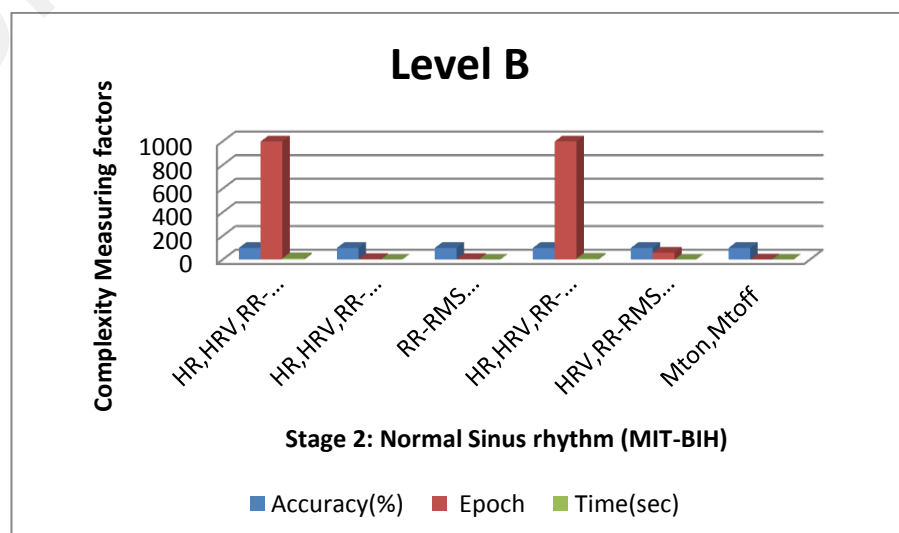
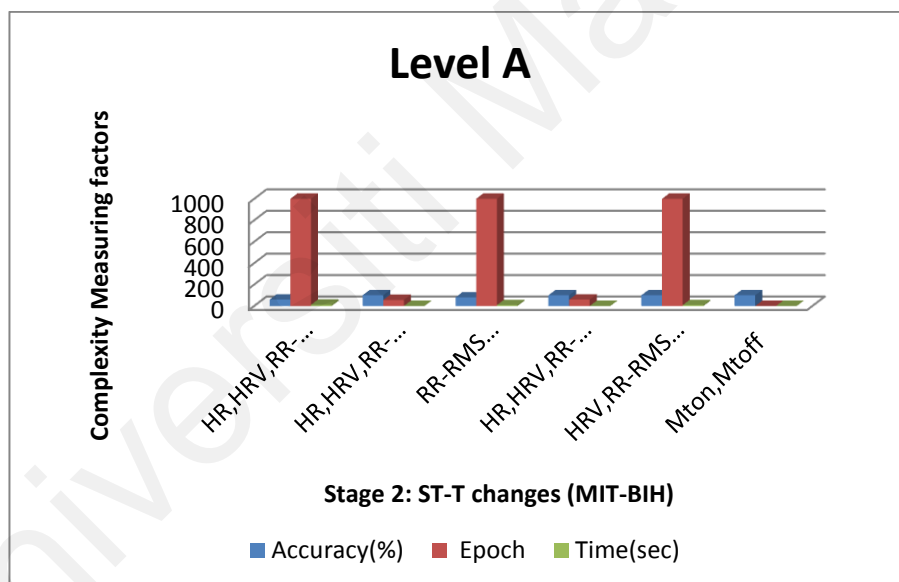


Figure 5.18. Case 3: Complexity between both *afib* subjects (UMMC and MIT-BIH)

5.5.1 Discussion

This section covers the scanning process of DDL method through keen observations in context of complexity factor. Figure 5.19 and Figure 5.20 shows two different categories of MIT-BIH and UMMC. Figure 5.19 highlights the workflow of the three different levels of MIT-BIH. In *Level A*, the operational processes are applied to six different feature combinations. According to the scope of the critical analysis, the complexity factor is least in the last combination (mt_{on} and mt_{off}), and similar to the previous results of Stage 3 as highlighted in figure 5.16. As long as the concern is the

high complexity rate of *Level A*, the combination of the first, third, and fifth features yields a high value, and an epoch with a value of 1,000 is obtained. Similarly, *Levels B* and *C* in Figure 5.19 highlights the same best complexity factor discussed in previous results (see Figure 5.17 and Figure 5.18). The feature combination of mt_{on} and mt_{off} delivers the best results when compared with other combinations. The epoch values that almost reach the zero level reflect the best conditions of time complexity. By contrast, at *Level B*, the worst cases, with a high rate of epoch that reaches level 1,000 include combination of the first and fourth features. At *Level C* in Figure 5.19, all feature combinations result in an epoch level of 1,000 except the last combination (mt_{on} and mt_{off}).



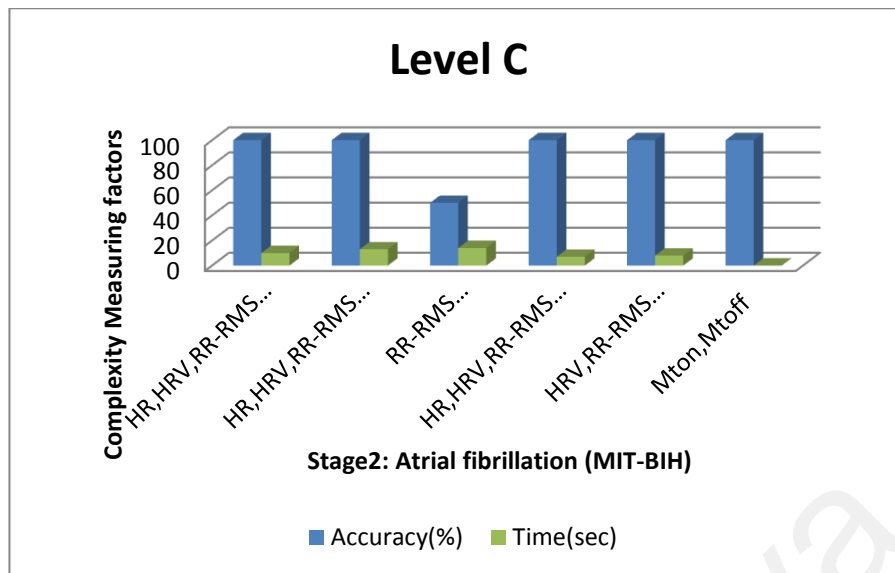


Figure 5.19. Stage 2 (MIT-BIH): Complexity measurement and pattern matching of all levels (*ST-T changes, nsr, and afib*)

Figure 5.20 shows a workflow similar to Figure 5.19 which is applied on Stage 2 of the UMMC dataset. At *Level A* of the *flattened T wave*, feature combination of mt_{on} and mt_{off} is the best in terms of time complexity. Figure 5.20 also shows that the combination of the first, third, and fifth features is the worst case in the context of time complexity.

With regard to time complexity of the other UMMC levels, combination of the last two features (mt_{on} and mt_{off}) in *Level B* is the least time complex. By contrast, the combination of first and fourth features is the worst in terms of complexity due to the high epoch (1,000 epochs). Finally, *Level C* of *afib* presents the same scenario in terms of best complexity ratio as observed in above levels of Figure 5.19, but in the scenario of the worst condition all other feature combinations represent 1000 epochs level. Due to similarity concern of epoch level in worst conditions, we ignored the epoch representation in *Level C* of Figure 5.20.

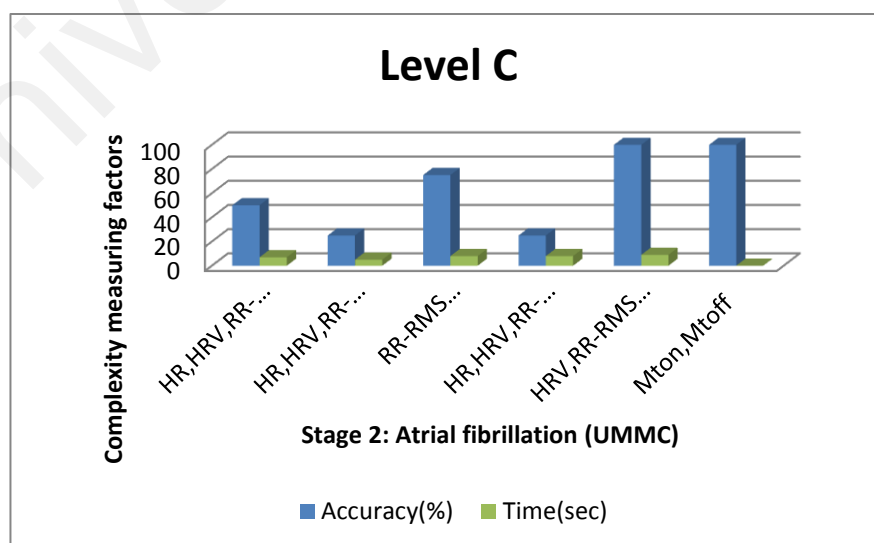
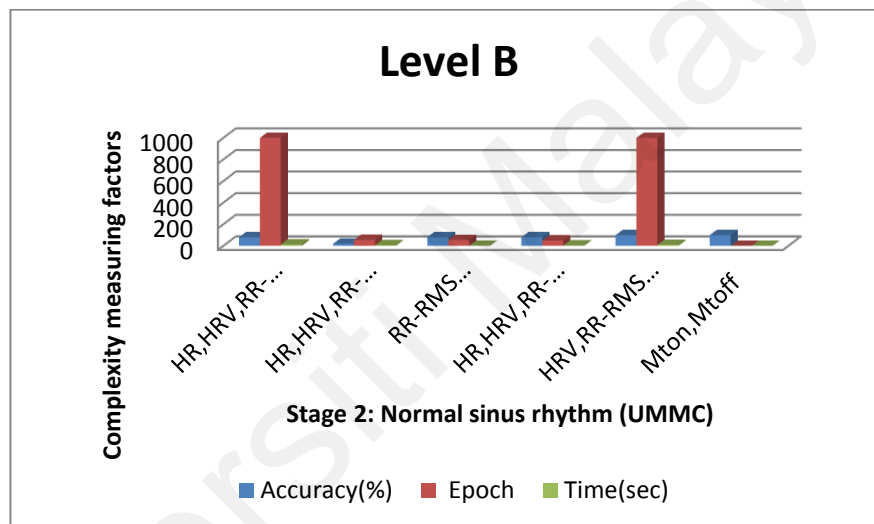
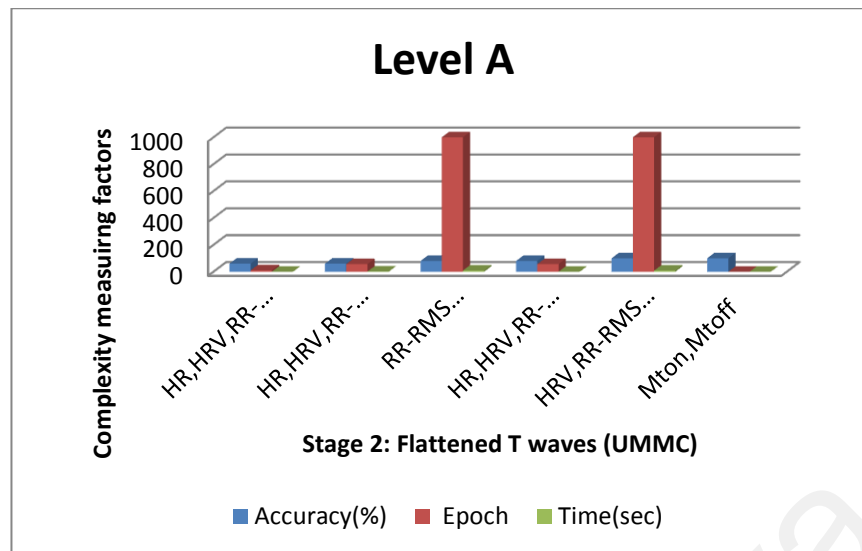


Figure 5.20. Stage 2 (UMMC): Complexity measurement and pattern matching of all levels (*flattened T wave, nsr, and afib*)

After critical analysis of DDL method, it was observed that the features mt_{on} and mt_{off} in all stages and levels was found to be the most ideal in terms of accuracy and least epoch values as compared with other feature combinations. However, this analysis lacks to discuss the net error of whole ANN in DDL which plays a vital role in evaluation of the complexity and accuracy factors.

Therefore, the next section discusses the mathematical evaluation of DDL operations in terms of net error estimation of whole ANN via an error measurement of feed forward propagation and backward propagation along with constant weights

5.6 Complexity evaluation via mathematical model

This section covers the mathematical evaluation of proposed DDL model by calculating the computational complexity in perspective of cost function (CF) which is associated with the measurement of Mean square error (MSE) on the biases of epoch values. For computational complexity calculation, the low MSE and epoch values highlight the minimum CF value and conversely high values of MSE and epoch indicates the maximum CF value(Garza-Ulloa, 2018). In DDL model, the systematic operations are performed on two different datasets with two successive stages of Multi-layer perceptron's (MLP) or ANN. This is used under the concepts of deterministic learning theory(Cong Wang & Hill, 2007). The weights of whole neural model are based on constant input feed by using the deterministic learning (see above Section 5.3.2). It is used to recognize the cardiac diseases. Additionally, pre-defined arranged feature set size by using the different fc as discussed in above Section 5.3.1(see Appendix–A for six fc). Such different fc 's provides the CF by compute the MSE and epoch value of MLP in DDL model. The net CF is measured by following the outcomes of ECG anomalies are categorized as DDL

5.6.1 Feed Forward Propagation

According to DDL model, the five hidden layers are utilized for operational activities. Firstly, in feed forward propagation, the output of hidden layer is calculated through sigmoid function $f(ln)$ by using input feed (x), biased value (b), and the constant weights (W_c) at one input cycle, as presented in equation 5.11 and equation 5.12. Figure 5.21 further narrates both these equations (5.11 and 5.12).

$$In = W_c \cdot x_1 \cdot b + W_c \cdot x_2 \cdot b + \dots W_c \cdot x_n \cdot b \quad (5.11)$$

$$f(ln) = \frac{1}{1+e^{-ln}} \quad (5.12)$$

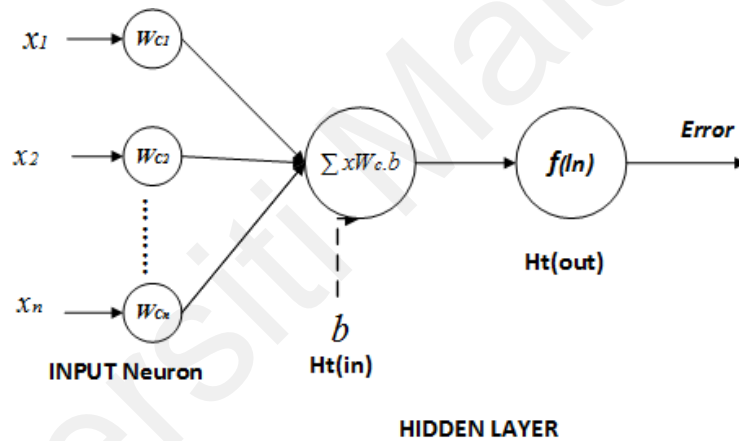


Figure 5.21. View of input and hidden layers in feed forward propagation

According to figure 5.21, error estimation of each five hidden layers adjust a platform for error calculation at output layer in DDL feed forward propagation. For starting the error estimation on hidden layers, in equation 5.13, $H_{t1}(in)$ represents the given input of first hidden layer with constant weight W_c , biased value $b1$ and input feed $x(i)$ where i represents number of features that used in different fc . By following equation 5.14 is a sigmoid function which represents the output of first hidden layer ($H_{t1}(out)$).

$$H_{t1}(in) = W_c \sum_{i=2}^n x(i) \cdot b1 \quad , \quad (5.13)$$

$$H_{t1}(out) = \frac{1}{1+e^{-H_{t1}(in)}} \quad (5.14)$$

Similar to above equation 5.13, in equation 5.15, $(H_{t2}(in))$ represents the given input of second hidden layer with biased value $b2$ and input feed $x(i)$. Furthermore, equation 5.16 is a sigmoid function $(H_{t2}(out))$ which represents the output of second hidden layer.

$$H_{t2}(in) = W_c \sum_{i=2}^n x(i).b2 \quad (5.15)$$

$$H_{t2}(out) = \frac{1}{1+e^{-H_{t2}(in)}} \quad (5.16)$$

Like the first two hidden layers, equation 5.17 highlights the given input of third hidden layer $(H_{t3}(in))$ with biased value $b3$. Equation 5.18 highlight the sigmoid function $(H_{t3}(out))$ as an output of third hidden layer.

$$H_{t3}(in) = W_c \sum_{i=2}^n x(i).b3 \quad (5.17)$$

$$H_{t3}(out) = \frac{1}{1+e^{-H_{t3}(in)}} \quad (5.18)$$

Moreover, equation 5.19 shows the input $(H_{t4}(in))$ of forth hidden layer with biased value $b4$ and equation 5.20 highlighted the output $(H_{t4}(out))$ of fourth hidden layer

$$H_{t4}(in) = W_c \sum_{i=2}^n x(i).b4 \quad (5.19)$$

$$H_{t4}(out) = \frac{1}{1+e^{-H_{t4}(in)}} \quad (5.20)$$

Lastly, equation 5.21 highlight input of fifth hidden layer $(H_{t5}(in))$ and equation 5.22 represents the output of fifth layer $(H_{t5}(out))$.

$$H_{t5}(in) = W_c \sum_{i=2}^n x(i).b5 \quad (5.21)$$

$$H_{t5}(out) = \frac{1}{1+e^{-H_{t5}(in)}} \quad (5.22)$$

In error estimation of feed forward propagation, the next phase is to highlight the status of feature patterns recognized (r) or unrecognized (ur) through output layer that are measured with results of five hidden layers. With this concern, in equation 5.23 represents the input portion at Output layer (Out_{in}) for r status that is equal to calculated sum of outputs of five hidden layer ($\sum_{k=1}^5 h_{tk}(out)$), where k represents the number of hidden layers that are up to five hidden layers. Out_r highlight the recognized output through sigmoid function. Along with features pattern recognition status, the error is calculated through equation 5.24

$$Out_{in} = W_c \sum_{k=1}^5 h_{tk}(out) \quad (5.23)$$

$$Out_r := \frac{1}{1+e^{-Out_{in}}} \quad (5.24)$$

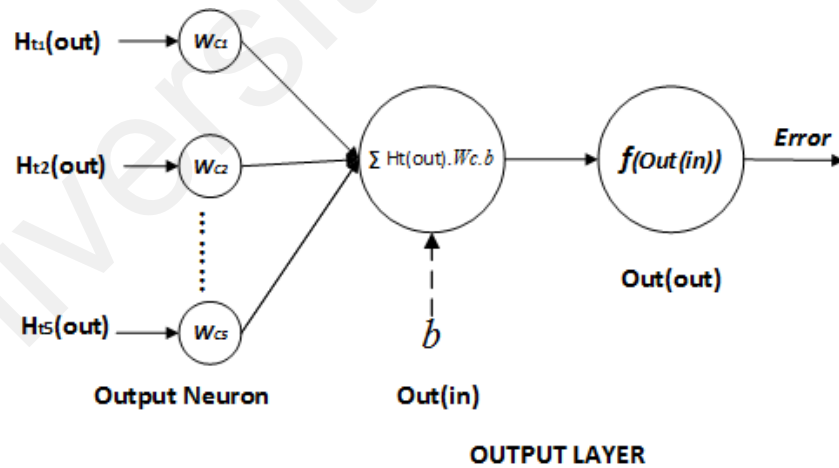


Figure 5.22. View Output layer in feed forward propagation

The next step is error calculation at features recognition status which represented in equation 5.25

$$Error_r = \sum \frac{1}{2} (T.Out_r - A.Out_r)^2 \quad (5.25)$$

Where, $T.Out_r$ represents the Target output of recognition status and $A.Out_r$ shows the Actual output of recognition status.

Similar to feature recognition status, equation 5.26 and equation 5.27 shows the findings for ur status and then equation 5.28 highlight the error calculated for unrecognized pattern matching

$$Out_{in} = W_c \sum_{k=1}^5 h_{tk}(out) \quad (5.26)$$

$$Out_{ur} = \frac{1}{1+e^{-Out_{in}}} \quad (5.27)$$

$$Error_{ur} = \sum \frac{1}{2} (T.Out_{ur} - A.Out_{ur})^2 \quad (5.28)$$

Finally, calculate the net or total error at feed forward propagation through the sum up of the error rate of recognized and unrecognized outputs. Such summation is represented in equation 5.29 highlighting the net error that provides direction to calculate the backward propagation errors.

$$Error_{(total)} = Error_r + Error_{ur} \quad (5.29)$$

5.6.2 Backward propagation

For measuring CF of MLP structure in DDL model, next phase is to calculate net error of back ward propagation at output layer with the constant weights (W_c). The total error of forward propagation ($Error_{(total)}$) partially derivates with respect to constant weight W_c in equation 5.30 by using the Chain rule(Lv et al., 2018)

$$\frac{\partial Error_{(total)}}{\partial W_c} = \frac{\partial Error_{(total)}}{\partial Out_r} * \frac{\partial Out_r}{\partial net_r} * \frac{\partial net_r}{\partial W_c} \quad (5.30)$$

Above chain rule in equation 5.30 is segmented into three parts, equation 5.31 represent the solved form of first segment where total calculated error($Error_{(total)}$) is partial derivate with respect to output of the recognized features pattern (Out_r) (Wee, Min, Arooj, & Supriyanto, 2010)

$$\frac{\partial Error_{(total)}}{\partial Out_r} = (T. Out_r - A. Out_r) \quad (5.31)$$

Next, equation 5.32 highlighted the solved form of equation 5.30 second segment, where output of recognized features pattern (Out_r) partial derivatives with respect to network of recognized status (net_r),

$$\frac{\partial Out_r}{\partial net_r} = Out_r(1 - Out_r) \quad (5.32)$$

Furthermore, the two segments in form of equation 5.31 and equation 5.32 are added in equation 5.30 along with solution of third segment. As a result of addition, below equation 5.33 highlights the net error gain of recognized output.

$$\frac{\partial Error_{(total)}}{\partial W_c} = [T. Out_r - A. Out_r] * [Out_r(1 - Out_r)] * Out_r \quad (5.33)$$

Similarly, same procedure is followed for calculation of the net error for unrecognized output in backward propagation as followed in equations 5.30 to 5.33. With net error concern of unrecognized output, equation 5.34 highlights the partial derivate of total net error ($Error_{(total)}$) with respect to constant weight W_c through using the chain rule.

$$\frac{\partial Error_{(total)}}{\partial W_c} = \frac{\partial Error_{(total)}}{\partial Out_{ur}} * \frac{\partial Out_{ur}}{\partial net_{ur}} * \frac{\partial net_{ur}}{\partial W_c} \quad (5.34)$$

Equation 5.35 shows the expansion of chain rule same like equation 5.31 and equation 5.32

After the chain rule expansion of equation 5.34, below equation 5.35 is the explanatory form of net error calculated ($Error_{(total)}$) at unrecognized output.

$$\frac{\partial Error_{(total)}}{\partial W_{kc}} = [T. Out_{ur} - A. Out_{ur}] * [Out_{ur}(1 - Out_{ur})] * Out_{ur} \quad (5.35)$$

Furthermore, in backward propagation, these net error estimations for both recognized and unrecognized output status is further useful for error measurement of five hidden layers

Hidden layer: Next phase in back propagation is to measure the net error on hidden layers of DDL model. Firstly, estimate the error of first hidden layer (Ht_1). For error estimation Ht_1 , equation 5.36 shows the total error is partial derivate with respect to constant weight which is measured through use of chain rule(Lv et al., 2018; Ngia & Sjöberg, 2000)

$$\frac{\partial Error_{(total)}}{\partial W_c} = \frac{\partial Error_{(total)}}{\partial Out_{Ht_1}} * \frac{\partial Out_{Ht_1}}{\partial net_{Ht_1}} * \frac{\partial net_{Ht_1}}{\partial W_c} \quad (5.36)$$

To measure the net error at first hidden layer, first segment of equation 5.36 total error is partial derivate with respect to output of first hidden layer ($\frac{\partial Error_{(total)}}{\partial Out_{Ht_1}}$) that is further segmented into two parts in equation 5.37. In equation 5.37, the total error of recognized status ($Error_r$) partial derivate with respect to output of first hidden layer (Out_{Ht_1}) sums up to partial derivate total error unrecognized status ($Error_{ur}$) with respect to output of first hidden layer (Out_{Ht_1}).

$$\frac{\partial Error_{(total)}}{\partial Out_{Ht_1}} = \frac{\partial Error_r}{\partial Out_{Ht_1}} + \frac{\partial Error_{ur}}{\partial Out_{Ht_1}} \quad (5.37)$$

Furthermore, these two segments of equation 5.37 are reflected in equation 5.38 and equation 5.39. Whereas, total $Error_r$ partial derivate with respected to Out_{Ht_1} is computed with the help of below expansion by using the chain rule.

$$\frac{\partial Error_r}{\partial Out_{Ht_1}} = \frac{\partial Error_r}{\partial Out_r} * \frac{\partial Out_r}{\partial net_{Ht_1}} * \frac{\partial net_{Ht_1}}{\partial Out_{Ht_1}} \quad (5.38)$$

Similarly, equation 5.39 represented second segmented of equation 5.37 that compute the net error for unrecognized $Error_{ur}$ is partially derivate with respect Out_{Ht_1} . So, compute the net $Error_{ur}$ via below chain rule formation.

$$\frac{\partial Error_{ur}}{\partial Out_{Ht_1}} = \frac{\partial Error_{ur}}{\partial Out_{ur}} * \frac{\partial Out_{ur}}{\partial net_{Ht_1}} * \frac{\partial net_{Ht_1}}{\partial Out_{Ht_1}} \quad (5.39)$$

Finally, below equation 5.40 is the complete form of net error computation at first hidden layer in backward propagation by merging the equations 5.37 to 5.39 in equation 5.36.

$$\frac{\partial Error_{(total)}}{\partial W_c} = \left[\left[\left(\frac{\partial Error_r}{\partial Out_r} * \frac{\partial Out_r}{\partial net_{Ht_1}} * \frac{\partial net_{Ht_1}}{\partial Out_{Ht_1}} \right) + \left(\frac{\partial Error_{ur}}{\partial Out_{ur}} * \frac{\partial Out_{ur}}{\partial net_{Ht_1}} * \frac{\partial net_{Ht_1}}{\partial Out_{Ht_1}} \right) \right] * \frac{\partial Out_{Ht_1}}{\partial net_{Ht_1}} * \frac{\partial net_{Ht_1}}{\partial W_c} \right] \quad (5.40)$$

Moreover, second hidden layer compute the net error in same way as computed first hidden layer. For second hidden layer(Ht_2), the below highlighted equation 5.41 computes the partial derivate of $Error_{(total)}$ with respect constant weight W_c . Such computation is performed with the help of chain rule as discussed in above equation 5.36.

$$\frac{\partial Error_{(total)}}{\partial W_c} = \frac{\partial Error_{(total)}}{\partial Out_{Ht_2}} * \frac{\partial Out_{Ht_2}}{\partial net_{Ht_2}} * \frac{\partial net_{Ht_2}}{\partial W_c} \quad (5.41)$$

Like Ht_1 above operations, equations from 5.42 to 5.44 is the expansion of equation 5.41 for second hidden layer (Ht_2). For more detail, the highlighted equation 5.42 represents the partial derivate of $Error_{(total)}$ with respect to output of Ht_2 (Out_{Ht_2}) which is equal to sum of partial derivatives of $Error_r$ with respect to Out_{Ht_2} and partial derivate of $Error_{ur}$ with respect to output of Out_{Ht_2} .

$$\frac{\partial Error_{(total)}}{\partial Out_{Ht_2}} = \frac{\partial Error_r}{\partial Out_{Ht_2}} + \frac{\partial Error_{ur}}{\partial Out_{Ht_2}} \quad (5.42)$$

The first segment of equation 5.42 narrates the partial derivative of recognized state error with respect to output of Ht_2 . In below equation 5.43 highlighted the first segment of equation 5.42 that is computed by applying chain rule, like as we discussed in Ht_1 (see equation 5.38).

$$\frac{\partial Error_r}{\partial Out_{Ht_2}} = \frac{\partial Error_r}{\partial Out_r} * \frac{\partial Out_r}{\partial net_{Ht_2}} * \frac{\partial net_{Ht_2}}{\partial Out_{Ht_2}} \quad (5.43)$$

Similarly, equation 5.44 in below computes the net error of unrecognized state with respect to output of Ht_2 through applying chain rule, like as we discussed in Ht_1 (see equation 5.39).

$$\frac{\partial Error_{ur}}{\partial Out_{Ht_2}} = \frac{\partial Error_{ur}}{\partial Out_{ur}} * \frac{\partial Out_{ur}}{\partial net_{Ht_2}} * \frac{\partial net_{Ht_2}}{\partial Out_{Ht_2}} \quad (5.44)$$

Lastly, below equation 5.45 is the updated version of equation 5.41 after merging of equations 5.42 to 5.44, like as discussed in above (see equation 5.40).

$$\frac{\partial Error_{(total)}}{\partial W_c} = \left[\left[\left(\frac{\partial Error_r}{\partial Out_r} * \frac{\partial Out_r}{\partial net_{Ht_2}} * \frac{\partial net_{Ht_2}}{\partial Out_{Ht_2}} \right) + \left(\frac{\partial Error_{ur}}{\partial Out_{ur}} * \frac{\partial Out_{ur}}{\partial net_{Ht_2}} * \frac{\partial net_{Ht_2}}{\partial Out_{Ht_2}} \right) \right] * \frac{\partial Out_{Ht_2}}{\partial net_{Ht_2}} * \frac{\partial net_{Ht_2}}{\partial W_{kc}} \right] \quad (5.45)$$

Next, same procedure is followed for net error rate of third hidden layer (Ht_3) as followed in above for above Ht_1 and Ht_2 . Equation 5.46 represents the total error is partial derivate with respect to constant weight for estimation error rate at Ht_3 by using chain rule.

$$\frac{\partial Error_{(total)}}{\partial W_c} = \frac{\partial Error_{(total)}}{\partial Out_{Ht_3}} * \frac{\partial Out_{Ht_3}}{\partial net_{Ht_3}} * \frac{\partial net_{Ht_3}}{\partial W_c} \quad (5.46)$$

Afterward, below equation 5.47 is the primary part of equation 5.46 that represents the sum up of recognized error state and unrecognized error state at the output of Ht_3 like we discussed in Ht_1 and Ht_2 (see equation 5.37 and equation 5.42).

$$\frac{\partial Error_{(total)}}{\partial Out_{Ht_3}} = \frac{\partial Error_r}{\partial Out_{Ht_3}} + \frac{\partial Error_{ur}}{\partial Out_{Ht_3}} \quad (5.47)$$

Similar to above hidden layers (t_1 and Ht_2), equation 5.48 presents the net error of recognized state is partial derivate with respect to output at Ht_3 through using the chain rule.

$$\frac{\partial Error_r}{\partial Out_{Ht_3}} = \frac{\partial Error_r}{\partial Out_r} * \frac{\partial Out_r}{\partial net_{Ht_3}} * \frac{\partial net_{Ht_3}}{\partial Out_{Ht_3}} \quad (5.48)$$

Onwards, equation 5.49 presents the net error of unrecognized state at Ht_3 with compute the below expression of chain rule like as discussed in first two hidden layers.

$$\frac{\partial Error_{ur}}{\partial Out_{Ht_3}} = \frac{\partial Error_{ur}}{\partial Out_{ur}} * \frac{\partial Out_{ur}}{\partial net_{Ht_3}} * \frac{\partial net_{Ht_3}}{\partial Out_{Ht_3}} \quad (5.49)$$

Equation 5.50 in below is the expanded version of equation 4.6, same as above expanded equations like equation 5.40 and equation 5.45.

$$\frac{\partial Error_{(total)}}{\partial W_c} = \left[\left(\frac{\partial Error_r}{\partial Out_r} * \frac{\partial Out_r}{\partial net_{Ht_3}} * \frac{\partial net_{Ht_3}}{\partial Out_{Ht_3}} \right) + \left(\frac{\partial Error_{ur}}{\partial Out_{ur}} * \frac{\partial Out_{ur}}{\partial net_{Ht_3}} * \frac{\partial net_{Ht_3}}{\partial Out_{Ht_3}} \right) \right] * \frac{\partial Out_{Ht_3}}{\partial net_{Ht_3}} * \frac{\partial net_{Ht_3}}{\partial W_{kc}} \quad (5.50)$$

Furthermore, from equation 5.51 to equation 5.54 highlight the computation of net error rate of fourth hidden layer (Ht_4) same as above hidden layers.

$$\frac{\partial Error_{(total)}}{\partial W_c} = \frac{\partial Error_{(total)}}{\partial Out_{Ht_4}} * \frac{\partial Out_{Ht_4}}{\partial net_{Ht_4}} * \frac{\partial net_{Ht_4}}{\partial W_c} \quad (5.51)$$

Similarly, below equation 5.52 highlighted the sum up of recognized and unrecognized states partial derivate with respect to output of Ht_4 .

$$\frac{\partial Error_{(total)}}{\partial Out_{Ht_4}} = \frac{\partial Error_r}{\partial Out_{Ht_4}} + \frac{\partial Error_{ur}}{\partial Out_{Ht_4}} \quad (5.52)$$

Equation 5.53 narrates the first segment of equation 5.52. In equation 5.53, computes the partial derivate of recognized error state with respect to output of Ht_4 .

$$\frac{\partial Error_r}{\partial Out_{Ht_4}} = \frac{\partial Error_r}{\partial Out_r} * \frac{\partial Out_r}{\partial net_{Ht_4}} * \frac{\partial net_{Ht_4}}{\partial Out_{Ht_4}} \quad (5.53)$$

Similar to computation of recognized state error in equation 5.53, below equation 5.54 highlights the second segment of equation 5.52 and computed the net error of unrecognized state output error through applying the chain rule as performed in above hidden layers (see equation 5.39, equation 5.44 and equation 5.49).

$$\frac{\partial Error_{ur}}{\partial Out_{Ht_4}} = \frac{\partial Error_{ur}}{\partial Out_{ur}} * \frac{\partial Out_{ur}}{\partial net_{Ht_4}} * \frac{\partial net_{Ht_4}}{\partial Out_{Ht_4}} \quad (5.54)$$

Additionally, below equation 5.55 is the expanded form of equation 5.51 just like first three hidden layers.

$$\frac{\partial Error_{(total)}}{\partial W_c} = \left[\left(\frac{\partial Error_r}{\partial Out_r} * \frac{\partial Out_r}{\partial net_{Ht_4}} * \frac{\partial net_{Ht_4}}{\partial Out_{Ht_4}} \right) + \left(\frac{\partial Error_{ur}}{\partial Out_{ur}} * \frac{\partial Out_{ur}}{\partial net_{Ht_4}} * \frac{\partial net_{Ht_4}}{\partial Out_{Ht_4}} \right) \right] * \frac{\partial Out_{Ht_4}}{\partial net_{Ht_4}} * \frac{\partial net_{Ht_4}}{\partial W_c} \quad (5.55)$$

Moreover, from equation 5.56 to equation 5.60 narrates the computation of net error rate of fifth hidden layer (Ht_5) are same as we discussed in above hidden layers

$$\frac{\partial Error_{(total)}}{\partial W_c} = \frac{\partial Error_{(total)}}{\partial Out_{Ht_5}} * \frac{\partial Out_{Ht_5}}{\partial net_{Ht_5}} * \frac{\partial net_{Ht_5}}{\partial W_c} \quad (5.56)$$

$$\frac{\partial Error_{(total)}}{\partial Out_{Ht_5}} = \frac{\partial Error_r}{\partial Out_{Ht_5}} + \frac{\partial Error_{ur}}{\partial Out_{Ht_5}} \quad (5.57)$$

$$\frac{\partial Error_r}{\partial Out_{Ht_5}} = \frac{\partial Error_r}{\partial Out_r} * \frac{\partial Out_r}{\partial net_{Ht_5}} * \frac{\partial net_{Ht_5}}{\partial Out_{Ht_5}} \quad (5.58)$$

$$\frac{\partial Error_{ur}}{\partial Out_{Ht_5}} = \frac{\partial Error_{ur}}{\partial Out_{ur}} * \frac{\partial Out_{ur}}{\partial net_{Ht_5}} * \frac{\partial net_{Ht_5}}{\partial Out_{Ht_5}} \quad (5.59)$$

$$\frac{\partial Error_{(total)}}{\partial W_{kc}} = \left[\left(\frac{\partial Error_r}{\partial Out_r} * \frac{\partial Out_r}{\partial net_{Ht_5}} * \frac{\partial net_{Ht_5}}{\partial Out_{Ht_5}} \right) + \left(\frac{\partial Error_{ur}}{\partial Out_{ur}} * \frac{\partial Out_{ur}}{\partial net_{Ht_5}} * \frac{\partial net_{Ht_5}}{\partial Out_{Ht_5}} \right) \right] * \frac{\partial Out_{Ht_5}}{\partial net_{Ht_5}} * \frac{\partial net_{Ht_5}}{\partial W_c} \quad (5.60)$$

Finally, the MSE of whole MLP is measurement through feed forward propagation and back propagation net errors for each feature combination (fc).

5.6.3 Determinate Cost function:

This section proceeds the results of feed forward propagation (section 5.6.1) and backward propagation (section 5.6.2) for each defined fc (see Appendix-A for feature combinations). Next, the CF is measured by calculating the MSE and epoch values of whole MLP structure by summation the net error of feed forward propagation (FFP) and backward propagation (BWP) for one input feed means one defined fc . Therefore, equation 5.61 represents the $\Delta Error$ that is sum of net FFP error and BWP net error.

$$\Delta Error = FFP (Error_{(total)}) + BWP (Error_{(total)}) \quad (5.61)$$

Thus, equation 5.62 given below highlights the MSE of each selected fc (see Section 5.2 for algorithm of feature combination selection). In equation 5.62, $T.Error$ represents the target error and $\Delta Error$ shows the actual error of whole MLP as highlighted in equation 6.61

$$MSE = \frac{1}{2} \sum (\Delta Error - T.Error)^2 \quad (5.62)$$

Furthermore, the learning rate (α) lies in range of 0.0 to 1.0 that delivers different neural model response with respect to different learning rate values. The learning rate is set according to state-of-the-art approach, means smaller α requires more epoch values that means more computational complex and larger the α requires less epoch values which means low computational complex (Kim, Shin, Shin, & Lee, 2009). However, DDL model follows the convention of MLP structure like, the upgradation of weights and α associated with defined condition means adjust optimal α value with constant weights (Ghongade & Ghatol, 2008; Kandil, Khorasani, Patel, & Sood, 1993; Lai et al.,

2019). In DDL, the optimal α value with constant weights delivered the least computational complex plus accurate recognition results. Below equation 5.63 summarized the above statements; equation 5.63 represents the next input feed that take other fc with upgraded constant weights (W_{c+1}).

$$W_{c+1} = W_c - \alpha \cdot \sum_{j=fc}^{fcn} \left(\frac{\partial Error_{(total)}}{\partial W_c} \right)_j \quad (5.63)$$

Above equation 5.63 highlighted the constant weights upgradation (W_{c+1}) of whole MLP structure for other fc (another input feed) along with optimal change of α value.

To further support the computational complexity or CF of DDL, below graphical representation (figure 5.23 and figure 5.24) of DDL and deep learning (DL) models summarized the complexity factor and other parameters. Figure 5.23 narrates the CF of DDL against different fc factors with optimal α value, whereas fcn is the defined feature combination of DDL which highlight the least CF (least MSE and epoch value) for features pattern recognition process along with high accuracy ratio. For more detail of CF against different defined fc factor, the epoch values (CF) of each fc is highlighted in critical analysis of feature selection in DDL(see Appendix-A)

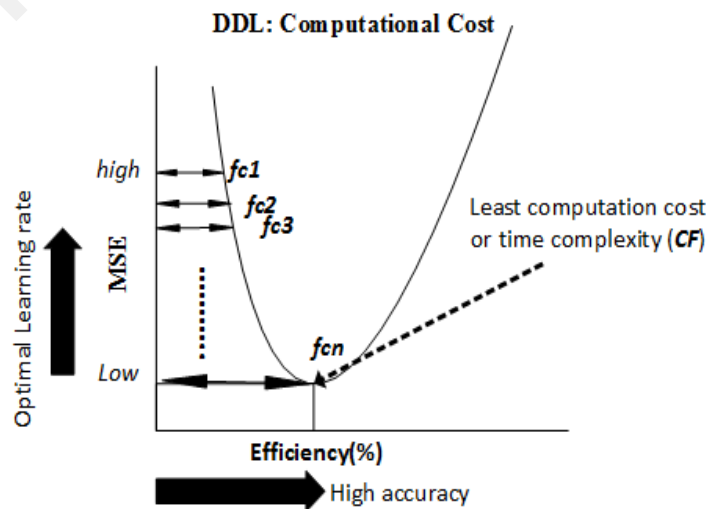


Figure 5.23. Computation Complexity representation of DDL

Similarly, in figure 5.24 highlights the *CF* of different DL models that is quite high due to the low α value. However, different DL models contributed the high accuracy ratio in ECG features recognition (recognition of different cardiac diseases).

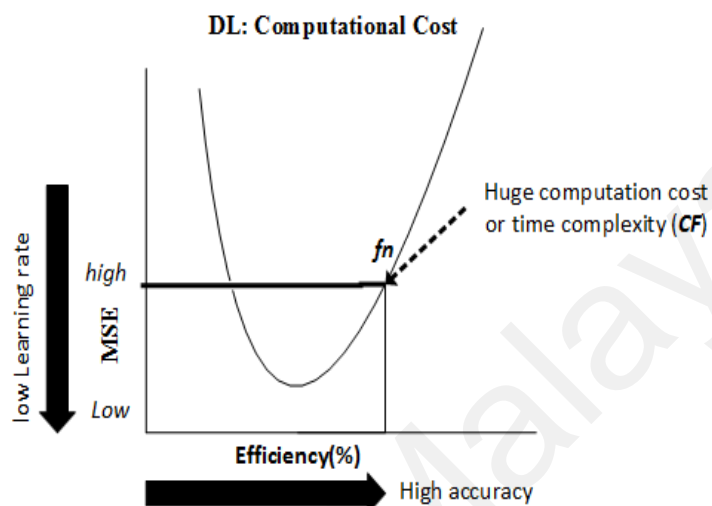


Figure 5.24. Computational Complexity representation of DL

Finally, Table 5.15 highlights the comparison of DDL with different DL models. Such comparison is the critical step of evaluation which highlights the significance of DDL in context of computation cost along with high accuracy ratio.

Table 5.15: DDL computation complexity comparison

<i>Deep Deterministic Learning vs Deep Learning models</i>						
<i>References</i> (DL models)	<i>MI</i>			<i>Afib</i>		
	<i>Dataset</i>	<i>CF(Eph)</i>	<i>Acc</i>	<i>Dataset</i>	<i>CF(Eph)</i>	<i>Acc</i>
(Buscema, Grossi, Massini, Breda, & Della Torre, 2020)	<i>N.A</i>	<i>N.A</i>	<i>N.A</i>	MIT-BIH	1000	95%
(Acharya, Oh, et al., 2017)	<i>N.A</i>	<i>N.A</i>	<i>N.A</i>	MIT-BIH	20	94.03%
(Acharya, Fujita, Oh, et al., 2017)	PTB	60	95.22 %	<i>N.A</i>	<i>N.A</i>	<i>N.A</i>
(Baloglu et al., 2019)	PTB	100	99.00%	<i>N.A</i>	<i>N.A</i>	<i>N.A</i>
(Oh, Ng, San Tan, & Acharya, 2018)	MIT-BIH	150	98.10%	<i>N.A</i>	<i>N.A</i>	<i>N.A</i>
The proposed work (DDL)	MIT-BIH, UMMC	57	99.98%	MIT-BIH, UMMC	1	99.97%

**Eph(Number of epoch value), Acc(Accuracy), CF(Cost Function)

According to table 5.15, the accuracy and epoch value (computation complexity or CF) findings of DDL are far better than other existing methods. In MI case, the factors of epoch value (57) and accuracy (99.98%) of DDL shows efficient results as compared to other existing methods. Similarly, in afib case, the factors of epoch value (0) and accuracy(99.97%) of DDL presents much better results as compared to other existing methods.

5.6.4 Big O Notation Calculation

This section covers the validation of computational complexity or CF in context of measuring the Big O notation of proposed DDL and state-of-the-art DL models that highlighted in table 5.15. From literature survey, Big O notation are measured the upper bound of the algorithm and is dependent on the size of input that is provided on the particular algorithm or model and time taken for operations of input(Bae, 2019; Chivers & Sleightholme, 2015). From instance (Imtiaz, Mardell, Saremi-Yarahmadi, & Rodriguez-Villegas, 2016), two state-of-the-art algorithms OSEA(open source ECG analysis) and low SNR identification are compared on the accuracy and Big O notation for computational complexity. OSEA algorithm highlighted the linear time Big O notation that is $O(n)$, where n is the input size and low SNR identification algorithm represented the Big O notation in terms of $O(\log n)$.

Moreover, time series classification (TSC) via deep learning models that are used in existing studies highlight the Big O notation(upper bound) as $O(N^2T^4)$, $O(N^2T^3)$ and $O(N^2)$, where N defines the size of dataset and T shows the length of the time series(number of samples)(Ismail Fawaz, Forestier, Weber, Idoumghar, & Muller, 2019; Ismail Fawaz et al., 2020; Schäfer, 2015). Table 5.16 summarized the existing approaches that measured the Big O notations.

Table 5.16: Big O notations of existing approaches

References	Approach	Big O Notation
(Ismail Fawaz et al., 2019)	TSC (CNN)	$O(N^2T^4)$
(Ismail Fawaz et al., 2020)	TSC(Shapelet transform) TSC(Elastic Ensemble) TSC(BOSS)	$O(N^2T^4), O(N^2T^3)$ $O(N^2)$
(Schäfer, 2015)	TSC(BOSS)	$O(N^2)$
(Imtiaz et al., 2016)	OSEA Algorithm , low SNR identification algorithm	$O(n), O(\log n)$

**BOSS (Bag-of-SFA-Symbols), CNN(convolution neural network)

Furthermore from different instances (Brand, Peng, Song, & Weinstein, 2020; Du, Poczós, Zhai, & Singh, 2019; Zhang, Martens, & Grosse, 2019), different gradient decent methods are employed in MLP structure and highlighted the complexity as $O(mn), O(mn^2), O(m)$ where n is input size and m belongs to width of neural network or MLP. In proposed DDL, optimal gradient descent value along with minimum epoch values (see Algorithm feature selection combination) defines the complexity factor and Big O highlighted as a $O(nmd)$, Where n is the input size(number of selected features), m is the width of MLP(number of neurons) and d are used for classification purposes. So, the Big O notation of DDL model is measured through Equation 5.64 and Big O for state-of-the-art DL models in Table 5.15 measured the Big O notations of Table 5.16.

$$O(nmd) \tag{5.64}$$

To measure the Big O notation of DDL for MI and afib, equation 5.64 and use Big O notations of Table 5.16 to measure the state-of-the-art DL models that highlighted in Table 5.15. Table 5.17 highlighted the state-of-the-art comparison of Big O values of

DL models with proposed DDL model by using the same existing DL models of Table 5.15.

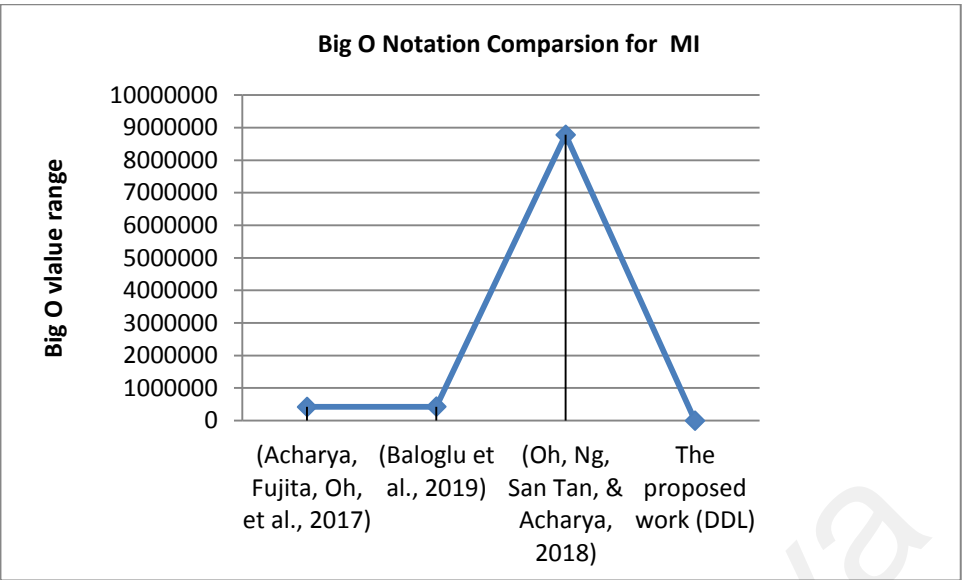
Table 5.17: Comparison of Big O notations for MI and afib

Big O Notation for MI				
Reference	N/d	T/n	Big O Notations and findings	Accuracy
(Acharya, Fujita, Oh, et al., 2017)	650	0.7	$O(N^2T^4) = 101442.25$ $O(N^2T^3) = 144917.5$ $O(N^2) = 422500$	95%
(Baloglu et al., 2019)	651	0.56	$O(N^2T^4) = 42095.47$ $O(N^2T^3) = 74426.23$ $O(N^2) = 423801$	99%
(Oh, Ng, San Tan, & Acharya, 2018)	2963	0.9	$O(N^2T^4) = 5760144.0009$ $O(N^2T^3) = 6400160.001$ $O(N^2) = 8779369$	98.10%
The proposed work (DDL)	6	0.7 m=10	$O(mnd) = 42$	99.98%
Big O Notation for afib				
Reference	N/d	T/n	Big O Notations and findings	Accuracy
(Buscema, Grossi, Massini, Breda, & Della Torre, 2020)	250	0.5	$O(N^2T^4) = 3906.25$ $O(N^2T^3) = 7812.5$ $O(N^2) = 62500$	95%
(Acharya, Oh, et al., 2017)	1250	0.9	$O(N^2T^4) = 1025156.25$ $O(N^2T^3) = 113962.5$ $O(N^2) = 1562500$	94.30%
The proposed work (DDL)	3	0.7 m=10	$O(mnd) = 21$	99.97%

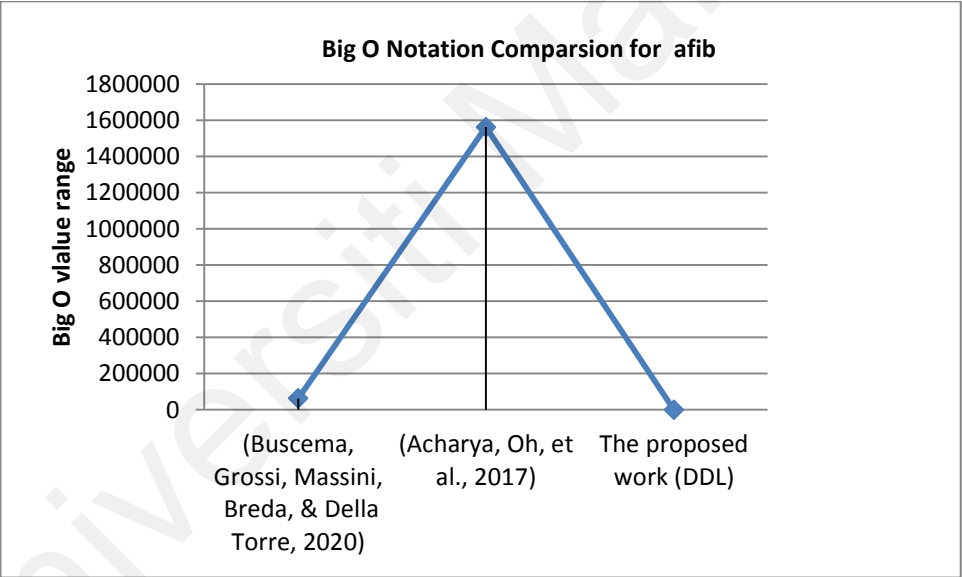
**N(number of samples),d(number of features),T /n (number of training dataset size), m(width of MLP)

According to Table 5.17, proposed DDL Big O value of MI is the best case as compared to other existing DL models that means DDL is least time or computational complexity. Similarly, proposed DDL model for afib also shows the best case in terms of Big O notation as compared to existing DL models.

Figure 5.25 (a) and Figure 5.25 (b) represents the summary of Table 5.17 which clearly highlighted the proposed DDL model is the least computational complex than other DL models.



(a) Big O for MI



(a) Big O for afib

Figure 5.25. Representation of Big O notation for MI and afib

Moreover, the valuable findings of DDL are further cross validate in prediction classification approach by using other public dataset(PTB) and UMMC dataset in next Chapter 6.

5.7 Conclusion

This chapter presented an effective deep deterministic learning model approach to recognize the different cardiac diseases from ECG data streams. Furthermore, in deep deterministic learning model a unique feature selection scheme is followed for recognition of different cardiac diseases. It was discovered that the proposed pattern recognition architecture empowered with deep deterministic learning model performed significantly well and achieved the higher accuracy (i.e. more than 98%) when compared with existing state of the art techniques. The results of proposed effective model highlighted the more accurate as well as robust as compared with existing methods (see Table 5.14 and Table 5.15). Such impressive results of proposed model are critically discussed (see Section 5.5) and then validates the robust factor of proposed model by mathematical evaluation, the computational complexity factor (see Section 5.6). Hence, to cross look such impressive results in different context through induction of different public dataset and predictive classification approach. Predictive classification model is proposed for cross look the impressive results of DDL and presented in Chapter 6.

CHAPTER 6: PROPOSED MODEL-DRIVEN DEEP DETERMINISTIC LEARNING FOR PREDICTIVE CLASSIFICATION

6.1 Introduction

This Chapter presents the Model Driven Deep Deterministic Learning (MDDDL) structural model that exploits the predictive classification of similarity between *flattened T wave* subjects (UMMC dataset) with time domain features pattern matching of *T wave alternans*(TWA) subjects(PTB dataset). This similarity index measures the predictive classification which helps in early diagnosis of the nature of Myocardial Infarction (MI). The section 6.2 and section 6.3 presents the complete operational activities description of MDDDL which includes the feature engineering in subsection 6.3.1. Section 6.4 covers the different form of MDDDL results that include the data fusion activities in subsection 6.4.1. These fusion activities are further drilled down into two settings, namely Setting I in subsection 6.4.1.1 and Setting II in subsection 6.4.1.2. Furthermore, the critical analysis is present in section 6.5 that covers the overlook for fusion activities results with different features combination. Section 6.6 covers the evaluation scheme of MDDDL through statistical diagnostic test evaluation and state-of-the-art comparison. Subsection 6.6.1 presents the statistical diagnostic test evaluation that is performed through different parameters of *MedCalc* software. Similarly, subsection 6.6.2 highlights the comparison of MDDDL with state-of-the-art predictive classification methods. Finally, this chapter concludes in section 6.7 with discussion of limitations and future work in MDDDL.

6.2 Model-Driven Deep Deterministic Learning

In the history of ECG features identification, the robust accurate classification techniques and methods of different cardiac diseases are already proposed in number of studies (Limaye & Adegbija, 2018; Ravi et al., 2017), but there are still some ambiguities in classifying process of these cardiac diseases that in the form of feature dependences factor (Mastoi, Wah, Raj, & Iqbal, 2018). However, the predictive classifications of these cardiac diseases are useful and will be further helpful for early diagnosis of these diseases. Similarly, predictive classification of MI with different ECG features plays a vital role in early diagnosis of the nature of MI. With the concern of early diagnosis through predictive classification, some cardiac diseases require special attention due to the risk factor namely, tachycardia cases, premature ventricular contraction, and different shapes of MI (Stub et al., 2015). Therefore, an early diagnosis with predictive classification of such cardiac problems helps the physicians in providing better treatment for cardiac patients. Similarly, predictive classification with similarity measurement of *flattened T wave* and other T wave anomalies is the most crucial step for early diagnosis the nature of MI.

In current era, deep learning (DL) techniques are normally used for recognition and predicative classification of different ECG features. In predictive classification of well-known MI cases, a Model Driven Deep Learning (MDDL) approach is a most suitable approach for the prediction of defined paradigm (Xu & Sun, 2018). However, to measure the predictive ratio of flattened anomalies, need some sort of predefined steps required to predict these anomalies. (Merode, Molema, & Goldschmidt, 2004). In predefined context; the concept of DDL is more suitable that already proposed in Chapter 5.

This Chapter presents the novel MDDDL method which is designed for the similarity based predictive classification between *flattened T wave* and T wave alternans(TWA) subjects. Furthermore, the formation of MDDDL is constructed after detail review of DL techniques. In DL techniques, the detection of different cardiac diseases is performed by skipping the feature engineering phases, thereby facilitating the reduction of the complexity factor. However, in actual cases, a particular paradigm for the identification of these cardiac diseases that might increase the complexity factor, such as extensive time, is necessary for the complete execution of convolutional neural network (CNN), recurrent neural network (RNN)and probabilistic neural network (PNN) models(Acharya, Fujita, Oh, et al., 2017; Acharya, Oh, et al., 2017; Ravi et al., 2017). By contrast, the DDL approach (See Chapter 5) is executed on the basis of pre-defined steps along with the feature engineering phase. The complexity factor of DDL is much lower relative to that of DL (See Section 5.6), and DDL is suitable for the identification of such anomalies that have no prior record. In this Chapter, a unique structure is designed in the form of an MDDDL, which achieves similarity based predictive classification of *flattened T waves*. The different feature fusion process of DDL is introduced in MDDDL for predictive classification with parametric MDDL structure. Moreover, the feature of the MDDL is replicated in MDDDL for the predicative classification of *flattened T wave*. A list of contributions is summarised below.

- 1) A novel MDDDL is constructed for the similarity based predictive classification of *flattened T waves* by using the feature fusion theme of DDL.
- 2) Extensive level feature exploration is introduced for the predictive classification of *flattened T waves* with the inclusion of a new feature namely, mean T-wave peak (mt_{pk}).

- 3) Deep traditional and newly derived feature combinations are included in fusion activities for the identification of the least complex combination of predictive classification of different T-wave anomalies (mt_{on} , mt_{off} and mt_{pk} are the least complex combinations in all scenarios).

6.3 Experimental Setup

This MDDDL model outlines the importance of MI prediction, especially for MI cases without previous records (*flattened T wave*). The most important part of this research is the proposed methodology and its workflow, which shows the prediction method of *flattened T waves*. The MDDDL is a model for the predictive classification of the *flattened T wave*. MDDDL applies the concept of DDL for the prediction of *flattened T waves* with the help of fusion activity. Figure 6.1 highlights the pictorial summary of MDDDL.

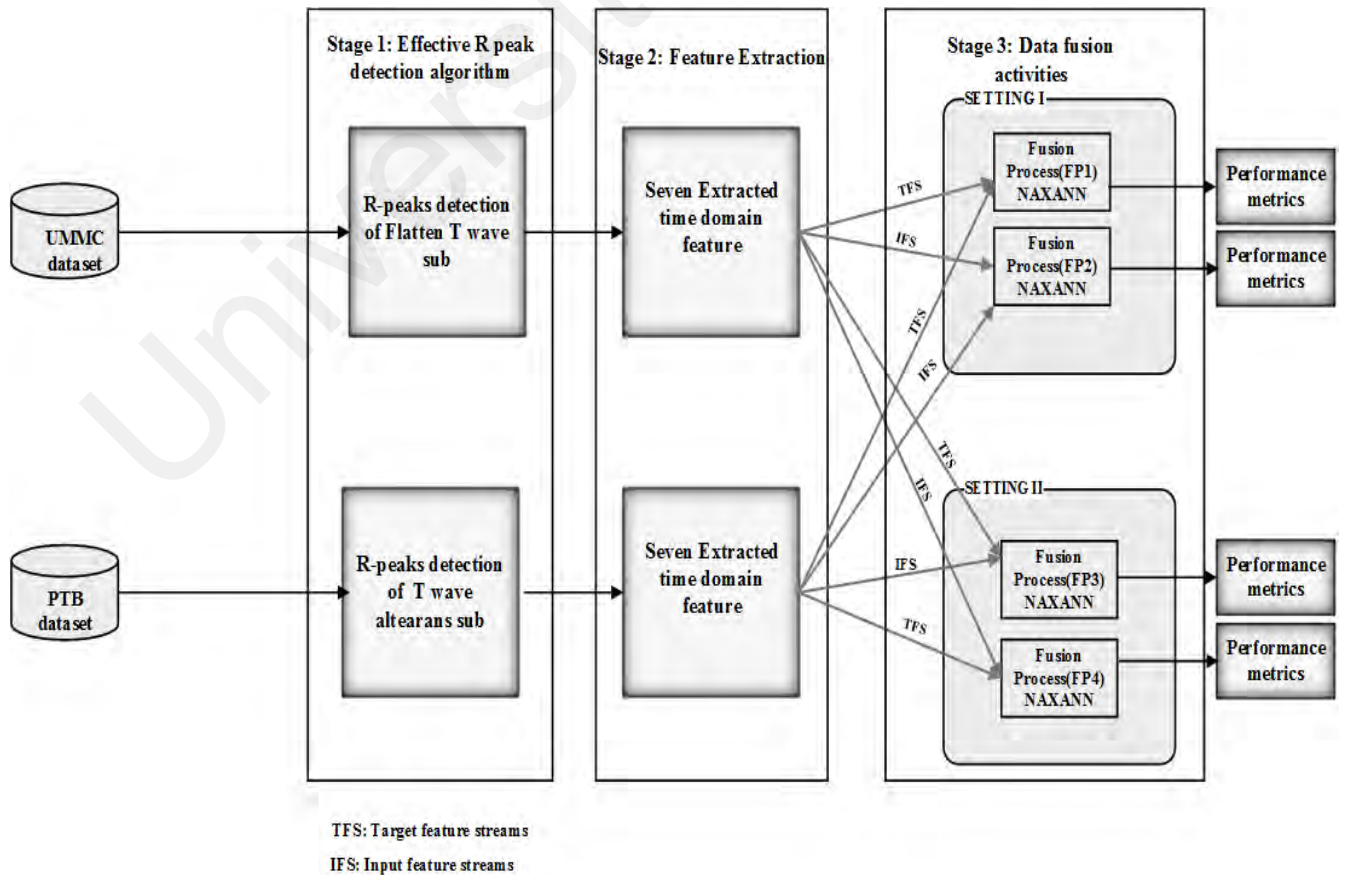


Figure 6.1. Architecture of MDDDL

MDDDL is a novel way for the measurement of predictive ratio of *flattened T wave* by using two different datasets (UMMC and PTB). In MDDDL, the fusion activity concept of DDL is coupled with best predictive classifier (scalable conjugate algorithm). Additionally, two small sample sizes of 10 different data streams of TWA and *flattened T wave* are adopted for MDDDL operations. The 10 data streams of TWA are obtained from the publicly available PTB ECG signal database. Similarly, the 10 data streams of *flattened T-wave* sample sizes were chosen from the UMMC exclusive dataset. In next phase, the feature engineering steps were imposed on both datasets by using the effective R-peak detection algorithm (discussed in Chapter 4, see Section 4.3) which is also a core part of MDDDL. The critical area of effective R-peak detection algorithm is the setting of the fixed threshold points that are used to measure efficiency of algorithm (as discussed in Section 4.4 of Chapter 4 and Section 5.4 in Chapter 5).

6.3.1 Feature Engineering

In this Chapter, the same representation of signal is followed as used in Chapter 5 (see Section 5.3.1). The complete ECG wavelet length is represented as a ln . Similarly, the detected R-peaks and RR intervals are highlighted as pi and $|(pi + 1) - (pi)|$, respectively. Equation 6.1 shows the mean value of the heart rate as follows:

$$mhrv = 60 / (ln - 1) \sum_{i=0}^{ln} |(pi + 1) - (pi)| \quad (6.1)$$

Equation 6.2 highlights the root mean difference value of RR intervals as

$$rr - rms = \sqrt{1 / (ln - 2) \sum_{i=3}^{ln} [|(pi + 1) - (pi)|] 1/2} \quad (6.2)$$

Equations 6.3(a) and 6.3(b) show the standard deviation of the RR interval ($sddn$), and Equation 6.4 covers the RR numbers of pairs larger than and equal to 50 ($nnrr$). Equations 6.5(a) and 6.5(b) highlight the mean value of T-onset (mt_{on}) detection.

Similarly, Equations 6.6(a) and 6.6(b) define the mean value of T-offset (mt_{off}). Finally, Equations 6.7(a) and 6.7(b) represent the mean value of T-peak (mt_{pk}) features.

$$\gamma = 1/ln \sum_{i=0}^{ln} |(pi + 1) - (pi)| \quad (6.3a)$$

$$sddn = \sqrt{1/(ln - 1) \sum_{i=2}^n [|(pi + 1) - (pi)| - \gamma |]} \quad (6.3b)$$

$$\Omega = RR \geq 50$$

$$nnrr = [\sum_{i=0}^{ln} |(pi + 1) - (pi)|] + \Omega \quad (6.4)$$

$$t_{on} = \vartheta = 40 + 1.33 \sum_{i=2}^n \sqrt{|(pi + 1) - (pi)|} \quad (6.5a)$$

$$mt_{on} = 1/(ln - 1) \sum_{i=2}^n |(\vartheta i + 1) - (\vartheta i)| \quad (6.5b)$$

$$t_{off} = \beta = 40 + 1.33 \sum_{i=3}^n [|(pi + 1) - (pi)|]1/6 \quad (6.6a)$$

$$mt_{off} = 1/(ln - 1) \sum_{i=2}^n |(\beta i + 1) - (\beta i)| \quad (6.6b)$$

$$\eta = (t_{on} + t_{off})/2 \quad (6.7a)$$

$$mt_{pk} = 1/(ln - 1) \sum_{i=2}^n |(\eta i + 1) - (\eta i)| \quad (6.7b)$$

6.4 Experimental Results

The defined schema of MDDDL is represented in two stages. The first stage completely belongs to the feature extraction stage implemented on *flattened T-wave* cases of the UMMC dataset and TWA cases of the PTB dataset. Table 6.1 presents the complete results of the 10 *flattened T waves*, which highlight the detected R-peaks with the different threshold values (tp , tn , tp and fn). Through these threshold values, the efficiency gages are calculated in the form of accuracy (ACC), Positive prediction value

(P^+), Sensitivity (Se) and False discovery ratio(F^{DR}). According to Table 6.1, the ECGRLIIDAT *flattened* stream represents the least R-peak detection by using the proposed effective R-peak detection algorithm. By contrast, the ECGRLIISAT *flattened* case highlights the largest detected R-peaks by using the same algorithm with the same frequency (250 Hz).

Table 6.1: Accuracy parameters of flattened T wave cases (UMMC)

$M_Subjects$	$Rpeaks$	tp	tn	fp	fn	RR <i>intervals</i>	$ACC(\%)$	$P+$ (%)	Se (%)	F^{DR} (%)
ECGRLIABD	26	16	0	0	0	25	100	100	100	0
ECGRLIANSI	27	25	0	0	0	26	100	100	100	0
ECGRLIIDAT	15	14	0	0	0	14	100	100	100	0
ECGRLIIFA	26	5	0	0	0	25	100	100	100	0
ECGRLIIHAJ	39	38	0	0	0	38	100	100	100	0
ECGRLIISAT	262	261	0	0	0	261	100	100	100	0
ECGRLIJUS	46	45	0	0	0	45	100	100	100	0
ECGRLIINAF	22	21	0	0	0	21	100	100	100	0
ECGRLIIRAF	19	17	0	0	0	18	100	100	100	0
ECGRLIIRAZ	26	25	0	0	0	25	100	100	100	0

Afterward, by using the results of the detected R-peaks, the second stage is the extraction of seven time-domain features by following the MDDDL methodology.

Table 6.2 lists the complete extracted features of *flattened T-wave* cases.

Table 6.2: Feature extraction unit of flattened T wave cases (UMMC)

$M_Subjects$	hrv	snn	$rmsdd$	$nn50$	mt_{on}	mt_{off}	mt_{pk}
ECGRLIABD	104.8873	1.2038	1.3679	22	0.69456	0.67132	0.68294
ECGRLIANSI	21.3446	2.161	3.2966	13	0.7046	0.67299	0.68879
ECGRLIIDAT	15.7831	5.1889	7.265	12	0.74111	0.67907	0.71009
ECGRLIIFA	90.2261	2.9735	3.3506	23	0.70582	0.67319	0.68951
ECGRLIIHAJ	17.1005	0.19156	0.1104	22	0.70778	0.67352	0.69065
ECGRLIISAT	19.8401	0.066472	0.030041	15	0.70519	0.67309	0.68914
ECGRLIJUS	36.0787	0.76027	0.6004	20	0.70392	0.67288	0.6884
ECGRLIINAF	18.0198	1.7666	2.0366	19	0.6999	0.67221	0.68605
ECGRLIIRAF	20.7079	0.54555	0.65265	9	0.70537	0.67312	0.68924
ECGRLIIRAZ	67.7357	3.1826	4.249	24	0.69848	0.67197	0.68523

The same work sets are implemented on 10 TWA streams of the PTB dataset, which includes similar R-peak detection scenarios, along with seven different extracted features. Table 6.3 shows the results from the effective R-peak detection algorithm on the TWA streams. The table also indicates that twa00 and twa10 streams demonstrates the worst cases in terms of detected R-peaks by using the same effective R-peak detection algorithm. Conversely, the twa05 stream exhibits the best case in terms of R-peak detection and twa06 represents the average case.

Table 6.3: Accuracy parameters of TWA cases (PTB)

<i>M_Subjects</i>	<i>R-peaks</i>	<i>tp</i>	<i>tn</i>	<i>fp</i>	<i>fn</i>	<i>RR intervals</i>	<i>ACC(%)</i>	<i>P+</i> <i>(%)</i>	<i>Se</i> <i>(%)</i>	<i>FDR</i> <i>(%)</i>
twa00.m	11	10	0	0	0	10	100	100	100	0
twa02.m	18	17	0	0	0	17	100	100	100	0
twa03.m	16	15	0	0	0	15	100	100	100	0
twa05.m	33	32	0	0	0	32	100	100	100	0
twa06.m	19	18	0	0	0	18	100	100	100	0
twa08.m	12	11	0	0	0	11	100	100	100	0
twa09.m	19	18	0	0	0	18	100	100	100	0
twa10.m	11	10	0	0	0	10	100	100	100	0
twa11.m	13	12	0	0	0	12	100	100	100	0
twa12.m	17	16	0	0	0	16	100	100	100	0

The extraction procedure is then implemented on the PTB dataset, and the seven features are extracted through these detected R-peaks and threshold values. Table 6.4 shows a complete list of these features.

Table 6.4: Feature extraction showcase of TWA cases (PTB)

<i>M_Subjects</i>	<i>hrv</i>	<i>snn</i>	<i>rmsdd</i>	<i>nn50</i>	<i>mt_{on}</i>	<i>mt_{off}</i>	<i>mt_{pk}</i>
twa00.m	30.8707	0.10505	0.12244	7	0.69792	0.67188	0.6849
twa02.m	105.9663	0.5538	0.72505	11	0.68361	0.66949	0.67655
twa03.m	61.3405	0.29362	0.2478	4	0.67687	0.66837	0.67262
twa05.m	310.4683	0.54452	0.72554	25	0.68296	0.66938	0.67617
twa06.m	55.4152	0.054415	0.053367	7	0.68936	0.67045	0.6799
twa08.m	37.0167	0.018854	0.02865	0	0.68936	0.67045	0.6799
twa09.m	55.7424	0.059502	0.065454	9	0.6882	0.67026	0.67923
twa10.m	32.2515	0.14689	0.082419	4	0.69767	0.67183	0.68475
twa11.m	38.4403	0.044198	0.037581	3	0.69505	0.6714	0.68323
twa12.m	50.8139	0.27709	0.4102	2	0.69066	0.67067	0.68067

The seven extracted features ($rr-rms$, $sddn$, $nn50$, hrv , mt_{on} , mt_{off} and mt_{pk}) are categorised into two groups: traditional and new feature combination. The four fusion activities of the MDDDL are performed through these extracted feature streams. The four fusion processes are further operated in two different settings. These extracted features play a vital role in the next module of the core part of MDDDL. The four different fusion activities are performed on Stage 2 under the section of the two different settings.

Two different datasets were used for the execution of the experimental setup of the proposed MDDDL method. The *flattened T wave* cases of the UMMC dataset and TWA cases of the PTB dataset are evaluated by using the MDDDL model through two different stages. These stages are further classified into two different settings. Figure 6.2 is a complete pictorial representation of the MDDDL evaluation shows two different settings, Setting I uses the customised non-linear input output artificial neural network (*NARX ANN*) for the measurement of the prediction ratio with the help of five hidden layers (hl) and two time delays (d). Data fusion activities are introduced in Setting 1 as the first two fusion processes. The first fusion process ($fp1$) takes the stream of UMMC and PTB features as target and input cases, respectively. By contrast, the second fusion process ($fp2$) respectively takes the PTB and UMMC feature streams as the target and input cases. In both fusion processes, the target and input cases are considered on the basis of two types of feature combination, namely, traditional features combination ($fc1$) and new features combination ($fc2$). Setting II is a complete replication of Setting I, except for the changes in the 10 hidden layers in *NARX ANN*.

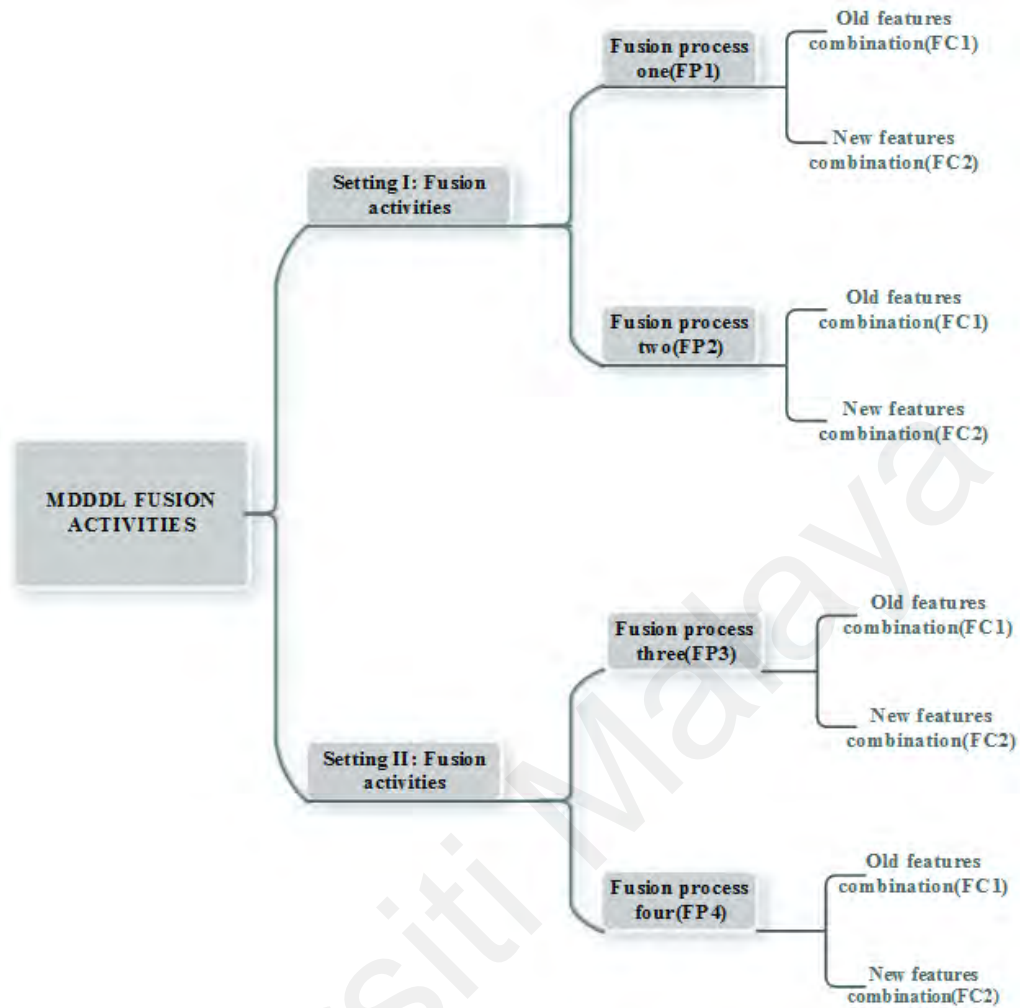


Figure 6.2. Complete MDDDL testbed classification

According to the proposed method of MDDDL, the evaluation or test bed scenarios are launched. The *flattened T wave* cases of UMMC dataset and TWA cases of PTB dataset are evaluated by using the MDDDL model which covers two different stages. Such stages are further classified into further two different settings that are briefly discussed in next subsection 6.4.1

6.4.1 Data Streams Fusion

The complete structure of MDDDL depends on the outcome of core operational activities that belong to the results of fusion activities. In this subsection, the fusion activities are categorised into two different sub-parts: Settings I and II. Setting I deals

with the first and second fusion processes, which use *flattened T-wave* (UMMC dataset) and TWA feature streams (PTB dataset) with five *hl*. Similarly, Setting II covers the third and fourth fusion processes with the same feature streams, except for the hidden layer structure(ten *hl*).

6.4.1.1 Setting I

The first evaluation activity of the MDDDL is based on two fusion processes. Setting I uses a customised *NARX ANN* with defined conditions, such as *hl* of five and *d* of two, and the best predictive algorithm scaled conjugate gradient (*trainscg*) is used for comparison of the large feature streams. Table 6.5 presents the *fp1* results.

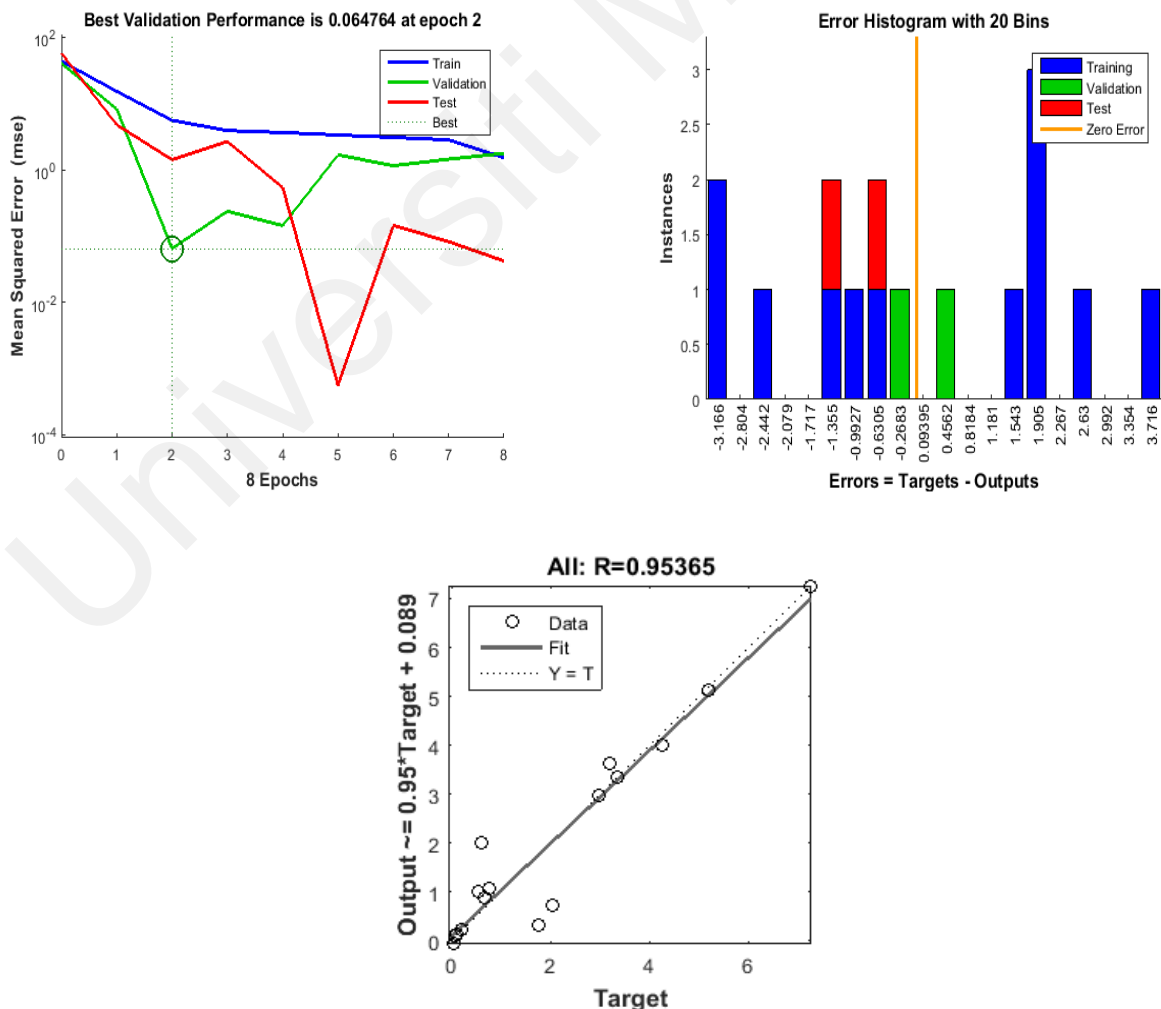
Table 6.5: Fusion activity process one with different feature streams

TARGET_STREAM: FLATTENED T-WAVE, INPUT_STREAM: T-WAVE ALTERANS FUSION ACTIVITY PROCESS 1											
<i>fc1</i>	Performance Matrics Hidden Layer (<i>hl</i>)=5 Delay(<i>d</i>)=2					<i>fc2</i>	Performance Matrics Hidden Layer (<i>hl</i>)=5 Delay(<i>d</i>)=2				
	perf	tim	eph	err	vad		perf	tim	eph	err	vad
hrv,rr-rms ,sddn,nn50	25.8	0	6	-0	6	hrv,rr-rms ,sddn,nn50,mt on,mt _{off} ,mt _{pk}	11	0	8	1.4	6
hrv,rr-rms	76.2	0	6	-1	6	nn50,mt _{on} , mt _{off} ,mt _{pk}	3.2	0	6	0.1	6
hrv,nn50	341	0	6	-2	6	hrv,mt _{on} , mt _{off} ,mt _{pk}	28	0	9	- 0.8	6
hrv, sddn	95.3	0	7	0.1	6	rr-rms ,sddn,mt _{on} , mt _{off} ,mt _{pk}	8	0	35	0	6
hr,rr-rms	27.7	0	7	0	6	sddn,mt _{on} , mt _{off} ,mt _{pk}	5	0	18	0	6
rr-rms ,sddn	20.1	0	6	0.1	6	mt _{on} ,mt _{off} , mt _{pk}	0	0	6	0	6

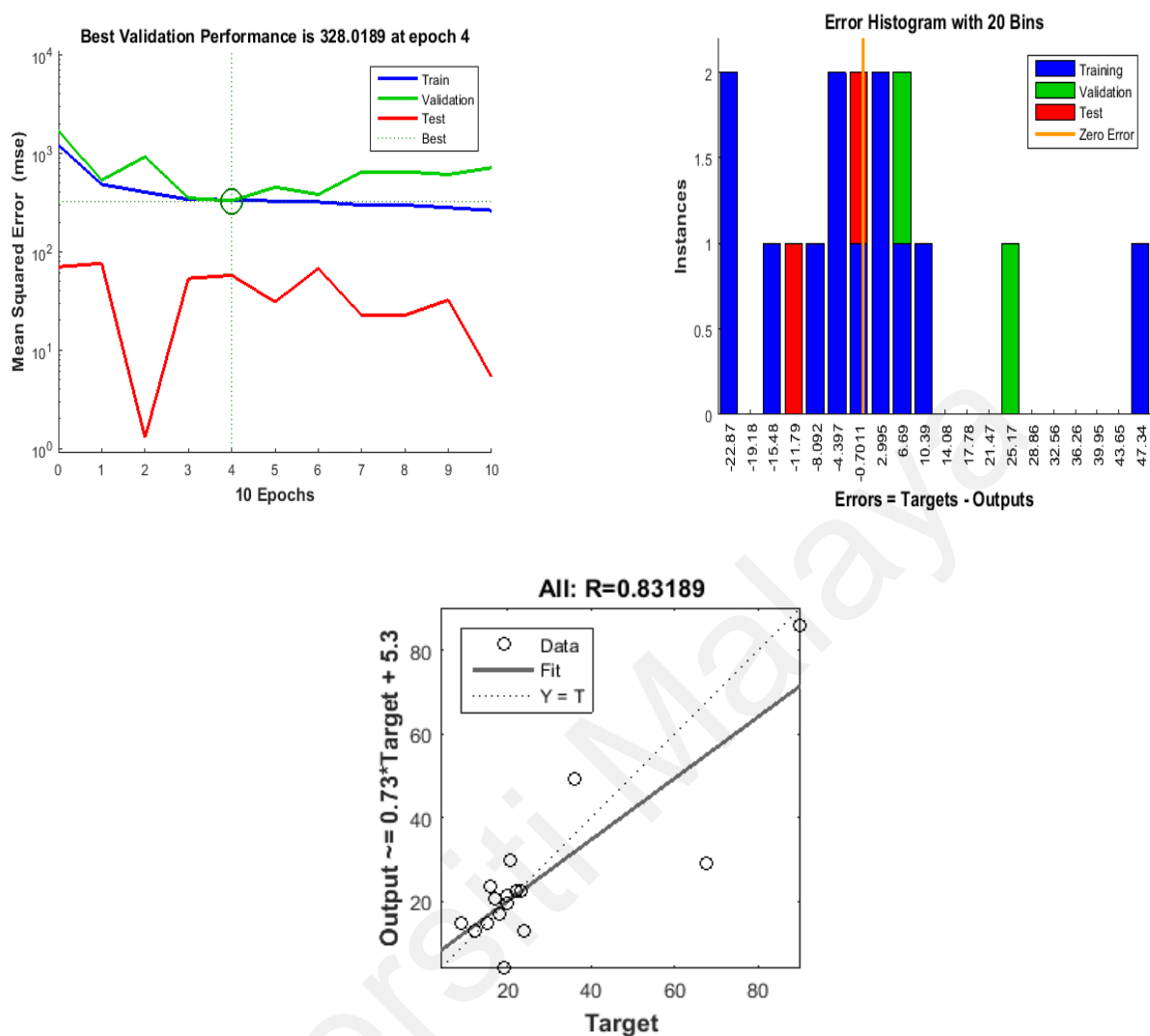
For *fp1*, two different feature combinations are executed on the basis of the aforementioned conditions with pre-set criteria, which indicate that the *flattened T-wave* feature stream is the target case and the TWA feature stream is the input case. In *fc1*, six different feature combinations are used for the fusion process. The efficiency of both

combinations is calculated through performance metrics, which include efficiency gages, performance (perf), time (tim), epoch (eph), error (err) and validation (vad). The validation and time parameters are constant throughout the *fcI* operations. Similarly, the relation of performance and epoch in all the *fcI* operations suggest the efficiency ratio.

Moreover, the accuracy of predictive classification is highlighted with features matching of target class and output class. In predictive classification, target class represents the desire results and output class refers the actual result which gets through experimental activities. The worst and best combinations of *fcI* are categorised according to the performance and epoch parameters, and such cases are highlighted in Figure 6.3.



(a) Best feature combination in terms performance (*rr-rms,sddn*)



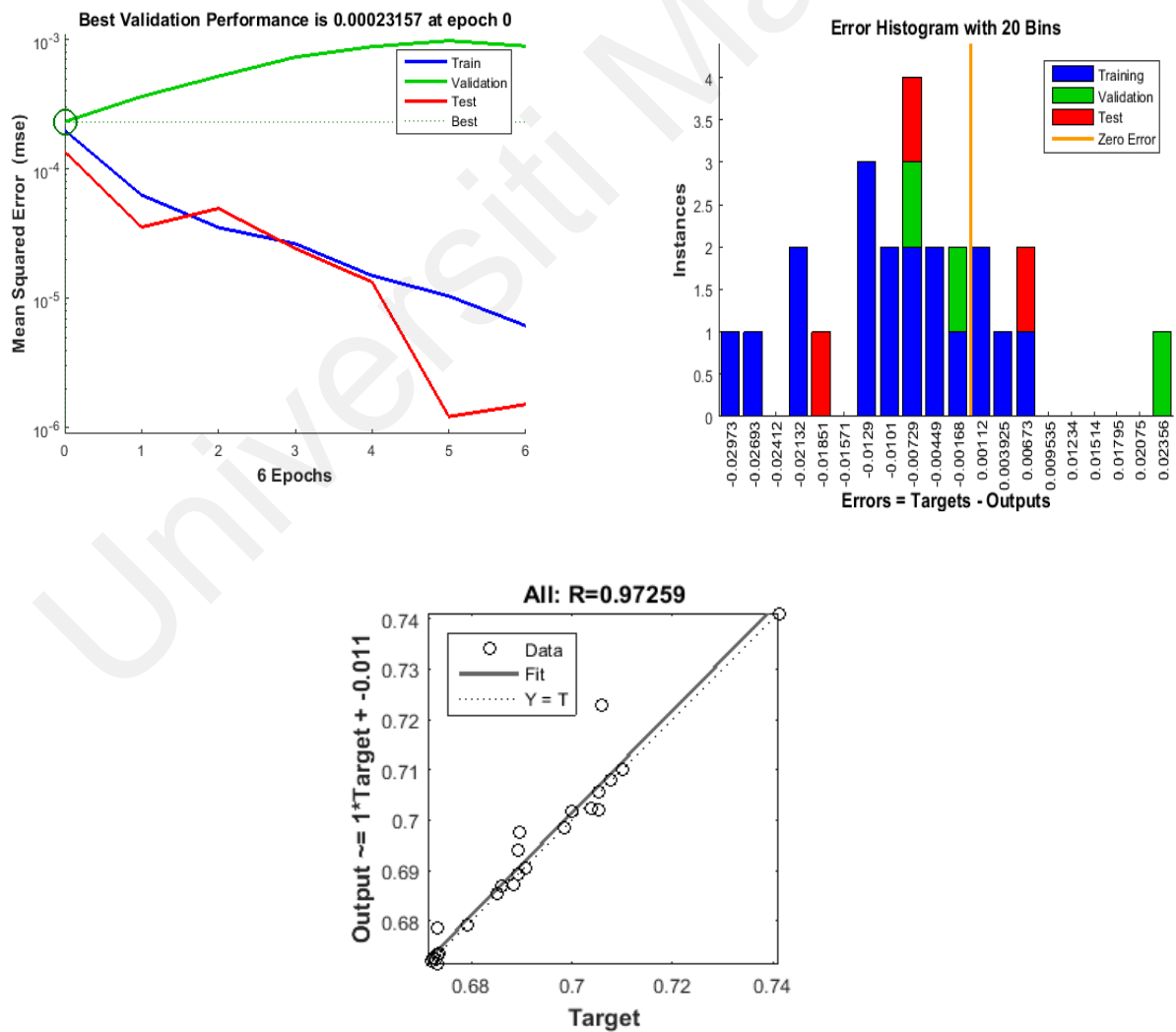
(b) worst feature combination in terms performance (*hrv,nn50*)

Figure 6.3. Efficiency gages of fusion process one with old features combination

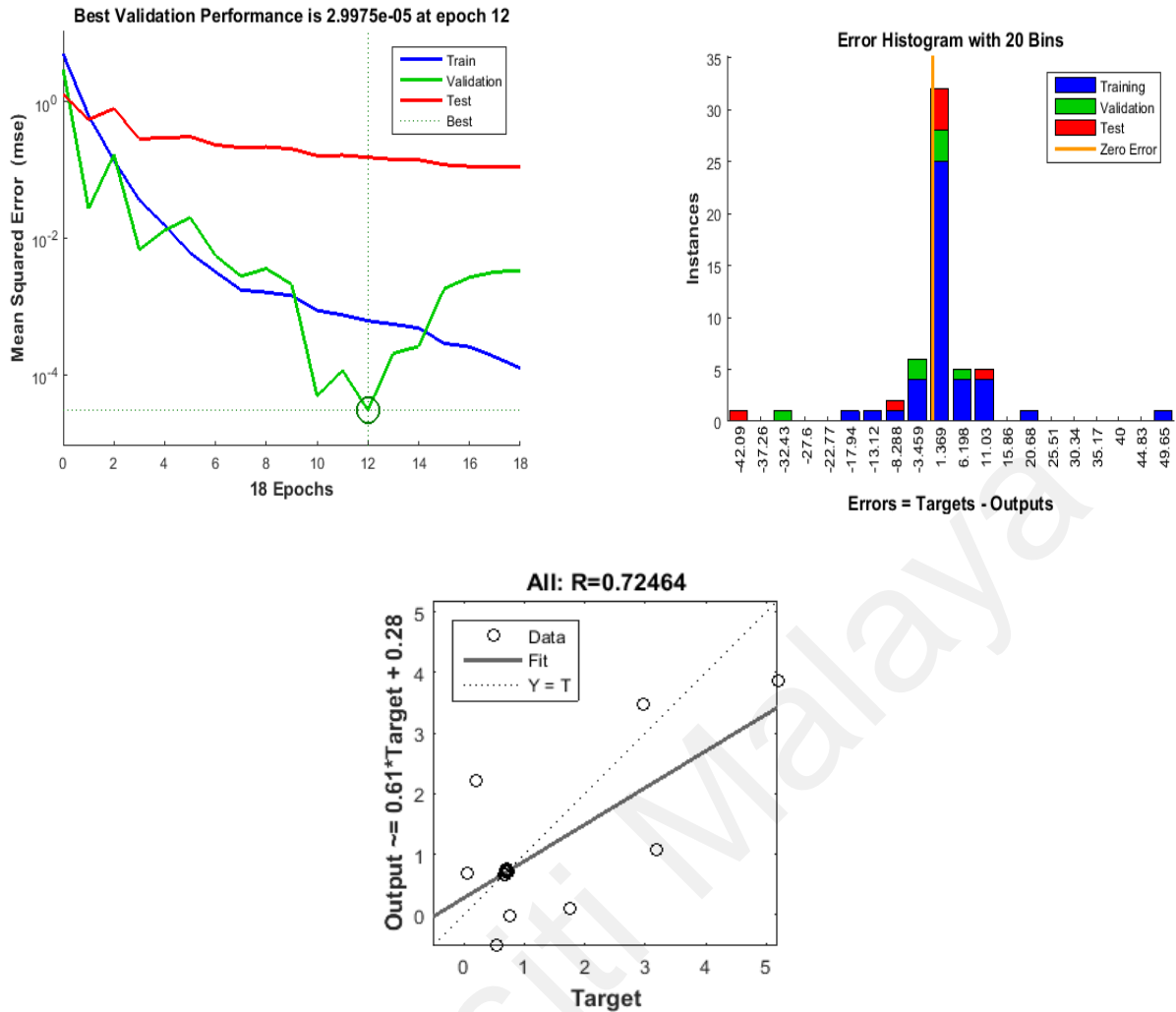
Figure 6.3 shows the efficiency gages of two different *fc1* cases of *fp1*. Figure 6.33(a) highlights the best feature combination (*rr-rms* and *sddn*) of *fp1* in terms of performance, the best validated performance point is at epoch 2 that highlight the computational cost or complexity, the error ratio reaches zero and regression value touches to almost one value ($R= 0.953$) that shows the accuracy ratio of predictive classification between target class and output class. Figure 6.3(b) shows the worst feature combination (*hrv* and *nn50*), in which the best validation performance point in

terms of computation cost is at epoch 4, the error ratio bit high to zero level and regression value $R=0.831$ indicates the ratio of accuracy of predictive classification

Furthermore, the $fc2$ in $fp1$ is similar to that in $fc1$ in terms of the parameters of validation and time. However, $fc2$ slightly differs in terms of performance and epoch parameters, thereby suggesting a better situation compared with that of $fc1$. The increased values of accuracy reveal improved efficiency of prediction. Figure 6.4 illustrates the worst and best combinations of $fc2$ on the basis of performance and epoch.



(a) Best feature combination in context performance (mt_{on} , mt_{off} , mt_{pk})



(b) Worst feature combination in light of performance ($sddn, mt_{on}, mt_{off}, mt_{pk}$)

Figure 6.4. Efficiency gages of fusion process one with new features combination

Figure 6.4 also shows the efficiency gages measurement of two different $fc2$ cases of $fp1$. Figure 6.4(a) illustrates the best feature combination (mt_{on}, mt_{off} and mt_{pk}) of $fp1$ in terms of the best validation performance point at epoch 0 which highlight the ideal computational complex value, error ratio which is exactly equal to zero and regression value R touches to almost one ($R=0.972$) which shows the high accuracy ratio of predictive classification. Figure 6.4(b) highlights the worst feature combination ($sddn, mt_{on}, mt_{off}$ and mt_{pk}), wherein the best validation performance point is at epoch 12 that highlight the worst computational cost as compared to figure 6.4(a), error ratio is far

above zero and regression value is $R=0.7246$ which highlight the least predictive classification accuracy ratio as compared to above features combination.

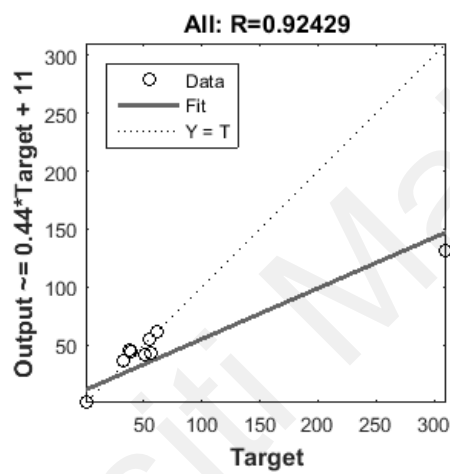
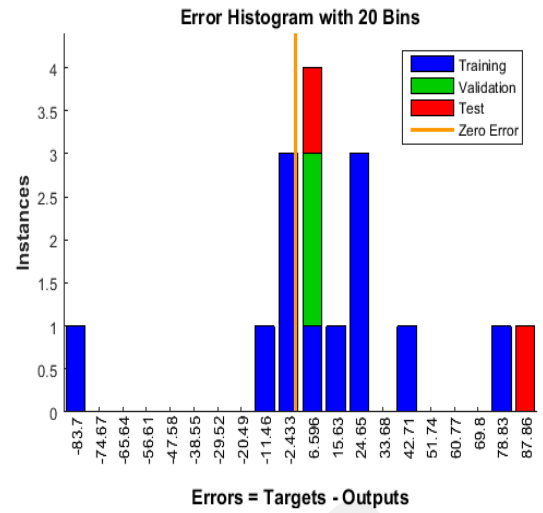
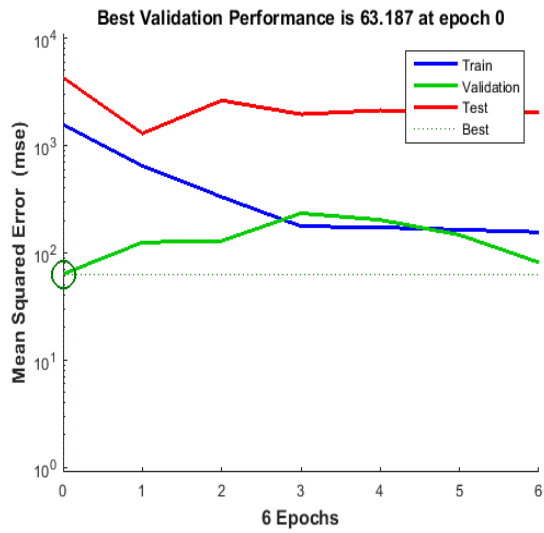
Furthermore, both same $fc1$ and $fc2$ are used with same defined conditions for $fp2$ ($hl = 5$, $d = 2$ and $trainscg$), except for the target and input feature streams. Table 6.6 lists the results of the entire operational investigations of $fp2$.

Table 6.6: Fusion activity process two with different feature streams

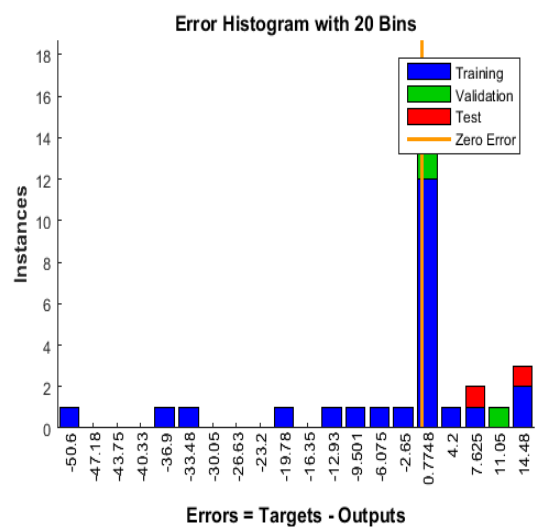
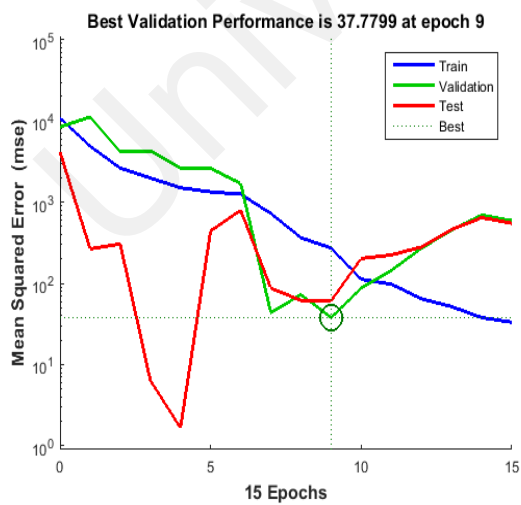
TARGET_STREAM: T-WAVE ALTERNANS, INPUT_STREAM: FLATTENED T WAVE FUSION ACTIVITY PROCESS 2											
$fc1$	Performance Matrics Hidden Layer (hl)=5 Delay(d)=2					$fc2$	Performance Matrics Hidden Layer (hl)=5 Delay(d)=2				
	perf	tim	eph	err	vad		perf	tim	eph	err	vad
hrv,rr-rms ,sddn,nn50	33.3	0	15	0.8	6	hrv,rr-rms ,sddn,nn50,mt _{on} , mt _{off} ,mt _{pk}	0.36	0	57	2.2	6
hrv,rr-rms	63.6	0	6	12	6	nn50,mt _{on} , mt _{off} ,mt _{pk}	0.24	0	9	-0	6
hrv,nn50	190	0	14	0	6	hrv,mt _{on} , mt _{off} ,mt _{pk}	40	0	9	0.5	6
hrv,sddn	1.02	0	29	1.2	6	rr-rms ,sddn,mt _{on} , mt _{off} ,mt _{pk}	0	0	8	-0	6
hr,rr-rms	9.1	0	9	1.6	6	sddn,mt _{on} , mt _{off} ,mt _{pk}	0	0	6	0	6
rr-rms ,sddn	0	0	13	0	6	mt _{on} ,mt _{off} ,mt _{pk}	0	0	7	0	6

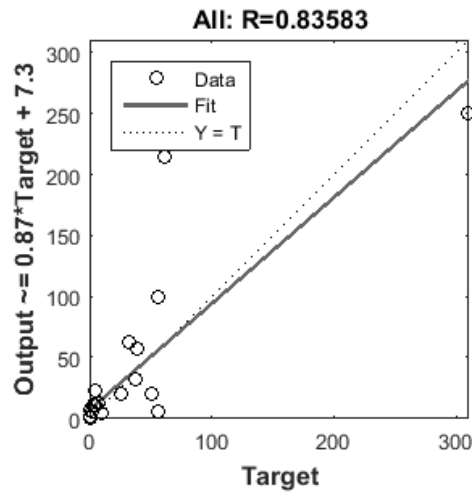
In the second fusion process, the same performance matrices are used for $fc1$ and $fc2$.

The results of $fp2$ for the two parameters of time and validation are evidently similar to those of $fp1$. The constant and minimum value range of time and validation on $fc1$ and $fc2$ shows the least time complexity factor. However, for the scenario of $fc1$ in $fp2$, the parameters of performance and epoch are low in range (the direct relation of performance and epoch), thereby indicating a low level of efficiency. Figure 6.5 depicts the worst and best cases of $fc1$ $fp2$ in terms of performance and epoch parameters.



(a) Best feature combination in aspect performance(*hrv,sddn*)



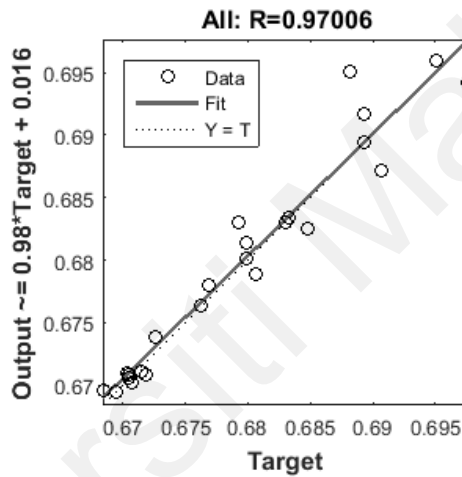
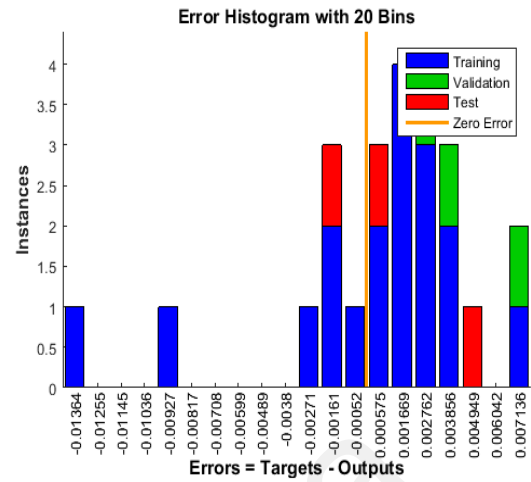
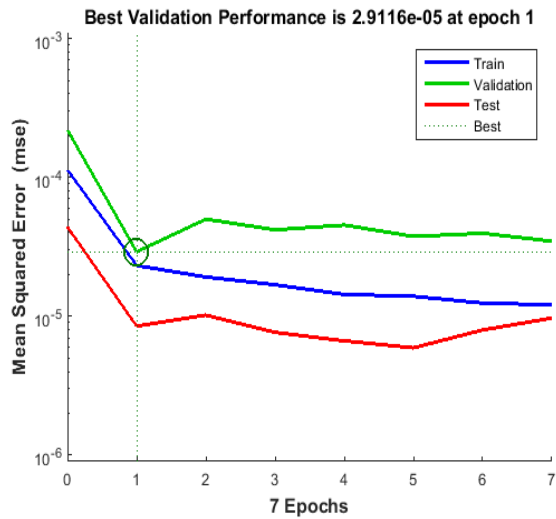


(b) Worst feature combination in performance (*hrv, rr-rms, sddn, nn50*)

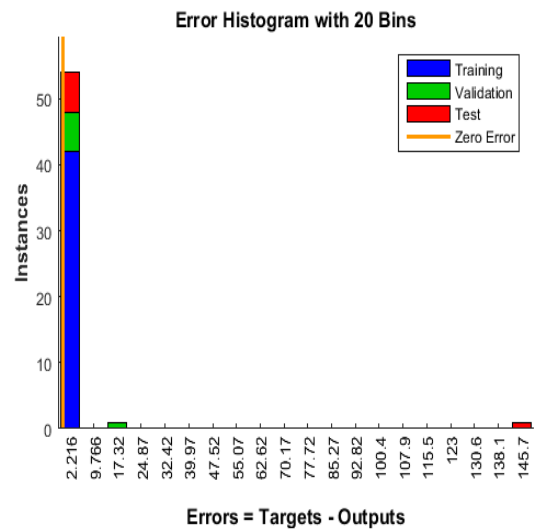
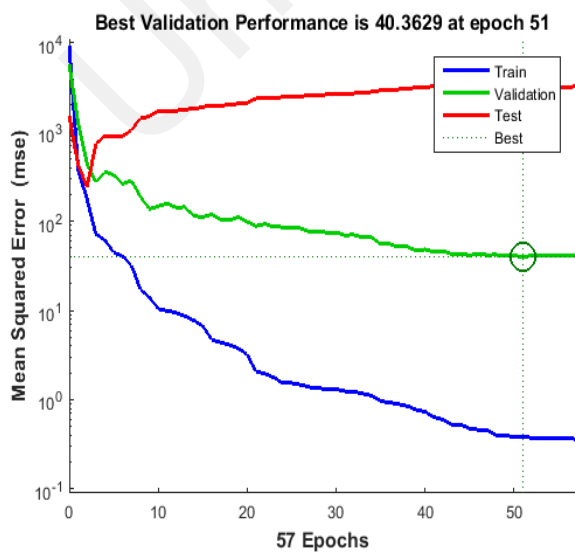
Figure 6.5. Efficiency gages of fusion process two with old features combination

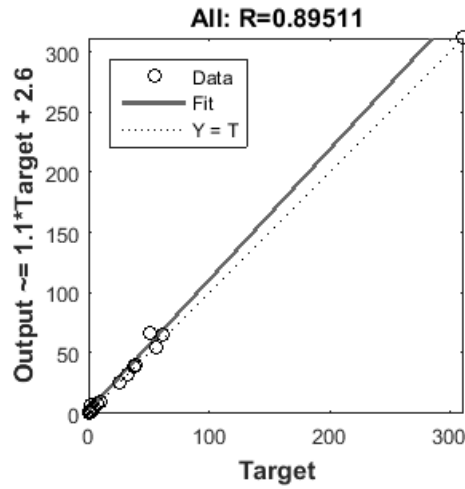
The pictorial representation in Figure 6.5 highlights the efficiency gages of *fp2*. Figure 6.5(a) represents the best feature combination (*hrv* and *sddn*) of *fp2*, which delivers the optimal validation performance point or ideal computation cost at epoch 0 value, an error ratio almost touches to zero and predictive classification accuracy ratio highlight in terms of regression value is equal to almost one ($R=0.924$). By contrast, Figure 6.5(b) represents the worst feature combination (*hrv, rr-rms, sddn* and *nn50*), in which the best validation performance point is at epoch 9 which means more computational complex as compared to above feature combination in Figure 6.5(a), and the error ratio almost reaches zero. Moreover, regression value ($R=0.835$) in Figure 6.5(b) shows the predictive accuracy ratio is low to above feature combination in Figure 6.5(a).

In *fc2*, the same defined conditions are also used to obtain valuable results. The similar results of *fc2* are observed in terms of the parameters of validation and time. Thus, the other parameters show different results compared with those of *fc1*. The parameters of performance and epoch indicate a slightly different outcome that improves the efficiency level, especially in the first combination. Figure 6.6 illustrates the best and worst cases of efficiency of *fc2* in *fp2*.



(a) Best feature combination in aspect performance ($mt_{on}, mt_{off}, mt_{pk}$)





(b) Worst feature combination in aspect performance ($hrv, rr-rms, sddn, nn50, mt_{on}, mt_{off}, mt_{pk}$)

Figure 6.6. Efficiency gages of fusion process two with new features combination

Figure 6.6 presents the efficiency measurement gauges of $fp2$ in context of $fc2$. Figure 6.6(a) shows the best feature combination (mt_{on} , mt_{off} and mt_{pk}) of $fp2$, which delivers the least computational complex value in terms of best validation performance point at epoch 1, error ratio is equal to zero level and high accuracy of predictive classification in aspect of regression value is $R=0.9700$. By contrast, Figure 6.6(b) depicts the worst feature combination (hrv , $rr-rms$, $sddn$, $nn50$, mt_{on} , mt_{off} and mt_{pk}), which delivers the best validation performance point at epoch 51 that shows more computational complex as compared to above feature combination (mt_{on} , mt_{off} and mt_{pk}), error ratio that reaches 2 and regression value is $R=0.89511$ shows least predictive classification accuracy.

6.4.1.2 Setting II

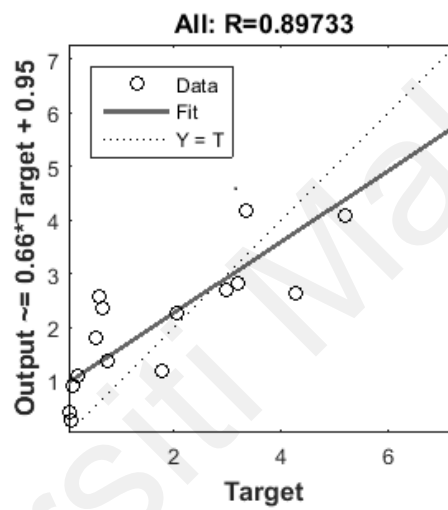
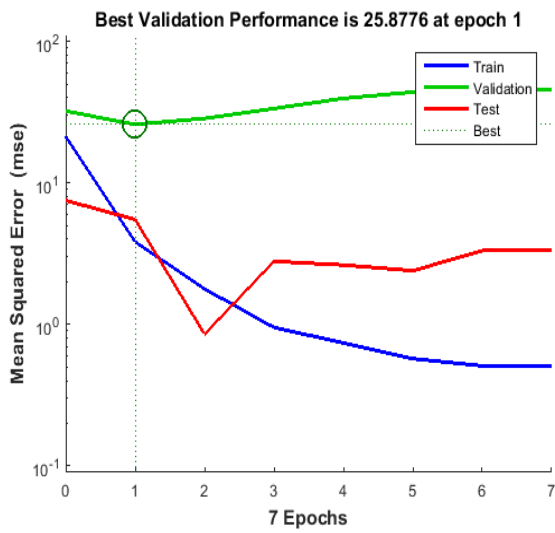
In this section, two additional fusion process activities are performed with same customized $NARX ANN$ for the prediction ratio of MI. However, a different $NARX ANN$ layer structure, such as ten hl is used.

Similar to the operational investigations of the first two fusion processes in setting I, the two feature combination schemas are also introduced in setting II. Table 6.7 highlights the complete operational investigations of fusion process three (*fp3*).

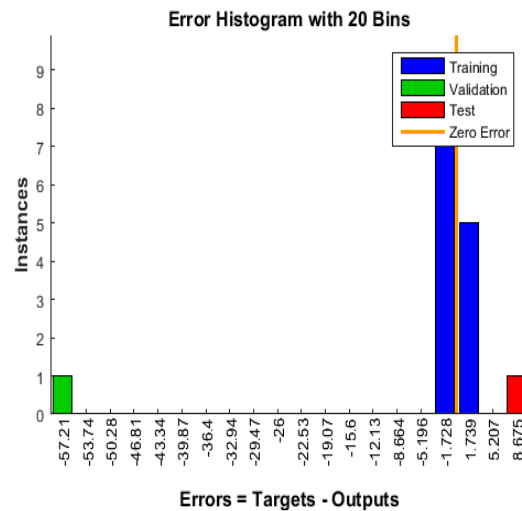
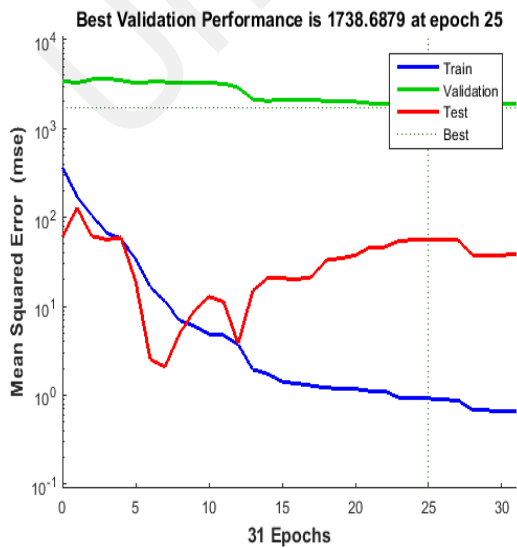
Table 6.7: Fusion activity process three with different feature streams

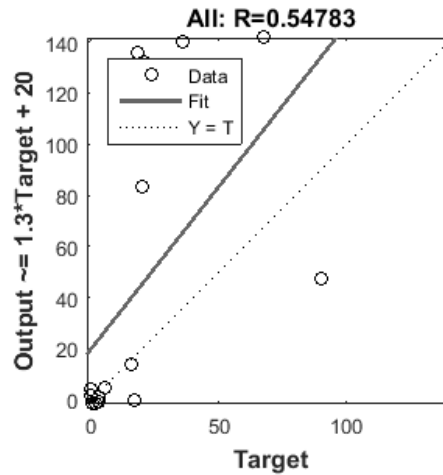
TARGET_STREAM: FLATTENED T-WAVE, INPUT_STREAM: T-WAVE ALTERANS FUSION ACTIVITY PROCESS 3											
<i>fc1</i>	Performance Matrices Hidden Layer (hl) = 10 Delay (d) = 2					<i>fc2</i>	Performance Matrices Hidden Layer (hl) = 10 Delay (d) = 2				
	perf	tim	eph	err	vad		perf	tim	eph	err	vad
hrv,rr-rms ,sddn,nn50	3.37	0	8	1.2	6	hrv,rr-rms ,sddn,nn50,mt _{on} , mt _{off} ,mt _{pk}	8.4	0	7	0.45	6
hrv,rr-rms	7.97	0	10	-0	6	nn50,mt _{on} , mt _{off} ,mt _{pk}	0.19	0	6	0	6
hrv,nn50	15.6	0	6	-1.2	6	hrv,mt _{on} , mt _{off} ,mt _{pk}	15.9	0	8	0.67	6
hrv, sddn	0.66	0	31	0	6	rr-rms ,sddn,mt _{on} , mt _{off} ,mt _{pk}	0.001	0	18	-0	6
hr,rr-rms	33.7	0	6	0	6	sddn,mt _{on} , mt _{off} ,mt _{pk}	2.94	0	9	0.02	6
rr-rms ,sddn	21.3	0	7	0	6	mt _{on} ,mt _{off} , mt _{pk}	4E-04	0	10	0	6

The same two feature combinations are used in *fp3* for the analysis of fusion activities with the help of defined conditions. The efficiency level is estimated through the performance metrics of *fc1*. In *fc1* of *fp3*, the parameters of time and validation remain at constant and minimum values, thereby indicating low time complexity factor. The parameters of performance and epoch have low ratio values, suggesting a low efficiency level. Figure 6.7 depicts the best and worst cases



(a) Best feature combination in aspect performance (*rr-rms,sddn*)



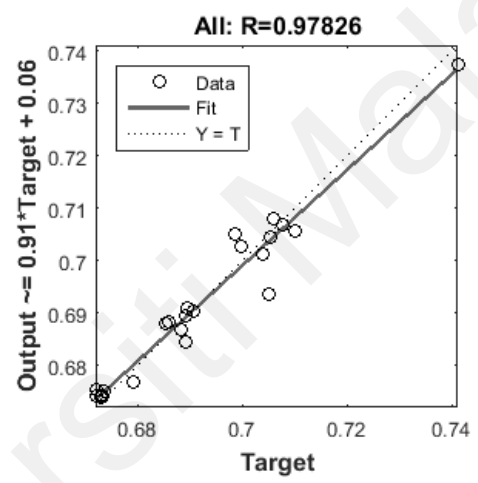
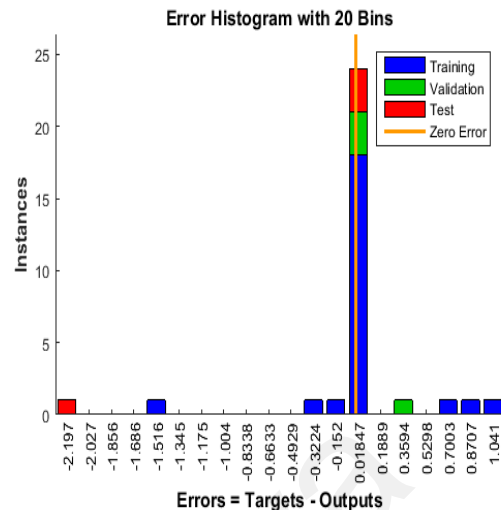
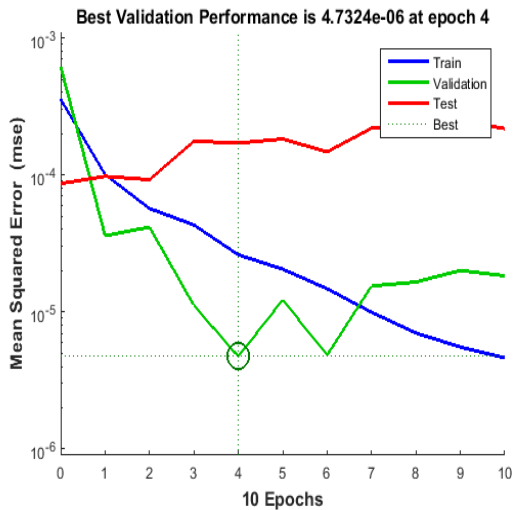


(b) Worst feature combination in aspect performance (*hrv, sddn*)

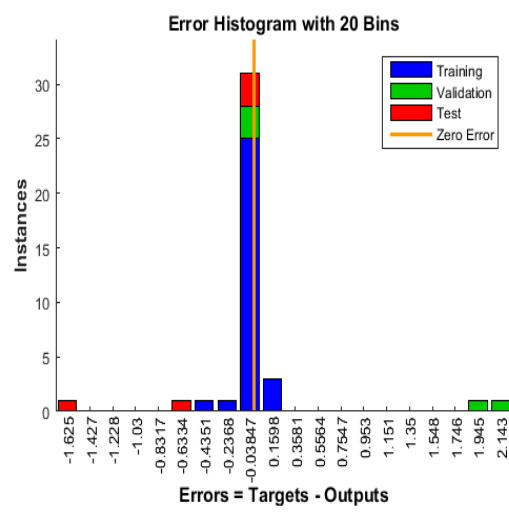
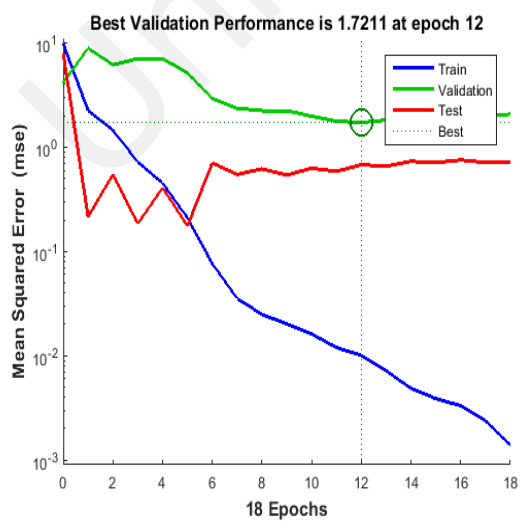
Figure 6.7. Efficiency gages of fusion process three with old features combination

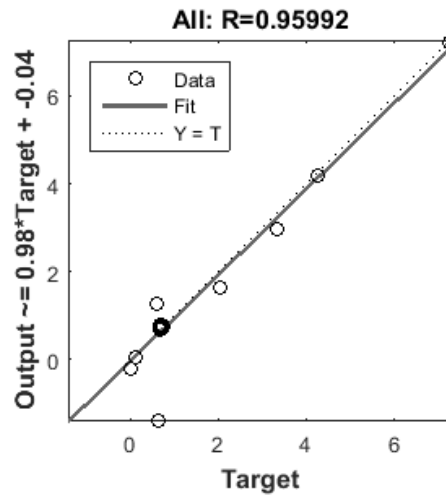
Figure 6.7 depicts *fp3*, which represents the efficiency measurement gages of *fc1*. Figure 6.7(a) represents the best feature combination (*rr-rms* and *sddn*) of *fp3*, which highlights the least computational complex in terms of optimal validation performance point at epoch 1, error ratio lies below zero level and regression value is $R=0.8973$ which represented the least accurate predictive ratio as compared to above fusion processes(*fp1, fp2*). By contrast, Figure 6.7(b) shows the worst feature combination (*hrv* and *sddn*), indicating that the best validation performance point is at epoch 25, error ratio is equal to zero level, and regression value ($R= 0.5478$) indicates the lowest accuracy ratio.

In *fc2* of *fp3*, the same results are acquired in the parameters of time and validation. However, different outcomes are achieved in terms of performance and epoch. Figure 6.8 highlights the best and worst cases. These worst and best cases belongs to same efficiency gages that are used in above fusion processes and gets the handy results in terms of regression value .The outcome are achieved through these regression values are further handy for features analysis.



(a) Best feature combination in context of performance ($mt_{on}, mt_{off}, mt_{pk}$)





(b) Worst feature combination in context of performance ($rr-rms, mt_{on}, mt_{off}, mt_{pk}$)

Figure 6.8. Efficiency gages of fusion process three with new features combination

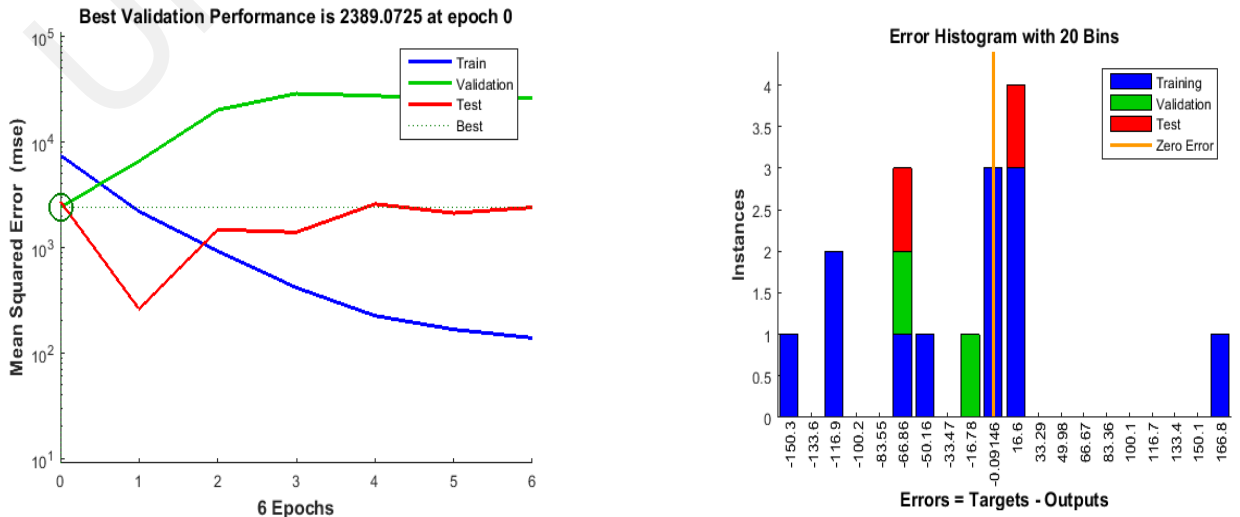
Figure 6.8 shows the efficiency measurement gages of $fp3$ in terms of $fc2$. Figure 6.8(a) highlights the best feature combination (mt_{on} , mt_{off} and mt_{pk}) of $fp3$, which reflects the best validation at epoch 4 (least complexity value), error ratio is below zero level and predictive classification accuracy in form of regression level touches to ideal case ($R=0.9782$). Conversely, figure 6.8(b) illustrates the worst feature combination ($rr-rms$, mt_{on} , mt_{off} and mt_{pk}), indicating that the computational complexity in aspect of best validation point is at epoch 12, error ratio is far below zero and accuracy ratio in form of regression level touches to same ideal case ($R=0.9583$).

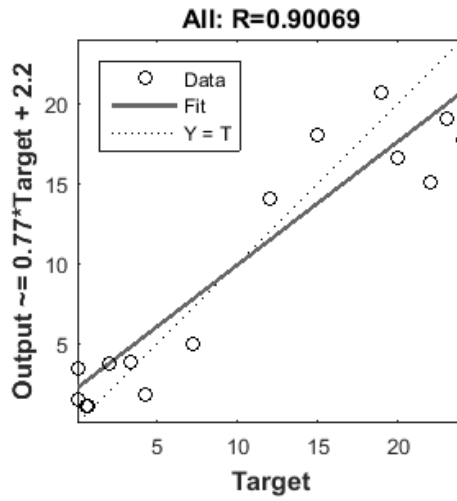
Finally, $fp4$ performs the same operational investigations with the same defined conditions, including the ten hidden layers, two delays and predictive algorithm scaled conjugate gradient. However, the feature stream scenarios differ in $fp4$; the TWA feature stream acts as the target case and the *flattened T-wave* feature stream behaves as the input case. Table 6.8 lists the results of all the operational investigations of $fp4$.

Table 6.8: Fusion activity process four with different feature streams

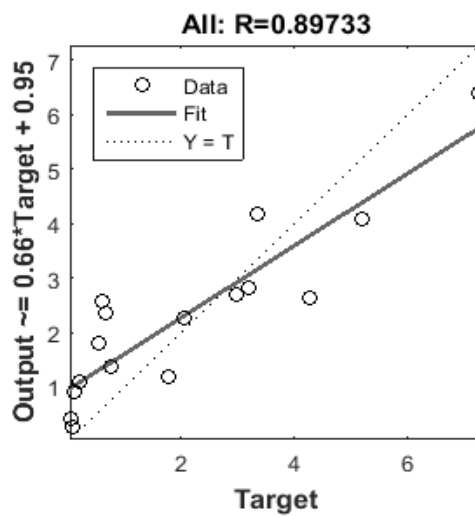
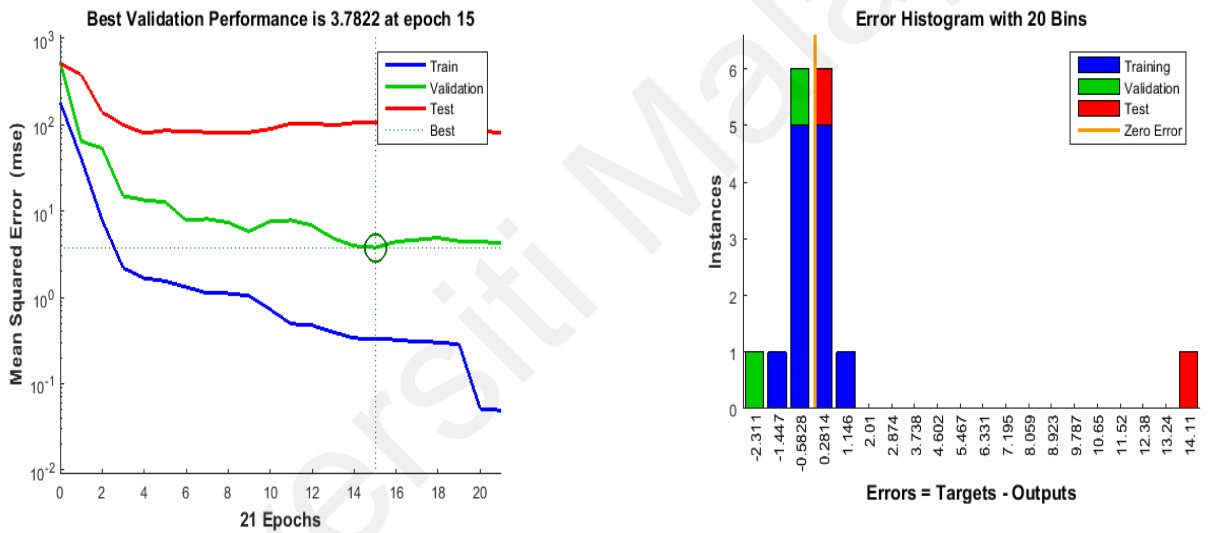
TARGET_STREAM: T-WAVE ALTERNANS, INPUT_STREAM: FLATTENED T-WAVE FUSION ACTIVITY PROCESS 4											
<i>fc1</i>	Performance Matric Hidden Layer (<i>hl</i>)=10 Delay(<i>d</i>)=2					<i>fc2</i>	Performance Matrics Hidden Layer (<i>hl</i>)=10 Delay(<i>d</i>)=2				
	perf	tim	eph	err	vad		perf	tim	eph	err	vad
hrv,rr-rms ,sddn,nn50	3.37	0	8	1.2	6	hrv,rr-rms ,sddn,nn50 mt _{on} ,mt _{off} ,mt _{pk}	8.4	0	7	0.45	6
hrv,rr-rms	7.97	0	10	- 0	6	nn50,mt _{on} , mt _{off} ,mt _{pk}	0.19	0	6	0	6
hrv, ,nn50	15.6	0	6	- 1.2	6	hrv, mt _{on} ,mt _{off} ,mt _{pk}	15.9	0	8	0.67	6
hrv ,sddn,	0.66	0	31	0	6	,rr-rms ,sddn, mt _{on} ,mt _{off} ,mt _{pk}	0.001	0	18	0	6
hr,rr-rms	33.7	0	6	0	6	sddn, mt _{on} ,mt _{off} ,mt _{pk}	2.94	0	9	0.02	6
rr-rms,sddn	21.3	0	7	0	6	mt _{on} ,mt _{off} ,mt _{pk}	4E- 04	0	10	0	6

In *fc1*, the parameters of time and validation indicate the same situation as above three fusion processes. Thus, the parameters of performance and epoch do not show exceptional results. The results of the two parameters are quite similar to those of previous fusion processes. According to Table 6.8, the same variation of performance and epoch values are highlighted as above fusion processes. Figure 6.9 highlights the two different cases of feature combination performances.





(a) Best feature combination in aspect of performance (*rr-rms, sddn*)

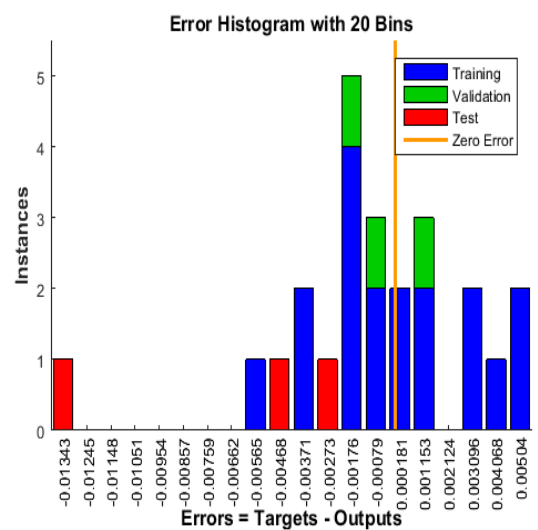
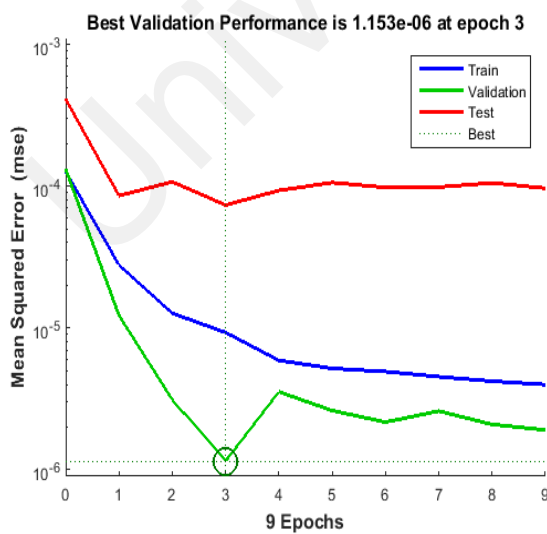


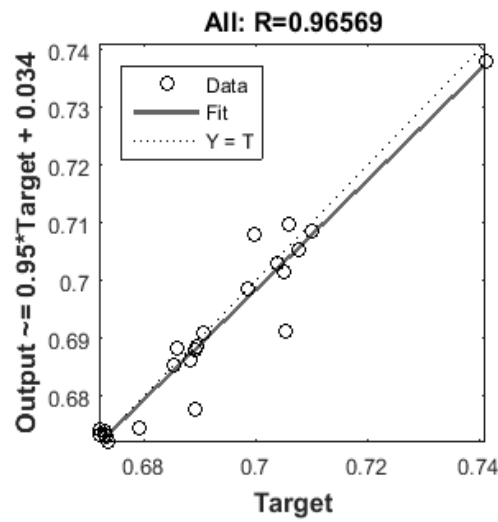
(b) Worst combination in aspect of performance (*rr-rms, nn50*)

Figure 6.9. Efficiency gages of fusion process four with old features combination

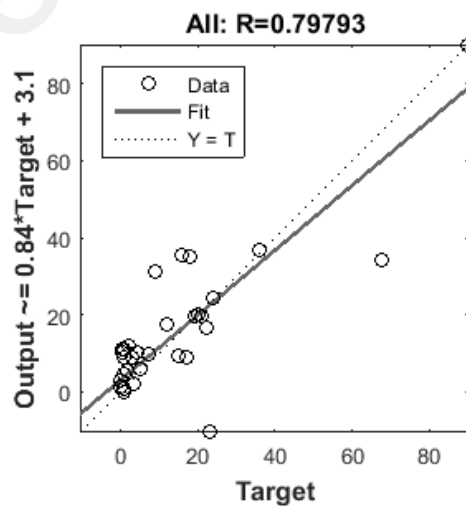
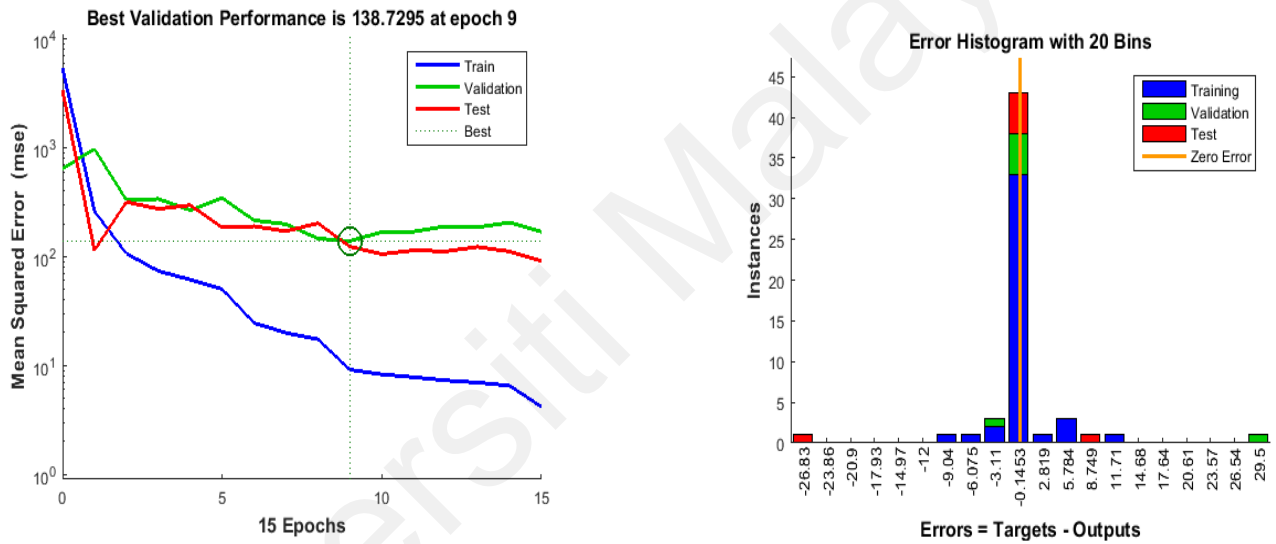
Figure 6.9 depicts the similar two *fc1* and *fc2* cases, which represent efficiency measurement gages of *fp4*. In *fc1*, Figure 6.9(a) reflects the best feature combination (*rr-rms* and *sddn*) of *fp4*. Feature combination of *rr-rms* and *sddn* delivers the epoch 0 that highlight the least computational complex value with far below zero error ratio level and accuracy of predictive classification in form of regression values reaches to bit satisfactory level $R=0.900$. In terms of worst scenario, Figure 6.9(b) illustrates the worst feature combination (*rr-rms* and *nn50*), which indicates that the best validation point is at epoch 15 (bit high computational complex value), error ratio is above to zero level and regression value ($R=0.8970$) highlights the accuracy which is almost near to above best feature combination in Figure 6.9(a).

By contrast, the trend *fc2* of *fp4* is a complete replica of *fc1* of *fp4* in terms of time and validation. However, the results of performance and epoch parameters are the same as the above fusion processes, except for the first and last combination of *fc2* of *fp4*. Figure 6.10 lists the outcomes for the three different conditions.





(a) Best combination in aspect of performance ($mt_{on}, mt_{off}, mt_{pk}$)



(b) Worst combination in aspect of performance ($hrv, rr-rms, sddn, nn50, mt_{on}, mt_{off}, mt_{pk}$)

Figure 6.10. Efficiency gages of fusion process four with new features combination

In the last part of the fusion activities, Figure 6.10 captured the efficiency measurement gages of *fp4* in context of best and worst cases in similar *fc1* and *fc2* cases. Figure 6.10(a) shows the best feature combination (mt_{on} , mt_{off} and mt_{pk}) of *fp4*, which indicates that epoch 3 is the computational complexity value with almost zero error ratio level and regression value ($R=0.966$) shows the high accuracy of predictive classification. Conversely, Figure 6.10(b) depicts the worst feature combination (*hrv*, *rr-rms*, *sddn*, *nn50*, mt_{on} , mt_{off} and mt_{pk}), which highlight the least computational complex value at epoch 9, error ratio is above than zero level and regression value $R=0.79$ indicates the least accurate prediction result.

The important part of this MDDDL is the fusion results, in which all fusion processes produce different outcomes, thereby showing some similarities for each parameter of each fusion processes. The experimental setup highlights the positive and negative results, especially in terms of new feature combinations, including three core features of the T wave (mt_{on} , mt_{off} and mt_{pk}). These findings are further discussed in critical analysis which highlight the similarities between four fusion processes as well as efficiency parameters of *fc1* and *fc2* in each fusion process.

6.5 Feature Critical Analysis

As discussed in Section 6.4, the most striking part of this research is the results that show positive elements of MDDDL. The performances metrics of each fusion process highlights the different efficiency level that is further segmented into two different features combinations (*fc1* and *fc2*). Through different combinations of features, the significance of three new features of T wave is clearly highlighted in all fusion processes. Figure 6.11 is a showcase of traditional features combination of fusion process one.

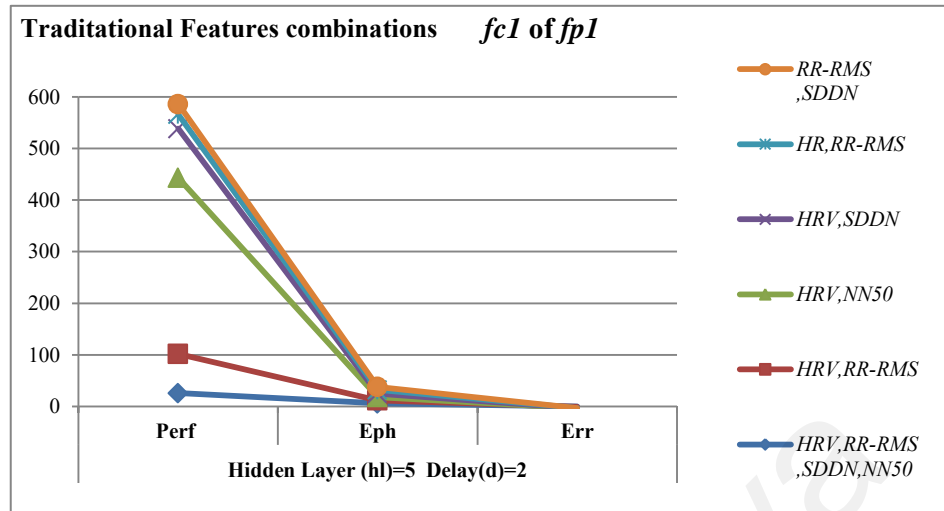


Figure 6.11. Features analytics of fusion process one (fc1)

According to the figure 6.11, the combination of features *rrrms*, *sddn* is indicate the best case in terms of efficiency level. The performance is high and an epoch value is low one in this combination. By contrast, the features combination of *hrv*, *rrrms*, *sddn*, *nn50* is worst one that present the low value of performance and epoch. Similarly, figure 6.12 highlights the different performance ratio of traditional feature combination by using the same pre-defined condition(*fc1* of *fp2*)

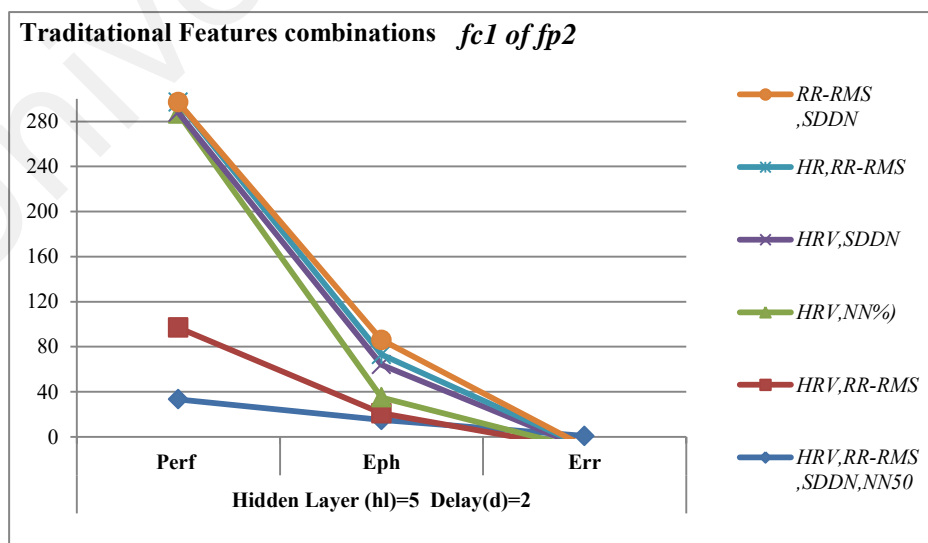


Figure 6.12. Features analytics of fusion process two (fc1)

In figure 6.12, the last combination *hrv* and *sddn* indicates the best in terms of efficiency due to the high rate of performance and epoch. With respect to last combination, features combination (*hrv,rr-rms,sddn,nn50*) shows the least in efficiency. The performance and epoch parameters are too low as compared to other features combination.

Furthermore, the next two fusion process highlights the different pre-defined condition (*hl=10*) as compared to first two fusion processes. Similar to *fp1* and *fp2*, the *fc1* and *fc2* are operated to analyses the performance of fusion activities in aspect of different features. However, the features streams are vice versa like in fusion process three(*fp3*), the target stream is *flattened T wave* features and input stream is TWA features. Similarly, in process four (*fp4*), the target stream is TWA and input stream is *flattened T wave* features. Figure 6.13 is a display unit of *fc1* results in context of *fp3*.

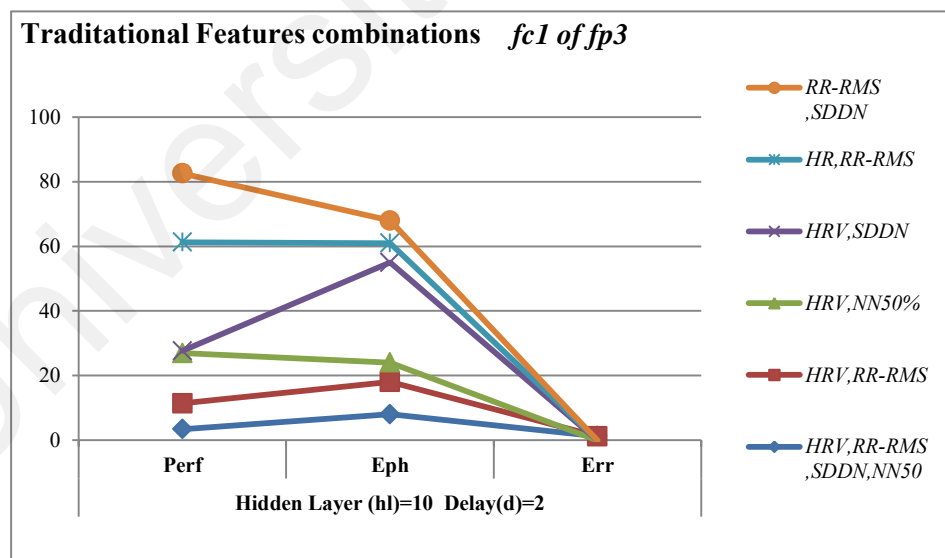


Figure 6.13. Features analytics of fusion process three (*fc1*)

According to figure 6.13, the results of *fp3* indicate the features combination of *rr-rms, sddn* is the best in efficiency. Conversely, features combination of *hrv,rr-rms,sddn,nn50* in figure 6.13 shows the low level of efficiency. Additionally, figure 6.14 is a graphical

representation of $fc1$ of $fp4$. The results of $fp4$ $fc1$ deliver the surprise element in context of all the feature combinations which are closely related to high efficiency level expect the features combination of $nn50,rr-rms$ (shows low efficiency level). It is observed that the condition of $hl=5,d=2$ and defined features streams are perfect one for predictive classification of MI in terms of traditional feature combination.

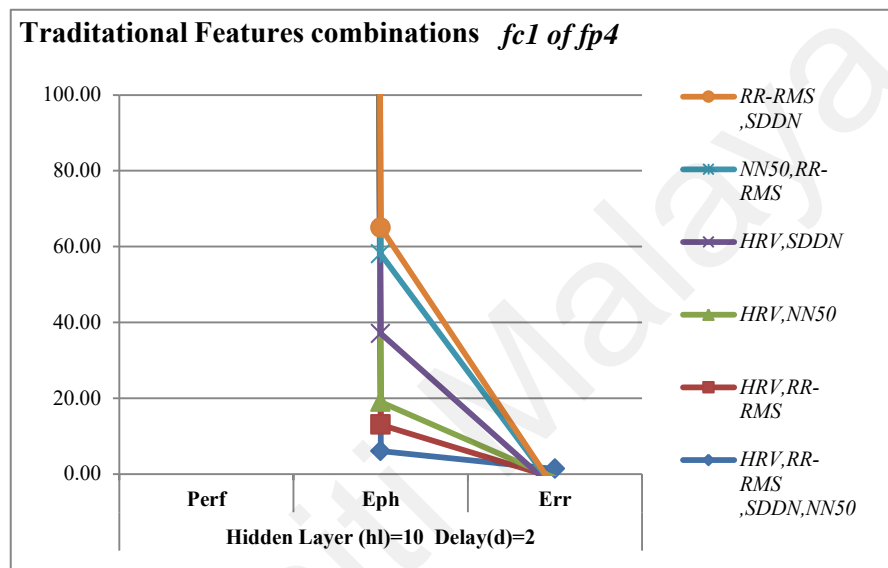


Figure 6.14. Features analytics of fusion process four ($fc1$)

Moreover, the next part of this analysis is the MDDDL $fc2$ results of all fusion processes. Figure 6.15 is showcase of $fc2$ $fp1$ that shows the true positive results. A feature combination of mt_{on}, mt_{off} and mt_{pk} shows the most efficient result in terms of performance and epoch. The second best in similar in figure 6.15 is the combination of $sddn, mt_{on}, mt_{off}$ and mt_{pk} that is bit low efficient as compared to above one. Conversely, the features combination of $sddn, mt_{on}, mt_{off}, mt_{pk}$ ($fp4fc2$) shows the worst combination in terms efficiency, such combination show the performance and epoch values are too low.

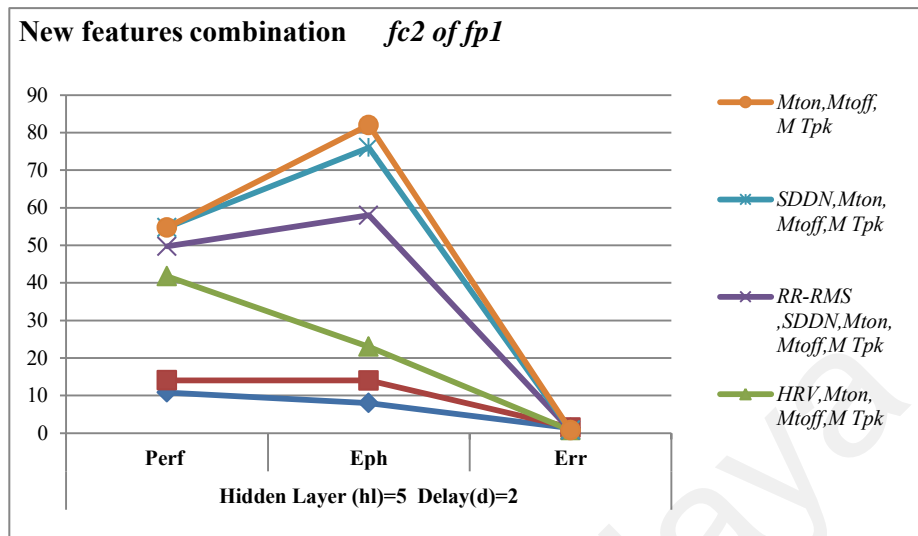


Figure 6.15. Features analytics of fusion process one (fc2)

The contest of efficiency comparison is still on going in the form of next two fusion processes. In display unit of figure 6.16 highlights the replica shape of *fp2 fc2*, in terms of best result. The features combination of $mt_{on}, mt_{off}, mt_{pk}$ and $sddn, mt_{on}, mt_{off}, mt_{pk}$ shows the best and second best combinations as compared to other combinations.

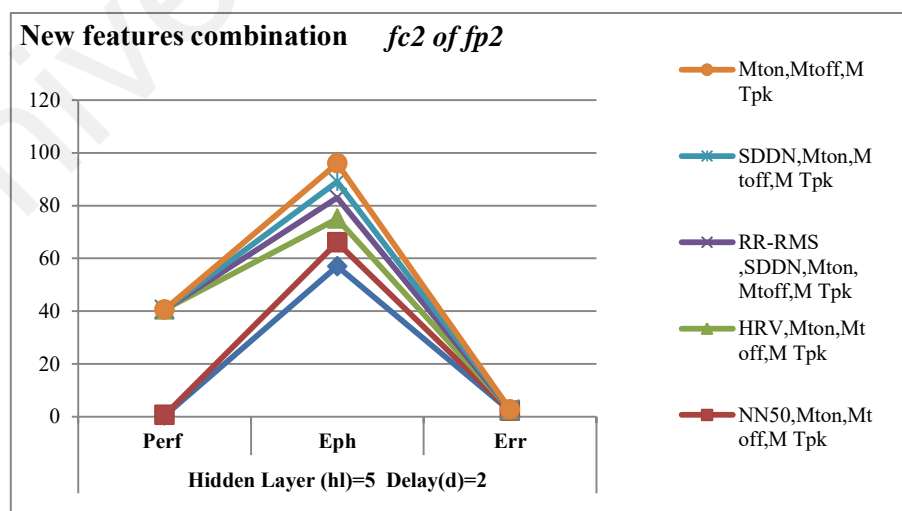


Figure 6.16. Features analytics of fusion process two (fc2)

Similarly, in $fc2\ fp3$ the replicated results are shown in below display unit highlighted in figure 6.17. Again the combination of mt_{on} , mt_{off} and mt_{pk} shows the best in terms of performance and epoch values.

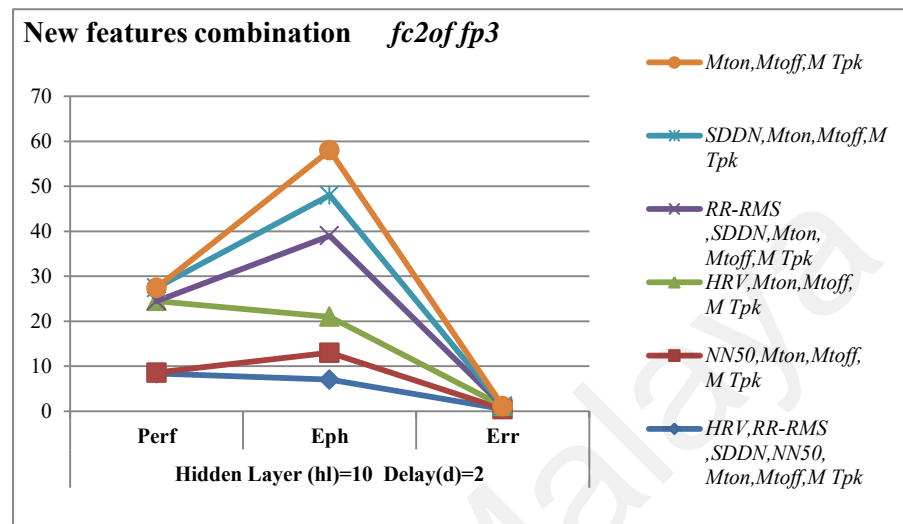


Figure 6.17. Features analytics of fusion process three (fc2)

Finally, the features combinations of $fp4\ fc2$ show the unique results of whole operational activities. According to figure 6.18, all features combinations represent the idea condition which means the performance parameter of all the features combinations are at peak value. By contrast, the epoch parameters of all the combinations are at position of zero level.

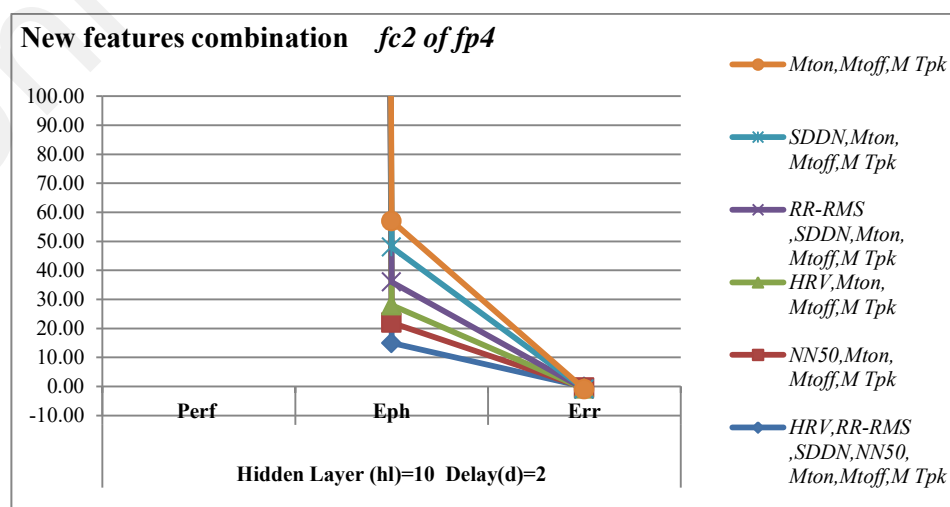


Figure 6.18. Features analytics of fusion process four (fc2)

The unique results in figure 6.18 are not only the ideal condition. According to literature, the performance and epoch values are directly related, but in result of *fp4.fc2* totally represent the opposite case. The inversely proportional of performance and epoch in figure 6.18 indicates the some hide errors in the scenario of *fp4.fc2*.

Furthermore, to validate the MDDDL each fusion process results through follow the statistical diagnostic test evaluation and state-of-the-art comparison of MDDDL. The next two subsections 6.6.1 and 6.6.2 of section 6.6 covers the evaluation schemes. Subsection 6.6.1 presents the parameters of statistical diagnostic test evaluation (*MedCalc* software) that includes positive prediction value (*PPV*), negative prediction value(*NPV*), specificity(*Sp*), Sensitivity(*Se*), Diseases Prevalence(*DisP*), Positive ratio (*PR*), Negative Ratio (*NR*) and accuracy(*Acc*). Secondly, subsection 6.6.2 cover the state-of-the-art methods are compared with MDDDL.

6.6 MDDDL Evaluation Schema:

This section presents the wrap up of MDDDL in form of validation. Such validation covers two different evaluation schemes namely, statistical diagnostic test evaluation and evaluation of MDDDL through comparison of state-of-the-art predictive classification methods.

6.6.1 Statistical Diagnostic Test Evaluation

A statistical diagnostic test evaluation was performed by using the *MedCalc* software (Gardner & Greiner, 2006; Mercaldo, Lau, & Zhou, 2007). For statistical evaluation of MDDDL, the parameters of diagnostic test evaluation namely, *PPV*, *NPV*, *PR*, *NR*, *Sp*, *Se*, *Acc* and *DisP* were the indicators of efficiency calculator. The threshold points of detected R peaks were used for calculation of the parameters of statistical diagnostic test evaluation. The threshold points of effective R peaks detection algorithm

namely, true positive R Peaks detected(TP), negative positive R peaks detected(NP), false positive R peaks detected(FP) and False negative R peaks detected(FN) were used to measure the parameters of evaluation test. Equations 6.8 to 6.15 highlighted the parameters of diagnostic test evaluation.

$$\text{Sensitivity } (Se) = \frac{TP}{TP + FN} * 100 \quad (6.8)$$

$$\text{Specificity } (Sp) = \frac{TN}{FP + TN} * 100 \quad (6.9)$$

$$\text{Positive Ration } (PR) = \frac{SE}{1 - SP} * 100 \quad (6.10)$$

$$\text{Negative Ratio } (NR) = \frac{1 - SE}{SP} * 100 \quad (6.11)$$

$$\text{Positive Prediction value } (PPV) = \frac{TP}{TP + FP} * 100 \quad (6.12)$$

$$\text{Negative Prediction value } (NPV) = \frac{TN}{FN + TN} * 100 \quad (6.13)$$

$$\text{Accuracy } (ACC) = \frac{TP + TN}{TP + TN + FP + FN} * 100 \quad (6.14)$$

$$\text{Disease Prevalence } (DisP) = \frac{TP + FN}{TP + TN + FP + FN} * 100 \quad (6.15)$$

The parameters of statistical diagnostic test evaluation in equations 6.8 to 6.15 are relied on the fixed threshold points (discussed in Section 4.4 of Chapter 4). The significant part of statistical diagnostic test evaluation are the results. Such results claimed the proposed structure of the MDDDL is truly suitable for predictive classification of any type of T wave anomalies especially for *flattened T waves*.

Table 6.9 presents the complete statistical evaluation of UMMC data streams (*flattened T waves* subjects) by using the results of Table 6.1 and Equations 6.8 to 6.15.

Table 6.9: Data streams of UMMC evaluation through statistical test evaluation.

Flattened T wave (UMMC)											
<i>M_Subjects</i>	<i>PPV (%)</i>	<i>NPV (%)</i>	<i>PR</i>	<i>NR</i>	<i>Sp (%)</i>	<i>DisP 95% CI</i>		<i>ACC 95% CI</i>		<i>Se 95% CI</i>	
ECGRLIABD	100	<i>Nil</i>	1	<i>Nil</i>	<i>Nil</i>	100	79.41	100	79.41	100	79.41
ECGRLIANSI	100	<i>Nil</i>	1	<i>Nil</i>	<i>Nil</i>	100	86.28	100	86.28	100	86.28
ECGRLIIDAT	100	<i>Nil</i>	1	<i>Nil</i>	<i>Nil</i>	100	76.84	100	76.84	100	76.84
ECGRLIIFA	100	<i>Nil</i>	1	<i>Nil</i>	<i>Nil</i>	100	47.82	100	47.82	100	47.82
ECGRLIIHAJ	100	<i>Nil</i>	1	<i>Nil</i>	<i>Nil</i>	100	90.75	100	90.75	100	90.75
ECGRLIIISAT	100	<i>Nil</i>	1	<i>Nil</i>	<i>Nil</i>	100	98.60	100	98.60	100	98.60
ECGRLIIJUS	100	<i>Nil</i>	1	<i>Nil</i>	<i>Nil</i>	100	92.13	100	92.13	100	92.13
ECGRLIINAF	100	<i>Nil</i>	1	<i>Nil</i>	<i>Nil</i>	100	83.19	100	83.19	100	83.19
ECGRLIIRAF	100	<i>Nil</i>	1	<i>Nil</i>	<i>Nil</i>	100	80.49	100	80.49	100	80.49
ECGRLIIRAZ	100	<i>Nil</i>	1	<i>Nil</i>	<i>Nil</i>	100	86.28	100	86.28	100	86.28

Similarly, Table 6.10 covers the statistical evaluation of PTB data streams (TWA subjects) through couple the results of Table 6.3 in Equations 6.8 to 6.15.

Table 6.10: Data streams of PTB evaluation through statistical test evaluation

T wave Alternans (PTB)											
<i>M_Subjects</i>	<i>PPV (%)</i>	<i>NPV (%)</i>	<i>PR</i>	<i>NR</i>	<i>Sp (%)</i>	<i>DisP 95% CI</i>		<i>ACC 95% CI</i>		<i>Se 95% CI</i>	
tw00.m	100	<i>Nil</i>	1	<i>Nil</i>	<i>Nil</i>	100	69.15	100	69.15	100	69.15
tw02.m	100	<i>Nil</i>	1	<i>Nil</i>	<i>Nil</i>	100	80.49	100	80.49	100	80.49
tw03.m	100	<i>Nil</i>	1	<i>Nil</i>	<i>Nil</i>	100	78.20	100	78.20	100	78.20
tw05.m	100	<i>Nil</i>	1	<i>Nil</i>	<i>Nil</i>	100	89.11	100	89.11	100	89.11
tw06.m	100	<i>Nil</i>	1	<i>Nil</i>	<i>Nil</i>	100	81.47	100	81.47	100	81.47
tw08.m	100	<i>Nil</i>	1	<i>Nil</i>	<i>Nil</i>	100	71.51	100	71.51	100	71.51
tw09.m	100	<i>Nil</i>	1	<i>Nil</i>	<i>Nil</i>	100	81.47	100	81.47	100	81.47
tw10.m	100	<i>Nil</i>	1	<i>Nil</i>	<i>Nil</i>	100	69.15	100	69.15	100	69.15
tw11.m	100	<i>Nil</i>	1	<i>Nil</i>	<i>Nil</i>	100	73.54	100	73.54	100	73.54
tw12.m	100	<i>Nil</i>	1	<i>Nil</i>	<i>Nil</i>	100	79.41	100	79.41	100	79.41

However, the comparison between confidence interval level(95% CI) of parameters of *Se*, *Acc* and *DisP* are help out for further quantitative and qualitative improvements.

Moreover, figure 6.19 highlights the confidence interval comparison between

parameters of Se , Acc and $DisP$ that derived from flattened T wave subjects of UMMC dataset and TWA subjects of PTB dataset.

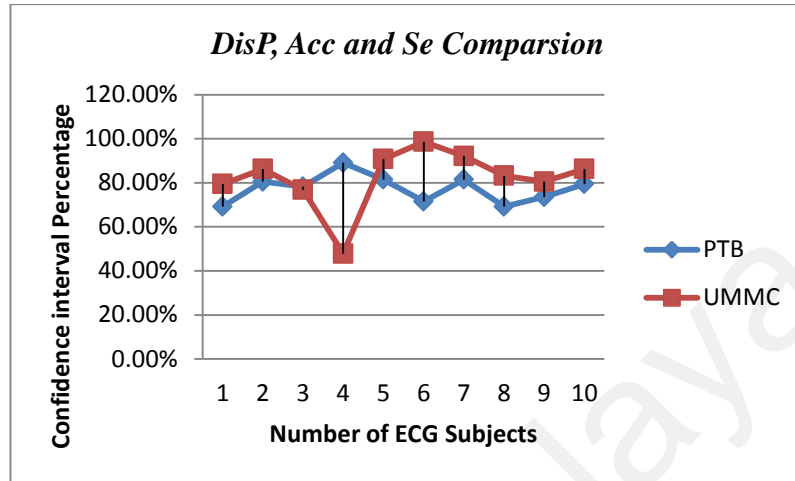


Figure 6.19. Confidence level comparison between parameters

6.6.2 State-of-the-art Comparison

This section highlights the comparison of proposed MDDDL with existing methods. The significant part of this MDDDL workflow is the execution of the second evaluation scheme namely, the evaluation of MDDDL through comparison with state-of-the-art techniques. Table 6.11 lists the state-of-the-art comparison.

Table 6.11: MDDDL Comparison with state-of-the-art.

Comparative results of MDDDL with other Predictive methods					
Sr #	Method	Dataset	Year	Accuracy ratio	Positive Prediction Value(PPV)
1	Prediction of MI with ANN(Kojuri, Boostani, Dehghani, Nowroozipour, & Saki, 2015)	Cardiax (SOT Sonotechnik, Maria Rain, Austria)	2015	95.63%	99.30%
2	Discrete Cosine Transform(DCT)(Acharya, Fujita, Adam, et al., 2017)	PTB Diagnostic ECG Database	2017	98.50%	99.80%
3	Discrete Wavelet Transform(DWT)(Acharya, Fujita, Adam, et al., 2017)	PTB Diagnostic ECG Database	2017	98.16%	99.77%
4	Empirical Mode Decomposition(EMD)(Acharya, Fujita, Adam, et al., 2017)	PTB Diagnostic ECG Database	2017	81.34%	93.16%

<i>Sr #</i>	<i>Method</i>	<i>Dataset</i>	<i>Year</i>	<i>Accuracy ratio</i>	<i>Positive Prediction Value(PPV)</i>
5	Efficient Predictive Model for MI(Daraei & Hamidi, 2017)	Shahid Madani Specialized Hos-pital, Khorramabad, Iran	2017	93.30%	—
6	Proposed MDDDL (Predictive Classification)	PTB Diagnostic ECG Database and University of Malaya Medical Center	2019	100% (UMMC& PTB)	100% (UMMC & PTB)

Table 6.11 shows that the prediction model was designed to predict acute MI cases by using customized ANN with an overall accuracy of 95.63% and a positive prediction of 99.30%. The next three methods were selected from a comparative study of MI prediction models, which highlighted three different methods, namely, discrete cosine transform (DCT), discrete wavelet transform (DWT) and empirical mode decomposition (EMD), with their respective accuracy and positive prediction values (98.16 % and 99.80% for DCT, 98.16% and 99.77% for DWT, and 81.34% and 93.16% for EMD). The fourth method is an efficient cost-effective prediction model for MI cases that exhibits an accuracy of 93.30%.

Finally, the proposed MDDDL model for the prediction of different MI cases highlights the maximum efficiency level for predictive classification of various MI cases with high accuracy levels in all the aforementioned methods. Trend of unique $fc1$ and $fc2$ along with best predictive classification algorithm(*train scg*) is the lead factor to attain high ratio of prediction accuracy. However, some qualitative improvements required in the MDDDL should be covered in future works by extending the number of fusion activities with employment of other MI categories as well as embed other training algorithms for more identification the similarity nature of various MI cases and further refinement of computation cost.. Additionally, extensive levels of feature

engineering will be coupled with traceability factors of model-driven architecture that help to understand the other factors of *nsst-t* in MI.

6.7 Conclusion

This chapter deals with the predictive analytics of different causes of MI by using a public dataset (PTB dataset) and an exclusive dataset (UMMC). The current research proposes a novel approach in the form of MDDDL for the predicative classification of *flattened T-wave* such as that in MI cases without past records. The MDDDL uses the concept of DDL for the predictive classification of the *flattened T wave* with the help of fusion activities. In MDDDL, the effective R-peak detection algorithm is executed on both datasets. Then, with the help of these detected R-peaks, the subsequent feature extraction steps are performed. The seven extracted features (*rr-rms*, *sddn*, *nn50*, *hrv*, *mt_{on}*, *mt_{off}* and *mt_{pk}*) are categorised in two groups: the traditional feature combinations (*fc1*) and the new feature combinations (*fc2*). Through these extracted feature streams, the main part of MDDDL, the fusion activities, are performed as four fusion processes (*fp1*, *fp2*, *fp3* and *fp4*). These fusion processes are achieved in MDDDL in two different settings. In Setting I, the first two fusion processes (*fp1* and *fp2*) are conducted with two feature combinations (*fc1* and *fc2*) along with defined conditions, which include a customised *NARX ANN* with five hidden layers ($hl = 5$) and two delays ($d = 2$), the best predictive algorithm of scaled conjugate gradient (*trainscg*) and different feature stream scenarios. Setting II is a complete replica of the operational investigations executed in Setting I. However, Setting II differs in the defined conditions, such as the presence of 10 hidden layers ($hl = 10$) in this setting. Furthermore, a discussion of the last feature comparison is executed to analyse the performance metrics by using the parameters of performance, epoch, time, validation checks and error ratio. Overall, the performance metrics show productive prediction results of *flattened T wave* cases. Finally, evaluate

the complete structural results of MDDDL through statistical diagnostic test evaluation by using the *MedCalc* software and state-of-the-art comparison. The diagnostic test evaluation results were measured on the parameters of *PPV*, *NPV*, *PR*, *NR*, *Se*, *Sp*, *Acc* and *DisP*. According to these parameters of diagnostic test evaluation, the results delivered the positive results on both datasets(UMMC and PTB). Additionally, the confidence level intervals of *Acc*, *Se* and *DisP* of both datasets were compared for future improvements and enhancement. In last, state-of-the-art evaluation was performed by comparison the MDDDL predictive classification model with previous MI Predictive classification models However, some qualitative improvements required in MDDDL, namely, a scalable number of fusion processes that employ additional MI data (ECG) streams for comprehensive classification, will be covered in future works. Furthermore, extensive levels of feature engineering will be coupled with traceability factors of model-driven architecture that help in the backward tracing of *nsst-t*.

CHAPTER 7: CONCLUSION

7.1 Introduction

This Chapter concludes the thesis through highlighting the different paradigms which are used in diagnostics purposes for providing the better treatment to cardiac patients. In this thesis, existing recognition and predictive classification techniques of different cardiac diseases were deeply investigated along with complete exploitation of existing feature engineering techniques. Moreover, conventional features selection formation coupled with various traditional wavelet analysis and machine learning techniques were employed for accurate recognition of different cardiac diseases especially Myocardial Infraction (*MI*) and Atrial Fibrillation (*afib*) recognition. However, some situations of MI that belongs to Non Specific ST-T Changes (*nsst-t*) are unpredictable and unclassifiable by using state-of-the-art recognition methods. In context of *nsst-t* knowledge, flattened anomalies are one of the parts of such MI situation that related to *nsst-t*. The need and significance values of *flattened T wave* in terms of accurate recognition or classification were justified in Chapter 1(section 1.3).For the concern of different ECG analytics experiments, an exclusive dataset was obtained from one of the larger Medical Research Center in Kuala Lumpur, Malaysia (UMMC) and secondly two public datasets of MIT-BIH and PITB were used. Afterwards, the collection of extensive set of ECG datasets, the existing time domain feature extraction methods coupled with proposed machine learning approaches for the recognition of different cardiac diseases especially *MI* situation in *flattened T wave* and *afib*. Additionally, to enhance the recognition efficiency with consideration of complexity factors, this thesis proposed and developed an three effective methods namely, T-onset feature driven deterministic method (for *flattened T wave*), features pattern recognition of cardiac

diseases through deep deterministic learning model (DDL), and model driven deep deterministic learning (MDDDL) for predictive classification of different *MI* situations.

To obtain certain level of results in recognition the performance domain of ECG features, various studies have empirically investigated the different features engineering techniques and recognition techniques. Most of the studies reported outperform recognition results but some reported unique results in terms of recognition of the unseen cardiac diseases. Few of the studies reported the improper discussion of different shapes of *MI* that generate the impact on *nsst-t*. Additionally, the empirically investigations of these studies reported no significant values for recognition of the flattened anomalies. The detailed justifications of empirically investigations of these studies are also presented in Chapter 2 (see section 2.3 and section 2.4)

The formation of this thesis is completely lies on the foundation of those studies that reported the empirical investigations in review of the recognition of unjustifiable cardiac diseases recognition (especially of *flattened T wave*) along with complexity involved in the recognition process. Afterwards, the experimental results in this thesis show that the proposed methods outperformed the existing recognition or classification methods. Moreover, before proceeding the *flattened T wave* recognition, at very first determine the feature structure of *flattened T wave* through adoption of the deterministic method by using the core art of T-wave Alternans (TWA) algorithm (see Section 4.4).

In this thesis, each individual research query in terms of research question (RQ) answered properly and detail discussions of these queries are already covered in Chapter 2, Chapter 4, Chapter 5, and Chapter 6. To wrap up this thesis by revisiting the research objectives and RQs that presented in Chapter 1 briefly describe how they are achieved. The major contributions, limitations, and future directions of this thesis are also a part of this Chapter.

7.2 Recap of Research Objectives and Research Questions

This section reviews the research objectives and RQ's of this study. Furthermore, briefly discuss the findings of each objectives RQ in terms of contribution of this study.

Objective 1: To extract the different features of flattened T wave cases from UMMC dataset through investigating the state-of-the-art techniques of feature engineering.

To obtain this objective, the relevant literature reviewed in the domain of state-of-the-art feature engineering techniques such techniques are further fruitful for the recognition of different cardiac diseases in ECG signals. To gain the first objective, exploitation of the different feature sets of UMMC dataset by imposing the state-of-the-art feature extraction techniques. These extracted features are further used for the recognition of different cardiac diseases especially recognition for unjustifiable cardiac diseases namely, *flattened T wave*. To attain the level of extraction for fruitful features knowledge of UMMC dataset more than 190 main studies obtained from six core different bibliographic databases (namely, Web of Science, IEEE Xplore, ACM Digital Library, PubMed Science Direct and Springer Link) were systematically selected and reviewed from the perspective of defined aforementioned aspects. Furthermore, the findings of each RQ of the objective 1 briefly are discussed below. .

RQ1: What are the existing methods of feature engineering for recognition of cardiac diseases?

In exploration result of literature review, several existing time and frequency methods were used for the extraction of features. The detailed answer is mentioned in Chapter 2(see subsection 2.3.3)

RQ2: How useful are the existing feature extraction techniques for extraction of different features of UMMC dataset?

The literature exploitation deliver the existing feature engineering techniques which were deployed on different public dataset with the same method that indicate the concept of global acceptance. Thus, in the light of global acceptance the same feature engineering techniques were deployed on UMMC datasets and got fruitful results. The detail of complete extracted features schemas of UMMC dataset are discussed in Chapter 3 (see section 3.6), Chapter 4 (see section 4.2), Chapter 5(see subsection 5.3.1), and Chapter 6(see subsection 6.3.1).

RQ3: What are the limitations in existing features selection schema for the recognition of cardiac diseases and how such schemas affect the performance and complexity factor?

Two limitations are observed in existing features selection that may affect directly or indirectly in recognition of different cardiac diseases. The factors of dependences involved between features and enhancement features set for recognition of cardiac diseases are the two core limitations in features selection (see Section 2.7.1). Therefore, these limitations affected the performance in recognition process and large features sets may cause the enhancement in computational complexity. The detailed justification of this answer in Chapter 2(see Section 2.5 and Section 2.7)

Objective 2: To develop efficient R peaks detection algorithm; for recognition of different ECG anomalies that are helpful for detection of *afib* and MI cardiac diseases.

To achieve this objective, the systematic methodology was adopted for the formation of accurate and robotic R peaks detection algorithm. In construction of efficient R peaks

detection algorithm, at first, the exploration of literature was performed to review the state-of-the-art R peaks detection algorithm (See Chapter 2, subsection 2.2.3). For achievement of this objective, the efficient and robust R peaks detection algorithm was constructed on the basis of limitation of state-of-the art algorithms. Additionally, the complete constructional steps are briefly discussed in Chapter 3(see subsection 3.4.1) and secondly, justified the statement of how such algorithm played a vital role in Chapter 4, Chapter 5 and Chapter 6. The findings of this objective in terms of different RQs answered are highlighted below.

RQ4: What are the limitations in traditional R peaks detection algorithms?

The major concern in state-of-the-art R peaks detection algorithms are the alignment of fix threshold. According to the literature, the assignment of fix threshold values for the detection of R peaks are the limitations and through such limitation factor the generation of another limitation that belongs to recognition of the different cardiac diseases. The detail discussion of such limitations which belongs to traditional R peaks detection algorithms are presented in Chapter 2 (see Section 2.8). Moreover, how to get some handy results after fix out these limitations are detail discussed in Chapter 4, Chapter 5 and Chapter 6

RQ5: How can the performance of the developed R peaks detection algorithm be evaluated?

The performance of proposed and developed effective R Peaks detection was evaluated through different paradigms ,namely efficiency gauges of such algorithm and state-of-the-art comparison of developed effective R peaks algorithm. The details of performance evaluation of developed algorithm are discussed in results section of

Chapter 4(see Section 4.4). Furthermore, the evaluation in terms of state-of-the-art comparison is also highlighted in Chapter 4 as a tabular form (See Table 4.5).

Objective 3: To highlight the correlation between flattened T waves and other anomalies of T waves.

To accomplish this objective, the deterministic method was adopted for features exploitation of *flattened T wave* by using the dataset of UMMC. To measure the similarities of *flattened T wave* with other anomalies of T wave and nature of *flattened T wave*, the two pre-defined processes were followed. For nature identification of *flattened T wave*, T-onset feature extraction of *flattened T wave* was performed through employing the core part of TWA algorithm. The complete logical justification of this derivation of T-onset feature of *flattened T wave* is presented in Chapter 4 (see Table 4.2). To attain the complete shape of this objective, the other features of *flattened T wave* were also extracted for further features pattern matching of *flattened T wave* with other anomalies. For features pattern matching concerns, the exclusive dataset UMMC and public datasets of MIT-BIH, PITB were extensively used. All the operational investigations are truly discussed in results section of Chapter 4, Chapter 5 and Chapter 6. Moreover, the findings of each RQ of this objective are mentioned below

RQ6: What is the importance of flattened of T wave abnormality in the context of medical or clinical ontologies?

The significant value of accurate recognition of *flattened T wave* reflects one factor of *nsst-t*. In context of *nsst-t*, the accurate detection and recognition of the flattened anomalies plays a vital role for findings the other factors of *nsst-t*. The detailed discussion of *flattened T wave* significance in context of *nsst-t* is presented in Chapter 2(see Section 2.4)

RQ7: How useful are the existing techniques to identify the flattened T wave features?

To employ the traditional feature extraction methods in deterministic way for extraction the *flattened T wave* features. The core step of TWA algorithm was inducted to extract the T-onset feature of *flattened T wave* by considering the detected R Peaks a fiducial point. Chapter 3, subsection 3.5.1 declared the proper justification of such R peaks usage. Afterward, different sort of results in Chapter 4 (see section 4.4) were validated such justification.

RQ8: How much do the features of the flattened T wave depend on the other ECG Wavelet segments?

All the operational processes were followed in the deterministic way for the extraction of *flattened T wave* features through the help of other features of ECG wavelet. A detected R peak of TWA algorithm used for finding the *flattened T wave* T-onset feature is the claim of this research question, such claim is completely justified in Chapter 4 result section 4.4. Moreover, the critical analysis findings of Chapter 5 (see section 5.5) and Chapter 6 (see section 6.5) indicates different sort of these feature dependencies.

Objective 4: To develop (minimum time or computational complexity) models for recognition and predictive classification of different *afib* and MI cases.

To attain this objective, the structure of this objective breaks into two subsets which belong to proposed recognition model of different cardiac diseases especially *flattened T wave* (DDL) and predictive classification model of different MI cases especially *flattened T wave* (MDDDL). The structure of proposed model (DDL) was constructed in pre-defined manner that used for features patterns matching of *flattened T wave* with

ST-T changes. Similarly, other cardiac ambiguities were also matched in the same way that declared the positive results of proposed model in terms of global acceptance. Chapter 5 is a complete justification of all the operational activities of DDL that defines the logical structure of feature pattern matching. In Chapter 5 (see Section 5.5), a deep critical analysis was performed which highlights the different set features combinations for complexity analysis. The findings of such analysis helped to reduce the time space complexity factor in recognition of cardiac diseases. Furthermore, the second part of this objective is achievement in Chapter 6 that presented the proposed predictive classification model (MDDDL) of different cases of MI. The operational processes of proposed predictive model were constructed on the theme of model driven deep learning. The detailed findings of MDDDL are covered in Chapter 6 (see Section 6.4). The answers of each RQ of this objective are properly justified as below.

RQ9: How much of the recognition and prediction performance of cardiac diseases can be enhanced through developed recognition and prediction models?

The recognition processes of proposed models (DDL and MDDDL) have shown the better accuracy ratio results as compared to traditional models. The justification of this claim are presented as a state-of-the-art methods comparison at the end of Chapter 5 and Chapter 6 respectively. In Chapter 5, state-of-the-art comparison is presented in Table 5.14 and Table 5.15. Similarly, at Chapter 6, Table 6.11 covered the state-of-the-art the comparison.

RQ10: What are the limitations of the developed models of recognition and predictive classification of different cardiac diseases?

Two core limitations are observed in both proposed models. In recognition concern (DDL), least efficient results were observed in *afib* cases on stage 2 (see subsection

5.4.2 in Chapter 5). The concern of least efficient results in *afib* cases is a limitation in DDL that will be covered in future by employing special additional stage for *afib* cases with more hidden layers. Association of extra stage in DDL for *afib* cases may enhance computational cost and reduction of such computational cost up to desired position will be a challenging task in future. Furthermore, second limitation belongs to features dependencies that are involved on both DDL and MDDDL (see section 5.5 and section 6.5).

RQ11: What are the limitations in existing recognition models in the context of complexity factor?

It is observed during review session of literature, the existing recognition models of different cardiac diseases were least discussed the complexity factor namely, cardiac arrhythmias classification through CNN, wavelet transformation maxima minima approach for the classification of cardiac diseases, T wave alternans algorithm for the recognition of T wave anomalies, and MI classification through CNN (See Section 2.7 of Chapter 2). The detailed discussion of complexity factor in recognition of different cardiac diseases are covered in Chapter 5 and Chapter 6 in the form of different analysis (see section 5.5, Appendix-A and section 6.5).

Objective 5: To evaluate the performance of proposed models through efficiency measurement matrices.

To accomplish this objective, the performance of proposed models of recognition and predictive classification of cardiac diseases were evaluated through defined efficiency measurement metrics namely, confusion matrix, epoch values, time constraint, best validation point, and regression value. The findings of such metrics are reported in results sections of Chapter 5 and Chapter 6 respectively (see subsection 5.4.1,

subsection 5.4.2, subsection 6.4.1.1 and subsection 6.4.1.2). Moreover, at the end of Chapter 5 and Chapter 6, the state-of-the-art comparisons are also mentioned in context to evaluate these proposed models

RQ12: To what extent is the performance of the proposed recognition and predictive models improved relative to existing state-of-the-art techniques?

An overall recognition accuracy of different cardiac diseases especially the *flattened T wave* cases are bit high as compared to state-of-the-art methods. More details of different experiments and results are presented in Chapter 5 and Chapter 6 (see Section 5.4 and Section 6.4 respectively). The justification of achieving the high level of accuracy in DDL and MDDDL models was possible through the high rate results of proposed effective R Peaks detection algorithm and feature selection process. The findings of proposed effective R Peaks detection algorithm are presented in Chapter 4 (see Section 4.4).

RQ13: Why the proposed recognition or classification and prediction models are efficient??

The efficiency of proposed recognition and predictive classification models is attained through feature patterns matching of *flattened T wave* with other anomalies. To maintain the efficiency factor, feature patterns matching of other cardiac disease namely *afib* are performed in same way as for *flattened T wave*. The justification of efficiency of the proposed recognition and predictive classification models are presented in Chapter 5 and Chapter 6 (See section 5.4 and section 6.4).

RQ14: How can the time complexity factor be evaluated?

At the end of Chapter 5 and Chapter 6, the features combinations analyses of proposed models (DDL and MDDDL) were performed to evaluate the time complexity factor (see Section 5.6 and Section 6.5). The feature selection analysis is presented at the end of this thesis in Appendix-A.

7.3 Limitations

Few limitations were identified in current recognition and predictive classification models.

1. In scenario of different unseen MI situations, the current recognition and predictive classification models can only classify the *flattened T wave* cases other than remaining factors of *nsst-t* (see Section 3.3). Thus, these models can only determine significant value of *flattened T wave* in context of *nsst-t*.
2. To get the exact significant knowledge of *nsst-t*, all the anomalies that related to *ST segment changes* and *T wave changes* with inclusion of complete platform of flatten anomalies. However, the proposed models in the form of DDL and MDDDL are employed to highlight only *flattened T wave*. The complete knowledge platform of *nsst-t* is a limitation in proposed deterministic methods. Additionally, extensive level of feature engineering and recognition of other flatten anomalies are pending on these deterministic methods. To overcome the limitations in future, few more features of *flattened T wave* will be extracted for the execution of operational activities of proposed DDL for the recognition of cardiac diseases. The construction for improvement of DDL model is based on the theme of reduction of features dependences that will be covered in future. Moreover, the MDDDL model will also be improved through same reduction of feature dependencies.
3. The exploitation session of literature delivered the two core areas to proceeds this research work. Review process of literature firstly, highlighted the

recognition issues of unjustifiable cardiac disease especially the flattened T wave and secondly, ignorance of computational complexity in classification processes. The proposed DDL and MDDDL models were employed for these highlighted issues. However, there are few limitations in terms of qualitative improvements required in these models namely, in DDL case, least accurate results on stage 2 in *nsr* cases (see Chapter 5, section 5.4.1). Similarly, in MDDDL more fusion process, enhancement of hidden layers and retrained the model for further different MI cases (see Chapter 6, section 6.4).

7.4 Future Directions

This section highlights the future directions for the recognition of different sort of cardiac diseases.

7.4.1 Early detection of Neurogenic Stunned Myocardium via nsst-t

Over the complexity of different cardiac diseases, the malfunction of heart muscles with the direct linkage of human nervous system which lies in the serious life risk alarm and requires special attention in emergency department of hospital,. In domain of neurocardiology, accurate and knowledge based recognition of neurogenic stunned myocardium (*NSM*) injury is most desirable requirement of medical professional (Biso et al., 2017). Numerous causes involved in generation of *NSM* event like hypertension, huge variation in blood pressure, heart rate variability in form of tachycardia, chronic kidney diseases, and nsst-t MI (Biso et al., 2017; Callaghan & Anne, 2016). For the diagnosis of the different neurogenic disorders through neurological causes, heart related, different tests like echocardiogram observations, event monitor, and ECG findings have been used. Clinical studies highlight different cardiac arrhythmia (afib and pvc) and MI, through NSTEMI and T wave inversion commonly occur after brain stroke (Bhagat, Narang, Sharma, Dash, & Chauhan, 2009). Therefore, early diagnosis of

these cardiac morbidities and relation with neurological behaviors are helped out for further damage and crucial for survival of human's life.

Currently, in era of automation, different machine learning techniques delivered immense contributions in the domain of neurogenic disorders and cardiac morbidities detection (Baloglu et al., 2019; Putten, Olbrich, & Arns, 2018; Raghavendraa, Acharya, & Hojjat Adeli, 2019). Especially, deep neural networks techniques are most dominated ones for detection of above cases (J. X. Chen et al., 2019; Reasat & Shahnaz, 2017).

However, the events of *NSM* in aspect of *nsst-t* cardiac different situations are still unexplored and are a challenging job for researchers (Biso et al., 2017; Khechinashvili & Asplund, 2002; Zou et al., 2017). Explored the interconnectivity between *NSM* and different factors of *nsst-t* via using the optimal structure deep neural networks highlighted the future work for researcher's community. Moreover, the significance of robust early detection of *NSM* with *nsst-t* factors is highly desirable for medical professional which plays the vital role for surgical purposes.

7.4.2 Prediction of Sudden Cardiac Arrest via MLP learning

In emergency department of hospital the situation of sudden cardiac arrest declares special attention for cardiologists. The survival of human life in situation of sudden cardiac arrest is a bit difficult thorough medication. The trigger of sudden cardiac arrest leads towards the cause of sudden cardiac death (SCD). Different conditions that can initiate the trigger of sudden cardiac arrest like presence of coronary artery diseases, cardiomyopathy (thickness of heart muscles), irregular heart rhythm, and heart birth defects. Different gender age ranges also indicate the sudden cardiac arrest risk alarms on the basis of medical history like, in men the age above than 45 years and Women the age above than 55 along with history of diabetes and previous MI existence (Adabag & Langsetmo, 2020).

Existing computational techniques highlighted the impressive results in context of accurate detection of sudden cardiac arrest situation(Jang et al., 2020; Khazaei, Raeisi, Goshvarpour, & Ahmadzadeh, 2018). Existing studies highlighted different MLP approaches especially CNN deep learning model are most suitable for detection of sudden cardiac arrest(Jang et al., 2020; Nguyen, Nguyen, & Kim, 2018). However, existing methods are lacking to provide the optimal solution for early prediction of sudden cardiac arrest(Jang et al., 2020; Layeghian Javan, Sepehri, & Aghajani, 2018). Therefore, employment of different optimal methods in prediction of sudden cardiac arrest narrates the upcoming new research area that will be explored in future. Predictive analytics of sudden cardiac arrest with the medical history of patients is a significant factor in survival of human life.

7.4.3 Robust Recognition of Ventricular Arrhythmias via Optimal CNN model

The generation of cardiac arrhythmias is correlated with numerous cardiac situations that lead to the risk position of human life. Heterogeneous nature of cardiac arrhythmia's identification is demanded in emergency department of hospital. In domain of ventricular arrhythmia (VA), occurrence of premature ventricular contraction (PVC) is one of the life risk session that may generate with rapid heart rate more than 100 beats per minute(tachycardia)(Allami, 2019). Ventricular fibrillation(VF) cardiac situation is also under the coverage of VA and belongs to rapid heart rate (tachycardia)(Jekova & Krasteva, 2004). Similarly, Ventricular Flutter(VFL) belongs to the category of VA and is more severe due to high shoot up of heart rate, more than 250 beats per minute(Link et al., 2017). In occurrence of VFL, the existence of P wave and T wave in ECG signal is invisible which leads to the MI and other cardiac complexities. More of, the variations of ventricular tachycardia are the causes of PVC ,VF and VFL that leap into other crucial stages like NSTEMI and heart failure(Jekova & Krasteva, 2004; Link et al., 2017).

Different automated techniques are currently used for detection of ventricular arrhythmia and deliver immense contributions in context of accurate findings of tachycardia situation (Fujita & Cimr, 2019; Mohanty, Biswal, & Sabut, 2020). Different deep learning models played a remarkable role in accurate detection of ventricular arrhythmia in context of ventricular tachycardia (Acharya, Fujita, Lih, et al., 2017; Yildirim, Pławiak, Tan, & Acharya, 2018). However, to measure the robust detection of different variations of ventricular arrhythmias by using these current automated techniques are still a limitations (Acharya, Fujita, Lih, et al., 2017; Fujita & Cimr, 2019; Yildirim et al., 2018). Therefore, robust identification of the various variations of ventricular arrhythmia's like PVC, VF, VFL via optimal CNN model like shallow CNN is the opportunity where researchers will explore in future.

7.5 Conclusion

Finally, this chapter is summarizes the entire thesis by retrace of all the research objective with inclusion of each RQ in each objective. This Chapter also covers the various limitations in proposed models and highlighted the few key future directions for classification or recognition of cardiac diseases.

REFERENCES

- Acharya, U. R., Fujita, H., Adam, M., Oh, S. L., Sudarshan, V. K., Hong, T. J., ... San, T. R. (2017). Automated characterization and classification of coronary artery disease and myocardial infarction by decomposition of ECG signals: A comparative study. *Information Sciences*, 377, 17–29. <https://doi.org/10.1016/j.ins.2016.10.013>
- Acharya, U. R., Fujita, H., Lih, O. S., Hagiwara, Y., Tan, J. H., & Adam, M. (2017). Automated detection of arrhythmias using different intervals of tachycardia ECG segments with convolutional neural network. *Information Sciences*, 405, 81–90. <https://doi.org/10.1016/j.ins.2017.04.012>
- Acharya, U. R., Fujita, H., Lih, S., Yuki, O., Jen, H., Tan, H., ... Tan, R. S. (2019). Deep convolutional neural network for the automated diagnosis of congestive heart failure using ECG signals. *Applied Intelligence*, 49, 16–27. <https://doi.org/https://doi.org/10.1007/s10489-018-1179-1>
- Acharya, U. R., Fujita, H., Oh, S. L., Hagiwara, Y., Tan, J. H., & Adam, M. (2017). Application of deep convolutional neural network for automated detection of myocardial infarction using ECG signals. *Information Sciences*, 415, 190–198. <https://doi.org/10.1016/j.ins.2017.06.027>
- Acharya, U. R., Fujita, H., Sudarshan, V. K., Lih Oh, S., Muhammad, A., Koh, J. E. W., ... San Tan, R. (2017). Application of empirical mode decomposition (EMD) for automated identification of congestive heart failure using heart rate signals. *Neural Computing and Applications*, 28(10), 3073–3094. <https://doi.org/10.1007/s00521-016-2612-1>
- Acharya, U. R., Oh, S. L., Hagiwara, Y., Tan, J. H., Adam, M., Gertych, A., & Tan, R. S. (2017). A deep convolutional neural network model to classify heartbeats. *Computers in Biology and Medicine*, 89, 389–396. <https://doi.org/10.1016/j.combiomed.2017.08.022>
- Adabag, S., & Langsetmo, L. (2020). Sudden cardiac death risk prediction in heart failure with preserved ejection fraction. *Heart Rhythm*, 17(3), 358–364. <https://doi.org/10.1016/j.hrthm.2019.12.009>
- Alathr, K., Smith, J. D., & Vinocur, J. M. (2017). Atypical long QT syndrome phenotype in heterozygous/homozygous KCNQ1 Ala590Thr. *HeartRhythm Case Reports*, 3(4), 219–223. <https://doi.org/10.1016/j.hrcr.2017.01.007>
- Alex, D., Khor, H. M., Chin, A. V., Hairi, N. N., Othman, S., Khoo, S. P. K., ... Tan, M. P. (2018). Cross-sectional analysis of ethnic differences in fall prevalence in urban dwellers aged 55 years and over in the Malaysian Elders Longitudinal Research study. *BMJ Open*, 8(7), 1–6. <https://doi.org/10.1136/bmjopen-2017-019579>
- Allami, R. (2019). Premature ventricular contraction analysis for real-time patient monitoring. *Biomedical Signal Processing and Control*, 47, 358–365. <https://doi.org/10.1016/j.bspc.2018.08.040>

- Aloia, M. D., Longo, A., & Rizzi, M. (2019). Noisy ECG Signal Analysis for Automatic Peak Detection. *Information*, 10(2). <https://doi.org/10.3390/info10020035>
- Arabasadi, Z., Alizadehsani, R., Roshanzamir, M., Moosaei, H., & Yarifard, A. A. (2017). Computer aided decision making for heart disease detection using hybrid neural network-Genetic algorithm. *Computer Methods and Programs in Biomedicine*, 141, 19–26. <https://doi.org/10.1016/j.cmpb.2017.01.004>
- Arif, M., Malagore, I. A., & Afsar, F. A. (2012). Detection and Localization of Myocardial Infarction using K-nearest Neighbor Classifier. *Journal of Medical Systems*, 36(1), 279–289. <https://doi.org/10.1007/s10916-010-9474-3>
- Bae, S. (2019). Big-O Notation. In *JavaScript Data Structures and Algorithms* (pp. 1–11). <https://doi.org/10.1007/978-1-4842-3988-9>
- Baloglu, U. B., Talo, M., Yildirim, O., Tan, R. S., & Acharya, U. R. (2019). Classification of myocardial infarction with multi-lead ECG signals and deep CNN. *Pattern Recognition Letters*, 122, 23–30. <https://doi.org/10.1016/j.patrec.2019.02.016>
- Banerjee, S., & Mitra, M. (2014). Application of cross wavelet transform for ECG pattern analysis and classification. *IEEE Transactions on Instrumentation and Measurement*, 63(2), 326–333. <https://doi.org/10.1109/TIM.2013.2279001>
- Bao, H., Cai, H., Zhao, Y., Huang, X., Fan, F., Zhang, C., ... Cheng, X. (2017). Nonspecific ST-T changes associated with unsatisfactory blood pressure control among adults with hypertension in China. *Medicine*, 96(13). <https://doi.org/10.1097/MD.00000000000006423>
- Benhar, H., & Idri, A. (2019). A Systematic Mapping Study of Data Preparation in Heart Disease Knowledge Discovery. *Journal of Medical Systems*, 43(1), 17. <https://doi.org/10.1007/s10916-018-1134-z>
- Bhagat, H., Narang, R., Sharma, D., Dash, H. H., & Chauhan, H. (2009). ST elevation - An indication of reversible neurogenic myocardial dysfunction in patients with head injury. *Annals of Cardiac Anaesthesia*, 12(2), 149–151. <https://doi.org/10.4103/0971-9784.53446>
- Bhuiyan, T. A., Graff, C., Kanters, J. K., Nielsen, J., Melgaard, J., Matz, J., ... Struijk, J. J. (2015). The T-peak – T-end Interval as a Marker of Repolarization Abnormality: A Comparison with the QT Interval for Five Different Drugs. *Clinical Drug Investigation*, 35(11), 717–724. <https://doi.org/10.1007/s40261-015-0328-0>
- Bhuiyan, T. A., Graff, C., Kanters, J. K., Thomsen, M. B., & Struijk, J. J. (2013). Flattening of the Electrocardiographic T-wave is a Sign of Proarrhythmic Risk and a Reflection of Action Potential Triangulation. *Computing in Cardiology 2013*, 40, 353–356.
- Biso, S., Wongrakpanich, S., Agrawal, A., Yadlapati, S., Kishlyansky, M., & Figueredo, V. (2017). A Review of Neurogenic Stunned Myocardium. *Cardiovascular*

- Blanco-Velasco, M., Goya-Esteban, R., Cruz-Roldán, F., García-Alberola, A., & Rojo-Álvarez, J. L. (2017). Benchmarking of a T-wave alternans detection method based on empirical mode decomposition. *Computer Methods and Programs in Biomedicine*, 145, 147–155. <https://doi.org/10.1016/j.cmpb.2017.04.005>
- Bodisco, T., Netto, J. D., Kelson, N., Banks, J., & Hayward, R. (2014). Computation of ECG signal features using MCMC modelling in software and FPGA reconfigurable hardware. *Procedia - Procedia Computer Science*, 29, 2442–2448. <https://doi.org/10.1016/j.procs.2014.05.228>
- Brand, J. van den, Peng, B., Song, Z., & Weinstein, O. (2020). Training (Overparametrized) Neural Networks in Near-Linear Time. *ArXiv Preprint ArXiv:2006*, 11648. Retrieved from <http://arxiv.org/abs/2006.11648>
- Buscema, P. M., Grossi, E., Massini, G., Breda, M., & Della Torre, F. (2020). Computer Aided Diagnosis for atrial fibrillation based on new artificial adaptive systems. *Computer Methods and Programs in Biomedicine*, 191, 105401. <https://doi.org/10.1016/j.cmpb.2020.105401>
- Callaghan, S. O., & Anne, R. (2016). Focus: The Aging Brain: Neurocardiovascular Instability and Cognition. *The Yale Journal of Biology and Medicine*, 89(1), 59–71.
- Cervellera, C., & Muselli, M. (2004). Deterministic design for neural network learning: An approach based on discrepancy. *IEEE Transactions on Neural Networks*, 15(3), 533–544. <https://doi.org/10.1109/TNN.2004.824413>
- Cesari, M., Mehlsen, J., Mehlsen, A., Bjarup, H., & Sorensen, D. (2016). Application of a New Robust ECG T-wave Delineation Algorithm for the Evaluation of the Autonomic Innervation of the Myocardium. *38th Annual International Conference of the IEEE Engineering in Medicine and Biology Society (EMBC)*, 3801–3804.
- Chen, J. X., Zhang, P. W., Mao, Z. J., Huang, Y. F., Jiang, D. M., & Zhang, Y. N. (2019). Accurate EEG-based Emotion Recognition on Combined Features Using Deep Convolutional Neural Networks. *IEEE Access*, 7, 44317–44328. <https://doi.org/10.1109/ACCESS.2019.2908285>
- Chen, S. T., Guo, Y. J., Huang, H. N., Kung, W. M., Tseng, K. K., & Tu, S. Y. (2014). Hiding patients confidential data in the ECG signal via a transform-domain quantization scheme topical collection on mobile systems. *Journal of Medical Systems*, 38, 54. <https://doi.org/10.1007/s10916-014-0054-9>
- Chen, Y., & Yu, S. (2012). Artificial Intelligence in Medicine Selection of effective features for ECG beat recognition based on nonlinear correlations. *Artificial Intelligence In Medicine*, 54(1), 43–52. <https://doi.org/10.1016/j.artmed.2011.09.004>
- Cheng, P., & Dong, X. (2017). Life-threatening ventricular arrhythmia detection with personalized features. *IEEE Access*, 5, 14195–14203. <https://doi.org/10.1109/ACCESS.2017.2723258>

- Chivers, I., & Sleightholme, J. (2015). An Introduction to Algorithms and the Big O Notation. In *In Introduction to Programming with Fortran* (pp. 1–674). <https://doi.org/10.1007/978-3-319-17701-4>
- Comp, K. J., & Sumathi, S. (1997). Generalised parameters technique for identification of seasonal ARMA (SARMA) and non seasonal ARMA (NSARMA) models. *Korean Journal of Computational & Applied Mathematics*, 4(1), 135–146. <https://doi.org/10.1007/BF03011385>
- Czabanski, R., Horoba, K., Wrobel, J., Matonia, A., Martinek, R., Kupka, T., ... Leski, J. M. (2020). Detection of atrial fibrillation episodes in long-term heart rhythm signals using a support vector machine. *Sensors*, 20(3), 765. <https://doi.org/10.3390/s20030765>
- Dang, H. A. O., Sun, M., Zhang, G., & Qi, X. (2019). A Novel Deep Arrhythmia-Diagnosis Network for Atrial Fibrillation Classification Using Electrocardiogram Signals. *IEEE Access*, 7, 75577–75590. <https://doi.org/10.1109/ACCESS.2019.2918792>
- Daraei, A., & Hamidi, H. (2017). An Efficient Predictive Model for Myocardial Infarction Using Cost-sensitive J48 Model. *Iranian Journal of Public Health*, 46(5), 682.
- Deng, M., Wang, C., Tang, M., & Zheng, T. (2018). Extracting cardiac dynamics within ECG signal for human identification and cardiovascular diseases classification. *Neural Networks*, 100, 70–83. <https://doi.org/10.1016/j.neunet.2018.01.009>
- Deng, M., Wu, W., Cao, J., Tang, M., & Wang, C. (2019). Deterministic Learning-Based Methodology for Detecting Abnormal Dynamics of Cardiac Repolarization During Ischemia. In *2019 41st Annual International Conference of the IEEE Engineering in Medicine and Biology Society (EMBC)*, 1492–1495. <https://doi.org/10.1109/embc.2019.8857900>
- Desai, U., Nayak, C. G., Seshikala, G., Martis, R. J., & Fernandes, S. L. (2018). Automated Diagnosis of Tachycardia Beats. *Smart Computing and Informatics*, 421–429. https://doi.org/10.1007/978-981-10-5544-7_41
- Devi, I., Karpagam, G. R., & Kumar, B. V. (2017). A survey of machine learning techniques. *International Journal of Computational Systems Engineering*, 3(4), 203–212. <https://doi.org/10.1504/IJCSYSE.2017.089191>
- Dong, X., Si, W., & Huang, W. (2018). ECG-based identity recognition via deterministic learning. *Biotechnology and Biotechnological Equipment*, 32(3), 769–777. <https://doi.org/10.1080/13102818.2018.1428500>
- Dong, X., Wang, C., Hu, J., & Ou, S. (2014). Electrocardiogram (ECG) pattern modeling and recognition via deterministic learning. *Control Theory and Technology*, 12(4), 333–344. <https://doi.org/10.1007/s11768-014-4056-4>
- Dong, X., Wang, C., & Si, W. (2017). ECG beat classification via deterministic learning. *Neurocomputing*, 240, 1–12. <https://doi.org/10.1016/j.neucom.2017.02.056>

- Dorffner, G., Leitgeb, E., D, H. K. M., & Polten, A.-S. (1994). TOWARD IMPROVING EXERCISE ECG FOR DETECTING ISCHEMIC HEART DISEASE WITH RECURRENT AND FEEDFORWARD NEURALNETS. *In Proceedings of IEEE Workshop on Neural Networks for Signal Processing*, 499–508. <https://doi.org/10.1109/NNSP.1994.366016>
- Du, S. S., Poczós, B., Zhai, X., & Singh, A. (2019). Gradient descent provably optimizes over-parameterized neural networks. *7th International Conference on Learning Representations, ICLR 2019*, 1–19.
- Ebrahimzadeh, E., Manuchehri, M. S., Amoozegar, S., & Araabi, B. N. (2018). A time local subset feature selection for prediction of sudden cardiac death from ECG signal. *Medical & Biological Engineering & Computing*, 56, 1253–1270. <https://doi.org/10.1007/s11517-017-1764-1>
- Elgendi, M. (2013). Fast QRS Detection with an Optimized Knowledge-Based Method: Evaluation on 11 Standard ECG Databases. *PLoS ONE*, 8(9). <https://doi.org/10.1371/journal.pone.0073557>
- Elgendi, M., Eskofier, B., & Abbott, D. (2015). Fast T Wave Detection Calibrated by Clinical Knowledge with Annotation of P and T Waves. *Sensors*, 15(7), 17693–17714. <https://doi.org/10.3390/s150717693>
- Elhaj, F. A., Salim, N., Harris, A. R., Tian, T., & Ahmed, T. (2016). Arrhythmia recognition and classification using combined linear and nonlinear features of ECG signals. *Computer Methods and Programs in Biomedicine*, 127, 52–63. <https://doi.org/10.1016/j.cmpb.2015.12.024>
- Ellenius, J., & Groth, T. (2000). Methods for selection of adequate neural network structures with application to early assessment of chest pain patients by biochemical monitoring. *International Journal of Medical Informatics*, 57(2–3), 181–202. [https://doi.org/10.1016/S1386-5056\(00\)00065-4](https://doi.org/10.1016/S1386-5056(00)00065-4)
- Engin, M. (2004). ECG beat classification using neuro-fuzzy network. *Pattern Recognition Letters*, 25(15), 1715–1722. <https://doi.org/10.1016/j.patrec.2004.06.014>
- Faust, O., Hagiwara, Y., Jen, T., Shu, O., & Acharya, U. R. (2018). Deep learning for healthcare applications based on physiological signals: A review. *Computer Methods and Programs in Biomedicine*, 161, 1–13. <https://doi.org/10.1016/j.cmpb.2018.04.005>
- Feng, K., Pi, X., Liu, H., & Sun, K. (2019). Myocardial Infarction Classification Based on Convolutional Neural Network and Recurrent Neural Network. *Applied Sciences*, 9(9). <https://doi.org/10.3390/app9091879>
- Feng, N., Xu, S., Liang, Y., & Liu, K. U. N. (2019). A Probabilistic Process Neural Network and Its Application in ECG Classification. *IEEE Access*, 7, 50431–50439. <https://doi.org/10.1109/ACCESS.2019.2910880>
- Fujita, H., & Cimr, D. (2019). Computer Aided detection for fibrillations and flutters using deep convolutional neural network. *Information Sciences*, 486, 231–239.

<https://doi.org/10.1016/j.ins.2019.02.065>

- Fukuda, K., Kanazawa, H., Aizawa, Y., Ardell, J. L., & Shivkumar, K. (2015). Cardiac Innervation and Sudden Cardiac Death. *Circulation Research*, *116*(12), 2005–2019. <https://doi.org/10.1161/CIRCRESAHA.116.304679>
- Gardner, I. A., & Greiner, M. (2006). Receiver-operating characteristic curves and likelihood ratios: improvements over traditional methods for the evaluation and application of veterinary clinical pathology tests. *Veterinary Clinical Pathology*, *35*(1), 8–17. <https://doi.org/10.1111/j.1939-165X.2006.tb00082.x>
- Garza-Ulloa, J. (2018). Application of mathematical models in biomechanics: artificial intelligence and time-frequency analysis. In *Applied Biomechanics using Mathematical Models*. <https://doi.org/10.1016/b978-0-12-812594-6.00006-8>
- Ghongade, R., & Ghatol, A. (2008). A robust and reliable ECG pattern classification using QRS morphological features and ANN. In *TENCON 2008-2008 IEEE Region 10 Conference*, 1–6. <https://doi.org/10.1109/TENCON.2008.4766722>
- Ghoraani, B., Suszko, A. M., Selvaraj, R. J., Subramanian, A., Krishnan, S., & Id, V. S. C. (2019). Body surface distribution of T wave alternans is modulated by heart rate and ventricular activation sequence in patients with cardiomyopathy. *PLoS ONE*, *14*(4), 1–18. <https://doi.org/10.1371/journal.pone.0214729>
- Goh, C. H., Ng, S. C., Kamaruzzaman, S. B., Chin, A. V., & Tan, M. P. (2017). Standing beat-to-beat blood pressure variability is reduced among fallers in the Malaysian Elders Longitudinal Study. *Medicine*, *96*(42), 1–7. <https://doi.org/10.1097/MD.00000000000008193>
- Goldberger, A. L., Amaral, L. A. N., Glass, L., Hausdorff, J. M., Ivanov, P. C., Mark, R. G., ... Stanley, H. E. (2000). PhysioBank, PhysioToolkit, and PhysioNet: Components of a New Research Resource for Complex Physiologic Signals. *Circulation*, *101*(23), e215–e220. <https://doi.org/10.1161/01.CIR.101.23.e215>
- Gothwal, H., Kedawat, S., & Kumar, R. (2011). Cardiac arrhythmias detection in an ECG beat signal using fast fourier transform and artificial neural network. *Journal of Biomedical Science and Engineering*, *4*(04), 289–296. <https://doi.org/10.4236/jbise.2011.44039>
- Gutiérrez-Gnecchi, J. A., Morfin-Magaña, R., Lorias-Espinoza, D., Tellez-Anguiano, A. D. C., Reyes-Archundia, E., Méndez-Patiño, A., & Castañeda-Miranda, R. (2017). DSP-based arrhythmia classification using wavelet transform and probabilistic neural network. *Biomedical Signal Processing and Control*, *32*, 44–56. <https://doi.org/10.1016/j.bspc.2016.10.005>
- Hadjem, M., & Naït-Abdesselam, F. (2015). An ECG T-wave anomalies detection using a lightweight classification model for wireless body sensors. In *2015 IEEE International Conference on Communication Workshop (ICCW)*, 278–283. <https://doi.org/10.1109/ICCW.2015.7247191>
- Hameed, A. A., Karlik, B., & Salman, M. S. (2016). Back-propagation Algorithm with Variable Adaptive Momentum. *Knowledge-Based Systems*, *114*, 79–87.

<https://doi.org/10.1016/j.knosys.2016.10.001>

- Han, C., & Shi, L. (2019). Automated interpretable detection of myocardial infarction fusing energy entropy and morphological features. *Computer Methods and Programs in Biomedicine*, 175, 9–23. <https://doi.org/10.1016/j.cmpb.2019.03.012>
- Han, C., & Shi, L. (2020). ML–ResNet: a novel network to detect and locate myocardial infarction using 12 leads ECG. *Computer Methods and Programs in Biomedicine*, 185, 105138. <https://doi.org/10.1016/j.cmpb.2019.105138>
- Hannun, A. Y., Rajpurkar, P., Haghpanahi, M., Tison, G. H., Bourn, C., Turakhia, M. P., & Ng, A. Y. (2019). Cardiologist-level arrhythmia detection and classification in ambulatory electrocardiograms using a deep neural network. *Nature Medicine*, 25(1), 65. <https://doi.org/10.1038/s41591-018-0268-3>
- Harkness, W., Watts, P., Kopstein, M., Dziadkowiec, O., Hicks, G., & Scherbak, D. (2019). Correcting Hypokalemia in Hospitalized Patients Does Not Decrease Risk of Cardiac Arrhythmias. *Advances in Medicine*, 2019. <https://doi.org/10.1155/2019/4919707>
- He, R., Wang, K., Li, Q., Yuan, Y., Zhao, N., Liu, Y., & Zhang, H. (2017). A novel method for the detection of R-peaks in ECG based on K-Nearest Neighbors and Particle Swarm Optimization. *EURASIP Journal on Advances in Signal Processing*, 2017(1), 82. <https://doi.org/10.1186/s13634-017-0519-3>
- Hu, Y. H., Palreddy, S., & Tompkins, W. J. (1997). A patient-adaptable ECG beat classifier using a mixture of experts approach. *IEEE Transactions on Biomedical Engineering*, 44(9), 891–900. <https://doi.org/10.1109/10.623058>
- Imtiaz, S. A., Mardell, J., Saremi-Yarahmadi, S., & Rodriguez-Villegas, E. (2016). ECG artefact identification and removal in mHealth systems for continuous patient monitoring. *Healthcare Technology Letters*, 3(3), 171–176. <https://doi.org/10.1049/htl.2016.0020>
- Iqbal, U., Wah, T. Y., Habib Ur Rehman, M., & Mastoi, Q. U. A. (2018). Usage of Model Driven Environment for the Classification of ECG features: A Systematic Review. *IEEE Access*, 6, 23120–23136. <https://doi.org/10.1109/ACCESS.2018.2828882>
- Iqbal, U., Wah, T. Y., Habib Ur Rehman, M., & Mastoi, Q. U. A. (2019). A Deterministic Approach for Finding the T Onset Parameter of Flatten T Wave in ECG. *J. Inf. Sci. Eng.*, 35(2), 307–321. <https://doi.org/10.6688/JISE.201903>
- Iqbal, U., Wah, T. Y., Habib Ur Rehman, M., Mujtaba, G., & Imran, M. (2018). Deep Deterministic Learning for Pattern Recognition of Different Cardiac Diseases through the Internet of Medical Things. *Journal of Medical Systems*, 42(12), 252. <https://doi.org/10.1007/s10916-018-1107-2>
- Iqbal, U., Wah, T. Y., Habib Ur Rehman, M., & Shah, J. H. (2019). Prediction analytics of myocardial infarction through model-driven deep deterministic learning. *Neural Computing and Applications*, 1–20. <https://doi.org/10.1007/s00521-019-04400-9>

- Isaksen, J. L., Graff, C., Ellervik, C., Jensen, J. S., Andersen, H. U., Rossing, P., ... Jensen, M. T. (2018). Type 1 diabetes is associated with T-wave morphology changes. The Thousand & 1 Study. *Journal of Electrocardiology*, 51(6), S72–S77. <https://doi.org/10.1016/j.jelectrocard.2018.05.015>
- Ishikawa, J., Hirose, H., Schwartz, J. E., & Ishikawa, S. (2018). Minor electrocardiographic ST-T change and risk of stroke in the general Japanese population. *Circulation Journal*, 82(7), 1797–1804. <https://doi.org/10.1253/circj.CJ-17-1084>
- Ismail Fawaz, H., Forestier, G., Weber, J., Idoumghar, L., & Muller, P. A. (2019). Deep learning for time series classification: a review. *Data Mining and Knowledge Discovery*, 33(4), 917–963. <https://doi.org/10.1007/s10618-019-00619-1>
- Ismail Fawaz, H., Lucas, B., Forestier, G., Pelletier, C., Schmidt, D. F., Weber, J., ... Petitjean, F. (2020). InceptionTime: Finding AlexNet for time series classification. *Data Mining and Knowledge Discovery*, 34(6), 1936–1962. <https://doi.org/10.1007/s10618-020-00710-y>
- Jang, D. H., Kim, J., Jo, Y. H., Lee, J. H., Hwang, J. E., Park, S. M., ... Chang, H. (2020). Developing neural network models for early detection of cardiac arrest in emergency department. *American Journal of Emergency Medicine*, 38(1), 43–49. <https://doi.org/10.1016/j.ajem.2019.04.006>
- Jayant, H. K., Rana, K. P. S., Kumar, V., Nair, S. S., & Mishra, P. (2015). Efficient IIR Notch Filter Design using Minimax Optimization for 50Hz Noise Suppression in ECG. In *2015 International Conference on Signal Processing, Computing and Control (ISPCC)*, 290–295. <https://doi.org/10.1109/ISPCC.2015.7375043>
- Jekova, I., & Krasteva, V. (2004). Real time detection of ventricular fibrillation and tachycardia. *Physiological Measurement*, 25(5), 1167–1178. <https://doi.org/10.1088/0967-3334/25/5/007>
- Kaiser, W., Findeis, M., & Young, B. J. (2004). Improving T-Wave Alternans Measurement Quality by Reducing Noise and Artifacts. *Computers in Cardiology*, 31(1), 445–448.
- Kandil, N., Khorasani, K., Patel, R. V., & Sood, V. K. (1993). Optimum learning rate for backpropagation neural networks. *Canadian Conference on Electrical and Computer Engineering*, 465–468. <https://doi.org/10.1109/CCECE.1993.332193>
- Kang, J. G., Chang, Y., Su, K., Kim, J., & Shin, H. (2018). Association of isolated minor nonspecific ST-T abnormalities with left ventricular hypertrophy and diastolic dysfunction. *Scientific Reports*, 8(1), 1–7. <https://doi.org/10.1038/s41598-018-27028-6>
- Kaplan, S., Kursat, A., Sora, E., Ergin, S., Gunal, S., & Gulmezoglu, M. B. (2018). A survey on ECG analysis. *Biomedical Signal Processing and Control*, 43, 216–235. <https://doi.org/10.1016/j.bspc.2018.03.003>
- Kara, S., & Okandan, M. (2007). Atrial fibrillation classification with artificial neural networks. *Pattern Recognition*, 40(11), 2967–2973.

<https://doi.org/10.1016/j.patcog.2007.03.008>

- Karthik, R., Tyagi, D., Raut, A., & Saxena, S. (2019). Implementation of Neural Network and feature extraction to classify ECG signals. *Microelectronics, Electromagnetics and Telecommunications*, 317–326. https://doi.org/10.1007/978-981-13-1906-8_33
- Kaur, A., Agarwal, A., Agarwal, R., & Kumar, S. (2019). A Novel Approach to ECG R-Peak Detection. *Arabian Journal for Science and Engineering*, 44(8), 6679–6691. <https://doi.org/10.1007/s13369-018-3557-8>
- Kerro, A., Woods, T., & Chang, J. J. (2017). Neurogenic stunned myocardium in subarachnoid hemorrhage. *Journal of Critical Care*, 38, 27–34. <https://doi.org/10.1016/j.jcrc.2016.10.010>
- Kew, H., & Jeong, D. (2011). Variable Threshold Method for ECG R-peak Detection Variable Threshold Method for ECG R-peak Detection. *Journal of Medical Systems*, 35(5), 1085–1094. <https://doi.org/10.1007/s10916-011-9745-7>
- Khazaei, M., Raeesi, K., Goshvarpour, A., & Ahmadzadeh, M. (2018). Early detection of sudden cardiac death using nonlinear analysis of heart rate variability. *Biocybernetics and Biomedical Engineering*, 38(4), 931–940. <https://doi.org/10.1016/j.bbe.2018.06.003>
- Khechinashvili, G., & Asplund, K. (2002). Electrocardiographic Changes in Patients with Acute Stroke : A Systematic Review. *Cerebrovascular Diseases*, 14(2), 67–76. <https://doi.org/10.1159/000064733>
- Kim, J., Shin, H. S., Shin, K., & Lee, M. (2009). Robust algorithm for arrhythmia classification in ECG using extreme learning machine. *Biomedical Engineering Online*, 8(1), 31. <https://doi.org/10.1186/1475-925X-8-31>
- Koga, M., Kawamura, Y., Ito, D., Iseki, H., & Ikari, Y. (2016). CASE REPORT A case of ST segment-elevated myocardial infarction with less common forms of single coronary artery. *Cardiovascular Intervention and Therapeutics*, 31(4), 304–308. <https://doi.org/10.1007/s12928-015-0357-x>
- Koivikko, M. L., Kenttä, T., Salmela, P. I., Huikuri, H. V., & Perkiömäki, J. S. (2017). Changes in cardiac repolarisation during spontaneous nocturnal hypoglycaemia in subjects with type 1 diabetes: a preliminary report. *Acta Diabetologica*, 54(3), 251–256. <https://doi.org/10.1007/s00592-016-0941-2>
- Kojuri, J., Boostani, R., Dehghani, P., Nowroozpour, F., & Saki, N. (2015). Prediction of acute myocardial infarction with artificial neural networks in patients with nondiagnostic electrocardiogram. *Journal of Cardiovascular Disease Research*, 6(2), 51–59. <https://doi.org/10.5530/jcdr.2015.2.2>
- Krimi, S., Ouni, K., & Ellouze, N. (2006). T-Wave Detection Based on an Adjusted Wavelet Transform Modulus Maxima. *International Journal of Medical and Health Sciences*, 1(2).
- Lai, H., Deng, M., Tang, M., & Wang, C. (2019). Matlab-Based Myocardial Ischemia

Detection System Design via Deterministic Learning. *In Proceedings of 2018 Chinese Intelligent Systems Conference*, 615–625. <https://doi.org/10.1007/978-981-13-2291-4>

- Layeghian Javan, S., Sepehri, M. M., & Aghajani, H. (2018). Toward analyzing and synthesizing previous research in early prediction of cardiac arrest using machine learning based on a multi-layered integrative framework. *Journal of Biomedical Informatics*, 88, 70–89. <https://doi.org/10.1016/j.jbi.2018.10.008>
- Lee, M., Park, D., Dong, S. Y., & Youn, I. (2018). A Novel R Peak Detection Method for Mobile Environments. *IEEE Access*, 6, 51227–51237. <https://doi.org/10.1109/ACCESS.2018.2867329>
- Legarreta, I. R., Addison, P. S., Grubb, N., & Engineering, F. (2003). R-wave Detection Using Continuous Wavelet Modulus Maxima. *In Computers in Cardiology, 2003*, 565–568. <https://doi.org/10.1109/CIC.2003.1291218>
- Legarreta, I. R., Addison, P. S., Reed, M. J., Grubb, N., Clegg, G. R., Robertson, C. E., & Watson, J. N. (2005). Continuous wavelet transform modulus maxima analysis of the electrocardiogram: beat characterisation and beat-to-beat measurement. *International Journal of Wavelets, Multiresolution and Information Processing*, 3(1), 19–42. <https://doi.org/10.1142/S0219691305000774>
- Lemire, D., Pharand, C., Rajaonah, J., Dubé, B., & Leblanc, A. R. (2000). Wavelet Time Entropy, T Wave Morphology and Myocardial Ischemia. *IEEE Transactions on Biomedical Engineering*, 47(7), 967–970. <https://doi.org/10.1109/10.846692>
- Li, K., Pan, W., Jiang, Q., & Liu, G. (2018). A method to detect sleep apnea based on deep neural network and hidden Markov model using single-lead ECG signal. *Neurocomputing*, 294, 94–101. <https://doi.org/10.1016/j.neucom.2018.03.011>
- Limaye, A., & Adegbija, T. (2018). HERMIT: A Benchmark Suite for the Internet of Medical Things. *IEEE Internet of Things Journal*, 5(5), 4212–4222. <https://doi.org/10.1109/JIOT.2018.2849859>
- Lin, K. B., Shofer, F. S., McCusker, C., Meshberg, E., & Hollander, J. E. (2008). Predictive value of T-wave abnormalities at the time of emergency department presentation in patients with potential acute coronary syndromes. *Academic Emergency Medicine*, 15(6), 537–543. <https://doi.org/10.1111/j.1553-2712.2008.00135.x>
- Lin, W., Teo, S. G., & Poh, K. K. (2013). Electrocardiographic T wave abnormalities. *Singapore Medical Journal*, 54(11), 606–610. <https://doi.org/10.11622/smedj.2013218>
- Link, M. S., Bockstall, K., Weinstock, J., Alsheikh-Ali, A. A., Semsarian, C., Estes, N. A. M., ... Maron, B. J. (2017). Ventricular Tachyarrhythmias in Patients With Hypertrophic Cardiomyopathy and Defibrillators: Triggers, Treatment, and Implications. *Journal of Cardiovascular Electrophysiology*, 28(5), 531–537. <https://doi.org/10.1111/jce.13194>
- Liu, X., Yang, J., Zhu, X., Zhou, S., Wang, H., & Zhang, H. (2014). A novel R-Peak

- detection method combining energy and wavelet transform in electrocardiogram signal. *Biomedical Engineering - Applications, Basis and Communications*, 26(1), 1–9. <https://doi.org/10.4015/S1016237214500070>
- Llamedo, M., & Mart, J. P. (2011). Heartbeat Classification Using Feature Selection Driven by Database Generalization Criteria. *IEEE TRANSACTIONS ON BIOMEDICAL ENGINEERING*, 58(3), 616–625.
- Lobodzinski, S. S. (2013). ECG patch monitors for assessment of cardiac rhythm abnormalities. *Progress in Cardiovascular Diseases*, 56(2), 224–229. <https://doi.org/10.1016/j.pcad.2013.08.006>
- Lourakis, M. (2005). A Brief Description of the Levenberg-Marquardt Algorithm Implemented by levmar. *Foundation of Research and Technology*, 4(1), 1–6.
- Lv, C., Xing, Y., Zhang, J., Na, X., Li, Y., Liu, T., ... Wang, F. Y. (2018). Levenberg-marquardt backpropagation training of multilayer neural networks for state estimation of a safety-critical cyber-physical system. *IEEE Transactions on Industrial Informatics*, 14(8), 3436–3446. <https://doi.org/10.1109/TII.2017.2777460>
- Maggio, A. C. V., bonomini, P. M., Leber, E. L., & Arini, P. D. (2012). Quantification of Ventricular Repolarization Dispersion Using Digital Processing of the Surface ECG. In *Advances in Electrocardiograms - Methods and Analysis* (pp. 181–206). <https://doi.org/10.5772/23050>
- Martis, R. J., Acharya, U. R., & Min, L. C. (2013). ECG beat classification using PCA, LDA, ICA and Discrete Wavelet Transform. *Biomedical Signal Processing and Control*, 8(5), 437–448. <https://doi.org/10.1016/j.bspc.2013.01.005>
- Mastoi, Q.-U.-A., Wah, T. Y., Raj, R. G., & Iqbal, U. (2018). Automated Diagnosis of Coronary Artery Disease: A Review and Workflow. *Cardiology Research and Practice*, 2018, 9. <https://doi.org/10.1155/2018/2016282>
- Mathews, S. M., Kambhamettu, C., & Barner, K. E. (2018). A novel application of deep learning for single-lead ECG classification. *Computers in Biology and Medicine*, 99, 53–62. <https://doi.org/10.1016/j.compbiomed.2018.05.013>
- Mercaldo, N. D., Lau, K. F., & Zhou, X. H. (2007). Confidence intervals for predictive values with an emphasis to case – control studies. *Statistics in Medicine*, 26(10), 2170–2183. <https://doi.org/10.1002/sim>
- Merode, F. Van, Molema, H., & Goldschmidt, H. (2004). GUM and six sigma approaches positioned as deterministic tools in quality target engineering. *Accreditation and Quality Assurance*, 10(1–2), 32–36. <https://doi.org/10.1007/s00769-004-0876-0>
- Mika, S., Ratsch, G., Weston, J., Scholkopf, B., & Mullers, K. R. (1999). Fisher discriminant analysis with kernels. *IEEE Signal Processing Society Workshop*, 41–48. <https://doi.org/10.1109/NNSP.1999.788121>
- Minami, K. I., Nakajima, H., & Toyoshima, T. (1999). Real-time discrimination of

- ventricular tachyarrhythmia with fourier-transform neural network. *IEEE Transactions on Biomedical Engineering*, 46(2), 179–185. <https://doi.org/10.1109/10.740880>
- Minami, K., Nakajima, H., & Toyoshima, T. (1997). Arrhythmia diagnosis with discrimination of rhythm origin and measurement of heart-rate variation. *Computers in Cardiology*, (1997), 243–246. <https://doi.org/10.1109/cic.1997.647876>
- Miotto, R., Wang, F., Wang, S., Jiang, X., & Dudley, J. T. (2017). Deep learning for healthcare: review, opportunities and challenges. *Briefings in Bioinformatics*, 19(6), 1236–1246. <https://doi.org/10.1093/bib/bbx044>
- Mohanty, M., Biswal, P., & Sabut, S. (2020). Machine learning approach to recognize ventricular arrhythmias using VMD based features. *Multidimensional Systems and Signal Processing*, 31(1), 49–71. <https://doi.org/10.1007/s11045-019-00651-w>
- Nabar, S., Banerjee, A., Gupta, S. K. S., & Poovendran, R. (2011). GeM-REM: Generative Model-driven Resource efficient ECG Monitoring in Body Sensor Networks. In *2011 International Conference on Body Sensor Networks*, 1–6. <https://doi.org/10.1109/BSN.2011.29>
- Nabih-Ali, M., El-Dahshan, E.-S. A., & Yahia, A. S. (2017). Heart diseases diagnosis using intelligent algorithm based on PCG signal analysis. *International Journal of Biology and Biomedicine*, 2.
- Nagao, S., Watanabe, H., Sobue, Y., Kodama, M., Tanaka, J., Tanabe, N., ... Minamino, T. (2015). Electrocardiographic abnormalities and risk of developing cardiac events in extracardiac sarcoidosis. *International Journal of Cardiology*, 189, 1–5. <https://doi.org/10.1016/j.ijcard.2015.03.175>
- Naseer, N., & Nazeer, H. (2017). Classification of normal and abnormal ECG signals based on their PQRST intervals. In *2017 International Conference on Mechanical, System and Control Engineering (ICMSC)*, 388–391. <https://doi.org/10.1109/ICMSC.2017.7959507>
- Ngia, L. S. H., & Sjöberg, J. (2000). Efficient training of neural nets for nonlinear adaptive filtering using a recursive Levenberg-Marquardt algorithm. *IEEE Transactions on Signal Processing*, 48(7), 1915–1927. <https://doi.org/10.1109/78.847778>
- Nguyen, M. T., Nguyen, B. Van, & Kim, K. (2018). Deep Feature Learning for Sudden Cardiac Arrest Detection in Automated External Defibrillators. *Scientific Reports*, 8(1), 1–12. <https://doi.org/10.1038/s41598-018-33424-9>
- Nikan, S., Gwadry-Sridhar, F., & Bauer, M. (2017). Pattern Recognition Application in ECG Arrhythmia Classification. In *HEALTHINF*, 48–56.
- Nir FriedmanDan ,GeigerMoises, G. (1997). Bayesian Network Classifiers. *Machine Learning*, 29(2–3), 131–163.
- Oh, S. L., Ng, E. Y. K., San Tan, R., & Acharya, U. R. (2018). Automated diagnosis of

arrhythmia using combination of CNN and LSTM techniques with variable length heart beats. *Computers in Biology and Medicine*, 102, 278–287. <https://doi.org/10.1016/j.compbimed.2018.06.002>

Okin, P. M., Devereux, R. B., Fabsitz, R. R., Lee, E. T., Galloway, J. M., & Howard, B. V. (2002). Quantitative assessment of electrocardiographic strain predicts increased left ventricular mass: The strong heart study. *Journal of the American College of Cardiology*, 40(8), 1395–1400. [https://doi.org/10.1016/S0735-1097\(02\)02171-X](https://doi.org/10.1016/S0735-1097(02)02171-X)

Okin, P. M., Devereux, R. B., Nieminen, M. S., Jern, S., Oikarinen, L., Viitasalo, M., ... Dahlöf, B. (2001). Relationship of the electrocardiographic strain pattern to left ventricular structure and function in hypertensive patients: The LIFE study. *Journal of the American College of Cardiology*, 38(2), 514–520. [https://doi.org/10.1016/S0735-1097\(01\)01378-X](https://doi.org/10.1016/S0735-1097(01)01378-X)

Osowski, S., & Linh, T. H. (2001). ECG beat recognition using fuzzy hybrid neural network. *IEEE Transactions on Biomedical Engineering*, 48(11), 1265–1271. <https://doi.org/10.1109/10.959322>

Ousaka, D., Obara, N., & Fujiwara, M. (2018). Case Report A case of conservative management for left ventricular giant pseudoaneurysm without ST segment changes. *Journal of Cardiology Cases*, 17(5), 167–170. <https://doi.org/10.1016/j.jccase.2018.01.006>

Padmavathi, K., & Ramakrishna, K. S. (2015). Classification of ECG signal during Atrial Fibrillation using Autoregressive modeling. *Procedia - Procedia Computer Science*, 46(Icict 2014), 53–59. <https://doi.org/10.1016/j.procs.2015.01.053>

Pan, J., & Willis, J. (1985). A Real-Time QRS Detection Algorithm. *IEEE Transactions on Biomedical Engineering*, BME-32(3), 230–236.

Park, J. S., Lee, S. W., & Park, U. (2017). R Peak Detection Method Using Wavelet Transform and Modified Shannon Energy Envelope. *Journal of Healthcare Engineering*, 2017. <https://doi.org/10.1155/2017/4901017>

Park, Jinho, Pedrycz, W., & Jeon, M. (2012). Ischemia episode detection in ECG using kernel density estimation , support vector machine and feature selection. *Biomedical Engineering Online*, 11(1), 30. <https://doi.org/10.1186/1475-925X-11-30>

Park, Juyoung, & Kang, K. (2014). PcHD: Personalized classification of heartbeat types using a decision tree. *Computers in Biology and Medicine*, 54, 79–88. <https://doi.org/10.1016/j.compbimed.2014.08.013>

Patient, I., & Group, M. (2014). Crowd-Sourced Annotation of ECG Signals Using Contextual Information. *Annals of Biomedical Engineering*, 42(4), 871–884. <https://doi.org/10.1007/s10439-013-0964-6>

Patro, K. K., & Kumar, P. R. (2017). Effective Feature Extraction of ECG for Biometric Application. *Procedia Computer Science*, 115, 296–306. <https://doi.org/10.1016/j.procs.2017.09.138>

- Phillips, C. T., Wang, J., Celi, L. A., Zhang, Z., & Feng, M. (2019). Association of hypokalemia with an increased risk for medically treated arrhythmias. *PLoS ONE*, *14*(6). <https://doi.org/10.1371/journal.pone.0217432>
- Ponomariov, V., Chirila, L., Apipie, F.-M., Abate, R., Rusu, M., Wu, Z., ... Bucur, I. (2017). Artificial Intelligence versus Doctors' Intelligence: A Glance on Machine Learning Benefaction in Electrocardiography. *Discoveries*, *5*(3), e76. <https://doi.org/10.15190/d.2017.6>
- Pourbabaee, B., Roshtkhari, M. J., & Khorasani, K. (2017). Deep Convolution Neural Networks and Learning ECG Features for Screening Paroxysmal Atrial Fibrillation Patients. *IEEE Transactions on Systems, Man, and Cybernetics: Systems*, *48*(12), 2095–2104. <https://doi.org/10.1109/TSMC.2017.2705582>
- Prasad, G. K., & Sahambi, J. S. (2003). Classification of ECG Arrhythmias using Multi-Resolution Analysis and Neural Networks. *TENCON 2003. Conference on Convergent Technologies for Asia-Pacific Region*, 227–231. <https://doi.org/10.1109/TENCON.2003.1228899>
- Putten, M. J. A. M. Van, Olbrich, S., & Arns, M. (2018). Predicting sex from brain rhythms with deep learning. *Scientific Reports*, 1–7. <https://doi.org/10.1038/s41598-018-21495-7>
- Qayyum, H., Hemaya, S., Squires, J., & Adam, Z. (2018). Recognising the de Winter ECG pattern – A time critical electrocardiographic diagnosis in the Emergency Department. *Journal of Electrocardiology*, *51*(3), 392–395. <https://doi.org/10.1016/j.jelectrocard.2018.03.002>
- Qin, Q., Li, J., Yue, Y., & Liu, C. (2017). An Adaptive and Time-Efficient ECG R-Peak Detection Algorithm. *Journal of Healthcare Engineering*, 2017.
- Raghavendraa, U., Acharya, U. R., & Hojjat Adeli. (2019). Artificial Intelligence Techniques for Automated Diagnosis of Neurological Disorders. *European Neurology*, 1–24. <https://doi.org/10.1159/000504292>
- Rai, H. M., Trivedi, A., & Shukla, S. (2013). ECG signal processing for abnormalities detection using multi-resolution wavelet transform and Artificial Neural Network classifier. *Measurement*, *46*(9), 3238–3246. <https://doi.org/10.1016/j.measurement.2013.05.021>
- Raj, V. N. P. (2011). ECG Signal Denoising Using Undecimated Wavelet Transform. *In 2011 3rd International Conference on Electronics Computer Technology*, 94–98. <https://doi.org/10.1109/ICECTECH.2011.5941808>
- Ramirez, E., Melin, P., & Prado-arechiga, G. (2019). Hybrid model based on neural networks, type-1 and type-2 fuzzy systems for 2-lead cardiac arrhythmia classification. *Expert Systems With Applications*, *126*, 295–307. <https://doi.org/10.1016/j.eswa.2019.02.035>
- Rao, I. S. S., & Rao, T. S. (2016). Performance Identification of Different Heart Diseases Based On Neural Network Classification. *Int. J. Appl. Eng. Res*, *11*(6), 3859–3864.

- Ravi, D., Wong, C., Deligianni, F., Berthelot, M., Andreu-Perez, J., Lo, B., & Yang, G. Z. (2017). Deep Learning for Health Informatics. *IEEE Journal of Biomedical and Health Informatics*, 21(1), 4–21. <https://doi.org/10.1109/JBHI.2016.2636665>
- Reasat, T., & Shahnaz, C. (2017). Detection of Inferior Myocardial Infarction using Shallow Convolutional Neural Networks. *2017 IEEE Region 10 Humanitarian Technology Conference (R10-HTC)*, 718–721. <https://doi.org/10.1109/R10-HTC.2017.8289058>
- Rivera-Juárez, A., Hernández-Romero, I., Puertas, C., Zhang-Wang, S., Sánchez-Álamo, B., Martins, R., ... Atienza, F. (2019). Clinical Characteristics and Electrophysiological Mechanisms Underlying Brugada ECG in Patients With Severe Hyperkalemia. *Journal of the American Heart Association*, 8(3), e010115. <https://doi.org/10.1161/JAHA.118.010115>
- Rivero, D., Alhamaydeh, M., Faramand, Z., Alrawashdeh, M., Martin-Gill, C., Callaway, C., ... Al-Zaiti, S. (2019). Nonspecific electrocardiographic abnormalities are associated with increased length of stay and adverse cardiac outcomes in prehospital chest pain. *Heart and Lung*, 48(2), 121–125. <https://doi.org/10.1016/j.hrtlng.2018.09.001>
- Roza, V. C. C., De Almeida, A. M., & Postolache, O. A. (2017). Design of an artificial neural network and feature extraction to identify arrhythmias from ECG. In *2017 IEEE International Symposium on Medical Measurements and Applications (MeMeA)*, 391–396. <https://doi.org/10.1109/MeMeA.2017.7985908>
- Sadhukhan, D., & Mitra, M. (2012). R-peak detection algorithm for ECG using double difference and RR interval processing. *Procedia Technology*, 4, 873–877. <https://doi.org/10.1016/j.protcy.2012.05.143>
- Sankaran, A., Aralikkatte, R., Mani, S., Khare, S., Panwar, N., & Gantayat, N. (2017). DARVIZ : Deep Abstract Representation , Visualization , and Verification of Deep Learning Models. In *2017 IEEE/ACM 39th International Conference on Software Engineering: New Ideas and Emerging Technologies Results Track (ICSE-NIER)*, 47–50. <https://doi.org/10.1109/ICSE-NIER.2017.13>
- Sansone, M., Fusco, R., Pepino, A., & Sansone, C. (2013). Electrocardiogram pattern recognition and analysis based on artificial neural networks and support vector machines: A review. *Journal of Healthcare Engineering*, 4(4), 465–504. <https://doi.org/10.1260/2040-2295.4.4.465>
- Saritha, C., Sukanya, V., & Murthy, Y. N. (2008). ECG Signal Analysis Using Wavelet Transforms. *Bulg. J. Phys*, 35, 68–77.
- Savalia, S., Acosta, E., & Emamian, V. (2017). Classification of Cardiovascular Disease Using Feature Extraction and Artificial Neural Networks. *Journal of Biosciences and Medicines*, 5(11), 64–79. <https://doi.org/10.4236/jbm.2017.511008>
- Schäfer, P. (2015). The BOSS is concerned with time series classification in the presence of noise. *Data Mining and Knowledge Discovery*, 29(6), 1505–1530. <https://doi.org/10.1007/s10618-014-0377-7>

- Schillaci, G., Pirro, M., Pasqualini, L., Vaudo, G., Ronti, T., Gemelli, F., ... Mannarino, E. (2004). Prognostic significance of isolated, non-specific left ventricular repolarization abnormalities in hypertension. *Journal of Hypertension*, 22(2), 407–414. <https://doi.org/10.1097/00004872-200402000-00027>
- Sedova, K. A., Azarov, J. E., Artyeva, N. V., Ovechkin, A. O., Vaykshnorayte, M. A., Vityazev, V. A., ... Kneppo, P. (2017). Mechanism of electrocardiographic T-wave flattening in diabetes mellitus: Experimental and simulation study. *Physiological Research*, 66(5), 781–789.
- Shi, H., Sun, Y., & Li, J. (2018). Dynamical Motor Control Learned with Deep Deterministic Policy Gradient. *Computational Intelligence and Neuroscience*, 2018, 11. <https://doi.org/10.1155/2018/8535429>
- Shin, D. G., Cheol, S. Y., Sang, H. Y., Jun, H. B., Kim, Y.-J., Park, J. S., & Hong, G.-R. (2006). Prediction of Paroxysmal Atrial Fibrillation Using Nonlinear Analysis of the R-R Interval Dynamics Before the Spontaneous Onset of Atrial Fibrillation. *Circulation Journal Official Journal of the Japanese Circulation Society*, 70, 94–99.
- Sivaraks, H., & Ratanamahatana, C. A. (2015). Robust and accurate anomaly detection in ECG artifacts using time series motif discovery. *Computational and Mathematical Methods in Medicine*. <https://doi.org/10.1155/2015/453214>
- Soria, M. L., & Martínez, J. P. (2007). An ECG Classification Model based on Multilead Wavelet Transform Features. In *2007 Computers in Cardiology*, 105–108. <https://doi.org/10.1109/CIC.2007.4745432>
- Stub, D., Smith, K., Bernard, S., Nehme, Z., Stephenson, M., Bray, J. E., ... Kaye, D. M. (2015). Air Versus Oxygen in ST-Segment Elevation Myocardial Infarction. *Circulation*, 131(24), 2143–2150. <https://doi.org/10.1161/CIRCULATIONAHA.114.014494>
- Sun, Y., & Cheng, A. C. (2012). Machine learning on-a-chip : A high-performance low-power reusable neuron architecture for artificial neural networks in ECG classifications. *Computers in Biology and Medicine*, 42(7), 751–757. <https://doi.org/10.1016/j.combiomed.2012.04.007>
- Tan, M. P., Ho, Y. Y., Chin, A. V., Saedon, N. I., Abidin, I. Z., Chee, K. H., ... Kamaruzzaman, S. B. (2019). Ethnic differences in lifetime cumulative incidence of syncope: the Malaysian elders longitudinal research (MELoR) study. *Clinical Autonomic Research*, (0123456789). <https://doi.org/10.1007/s10286-019-00610-2>
- Touma, A. Al, Tafreshi, R., & Khan, M. (2016). Detection of Cardiovascular Abnormalities through 5-lead System Algorithm. *IEEE-EMBS International Conference on Biomedical and Health Informatics (BHI)*, 260–263. <https://doi.org/10.1109/BHI.2016.7455884>
- Tramèr, L., Becker, C., Hochstrasser, S., Marsch, S., & Hunziker, S. (2018). Association of electrocardiogram alterations of rescuers and performance during a simulated cardiac arrest: A prospective simulation study. *PLoS ONE*, 13(6). <https://doi.org/10.1371/journal.pone.0198661>

- Übeyli, E. D. (2009). Combining recurrent neural networks with eigenvector methods for classification of ECG beats. *Digital Signal Processing*, 19(2), 320–329. <https://doi.org/10.1016/j.dsp.2008.09.002>
- Vázquez-seisdedos, C. R., Neto, J. E., Reyes, E. J. M., Klautau, A., & De Oliveira, R. C. L. (2011). New approach for T-wave end detection on electrocardiogram: Performance in noisy conditions. *Biomedical Engineering Online*, 10(1), 77. <https://doi.org/10.1186/1475-925X-10-77>
- Vinyoles, E., Soldevila, N., Torras, J., Olona, N., & de la Figuera, M. (2015). Prognostic value of non-specific ST-T changes and left ventricular hypertrophy electrocardiographic criteria in hypertensive patients: 16-year follow-up results from the MINACOR cohort. *BMC Cardiovascular Disorders*, 15(1), 24. <https://doi.org/10.1186/s12872-015-0012-6>
- Wang, C, Dong, X., Ou, S., Wang, W., Hu, J., & Yang, F. (2016). A new method for early detection of myocardial ischemia: cardiodynamicsgram (CDG). *Science China Information Sciences*, 59(1), 1–11. <https://doi.org/10.1007/s11432-015-5309-7>
- Wang, C, & Guo, J. (2019). A data-driven framework for learners ' cognitive load detection A data-driven framework for learners ' cognitive load detection using ECG-PPG physiological feature fusion and XGBoost using ECG-PPG physiological feature fusion and XGBoost classification cl. *Procedia Computer Science*, 147, 338–348. <https://doi.org/10.1016/j.procs.2019.01.234>
- Wang, Cong, & Hill, D. J. (2007). Deterministic Learning and Rapid Dynamical Pattern Recognition. *IEEE Transactions on Neural Networks*, 18(3), 617–630.
- Wee, L. A. I. K., Min, T. Y., Arooj, A., & Supriyanto, E. (2010). Nuchal Translucency Marker Detection Based on Artificial Neural Network and Measurement via Bidirectional Iteration Forward Propagation. *WSEAS Transactions on Information Science and Applications*, 7(8), 1025–1036.
- World Health Organization. (2011). Global status report on noncommunicable diseases 2010. In *Geneva, World Health Organization*. [https://doi.org/ISBN 978 92 4 156422 9](https://doi.org/ISBN%20978%2092%204156422%209)
- World Health Organization. (2014). Global status report on noncommunicable diseases 2010. In *Google Scholar*.
- Wu, C. C., Hsu, W.-D., Islam, M. M., Poly, T. N., Yang, H.-C., Nguy, P.-A. A., ... Li, Y.-C. J. (2019). An artificial intelligence approach to early predict non-ST-elevation myocardial infarction Patients with Chest Pain. *Computer Methods and Programs in Biomedicine*, 173, 109–117. <https://doi.org/10.1016/j.cmpb.2019.01.013>
- Xia, Y., Zhang, H., Xu, L., Gao, Z., Zhang, H., Liu, H., & Li, S. (2018). An Automatic Cardiac Arrhythmia Classification System with Wearable Electrocardiogram. *IEEE Access*, 6, 16529–16538. <https://doi.org/10.1109/ACCESS.2018.2807700>
- Xu, Z., & Sun, J. (2018). Model-driven deep-learning. *National Science Review*, 5(1),

- Yaghouby, F., Ayatollahi, A., Bahramali, R., & Yaghouby, M. (2012). Robust genetic programming-based detection of atrial fibrillation using RR intervals. *Expert Systems*, 29(2), 183–199. <https://doi.org/10.1111/j.1468-0394.2010.00571.x>
- Yakovlev, A. N. (2016). Distributed data-driven platform for urgent decision making in cardiological ambulance control. *Future Generation Computer Systems*, 79, 144–154. <https://doi.org/10.1016/j.future.2016.09.017>
- Yamada, T., Fukunami, M., Shimonagata, T., & Kumagai, K. (2000). Prediction of Paroxysmal Atrial Fibrillation in Patients With Congestive Heart Failure: A Prospective Study. *Journal of American College Cardiology*, 35(2), 405–413. [https://doi.org/10.1016/S0735-1097\(99\)00563-X](https://doi.org/10.1016/S0735-1097(99)00563-X)
- Yan, G., Geng, T., Deng, M., & Wang, C. (2019). Research of CDG to identify individuals via deterministic learning theory. In *In Proceedings of 2018 Chinese Intelligent Systems Conference* (Vol. 529). https://doi.org/10.1007/978-981-13-2291-4_63
- Yang, T. F., Devine, B., & Macfarlane, P. W. (1994). Artificial neural networks for the diagnosis of atrial fibrillation. *Medical & Biological Engineering & Computing*, 32(6), 615–619. <https://doi.org/10.1007/BF02524235>
- Yeh, Y., Wang, W., & Wun, C. (2010). Expert Systems with Applications Feature selection algorithm for ECG signals using Range-Overlaps Method. *Expert Systems With Applications*, 37(4), 3499–3512. <https://doi.org/10.1016/j.eswa.2009.10.037>
- Yıldırım, Ö., Pławiak, P., Tan, R. S., & Acharya, U. R. (2018). Arrhythmia detection using deep convolutional neural network with long duration ECG signals. *Computers in Biology and Medicine*, 102, 411–420. <https://doi.org/10.1016/j.combiomed.2018.09.009>
- Yoon, D., Lim, H. S., Jeong, J. C., Kim, T. Y., Choi, J. G., Jang, J. H., ... Park, C. M. (2018). Quantitative evaluation of the relationship between t-wave-based features and serum potassium level in real-world clinical practice. *BioMed Research International*, 2018. <https://doi.org/10.1155/2018/3054316>
- Yu, Q., Liu, A., Liu, T., Mao, Y., Chen, W., & Liu, H. (2019). ECG R-wave peaks marking with simultaneously recorded continuous blood pressure. *PLoS ONE*, (1), 1–17.
- Yuan, N., Yang, W., Kang, B., Xu, S., & Li, C. (2018). Signal fusion-based deep fast random forest method for machine health assessment. *Journal of Manufacturing Systems*, 48(February), 1–8. <https://doi.org/10.1016/j.jmsy.2018.05.004>
- Zhang, G., Martens, J., & Grosse, R. (2019). Fast convergence of natural gradient descent for overparameterized neural networks. *Advances in Neural Information Processing Systems*, 32(NeurIPS), 1–12.
- Zheng, Q., Chen, C., Li, Z., Huang, A., Jiao, B., Duan, X., & Xie, L. (2013). A novel

multi-resolution SVM (MR-SVM) algorithm to detect ECG signal anomaly in WE-CARE project. *ISSNIP Biosignals and Biorobotics Conference, BRC*. <https://doi.org/10.1109/BRC.2013.6487453>

Zou, R., Shi, W., Tao, J., Li, H., Lin, X., Yang, S., & Hua, P. (2017). Neurocardiology: Cardiovascular Changes and Specific Brain Region Infarcts. *BioMed Research International*, 2017. <https://doi.org/10.1155/2017/5646348>

Universiti Malaya